

A Groundwater-Surface Water Interaction Study of an Alluvial Channel aquifer

Modreck Gomo

Thesis submitted in fulfillment of the requirements for the degree of

Philosophiae Doctor

in the

Faculty of Natural and Agricultural Sciences

(Institute for Groundwater Studies)

University of the Free State

Supervisor: Prof G. J. van Tonder

November 2011



Declaration

To my best knowledge and understanding, the thesis contains no material which has been previously published or written by another person except where due references has been given.

I, Modreck Gomo declare that; this thesis hereby submitted by me for the Philosophiae Doctor degree in the Faculty of Natural and Agricultural Sciences, Institute for Groundwater Studies at the University of the Free State is my own independent work. The work has not been previously submitted by me or anyone at any university. Furthermore, I cede the copyright of the thesis in favour of the University of the Free State.

Acknowledgments

I would like to express my sincere and special thanks to my academic supervisor Prof G. J. Van Tonder for all his academic and technical guidance. More importantly I thank Prof G. J. Van Tonder for his “always” positive attitude that has immensely contributed my overly motivation and academic development. The project manager Prof G. Steyl, I sincerely thank him for the academic guidance, overall funding support and management of the project.

Sincere thanks are also given to Prof. Joe Magner of the University of Minnesota (USA) for his input on the surface water flow processes and measurements. Technical assistance and support in various forms from **all** Institute of Groundwater Studies staff members is greatly appreciated. The study could have been impossible without technical field assistance from Stephanus De Lange (PhD Student), Teboho Shakhane (MSc student) and Leketa C Khahliso (MSc student). Assistance from Dora du Plessis on technical editing is greatly appreciated. This thesis emanated from a Water Research Commission (WRC) funded K5/2054 Surface water/groundwater hydrology project. Sincere thanks are given to WRC for financing this project.

I would also like to thank my family and friends for all their prayers and encouragements. Great praise to God who has given me the ability!

Keywords

Alluvial channel aquifer

Channel deposits

Gravel-sand

Groundwater-surface water interaction

Recharge mechanisms

Natural gradient tracer testing

Water balance mode

Hydrogeochemical processes

TABLE OF CONTENTS

TABLE OF CONTENTS.....	I
LIST OF FIGURES.....	VII
LIST OF TABLES	XII
LIST OF EQUATIONS	XIV
LIST OF ACRONYMS.....	XV
LIST OF QUANTITIES AND UNITS.....	XVI
1 INTRODUCTION	1
1.1 BACKGROUND.....	1
1.2 STUDY AIMS AND OBJECTIVES.....	4
1.2.1 <i>Geological characterization</i>	4
1.2.2 <i>Aquifer tests</i>	5
1.2.3 <i>Hydrogeochemical investigations</i>	5
1.2.4 <i>Recharge investigations</i>	5
1.2.5 <i>Tracer tests</i>	6
1.2.6 <i>GW-SW investigations</i>	6
1.2.7 <i>Conceptual discussion of alluvial channel aquifers</i>	6
1.3 CASE STUDY SITE.....	7
1.3.1 <i>Location</i>	7
1.3.1.1 <i>Field setting</i>	7
1.3.2 <i>Climate and topography</i>	8
1.3.3 <i>Water resources and use</i>	10
1.4 DATA COLLECTION STRATEGY	10
1.5 SIGNIFICANCE OF THE RESEARCH.....	11
1.6 LIMITATIONS OF THE STUDY	13
1.7 SUMMARY	13
2 ALLUVIAL CHANNEL AQUIFERS AND GW-SW INTERACTIONS STUDIES.....	14
2.1 ALLUVIAL CHANNEL AQUIFER	14
2.1.1 <i>Bedrock river channel</i>	15
2.1.1.1 <i>Aquifers along a bedrock river channel</i>	17

2.1.1.1.1	Idealized alluvial cover channel aquifer model.....	17
2.1.1.1.1.1	Geohydrological properties	19
2.1.1.1.1.2	Groundwater-river interactions.....	20
2.1.1.1.2	Alluvial cover and fractured-bedrock idealized aquifer model.....	21
2.1.2	<i>Alluvial river channel</i>	22
2.2	GW-SW INTERACTIONS	23
2.2.1	<i>GW-SW interactions studies</i>	24
2.2.2	<i>Mechanism of GW-SW interactions</i>	26
2.2.3	<i>Components of GW-SW interaction studies</i>	27
2.2.3.1	Aquifer system	27
2.2.3.2	Groundwater discharge measurements	27
2.2.3.2.1	Hydraulic measurements	28
2.2.3.2.2	Tracer test	28
2.2.3.2.3	Seepage flow meters.....	29
2.2.3.2.4	Stream flow measurements.....	30
2.2.3.3	Riparian zone	30
2.3	SUMMARY.....	31
3	GEOLOGICAL CHARACTERISATION	32
3.1	INTRODUCTION	32
3.2	REGIONAL GEOLOGY.....	33
3.2.1	<i>Quaternary deposits</i>	34
3.3	FIELD METHODS AND MATERIALS.....	35
3.3.1	<i>Outcrop mapping</i>	35
3.3.2	<i>Borehole drilling</i>	36
3.4	SITE GEOLOGY	39
3.4.1	<i>Outcrops</i>	39
3.4.2	<i>Geological logs and borehole construction</i>	40
3.4.2.1	Alluvial channel aquifer.....	40
3.4.2.1.1	BH1 borehole	40
3.4.2.1.2	BH2, BH3 and BH4.....	42
3.4.2.1.3	Other boreholes	43
3.4.2.1.4	Lithological hydrofacies	44
3.4.2.1.5	Grain size analysis	45
3.4.2.2	Background terrestrial aquifer.....	46

3.4.3	<i>Conceptual model</i>	48
3.4.3.1	Evolution of the alluvial channel aquifer	48
3.4.3.1.1	Geological conceptual model.....	50
3.4.3.2	Unconsolidated sediments	52
3.4.3.2.1	Calcrete	52
3.4.3.2.2	Clay-silt sediments	53
3.4.3.2.3	Gravel-sand deposits.....	55
3.4.3.2.4	Shale consolidated sediments.....	56
3.4.4	<i>Delineation of the aquifer system</i>	56
3.5	SUMMARY	58
4	HYDRAULIC TESTS IN A TYPICAL ALLUVIAL CHANNEL AQUIFER	59
4.1	FIELD MEASUREMENTS	60
4.1.1	<i>Groundwater flow directions</i>	60
4.1.2	<i>Infiltration tests</i>	64
4.1.2.1	Infiltration rates	66
4.1.3	<i>Slug tests</i>	66
4.1.3.1	Borehole yields and hydraulic parameters	67
4.1.4	<i>Aquifer pump testing</i>	68
4.1.4.1	Shallow main aquifer system	68
4.1.4.1.1	Aquifer pump test design.....	68
4.1.4.1.1.1	Selection of constant pumping rate (Q).....	68
4.1.4.1.1.2	Equipment set-up and measurements	69
4.1.4.1.1.3	Aquifer model selection.....	69
4.1.4.1.1.4	Pseudo-steady state conditions.....	70
4.1.4.1.1.5	Cone of depression movement.....	71
4.1.4.1.1.6	Aquifer lithology.....	71
4.1.4.1.1.7	Derivative flow characterization	72
4.1.4.1.1.8	Groundwater flow phases.....	73
4.1.4.1.1.9	Aquifer parameters.....	75
4.1.4.1.1.10	Transmissivity and storage	78
4.1.4.2	Deep aquifer system	81
4.2	SUMMARY	82
5	HYDROGEOCHEMICAL PROCESSES IN AN ALLUVIAL CHANNEL AQUIFER.....	83

5.1	INTRODUCTION	83
5.2	MATERIALS AND METHODS.....	84
5.2.1	<i>XRD and X-Ray analysis</i>	84
5.2.2	<i>Groundwater sampling and analysis</i>	84
5.3	RESULTS.....	85
5.4	DISCUSSION	87
5.4.1	<i>Hydrogeochemical processes</i>	87
5.4.1.1	Carbonate system	87
5.4.1.1.1	Stage 1.....	88
5.4.1.1.2	Stage 2.....	89
5.4.1.1.3	Stage 3.....	89
5.4.1.1.4	Stage 4.....	89
5.4.1.2	Nitrates as nitrogen $\text{NO}_3^-(\text{N})$	89
5.4.1.2.1	Nitrate evolution routes	90
5.4.1.2.1.1	Route A.....	90
5.4.1.2.1.2	Route B.....	91
5.4.1.3	Sodium	92
5.4.1.3.1	Ion exchange	92
5.4.1.3.2	Silicate weathering.....	95
5.4.1.4	Saturation indices	95
5.4.1.5	Sulphate and chloride	96
5.4.2	<i>Groundwater quality</i>	98
5.4.2.1	Hardness	98
5.4.2.2	Irrigation water quality	99
5.4.2.3	Trace elements.....	100
5.5	SUMMARY	100
6	GROUNDWATER RECHARGE INVESTIGATIONS IN AN ALLUVIAL CHANNEL AQUIFER.....	102
6.1	INTRODUCTION	102
6.1.1	<i>Methods and materials</i>	103
6.1.1.1	Water level fluctuation method.....	103
6.1.1.2	Chloride mass balance method.....	104
6.2	RESULTS AND DISCUSSIONS	105
6.2.1	<i>Water level fluctuations</i>	105
6.2.2	<i>Groundwater level response to rainfall</i>	106

6.2.3	<i>Chloride mass balance</i>	108
6.2.4	<i>Stable environmental isotopes ($\delta^{18}O$ and δ^2H)</i>	109
6.3	RECHARGE CONCEPTUAL MODEL	110
6.4	SUMMARY	112
7	NATURAL GRADIENT TRACER TEST IN AN ALLUVIAL CHANNEL AQUIFER	114
7.1	NATURAL GRADIENT POINT DILUTION TRACER TEST	114
7.1.1	<i>Design of the experiment and salt solute injection system</i>	114
7.1.1.1	Tracer testing zone	115
7.1.1.2	Measurements and accuracy	116
7.1.1.3	Data analysis	116
7.1.1.3.1	Density effects	117
7.1.1.3.1.1	Qualitative analysis	118
7.1.1.4	Dilution plots	120
7.1.1.5	Summary NGPDTT in alluvial channel aquifers	122
7.2	NATURAL GRADIENT TRACER BREAKTHROUGH TEST	122
7.2.1	<i>Test field design</i>	123
7.2.2	<i>Tracer breakthrough</i>	124
7.2.3	<i>Challenges of the NGTBT</i>	127
7.2.4	<i>General guidelines for NGTBT</i>	127
7.3	SUMMARY	128
8	ALLUVIAL CHANNEL AQUIFER AND RIVER/STREAM INTERACTIONS	130
8.1	INTRODUCTION	130
8.2	WATER BALANCE MODEL	130
8.2.1	<i>GW-SW water balance system</i>	131
8.2.2	<i>Methods and materials</i>	132
8.2.2.1	Discharge measurements	132
8.2.2.2	Isotopes and solute measurements	133
8.2.3	<i>Results and discussion</i>	134
8.2.3.1	Model inflow	134
8.2.3.1.1	River inflow (Q_{RI})	134
8.2.3.1.2	Groundwater inflow (Q_{GI})	135
8.2.3.1.3	River outflow (Q_{RO})	136
8.2.3.1.4	Model net balance	138
8.2.3.1.5	Model reliability	140
8.3	STABLE ISOTOPE ANALYSIS	141

8.4	GW-SW INTERACTION MECHANISMS AT THE SITE	144
8.5	GENERAL GUIDELINES FOR GW-SW INTERACTION STUDIES.....	145
8.6	SUMMARY	148
9	CONCLUSIONS AND RECOMMENDATIONS.....	149
9.1	CONCLUSIONS.....	149
9.1.1	<i>Geological characterisation</i>	<i>149</i>
9.1.2	<i>Hydraulic processes and groundwater flow.....</i>	<i>150</i>
9.1.3	<i>Hydrogeochemical processes</i>	<i>151</i>
9.1.4	<i>Groundwater recharge processes and mechanisms</i>	<i>152</i>
9.1.5	<i>Natural gradient tracer tests in an alluvial channel aquifer</i>	<i>152</i>
9.1.6	<i>GW-SW interactions along the alluvial channel aquifer</i>	<i>153</i>
9.1.7	<i>Proposed classification of alluvial channel aquifers</i>	<i>154</i>
9.2	RECOMMENDATIONS	155
9.3	MAIN CONTRIBUTION OF THE THESIS.....	157
10	REFERENCES	158
	APPENDICES.....	169
	APPENDIX 1 HYDRAULIC TESTS.....	169
	APPENDIX 1.1 INVERSE AUGER METHOD.....	169
	APPENDIX 1.2 DERIVATIVE PLOTS.....	172
	APPENDIX 1.3 SEMI-LOG PLOTS	173
	APPENDIX 2 GROUNDWATER AND RIVER WATER CHEMISTRY	174
	APPENDIX 2.1 JULY 2010.....	174
	APPENDIX 2.2 FEBRUARY 2011	175
	APPENDIX 2.3 MAY 2011	176
	APPENDIX 2.4 AUGUST 2011.....	177
	APPENDIX 2.5 DECEMBER 2011.....	178
	APPENDIX 3 GROUNDWATER LEVELS	179
	APPENDIX 3.1 ALLUVIAL CHANNEL AQUIFER.....	179
	APPENDIX 3.2 BACKGROUND TERRESTRIAL AQUIFER.....	179
	APPENDIX 4 ISOTOPES	180
	APPENDIX 4.1 FEBRUARY AND MAY 2011.....	180
	ABSTRACT	181

LIST OF FIGURES

Figure 1-1 Location of the case study site; the small square on the inserted Africa map shows the location of Bloemfontein city in the Free State Province of South Africa; letter A shows the location of the weir downstream of the case study site.	3
Figure 1-2 Location of the terrestrial aquifer and alluvial channel aquifers on the terrestrial land and riparian zone respectively; also shown is the location of the groundwater discharge zone and boreholes that were drilled into the two aquifers systems.....	8
Figure 1-3 Monthly rainfall for the study area recorded during the 2010/2011 rain season (<i>WeatherSA</i> 2011).....	9
Figure 1-4 An image showing surface topography from the background terrestrial aquifer to the alluvial channel aquifer; also shown is the location of the boreholes drilled into the alluvial channel aquifer and terrestrial aquifer.	9
Figure 1-5 A 3-dimensional image showing the surface topography from the riparian zone towards the river; also shown in the image is the seepage face where groundwater discharges into the river (the image is not to scale in the vertical direction).	10
Figure 2-1 A plan showing the idealized location of a typical alluvial channel aquifer between the river bank and terrestrial aquifer.....	14
Figure 2-2 Image of alluvial cover along the bedrock channel reaches (Taken from Keen-Zebert 2007).	16
Figure 2-3 Photos showing an (a) outcrop of shale bedrock and (b) the thin alluvial cover along the river bank adjacent to the alluvial channel aquifer.	16
Figure 2-4 Idealized groundwater flow in the alluvial cover channel aquifer occurring along a bedrock river channel; the aquifer locally discharges groundwater into a “gaining river” at the seepage face created between the alluvial cover and bedrock contact plane; arrows shows flow directions.	18
Figure 2-5 A photo showing the shale bedrock at the case study site that has been subjected to fracturing and weathering processes.	19
Figure 2-6 Idealized groundwater flow conditions in an alluvial cover channel aquifer occurring along a bedrock river channel where the river is losing water to the aquifer; the river stage elevation rises above the groundwater elevations thereby reversing the gradient and the losing river discharges water into the alluvial channel aquifer; arrows show the flow directions.	20
Figure 2-7 Idealized groundwater flow conditions in an alluvial channel aquifer occurring along a bedrock river channel; the groundwater resource occurs and flows in both the alluvial cover and fractured-bedrock; arrows show the flow directions.	21
Figure 2-8 An image showing an alluvial valley of the Paria River in Arizona (Hereford 2000); thick alluvial channel deposits can be seen on opposite sides of the current river channel.	23
Figure 2-9 A schematic representation of GW-SW interactions occurring through the river/stream bed for; (A) gaining and (B) losing stream system (Taken from Winter <i>et al.</i> 1999).	26
Figure 3-1 A schematic showing the Karoo Supergroup sequence (after Tankard <i>et al.</i> 1982).	33
Figure 3-2 Models showing the fluvial processes associated with (a) braided stream and (b) Meandering streams (Botha <i>et al.</i> 1998).	35
Figure 3-3 Location of the boreholes that were drilled into the alluvial channel aquifer and terrestrial background aquifer of the study site; also shown is the location of shale and calcrete outcrops.	37

Figure 3-4 Photos of the showing: (a) Air percussion drilling equipment used for borehole drilling and (b) Poly Vinyl Chloride pipes used for boreholes casing; perforations on the pipe were handmade using a grinder machine.....	38
Figure 3-5 A schematic diagram showing the lithology and construction of BH1; the bold and dashed lines shows the average water levels measured before and after sealing with concrete respectively.	41
Figure 3-6 Geological logs showing the lithologies intersected in 24 m deep boreholes (BH2, BH3 and BH4).....	42
Figure 3-7 Geological logs showing the lithology intersected in BH6, BH5, BH7, BH9 and BH8 boreholes; the groundwater levels shown in bold lines were measured after borehole construction.	44
Figure 3-8 Geological logs showing the lithologies intersected in the background boreholes.	47
Figure 3-9 Scatter plots of groundwater level against ground surface elevation of the boreholes drilled into the terrestrial (a) and shallow alluvial channel main aquifer (b); these water levels were measured 5 days after drilling of each borehole.	47
Figure 3-10 A plot showing the relationship between surface topography elevation and groundwater level elevation of the background terrestrial aquifer and the alluvial channel aquifer; groundwater level were measured 5 days after drilling of each borehole.	48
Figure 3-11 A schematic showing the idealized old river channel that was flowing on top of the shale bedrock; the arrow shows the direction towards which the river channel was shifting.	49
Figure 3-12 A schematic showing the idealized position of the current river channel and the alluvial channel aquifer system; the horizontal arrow shows the groundwater flow direction in the alluvial channel aquifer that eventually discharges into the river at the contact plane.	49
Figure 3-13 Location of boreholes drilled into the alluvial channel aquifer from which the geological cross sections were constructed.....	50
Figure 3-14 Idealized geological cross-section from point A to point B.	51
Figure 3-15 Idealized geological cross-section from point C to point D; the arrow shows the position of groundwater discharge that occurs through a seepage face created at the contact plane of the unconsolidated sediments and shale impermeable bedrock.	52
Figure 3-16 A schematic of deep soil horizon showing the clay-silt soils sediments located below the calcrete layer.....	54
Figure 3-17 Washed samples of coarse sand and gravel channel deposits that were intersected in BH7 borehole between 6-9 mbgl.....	55
Figure 3-18 Shale bedrock outcropping at the site river bank.	56
Figure 3-19 EC profiles showing anomalies associated with the groundwater flow in the gravel-sand geohydrologic zone between 5-8 mbgl; the arrow indicates the position of the main anomaly.	57
Figure 4-1 Location of the boreholes drilled into the alluvial channel aquifer.	59
Figure 4-2 Time series principal natural groundwater flow directions monitored for 13 months (August 2010-September 2011) in the: (a) alluvial channel aquifer and (b) terrestrial aquifer; each arrow shows the principal flow direction for a specific month.	60
Figure 4-3 Time series principal natural groundwater flow directions monitored for 13 months (August 2010-September 2011) between the alluvial channel aquifer and terrestrial background aquifer; each arrow shows the principal flow direction for a specific month.	62

Figure 4-4 Groundwater level contours (mams) and vectors on the study site showing groundwater flow directions; the insert shows location of the study area on the alluvial channel aquifer; the arrow in the insert shows the natural principle groundwater flow direction as determined using water level elevation from various combinations of borehole triangles.	63
Figure 4-5 Idealized schematic used in literature to show groundwater flow direction along a gaining stream (Adapted from Winter 1998).	64
Figure 4-6 Location of the infiltration sites on the riparian zone of the alluvial channel aquifer, IH represent infiltration hole.	65
Figure 4-7 Parallel drawdown time plots showing the pseudo-steady state conditions from 50 minutes to the end of the test; borehole BH7 was being pumped and observations were made in BH3, BH5 and BH6 boreholes.	70
Figure 4-8 Derivative drawdown plot showing early time Theis response (A), transition period (B), RAF (C) and impermeable boundary effects flow characteristics during the abstraction from borehole BH7.	72
Figure 4-9 Semi-log plot of drawdown (linear scale) against time (log scale) showing three distinct flow phases (A, B and C) during a four hour aquifer test.	74
Figure 4-10 Semi-log plot of drawdown against time showing the application of Cooper and Jacob equation (1946) to get transmissivity from pumping borehole between the 10-100 log cycle.	77
Figure 4-11 Semi-log plot of drawdown against time showing the application of Cooper and Jacob equation (1946) fit to determine aquifer transmissivity and storativity from an observation borehole between 10-100 log cycle.	77
Figure 4-12 Variation between the aquifer transmissivity determined from pumping and observation drawdown; BH7 was being pumped and observations made in (BH3, BH5, BH6 and BH9); T_p is the transmissivity obtained when the borehole is pumped and T_o is when used for observations; d is the average proportion % of gravel-sand grains of the aquifer material surrounding the borehole analysis.	79
Figure 4-13 Groundwater levels measured in deep and shallow aquifers of the alluvial channel aquifer system.	82
Figure 5-1 Groundwater and river samples plots on a piper diagram; groundwater samples are encircled by the dashed oval while the bold oval encircles the river water samples.	86
Figure 5-2 A flow diagram showing the idealised carbonate system reactions that occur during the recharge process as the water passes through the aquifer media of different chemical and physical properties.	88
Figure 5-3 Possible routes of nitrate evolution in the alluvial channel aquifer.	90
Figure 5-4 Bivariate plot of Na^+ against Cl^- at the study site; black arrows indicate the contribution of the ion-exchange process and deviation from the 1:1 evaporation line; meq/l – Milliequivalent per Liter.	92
Figure 5-5 Bivariate plot showing $(Ca^{+2}+Mg^{+2})$ against $(SO_4^{-2}+HCO_3^-)$ for the groundwater samples from the alluvial channel aquifer and terrestrial aquifer.	93
Figure 5-6 Relationship between $(Ca^{+2}+Mg^{+2}-SO_4^{-2}-HCO_3^-)$ against (Na^+-Cl^-) for groundwater sampled in February 2011 (a), May 2011 (b), August 2011(c) and December 2011 (d).	94

Figure 5-7 Relationship between the saturation indices for calcite and dolomite; quadrants define: A-Dolomite and calcite supersaturation, B-Dolomite undersaturation and calcite supersaturation, C-dolomite and calcite undersaturation; and D-dolomite supersaturation and calcite undersaturation.	96
Figure 5-8 Scatter diagrams showing Cl^- against SO_4^{2-} plots for groundwater samples collected in: (a) February, (b) May 2011, (c) August and (d) Dec2011.	97
Figure 5-9 Classification of groundwater based on salinity and alkalinity hazard of irrigation requirements.	99
Figure 6-1 Groundwater level responds to rainfall measured during the monitoring period from August 2010 to September 2011; rainfall amounts were derived qualitatively from historical rainfall maps of the South African weather service (<i>WeatherSA</i> 2011).	107
Figure 6-2 Plot of $\delta^2\text{H}$ against $\delta^{18}\text{O}$ for groundwater samples showing the deviation from the GMWL and LMWL; GMWL: $\delta^2\text{H} = 8 \cdot \delta^{18}\text{O} + 10$; LMWL Pretoria: $\delta^2\text{H} = 6.5 \cdot \delta^{18}\text{O} + 7.8$; (IAEA/WMO, 2004).	110
Figure 6-3 Idealized groundwater recharge processes for the alluvial channel aquifer and the terrestrial aquifer; big arrows represent large quantity parameters; the furthest borehole in the terrestrial land is located about 500 m from the river bank.	111
Figure 6-4 Photos showing some of the holes that have been created by burrowing animals on the riparian zone; arrows points at some of the identified holes and cavities.	112
Figure 7-1 A photo showing the perforated 1 litre plastic container that was used for injecting the salt solute into the testing borehole.	115
Figure 7-2 Borehole BH7 geological log and EC profiling showing EC anomaly between 6-9 mbgl that is associated with the gravel-sand main flow zone of the alluvial channel aquifer.	116
Figure 7-3 Typical influence of density effect on tracer initial dilution rates (Taken from Shakhane 2011).	118
Figure 7-4 NGPDTT dilution plots of EC against time; (a) The whole dilution plot from 0-3300 minutes; (b) Dilution plot from 400-3300 minutes and (c) Dilution plot from 1800-3300 minutes. .	119
Figure 7-5 NGPDTT measurements for test 1; (a) LTC levellogger EC measurements and (b) Standardized EC measurements.	120
Figure 7-6 NGPDTT measurements for test 2; (a) LTC levellogger EC measurements and (b) Standardized EC measurements.	121
Figure 7-7 A schematic of the NGTBT field design and the idealized tracer plume movement from the injection borehole BH7; the arrow shows the principal direction of natural groundwater flow.	123
Figure 7-8 EC profile in BH6 indicating an anomaly between 6-8 mbgl that is associated with the gravel-sand main flow zone.	124
Figure 7-9 Salt solute tracer breakthrough curve and rapid increase of water levels measured in BH6 during the NGTBT.	125
Figure 7-10 Schematic of tracer plume movement from the injection borehole towards monitoring boreholes in an ideal natural gradient testing field; the arrow shows the principal direction of natural groundwater flow.	127
Figure 8-1 An illustration showing components of the GW-SW water balance system.	131
Figure 8-2 Measured river cross-sectional area of flow at the inflow segment of the GW-SW system; the numbers indicate trapezoidal segments that were used to calculate the flow cross-sectional area.	134

Figure 8-3 Idealized schematic showing the components of the aquifer discharge zone at the seepage face; Δh is the hydraulic head differences between local aquifer and discharging zone groundwater levels; arrows indicate groundwater discharge into the aquifer.....	136
Figure 8-4 Measured cross-sectional area of flow (A) at the outflow segment of the GW-SW system; the numbers indicate trapezoidal segments that were used to calculate the flow cross-sectional area.	137
Figure 8-5 Measured cross-sectional area of flow (B) at the outflow segment of the GW-SW system; the numbers indicate the trapezoidal segments that were used to calculate the flow cross-sectional area.	138
Figure 8-7 Plot of δ^2H against $\delta^{18}O$ for ground and river water samples showing the deviation from the GMWL and LMWL; GMWL: $\delta^2H = 8 \cdot \delta^{18}O + 10$; LMWL Pretoria: $\delta^2H = 6.5 \cdot \delta^{18}O + 7.8$; (IAEA/WMO, 2004).	142
Figure 8-8 δ^2H and $\delta^{18}O$ that was measured for the water inflow and outflow of the GW-SW system measured in October 2011 during dry and low river flow conditions.....	143
Figure 8-9 A photo showing the seepage face where groundwater discharges from the alluvial channel into the river; arrows shows flow direction flow.	144
Figure 8-9 An illustration showing groundwater flow in the unconsolidated sediments of the alluvial channel main aquifer underlying the low permeable shale bedrock where discharges groundwater into the river at the seepage face; Δh is the average hydraulic head differences between alluvial channel aquifer and discharging zone; arrows shows direction of flow.	145
Figure 8-11 A flow diagram showing important steps and considerations for GW-SW interactions investigations.	147
Figure 9-1 A flow diagram showing the proposed classification of alluvial channel aquifers and typical attributes of geohydrological properties.....	154

LIST OF TABLES

Table 1 Information about borehole depth, casing and main water strikes, the boreholes were named according to their drilling order. The water levels were measured after one week after drilling but prior to construction.	39
Table 2 Properties of major sediment hydrofacies observed at the study site.....	45
Table 3 Results of grain size analysis and estimated hydraulic conductivity for representative gravel-sand aquifer materials.	45
Table 4 Average saturated hydraulic conductivities of the infiltrating front determined on the riparian zone.	66
Table 5 Borehole yield and hydraulic conductivity estimates values determined from the slug test for the boreholes drilled into the alluvial channel aquifer.....	67
Table 6 Spread rate of movement of the depression cone from the pumping boreholes to observation boreholes calculated based on the response time and observation distance (r).	71
Table 7 Transmissivity values determined for flow phases B and C when BH7 was being pumped and observations made in BH3, BH4, BH5 and BH9 boreholes.	75
Table 8 Aquifer parameters determined from single-borehole test analysis.....	78
Table 9 Aquifer parameters determined from multiple-borehole test analysis.	78
Table 10 Transmissivity values obtained when Cooper and Jacob is applied on pumping and observation boreholes.	80
Table 11 Transmissivity values determined from the boreholes drilled into the deep aquifer system.	81
Table 12 Maximum and minimum concentrations of major ions and other important ions measured in the groundwater during the monitoring period, also shown in the table is the South African National Standards (SANS 1996) of drinking water quality target concentrations.	85
Table 13 Major oxides elements detected in the channel deposits that makes the alluvial aquifer and their relative % content.	86
Table 14 Major minerals detected in the alluvial channel aquifer materials; XX - dominant (> 40 % per volume), X - major (10-40 % per volume), xx - Minor (2-10 % per volume) and x - accessory (1-2 % per volume).	87

Table 15 Classification of groundwater based on hardness (Sawyer and McMcarty 1967).....	98
Table 16 Maximum and minimum concentrations of trace elements analysed in the groundwater.	100
Table 17 Monthly groundwater recharge rates calculated using Equation 9 for the boreholes drilled into the alluvial channel aquifer during the (2010-2011) rainy season.....	105
Table 18 Monthly groundwater recharge values and rates calculated using Equation 9 for the boreholes drilled into the terrestrial aquifer channel aquifer during the (2010-2011) rain season..	105
Table 19 Average monthly groundwater chloride concentrations and the calculated recharge rate [mm] for the alluvial channel aquifer.	109
Table 20 Average monthly groundwater chloride concentrations and the calculated recharge rate for the terrestrial aquifer.....	109
Table 21 Groundwater flux (q) determined from the NGPDTT in BH7 borehole and other parameters used during the calculations.	121
Table 22 Measurements of the total cross-sectional area of flow, surface velocity, discharge, $\delta^2\text{H}$ stable isotopic ratio and EC at the inflow segment of the model.	135
Table 23 Calculated groundwater discharge from the alluvial channel aquifer into the river and parameters used for calculations; EC and $\delta^2\text{H}$ of the discharging waters.....	136
Table 24 Measurements of the cross-sectional area of flow, velocity, flow rate, $\delta^2\text{H}$ EC and at positions A and B along the outflow segment of the GW-SW model.....	138
Table 25 Measured and calculated components of the water balance model based on the mass, solute concentration and $\delta^2\text{H}$ isotopic ratio. A complete set of data and measured parameters used for the calculations is found in Appendix 5 of the appendices data disk.	139
Table 26 Water balance model lose rates calculated when aquifer thickness is varied from 0.1-2.0 m.	141

LIST OF EQUATIONS

Equation: 1 Groundwater flux (Darcy velocity).	29
Equation 2: Hazen (1911) hydraulic conductivity.	45
Equation 3: Cooper and Jacob (1946) aquifer transmissivity.	76
Equation 4: Cooper and Jacob (1946) aquifer storativity.	77
Equation 5: Nitrification of ammonium sulphate fertilizers.	91
Equation 6: Nitrification of urea fertilizer.	91
Equation 7: Nitrification of ammonia nitrate fertilizer.	91
Equation 8: Silicate weathering.	95
Equation 9: Recharge (Water level fluctuation method).	103
Equation 10: Groundwater recharge flux (Chloride mass balance method).	104
Equation 11: Groundwater flux (Darcy velocity).	117
Equation 12: Tracer concentration standardization.	117
Equation 13: Mass balance.	131
Equation 14: Solute mixing balance.	132
Equation 15 Stable Isotope mixing balance.	132
Equation 15: Darcy.	135

LIST OF ACRONYMS

GW-SW	Groundwater-Surface Water
GW-RW	Groundwater-River Water
LTC	Level Temperature Conductivity
mamsl	meters above mean sea level
mbgl	meters below ground level
mbws	meters below water surface
NGPDTT	Natural Gradient Point Dilution Tracer Test
NGTB	Natural Gradient Tracer Breakthrough
TDS	Total Dissolved Solids
PHREEQC	pH reaction Equilibrium calculation
ppp	parts per million
SAR	Sodium Adsorption Ratio

LIST OF QUANTITIES AND UNITS

Area (A)	m^2
Aquifer thickness (b)	m
Concentration	mg/l
Discharge (Q)	l/s or m^3/d
Drawdown (s)	m
Electrical conductivity (EC)	$\mu\text{S}/\text{cm}$ or mS/m
Groundwater flux (q)	m^2/d
Groundwater velocity (v)	m/d
Hydraulic conductivity (K)	m/d
Transmissivity (T)	m^2/d

1 INTRODUCTION

1.1 Background

Although considerable literature exist on the geomorphologic processes of alluvial and river channels (Richards 1982, Vigilar and Diplas 1998, Turowski et al. 2008 and Turowski 2010), very little effort has been devoted on describing the influence that these channel types have on the occurrence and properties of the alluvial channel aquifer. In literature, the term “alluvial aquifer” has been used in reference to aquifers that generally comprises of unconsolidated river channel deposits (Kelly 1997, Weng *et al.* 1999, Klingbeil *et al.* 1999, Mansell and Hussey 2005) without addressing the nature of the hosting river channel. In nature, alluvial aquifers can occur along both the alluvial and bedrock river channels. The nature of the river channel housing the alluvial channel aquifer has a huge influence on the properties of the aquifer system that will develop. An alluvial channel aquifer is hereby defined to exist when groundwater occurs within sediments adjacent to the river banks on the riparian zone. It is important for groundwater scientists to understand the differences between alluvial and bedrock river channels and the influence that they can have on properties of the alluvial channel aquifers.

In Southern Africa, groundwater from alluvial channel aquifers along both ephemeral and perennial rivers is reliably used to meet agricultural and domestic requirements (Seely *et al.* 2003). Ephemeral rivers are more common in Southern Africa due to extended periods (> 9 months) without significant rainfall events (Mansell and Hussey 2005). During these dry periods farmers heavily rely on groundwater, and alluvial aquifers offers the solution (Seely *et al.* 2003).

Alluvial channel aquifers located along the major rivers of the Southern Africa Karoo Basin typically comprises of unconsolidated calcrete, clay, silts and sand deposits. According to Woodford and Chevallier (2002), Quaternary deposits are a major characteristic along the main rivers of the Karoo Basin. Most of the alluvial channel aquifers are often characterised by shallow water table conditions and highly hydraulic conductive gravel-sand geohydrologic units. Such geohydrological characteristics although good for groundwater yield and abstractions, also present suitable conditions for contaminant access and migration into the aquifer. In general three typical geohydrological problems can be associated with alluvial channel aquifers. Firstly, the aquifers are often at risk from pollution given the typical shallow water table conditions and proximity to farming areas. Secondly, over abstraction from the aquifer can result in inflow from the surface water

resources depending on the connectivity and geohydrological properties. Thirdly, the dewatering of the alluvial channel aquifer can negatively affect the riparian vegetation and ecology (Rood *et al.* 2003). Alluvial channel aquifers are located in groundwater discharge zones thereby forming an important component of the groundwater-surface water (GW-SW) interaction system. Comprehensive studies of alluvial channel aquifer geohydrological properties at local scales (< 1000 m) have potential to improve the understanding of groundwater movement at large/regional scales.

Detailed geohydrological studies of alluvial channel aquifers and GW-SW interactions along the aquifer systems have not been conducted in Southern Africa. A few of the studies that have been reported were largely focused on assessing the potential yield and sustainable management of the aquifers (Benito *et al.* 2009; De Hamer *et al.* 2008; Moyce *et al.* 2006, Mansell and Hussey 2005). It is upon such a background that motivation was invoked for the PhD research thesis to focus on investigating the detailed geohydrological properties of the alluvial channel aquifer and GW-SW interactions along the aquifer. The case study site is located in the Modder River catchment, downstream of the Krugersdrift Dam which is situated about 30 km from the city of Bloemfontein, Free State Province in South Africa (Figure 1-1).

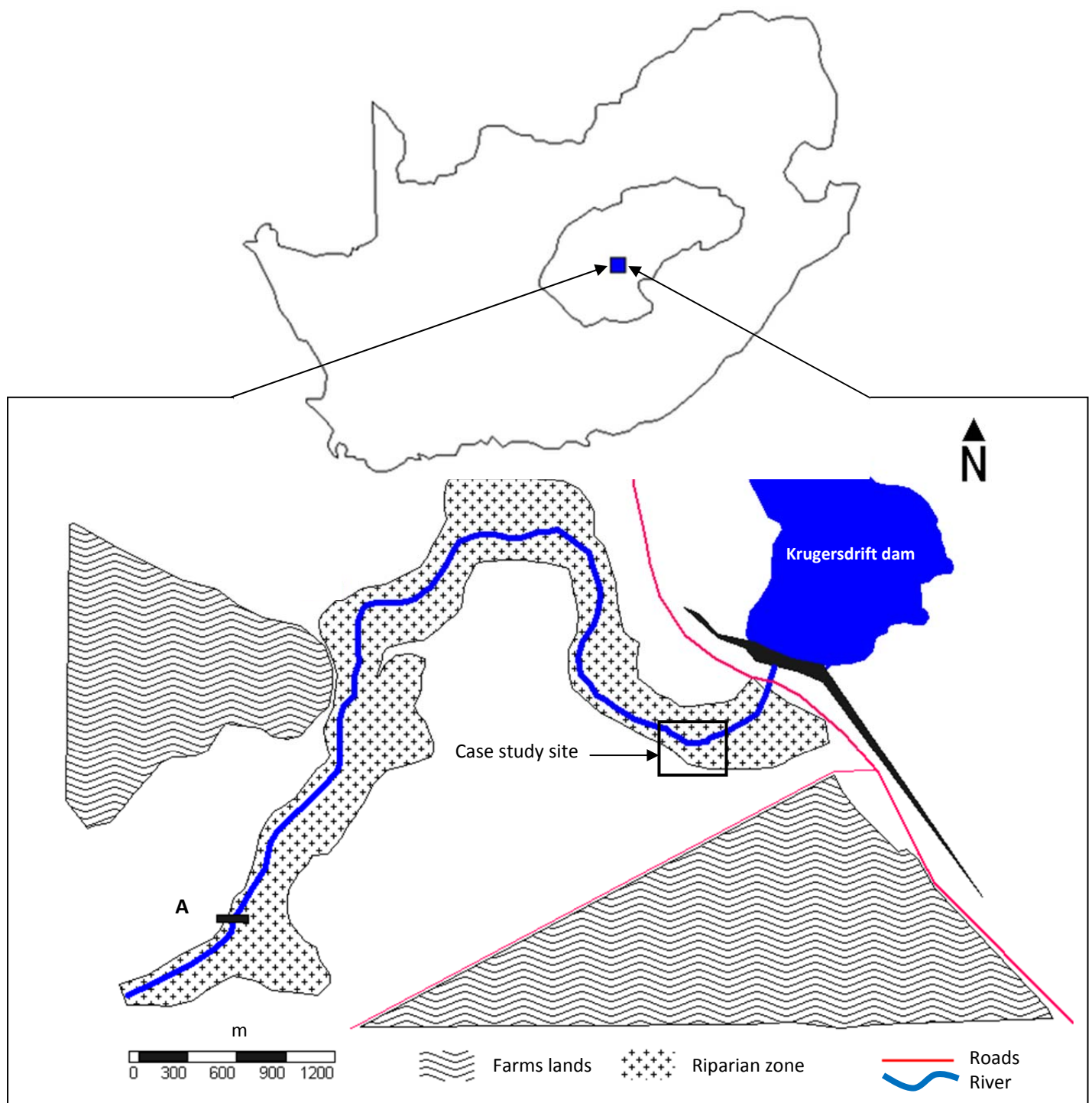


Figure 1-1 Location of the case study site; the small square on the inserted Africa map shows the location of Bloemfontein city in the Free State Province of South Africa; letter A shows the location of the weir downstream of the case study site.

Primary field investigations were designed to determine the geologic, hydraulic, hydrogeochemical and solute transport properties of the alluvial channel aquifer as an important component of the GW-SW interaction system. The secondary investigations were then aimed at assessing groundwater discharge and recharge mechanisms of the alluvial channel aquifer. The applicability of conventional

geohydrological tools to characterize an alluvial channel aquifer was also assessed as part of the study. A comprehensive comparison of the hydraulic, hydrogeochemical process and recharge mechanisms between the alluvial channel aquifer and terrestrial aquifer system was also conducted given their interdependence. Most of the work on the terrestrial background aquifer was covered by Leketa (2011) and will be used as the main reference for comparison purposes.

Because alluvial channel aquifers are often located in groundwater discharge zones, it was also important to include some basic aspects of GW-SW interaction studies in the last chapter of the thesis. A water balance model was developed for the GW-SW system as part of the tertiary level of investigation. The applications of the PhD thesis findings are not only limited to the case study site, but have important implications for GW-SW interaction studies, groundwater resource development and protection in areas where groundwater occurs in alluvial channel deposits.

When the title of the PhD thesis was registered, the project was initially aimed at GW-SW investigations. However as the project progresses, the major aim was adjusted to place emphasis on geohydrological characterization of the typical alluvial channel aquifer as an important component of GW-SW interaction system. The adjustment of the major aim was mainly motivated by the fact that no detailed groundwater studies have been conducted in typical alluvial channel aquifers in Southern Africa and the site offered a big opportunity for such a study. It was therefore considered important to place more emphasis on investigating the geohydrological properties of the aquifer system for the enhancement of scientific knowledge on typical alluvial channel aquifers.

1.2 Study aims and objectives

This PhD thesis is part of a broader study under the South African Water Research Commission aimed at assessing surface water/groundwater hydrology (K5/1760 Bulk Flow Project). The main aim of the study was to investigate the groundwater geohydrological properties of the alluvial channel aquifer and its interaction with the river at a local scale of investigation (< 1000 m). The study aim was achieved by conducting a systematic level of field investigations. A detailed description of the aims and specific objectives of each phase are given in the next subsections. This section of the report also serves as an outline for the rest of the thesis.

1.2.1 Geological characterization

Geological characterisation was aimed at achieving the following specific objectives:

- Identification and description of outcrops in the vicinity of the study area.

- Identification and description of the subsurface lithology.
- Assessment of the spatial variation of channel deposits aquifer materials.
- Identification of the main water strikes and delineation of the aquifer system.

1.2.2 Aquifer tests

Aquifer tests were conducted with the overall aim of understanding the groundwater flow properties in a typical alluvial channel alluvial aquifer. The aquifer tests were aimed at achieving the following specific objectives as important facets of the alluvial channel aquifer:

- Determining the infiltration rates and assessing its influence on recharge mechanisms and rates.
- Determining natural principal groundwater flow direction.
- Determining the typical drawdown behaviour of a typical alluvial channel aquifer during pumping.
- Selection of the appropriate aquifer model for the alluvial channel aquifer system.
- Determining aquifer transmissivity and storage properties of the alluvial channel aquifer.
- Assess the spatial variation of aquifer parameters as influenced by the subsurface heterogeneities.

1.2.3 Hydrogeochemical investigations

Hydrogeochemical investigations in the alluvial channel aquifer were conducted to achieve the following objectives:

- Identification and description of the groundwater hydrogeochemical processes.
- Assessment of the influence that hydrogeochemical processes has on the overall groundwater quality.
- Classification of groundwater quality of the alluvial channel aquifer.
- Qualitative assessment of recharge mechanisms.

1.2.4 Recharge investigations

Recharge investigations were conducted in order to:

- Test the applicability of various complimentary geohydrological tools on identifying recharge sources, mechanisms and quantification in a typical alluvial channel aquifer.
- Make quantitative and qualitative analysis of groundwater recharge mechanisms in the alluvial channel aquifer as an important component of the GW-SW interaction system.
- Compare the groundwater recharge rates and mechanisms between the alluvial channel aquifer and the background terrestrial aquifer.

1.2.5 Tracer tests

Natural gradient tracer tests (NGTT) were conducted with an overall aim of providing general guidance on performing and analysis of tracer tests in a typical alluvial channel alluvial aquifer under natural groundwater flow conditions. Tracer tests in the alluvial channel aquifer were also focused at achieving the following specific objectives:

- Quantification of groundwater flux and discharges.
- Determination of solute mass transport parameters in a 1-Dimensional direction under natural groundwater flow conditions.

1.2.6 GW-SW investigations

The GW-SW investigations were aimed at assessing the GW-SW interactions between the alluvial channel aquifer and the river surface water resource. The aim was achieved by performing the following specific objectives:

- Development of a GW-SW balance model based on mass conservation and solute mixing.
- Measurement of the river inflow into the GW-SW system.
- Measurement of the outflow from the GW-SW system.
- Quantification of the water losses out of GW-SW system.
- Quantification of the volume discharged from the alluvial channel aquifer into the GW-SW system.

1.2.7 Conceptual discussion of alluvial channel aquifers

The last phase of the thesis was aimed at giving a conceptual description of the typical alluvial channel aquifers that can occur along the bedrock and alluvial river channels. The following important aspects were addressed:

- Definition of alluvial channel aquifers.
- Development of the possible alluvial channel aquifer models that can occur along the two major river channels.
- Description of the typical groundwater flow properties in the alluvial channel aquifers that occurs along the alluvial and bedrock river channels.
- Groundwater- surface water interaction mechanisms along the alluvial channel aquifer.

1.3 Case study site

1.3.1 Location

The case study site is located in the Modder River catchment, downstream of the Krugersdrift Dam which is situated about 30 km from the city of Bloemfontein, in the Free State Province of South Africa (Figure 1-1). Modder River is a seasonal river in which the majority of the flow occurs during the rainy season. The study area is surrounded by farms that are mainly characterised by summer and winter crop production.

A weir was constructed downstream of the Krugersdrift dam (Figure 1-1) to support a nature conservation reserve area and to provide water for irrigation requirements. Large artificial pools have formed upstream of the weir. The main point here is that current nature of the river channel and flow adjacent to the alluvial channel aquifer does not reflect normal seasonal river flow conditions as it applies along the entire Modder River. The Modder River is also an important source of water for domestic, agricultural and industrial use to Bloemfontein, Botshabelo and Thaba N'chu areas (Seaman *et al.* 2001).

Farmers close to the study site have indicated that groundwater discharges continuously from the alluvial channel aquifer into the river throughout the year. The farmers further reported that the discharge which seeps through the contact plane of the unconsolidated sediment and impermeable shale bedrock has been occurring for at least 50 years. It was therefore an ideal site to use for investigating the geohydrology properties of a typical alluvial channel aquifer. The site also offered a great research opportunity to assess the groundwater contribution to river flow during low flow periods.

1.3.1.1 Field setting

Figure 1-2 shows the location of the case study site at local detailed scale. The terms study area and study site have been used interchangeably in this thesis. The local scale site of investigation consists of the following important components:

- The alluvial channel aquifer located along the riparian zone that is adjacent to the river bank (Figure 1-2).
- The terrestrial aquifer which is located in the background terrestrial land (Figure 1-2).
- The discharge zone (Figure 1-2) along the river banks at the seepage face (Figure 1-5).
- The river channel segment of interest stretches from Dam outflow platform (Figure 1-1) to the river outflow (RO) segment (Figure 1-2).

- The combination of the alluvial channel aquifer and river surface water resource which technically forms a “GW-SW system”.

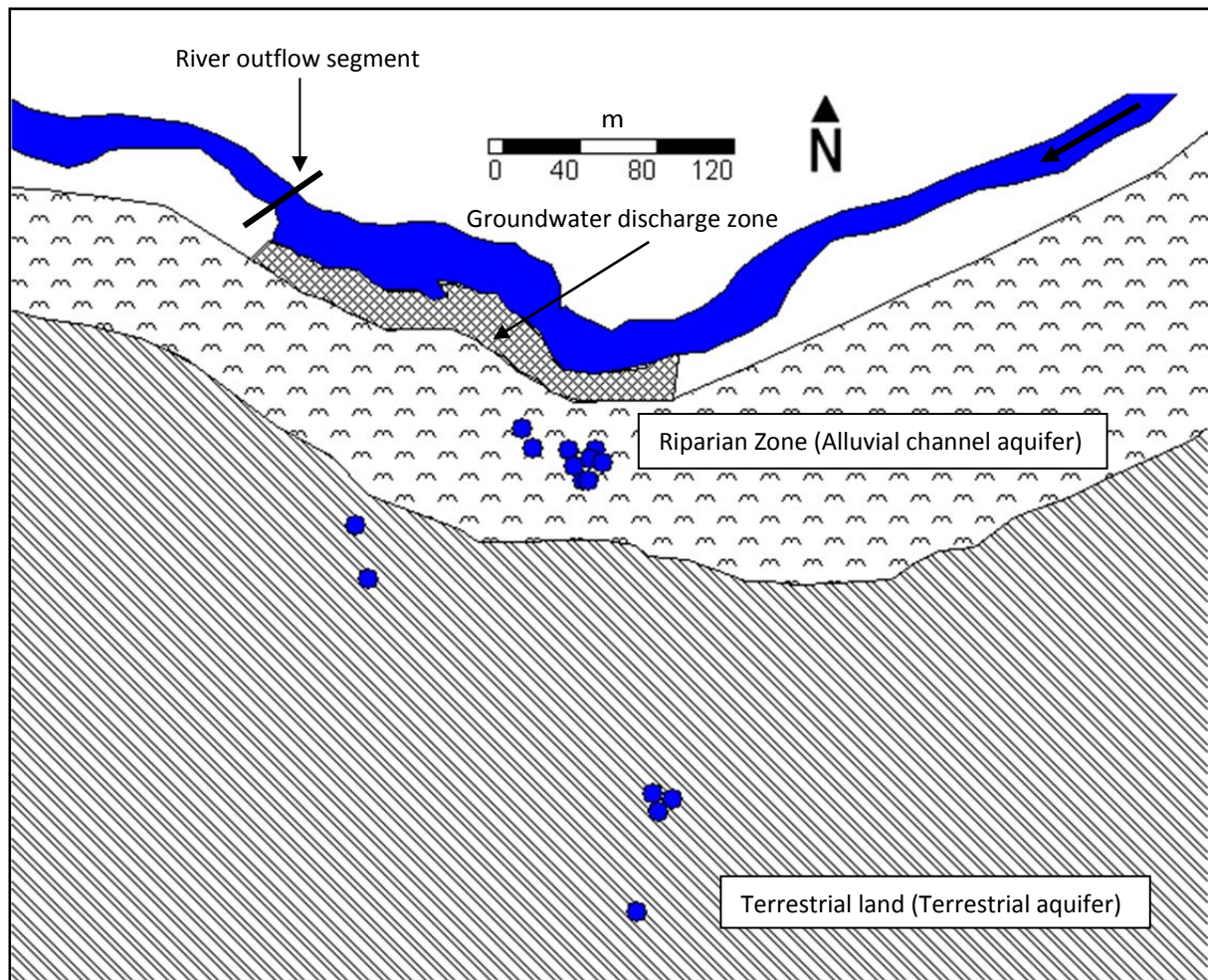


Figure 1-2 Location of the terrestrial aquifer and alluvial channel aquifers on the terrestrial land and riparian zone respectively; also shown is the location of the groundwater discharge zone and boreholes that were drilled into the two aquifers systems.

1.3.2 Climate and topography

The study area is generally characterised by arid to semi-arid climate with long periods of low rainfall events. The area is generally dry and on average receives about 600 mm of rainfall per annum. The rainfall is often associated with heavy thunderstorm activities. During the 2010/2011 rain season the study area received about 680 mm of rainfall (Figure 1-3, *WeatherSA* 2011). February and June 2011 were characterised by extremely high rainfall amounts in excess of 150 mm which resulted in flooding events. The riparian vegetation alongside the Modder River banks comprises of tall thorn trees, small Bushveld shrubs and thick grasses.

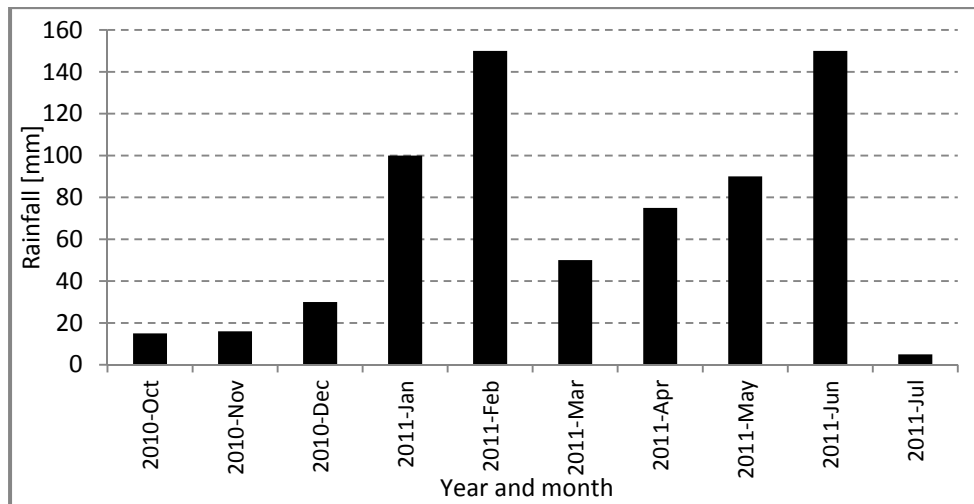


Figure 1-3 Monthly rainfall for the study area recorded during the 2010/2011 rain season (WeatherSA 2011).

Surface topography slopes towards the Modder River (Figure 1-4). The surface topography can have important influence on the natural groundwater flow direction, surface runoff and natural drainage. The groundwater is naturally expected to flow towards the river following topography from the background terrestrial aquifer to the alluvial channel aquifer.

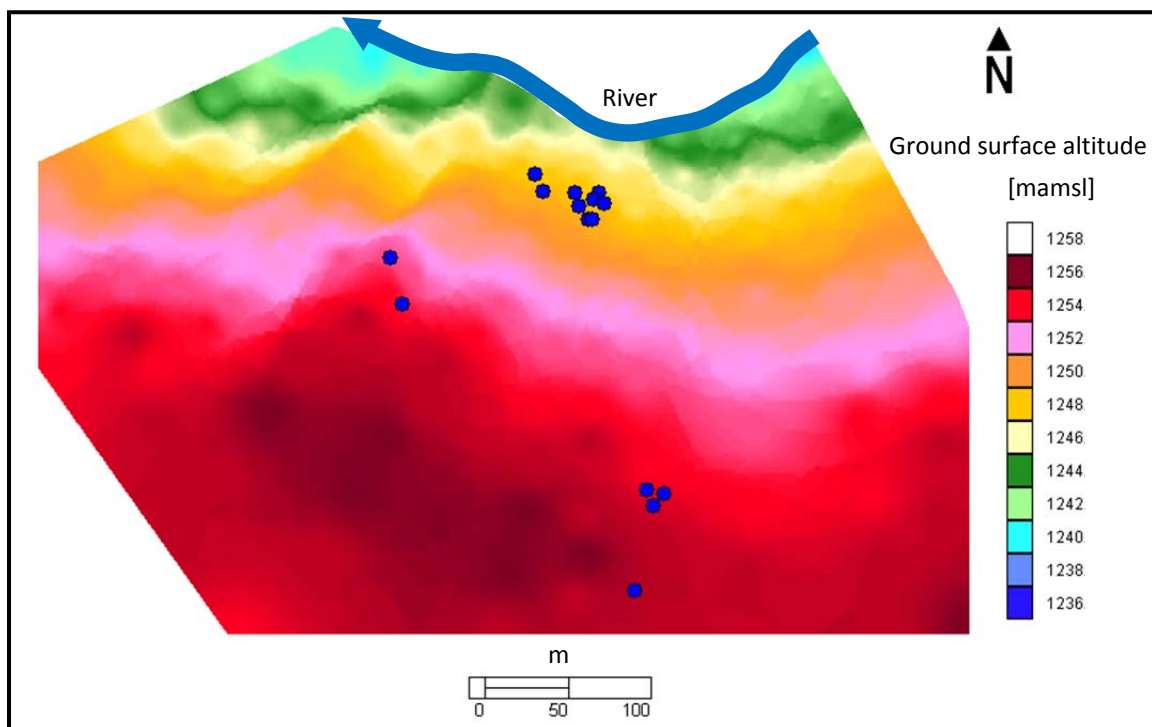


Figure 1-4 An image showing surface topography from the background terrestrial aquifer to the alluvial channel aquifer; also shown is the location of the boreholes drilled into the alluvial channel aquifer and terrestrial aquifer.

The sloping topography from the terrestrial land also assists in channeling of the surface runoff into the riparian zone. Figure 1-5 shows the surface topography on the riparian zone towards the river on a 3-dimensional image. Also shown in the image is the ideal location of the seepage face where groundwater continuously discharges into the river.

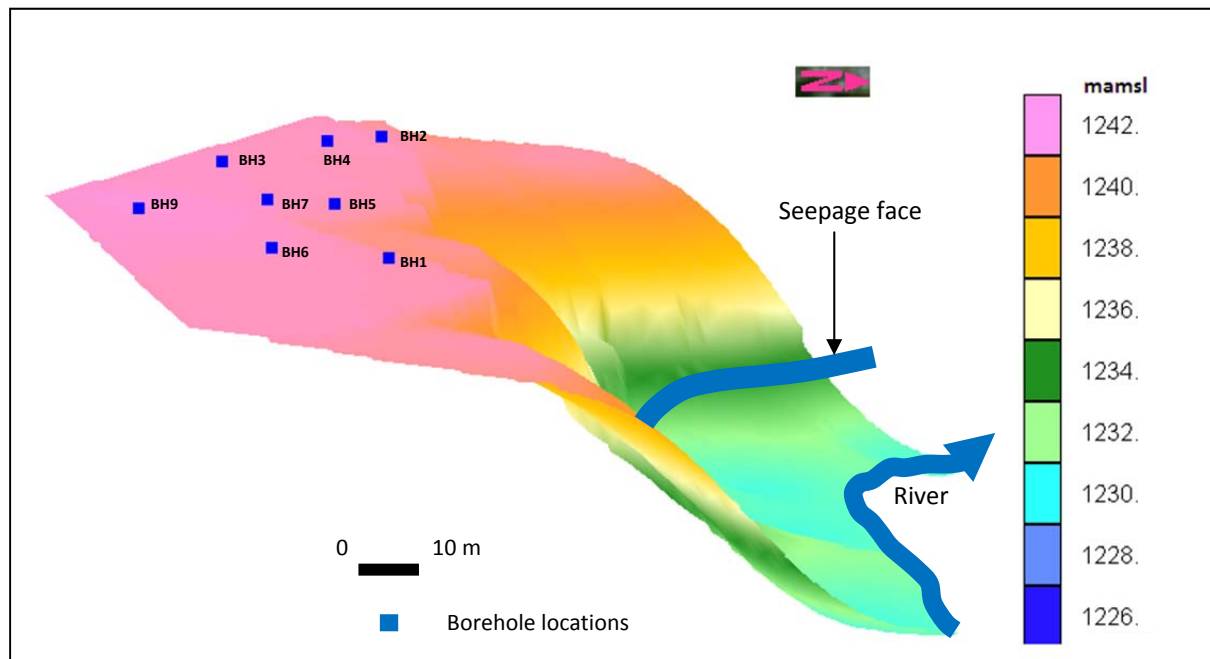


Figure 1-5 A 3-dimensional image showing the surface topography from the riparian zone towards the river; also shown in the image is the seepage face where groundwater discharges into the river (the image is not to scale in the vertical direction).

1.3.3 Water resources and use

The study area comprises of both surface and groundwater resources. Groundwater resources in the study area consist of the alluvial channel aquifer and background terrestrial aquifer (Figure 1-5). Besides a few farm house boreholes, no significant groundwater development and utilization were identified in the vicinity of the site. Modder River and the Krugersdrift dam are the two main surface water resources in the study area. Farmers around the site mainly use river water to meet their irrigation requirements. A weir (Figure 1-1, A) that was built on the downstream of the Krugersdrift dam assists in damming the water for irrigation and nature conservations.

1.4 Data collection strategy

The study was conducted over a period of two years. The work for the study was commenced in January 2010 with a review of literature and desktop studies and then planning for the fieldwork. In

May 2010, the field work started with visual site surveys and outcrop mapping as the preparatory phase for borehole drilling. The majority of geohydrology field work on the terrestrial aquifer was carried out by Leketa (2011) as part of his MSc studies.

Outcrop mapping and drilling of boreholes were used for geological characterisation. Drilling of boreholes is highly regarded as the principal means for geological characterization (USEPA 2001). A total of nine and six boreholes were drilled into the alluvial channel aquifer and terrestrial background aquifer respectively using the air percussion drilling method. Drilling chips were geologically logged to describe the subsurface lithology and texture in each borehole at an interval depth of 1 m.

Groundwater and river samples for the analysis of macro and micro elements were collected in July 2010, January 2011, May 2011, August and December 2011. The analysis of macro and micro elements was performed by the Institute for Groundwater Studies (IGS) laboratory of the Free State University in South Africa. Groundwater and river samples for stable isotope analysis were collected in February 2011 and May 2011. The analysis for stable isotope was performed by iThemba laboratory in the Johannesburg city of South Africa.

A number of hydraulic tests were conducted in the unsaturated and saturated zones respectively. A total of 12 infiltration tests were performed in the soil zone to assess the potential of piston recharge mechanism occurring in the riparian zone. Aquifer tests were conducted to determine the hydraulic and storage properties of the alluvial channel aquifer. A total of four tracer tests were conducted under natural groundwater flow conditions. A water balance model was developed to assess GW-SW interactions based measurements of flow, solute concentrations and stable isotopes made during the low river flow period in October 2011.

1.5 Significance of the research

The National Water Act (1998) compels water managers to consider all the water resources of a catchment as part of sustainable management. In practice, catchments are generally too large for investigating specific groundwater and surface water properties. Detailed studies at local scales provide a good platform for understanding groundwater flow properties at intermediate and regional scales. Comprehensive studies at local scales are important because the occurrence and properties of groundwater resources can be very complex to understand. Assessment of surface water resources is generally more objective in comparison to groundwater which is hidden in the subsurface. It is by no surprise that this thesis placed more emphasis on characterizing the alluvial channel aquifer as an important groundwater resource and component of GW-SW system.

Alluvial channel aquifers are naturally located in the groundwater discharge zones where interaction with the surface waters has important implications for both the riparian and surface water ecosystem. In practice, it is difficult to identify the locations where the groundwater and surface water resources are connected in order to characterize the nature of their connections. In a typical alluvial channel aquifer where groundwater is located in the alluvial sediment cover, the interaction mainly occurs through preferential flow pathways created at the contact plane of unconsolidated sediments and impermeable shale bedrock. The case study site provides the opportunity to characterise the geohydrological properties of the alluvial channel aquifer and assessment of GW-SW interactions under natural groundwater flow conditions.

A number of geohydrological studies have been conducted on alluvial channel aquifers in Southern Africa (Benito *et al.* 2009; De Hamer *et al.* 2008; Moyce *et al.* 2006 and, Mansell and Hussey 2005). Most of the studies focused on assessing the yield potential and sustainability of the alluvial channel aquifers with no effort being devoted to the detailed investigations of groundwater flow and solute transport phenomenon in the aquifers. In South Africa, most of the geohydrological studies have been focused on the typical Karoo fractured-rock aquifers and this has led to the development of significant knowledge and research base. Notable studies that have contributed to the development and expansion of scientific knowledge base on groundwater occurrence, flow and transport processes in typical Karoo fractured-rock aquifers include: Botha *et al.* 1998, Van Tonder *et al.* 2001 and Riemann 2002.

Geohydrological investigation techniques and guidelines manuals developed for typical Karoo fractured rock-aquifers are not always applicable to alluvial channel aquifers that mainly comprises of unconsolidated segments. It was therefore essential to test the applicability of conventional field and data analysis geohydrological tools on a typical alluvial channel aquifer at a local scale of investigation.

The results of this research have an overall contribution to the body of scientific knowledge and understanding of the groundwater and solute transport flow properties in a typical alluvial channel aquifer. The thesis is also expected to expand the knowledge of recharge mechanisms and hydrogeochemical characteristics in a typical alluvial channel aquifer. The conceptual understanding of GW-SW interactions mechanisms between the alluvial channel aquifer and rivers will also be enhanced.

1.6 Limitations of the study

The main limitation of this study is lack of long continuous monitoring data that can help to enhance the understanding of the seasonal effects on GW-SW interactions. The study was based on investigations at a small scale and the application of the findings is mainly confined to local hydrogeological scales. It is also important to mention the absence of surface geophysics investigations. Ideally surface geophysics investigations were expected to start before the actual drilling but that was not possible due to technical and financial constraints. Because this PhD thesis is part of a bigger research project, the geophysical aspect of the project was then earmarked for an MSc thesis that only started in August 2011. In general, surface geophysics investigations can be used to determine the thickness and extend of alluvial channel deposits as part of geological characterisation. Surface geophysics is also useful for determining the location of geological boundaries which can have significant influence on groundwater flow properties.

1.7 Summary

Chapter 1 gives the background information leading to the PhD research study. The main aim of the study was to investigate the groundwater geohydrological properties of the alluvial channel aquifer and its interaction with the river at a local scale (< 1000 m). Detailed studies at local scales provide a good platform for understanding groundwater flow properties at intermediate and regional scales. Alluvial channel aquifers are naturally located in the groundwater discharge zones where interaction with the surface waters has important implications for both the riparian and surface water ecosystems. The case study site is located in the Modder River catchment, downstream of the Krugersdrift Dam which is situated about 10 km from the city of Bloemfontein, in the Free State Province of South Africa.

The next chapter discusses the geohydrological properties of typical alluvial channel aquifers and conventional methods that are used to characterise GW-SW interactions.

2 ALLUVIAL CHANNEL AQUIFERS AND GW-SW INTERACTIONS STUDIES

This chapter gives a discussion of alluvial channel aquifers and typical aquifer models that can occur along the alluvial and bedrock river channels. The idealized aquifer models show the occurrence and typical groundwater flow process in alluvial channel aquifers. As part of the literature review, the chapter also discusses GW-SW interaction mechanisms and processes along a typical alluvial channel aquifer.

2.1 Alluvial channel aquifer

Although considerable literature exist on the geomorphologic processes of alluvial and bedrock river channels (Richards 1982, Vigilar and Diplas 1998, Turowski *et al.* 2008 and Turowski 2010), very little effort has been devoted to describe the influence that these channels has on the occurrence and properties of alluvial channel aquifers. In literature, the term “alluvial aquifer” has been used in reference to aquifers that generally comprises of unconsolidated river channel deposits (Kelly 1997, Weng *et al.* 1999, Klingbeil *et al.* 1999, Mansell and Hussey 2005) without addressing the nature of the hosting river channel. In nature, alluvial aquifers can occur along both the alluvial and bedrock river channels. The nature of the hosting river channel has a huge influence on the properties of the aquifer system. Figure 2-1 below shows the idealized location of a typical alluvial channel aquifer along the riparian zone between the river banks and the terrestrial background aquifer.

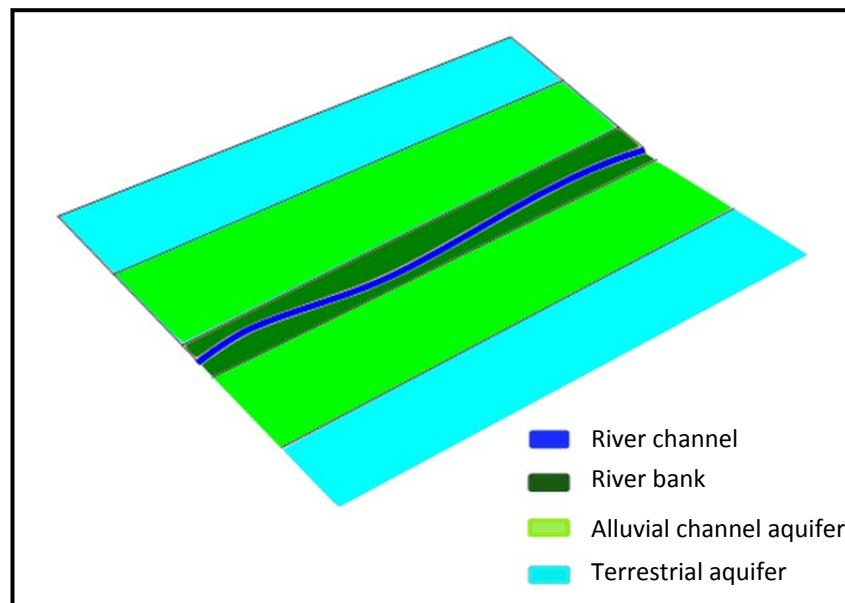


Figure 2-1 A plan view showing the idealized location of a typical alluvial channel aquifer between the river bank and terrestrial aquifer.

Alluvial channel aquifers constitute a worldwide important source of drinking and irrigation water, because they often have yields (Choi *et al.* 2009). In Southern Africa, Seely *et al.* (2003) reported huge reliance on groundwater from alluvial channel aquifers to meet agricultural and domestic water requirements. The aquifers are however often at risk from pollution given their typical shallow water table conditions. Overabstraction from alluvial channel aquifers can also occur especially in semi-arid and arid areas where groundwater serves as the main source of water. Alluvial channel aquifers also form an important component of the GW-SW interaction system because they are often located in the discharge zones. It is thus important for groundwater scientists to understand the differences between alluvial and bedrock river channels and their influence on the formation and properties of alluvial channel aquifers. The next subsections discuss the influence that the nature of river channels has on the occurrence and geohydrological properties of alluvial channel aquifers based on theoretical conceptualizations and field observations.

2.1.1 Bedrock river channel

It has long been acknowledged that the general understanding of the processes and evolution of bedrock river channels lags significantly behind that of alluvial channels (Howard 1998). In general, the bedrock or boundary resistant channels are limited with respect to the supply of sediment (Cenderelli and Cluer 1998). Along the bedrock channels, the capacity of the river to carry sediment often exceeds the supply of sediment material to the channel (Turowski *et al.* 2008). Recent studies by Turowski (2010), defines the bedrock river channel on the basis that it cannot substantially widen, lower, or shift its bed without eroding the bedrock. In this instance, the bedrock has significant control on the river capacity and sediment load relationships. Bedrock outcrops which are resistant to erosion often occur at intervals along the river course and this has a strong influence on the nature of the river processes within the immediate and upstream alluvial reaches (Tooth *et al.* 2002).

Turowski (2010) further argues that bedrock channels are in general semi-alluvial because they are partly composed of alluvium and bare rock. The alluvial sediments deposited on the bedrock river channel are hereby termed “alluvial cover” (Figure 2-2). Bedrock river channels are also exposed to extreme erosional effects which shapes the boundaries of the channel. If the bedrock is erosion and weathering resistant, the river would most likely deepen by shifting its course away from the bedrock.

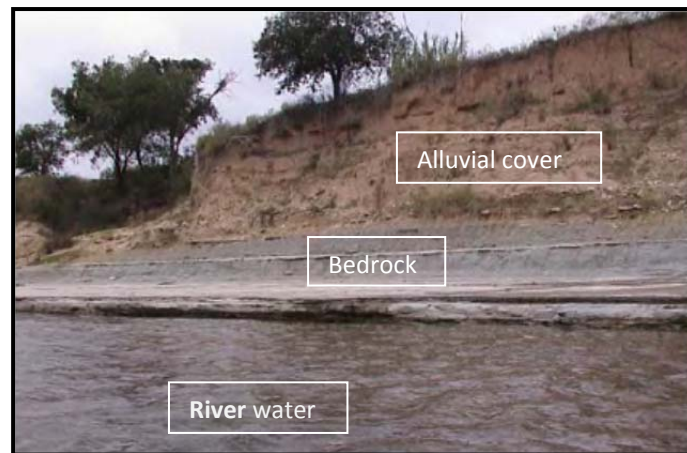


Figure 2-2 Image of alluvial cover along the bedrock channel reaches (Taken from Keen-Zebert 2007).

Based on the field observations, the river segment adjacent to the case study site was classified as a bedrock river channel. The following important observations were used for the classification:

- The shale consolidated formation outcropping along the river banks adjacent to the alluvial channel aquifer forms the river channel bedrock at the study site (Figure 2-3).
- Thin alluvial cover (< 10 m) of unconsolidated sediments that has been deposited on top of the underlying impermeable shale bedrock unit (Figure 2-3).

It is important to highlight that the bedrock river channel phenomenon existing at the case study area is only site specific. However the aquifer properties and other geohydrological findings from this study can still be applied at other sites where groundwater occurs in alluvial channel aquifers along bedrock river channels.



Figure 2-3 Photos showing an (a) outcrop of shale bedrock and (b) the thin alluvial cover along the river bank adjacent to the alluvial channel aquifer.

2.1.1.1 Aquifers along a bedrock river channel

A bedrock river channel potentially host different types of aquifer systems and these would require different geohydrological characterization approaches, tools and techniques. Aquifers formed on bedrock channels mainly consist of alluvial cover, fractured-bedrock aquifer or a combination of the two systems. In general, aquifers located along the bedrock river channels can behave as a typical porous media (alluvial cover deposits) and fractured-rock aquifer systems. The word bedrock is however misleading because it can be mistakenly associated with pure fractured-rock aquifers systems. In this instance, the term describes the geomorphologic nature of the river channel housing the alluvial channel aquifer.

2.1.1.1.1 Idealized alluvial cover channel aquifer model

The alluvial cover channel aquifer model in Figure 2-4 resembles groundwater flow conditions at the case study site. The alluvial cover channel aquifer consists of a thin unconsolidated alluvial cover (< 10 m) overlying the impermeable shale bedrock unit. The unconsolidated thin alluvial cover at the site comprise of calcrete, clay-silt and gravel-sand channel deposits. Groundwater flows in the unconsolidated sediments towards the river as driven by topography and hydraulic gradient. Groundwater flow conditions are generally under unconfined conditions. Semi-confined conditions however exist at local scales in segments of the aquifer where tight calcrete and clay-silt sediments overlie the gravel-sand main aquifer layer. Depending on the storage and hydraulic properties of the channel deposits, leaky aquifer conditions can also occur.

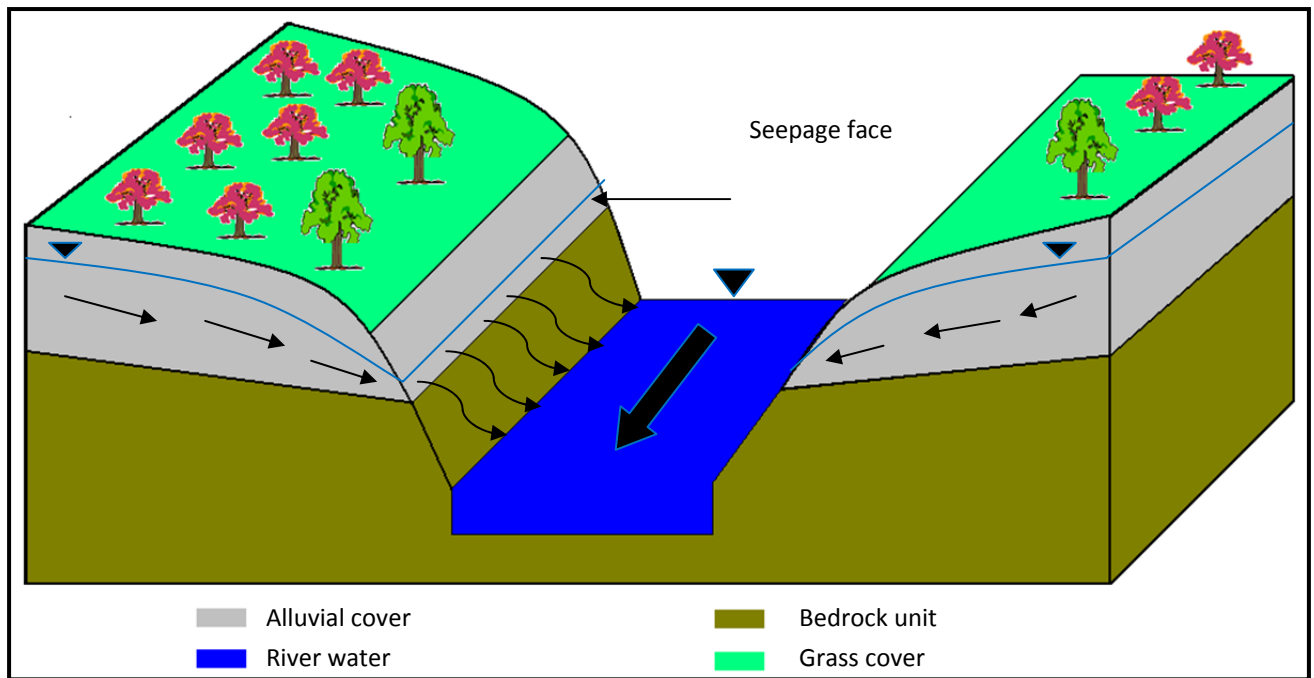


Figure 2-4 Idealized groundwater flow in the alluvial cover channel aquifer occurring along a bedrock river channel; the aquifer locally discharges groundwater into a “gaining river” at the seepage face created between the alluvial cover and bedrock contact plane; arrows shows flow directions.

The river stage elevation is lower than the groundwater elevation and as a result groundwater discharges into the gaining river at the seepage face (Figure 2-4). A seepage face has been created along the contact plane of the alluvial cover and the underlying low permeable bedrock unit. The impermeable underlying bedrock unit retards the vertical downward movement of groundwater from the unconsolidated sediments and as a result it preferentially moves along the contact plane to discharge into the river.

The section of shale bedrock unit outcropping at the river bank has been subjected to intense erosion and weathering resulting in the significant fracturing of the bedrock unit (Figure 2-5). The weathered and fractured outcropping bedrock unit can mislead one into hypothesizing the aquifer as a fractured-bedrock system. Without the understanding that can be derived from geological logs and aquifer testing, there are high chances of developing a wrong conceptual model for such a system. It is possible for the outcropping bedrock unit of a river channel to be weathered but it does not always imply it has significant contribution on groundwater flow conditions to warrant the use of the term “fractured-bedrock” aquifer.



Figure 2-5 A photo showing the shale bedrock at the case study site that has been subjected to fracturing and weathering processes.

2.1.1.1.1.1 Geohydrological properties

Groundwater mainly flows in the gravel-sand channel deposits which are typically characterised by high hydraulic conductivity properties. The hydraulic conductivity of the aquifers spatially varies depending on the sorting of the channel deposit aquifer materials and the amount of silt and clay present in the deposits. In other words, the sorting of gravel-sand aquifer materials and the silt-clay content has great influence on the aquifer hydraulic properties. Although high hydraulic conductivities of the gravel-sand deposits are good for groundwater yields, it can also accelerate contaminant migration.

Groundwater water recharge of the shallow alluvial cover aquifers occurs locally through normal and preferential infiltration as enhanced by the dense vegetation that often characterises riparian zones. Surface runoff and drainage from the terrestrial land also assist in the accumulation of water on the lower riparian zone thus enhancing the infiltration of water into the shallow alluvial cover aquifer system. Because of shallow water table conditions, the recharge process is often quick. The locally recharged groundwater of the alluvial cover aquifer typically has short residence time. High hydraulic properties of the channel deposits facilitate quick groundwater movement which consequently discharges into the river system. Geochemically, the shallow local groundwater system would be characterised by low Total Dissolved Solids (TDS) because of limited time in contact with the non-saline aquifer materials.

Coarse-grained alluvial channel aquifers can be approximated by a homogeneous porous media when estimating hydraulic and transport parameters. However groundwater and transport flow in the sediments is greatly controlled by aquifer material architecture (Zappa *et al.* 2006). It is therefore important to understand the effects that the physical properties of channel deposits has on the spatial variation of measured aquifer parameters. The influence that physical and chemical properties of geological material have on the spatial variation of geohydrological properties is collectively referred to as “heterogeneity”.

2.1.1.1.2 Groundwater-river interactions

Groundwater-river interaction is an important aspect of typical alluvial cover channel aquifers considering its location in the vicinity of existing river channels. In the alluvial cover channel aquifer, local groundwater discharges dominates the aquifer losses to the river. The local discharge occurs mainly through the shallow alluvial cover aquifer deposits that receive most of its water from the background terrestrial aquifer. When the river stage elevation exceeds the groundwater elevation of the alluvial cover channel aquifer, the river potentially becomes a losing one. For a direct hydraulic connection between the alluvial cover channel aquifer and the river to occur, the river stage elevation should be at least above the seepage discharge face (Figure 2-6). In the shallow alluvial cover channel aquifer system, direct hydraulic connection can only occur through the seepage face and high permeable unconsolidated deposits.

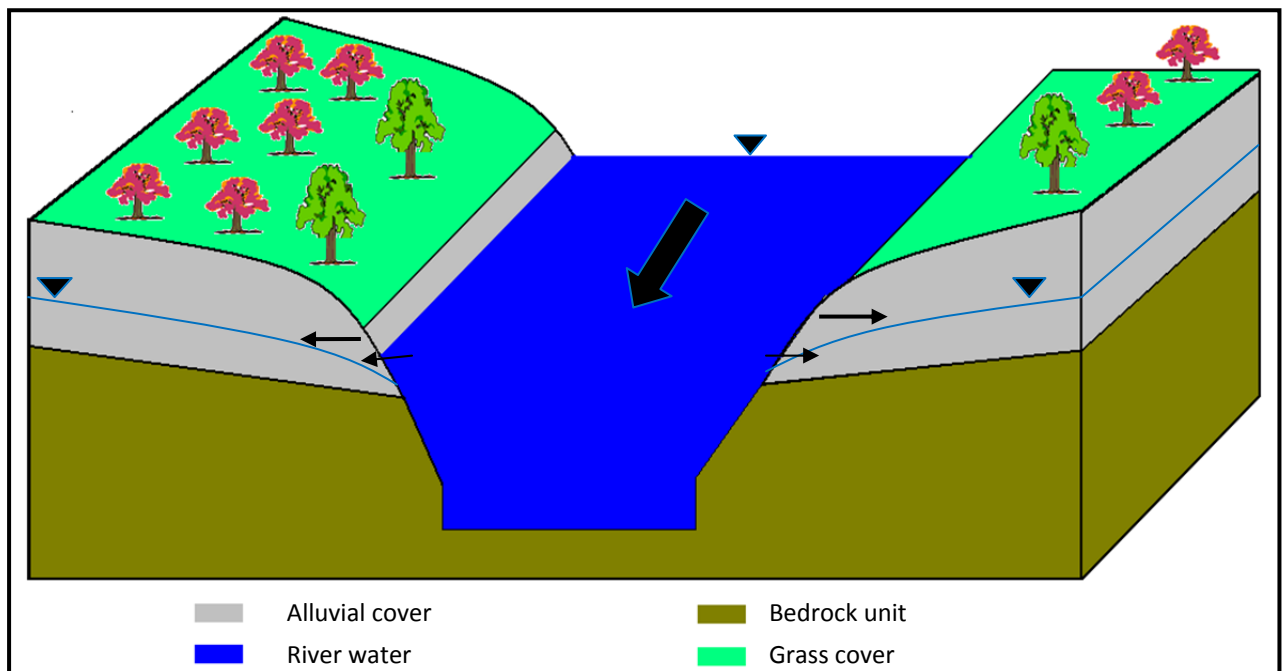


Figure 2-6 Idealized groundwater flow conditions in an alluvial cover channel aquifer occurring along a bedrock river channel where the river is losing water to the aquifer; the river stage elevation rises

above the groundwater elevations thereby reversing the gradient and the loosing river discharges water into the alluvial channel aquifer; arrows show the flow directions.

At the case study site, the seepage discharge face is located about 2 m height above the average river stage elevation. It is highly unlikely that the river stage will rise by more than 3 m during the average normal rainfall seasons considering the magnitude of the channel width (> 25 m). Conceptually, there will be no direct hydraulic connection between river and alluvial channel aquifer under normal rainfall patterns at the study site.

2.1.1.1.2 Alluvial cover and fractured-bedrock idealized aquifer model

It is possible that the bedrock underlying the alluvial cover can be significantly weathered creating fissures and fractures that can store and transmit groundwater in economic quantities (Figure 2-7). It is conceptualised that depositional unloading mainly activated fracturing of the bedrock unit. Other physical processes such as mass wasting and erosion can also contribute to fracturing of the bedrock.

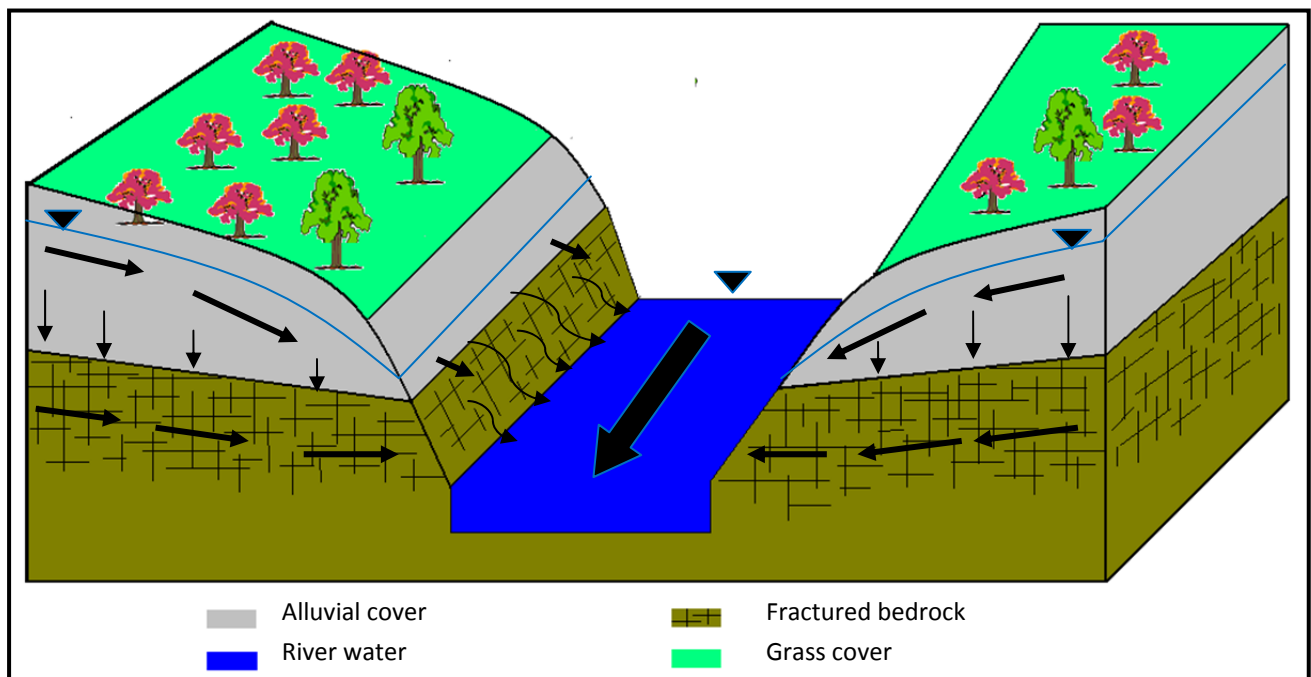


Figure 2-7 Idealized groundwater flow conditions in an alluvial channel aquifer occurring along a bedrock river channel; the groundwater resource occurs and flows in both the alluvial cover and fractured-bedrock; arrows show the flow directions.

Under such conditions, the groundwater resource would occur and flow in both the alluvial cover and fractured-bedrock aquifer systems. Ideally, the alluvial cover and fractured-bedrock aquifer system can respond as an interlinked or separate distinct system during groundwater abstraction conditions. The aquifer can respond as an interlinked system when the fractured-bedrock is

recharged from the overlying alluvial deposits during pumping. Emery and Cook (1984) observed deep fractured-bedrock aquifer that derived 80-100 % of its recharge during stressed (pumping) conditions from significant vertical and horizontal flow of the overlying deposits.

The system can constitute of two different aquifers when the fractured-bedrock aquifer is separated from the overlying alluvial cover by some form of confinement leading to the occurrence of a shallow and deep aquifer systems. The shallow and deep aquifer systems are characterised by local and regional groundwater flow respectively. Vertical hydraulic conductivity and drainage parameters are important properties in the aquifer model.

In this aquifer model, direct hydraulic connectivity of groundwater and the river can occur through the fractures and fissures of the bedrock which is most likely to be in contact with the river for most of the time. The bottom elevation of fractured-bedrock aquifer should be located at least below the river stage elevation for direct hydraulic connectivity to occur. The location of the fractured-bedrock bottom elevation would however depend on the weathering intensity and nature of the fracturing. More often, the fractured-rock aquifers of the Southern Africa Karoo basin are dominated by bedding plane fractures (Botha *et al.* 1998).

2.1.2 Alluvial river channel

Alluvial river channels are located in unconsolidated sediment with no underlying bedrock. According to Washington State Department of Ecology (1994-2011), an alluvial channel is a river channel that is formed in sediment material (sand, gravel, cobbles, or small boulders) that are mobile. The development of the channel is mainly regulated by; streamflow, sediment supply, and the nature of debris. According to Vigilar and Diplas (1998), alluvial river channels adjust their shape by entraining and redepositing bed material. Turowski *et al.* (2008) recognised that although there can be both gravel-bed bedrock channels and gravel-bed alluvial channels one cannot have a bedrock-bed alluvial channel. The existence of gravel deposited materials along the river channels is generally associated with both river channels. Although the focus of these definitions vary significantly, in summary it should be noted that alluvial channels are shaped by flow and sediment transport processes while the bedrock channels are developed by lithological and structural controls (Ashley *et al.* 1988). Figure 2-8 shows a picture of an alluvial valley occurring along an alluvial river channel in Arizona (USA). Along alluvial river channels the groundwater resource occurs and flows in unconsolidated the alluvial channel deposits. The typical geohydrological characteristics of the aquifer located along an alluvial river channel would be similar to that of the alluvial cover idealized model (Figure 2-4).

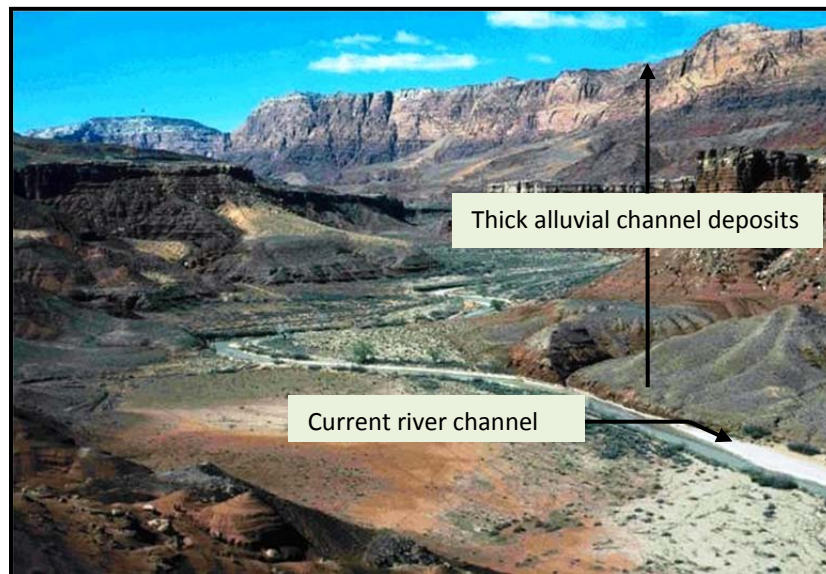


Figure 2-8 An image showing an alluvial valley of the Paria River in Arizona (Hereford 2000); thick alluvial channel deposits can be seen on opposite sides of the current river channel.

2.2 GW-SW interactions

The term GW-SW interaction defines the interrelationship between the groundwater and surface water resources. Groundwater and surface water resources rely on each other in various ways and sustainable management of these two interlinked resources requires a comprehensive understanding of their interactions. It is critical to understand the various components of the two water resources prior to investigating their interactions. Integrated management of groundwater and surface water resources is required in order to provide for the adequate protection of the resources (DWAF 2000). Groundwater can be best defined as water that occurs in saturated formations below the earth's surface. Surface water resource refers to water bodies such as lakes, river/streams, dams and wetlands that exist on the earth's surface. In this study, the river adjacent to the alluvial channel aquifer (groundwater) is main surface water resource.

Groundwater allocation requirements and provision for environments have immensely contributed to the development of GW-SW interaction studies. For instance in Australia, the maintenance of riparian and in-stream ecosystems has been the principal concern for groundwater allocations in the formulation of environmental flow regulations (Murray *et al.* 2003). In South Africa, research into aquifer-dependent ecosystems is hardly recognised in the national water legislation and ecological approaches in groundwater management are only implemented to a certain degree (e.g. the Reserve) (Knüppe 2011).

It is generally acknowledged that the groundwater requirements of terrestrial, riparian, wetland and stygian ecosystems is poorly understood in comparison to in-stream requirements (Murray *et al.* 2003). This poor understanding can be attributed to limited information and lack of proper research objectives and appropriate resources to undertake studies. Murray *et al.* (2003) further argues that the planning and management mechanisms of groundwater dependent ecosystems are generally not as advanced or sophisticated as the in-stream ecosystems. In other words, there is still a great need to place focus on understanding groundwater system behaviour and its influence on groundwater dependent ecosystems.

This section of the study gives a review of literature on various investigations that can be conducted when characterising the main facets of GW-SW interactions. Significant effort has been placed on investigating the groundwater resource components of the alluvial channel aquifer and their contributions to the river flow. By nature groundwater resources occur below the earth's surface which makes it difficult to investigate and quantify its properties as compared to the surface water. Geohydrological investigations in GW-SW interactions studies form the foundation to the development of physical and chemical conceptual understanding of the alluvial channel aquifer's contribution of surface waters.

2.2.1 GW-SW interactions studies

Groundwater-surface water interaction studies encompass a wide range of facets (Sophocleous 2002, Kalbus *et al.* 2006 and Smith, 2005). Critical components of groundwater-surface water interaction studies include:

- Hydraulic and geochemical properties of the aquifer system.
- Groundwater recharge and discharge qualities and quantities.
- Riparian and aquatic ecosystems.
- Aquifer and surface water hydraulic connectivity.
- Rainfall, runoff and stream flow processes.

The traditional investigation approach has been for geohydrologists to investigate geology, groundwater flow systems and climate within a river basin (Winter 1999) while on the other hand, hydrologists place emphasis on rainfall-runoff and stream flow processes. Ecological investigations are also important for assessing the influence of GW-SW interactions on the aquatic and riparian habitats. Although hydrological processes are useful for determining the quantity of water that the stream derives from the groundwater (base flow), enormous efforts in this study have been placed on geohydrological aspects of the GW-SW interactions based on the following reasoning:

- Groundwater resource allocation and managements can have important implications on the provisions that should be made for the surface water resource ecosystems. This makes groundwater an important resource thus understanding of its occurrence, flow, discharge and recharge in relation to the provision for river ecosystems becomes a prerequisite. Before groundwater allocations and provisions can be made a good conceptual understanding of both physical and chemical aspects of the groundwater system has to be made.
- Unlike other site conditions where base flow separation techniques have to be used to determine the existence of base flow and its quantification, the study site has different and unique physical conditions. It is evident from visual observations made on the Modder River bank adjacent to the case study site that the alluvial channel aquifer naturally discharges groundwater into the gaining river throughout the year. After visual observation of natural discharge, the secondary hydraulic investigation priority was then placed on quantifying the groundwater discharge at the seepage face.

Groundwater-surface water interaction can occur under both natural and stressed conditions, however the levels and nature of interactions significantly varies between the two conditions. Under natural conditions water exchanges is driven solely by natural hydraulic gradients and aquifer hydraulic properties. Groundwater abstraction from the alluvial channel aquifer has great influence on the hydraulic gradients distribution between the aquifer and connected river. It is important to have a comprehensive understanding of the natural GW-SW interactions prior to the investigation of the abstraction effects under stressed conditions. Based on the natural system behavior, numerical modelling programs such as MODFLOW (Chiang and Kinzelbach 1998) can be used to assess the influence of groundwater abstractions on GW-SW interactions under different scenarios.

Sophocleous (2002) raised a concern about the ability of the traditional approach to bring a holistic to the understanding of GW-SW interactions. Lack of an integrated approach among geohydrologists, hydrologists and ecological experts can contribute to poor field understanding of the interrelationships between several processes of GW-SW interactions. Attention has also been placed on the exchanges between near-channel and in-channel water, as part of evaluating the ecological structure of river systems (Sophocleous 2002). Understanding of the water quality and quantity exchanges between alluvial channel aquifers and rivers is important for riparian-zone management. A balanced GW-SW interaction system is important for supporting and sustaining the riparian and aquatic ecosystems.

2.2.2 Mechanism of GW-SW interactions

Groundwater-surface water interactions mechanism has been widely reported to occur through river/stream bed (Toth 1970, Winter *et al.* 1998 and Ivkovic 2009). Figure 2-9 shows the commonly used schematic representations of GW-SW interaction occurring through the stream/river bed for gaining and losing streams.

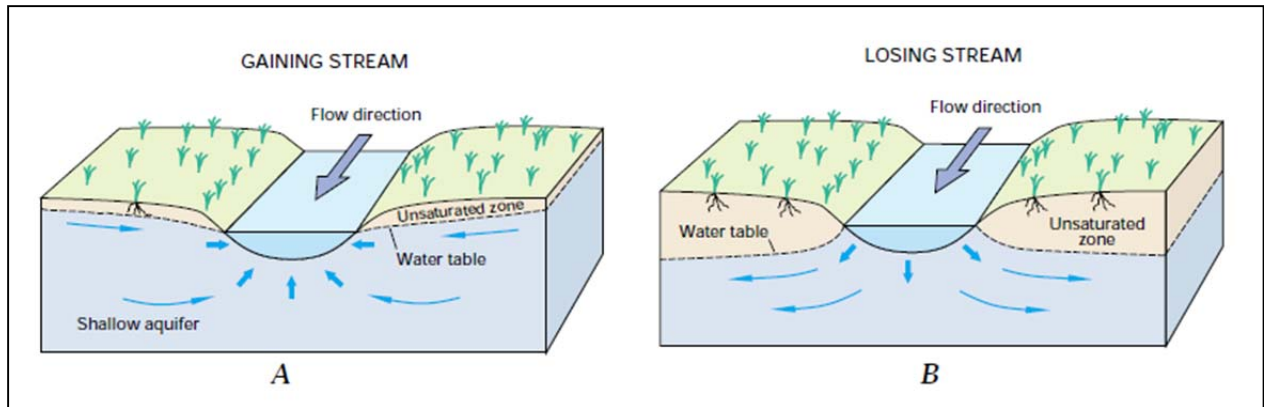


Figure 2-9 A schematic representation of GW-SW interactions occurring through the river/stream bed for; (A) gaining and (B) losing stream system (Taken from Winter *et al.* 1999).

Winter *et al.* (1999) identified three basic ways in which stream/river systems can interact with the groundwater:

- Streams gain water from inflow of ground water through the streambed (gaining stream). For this condition to exist the stream should be hydraulically connected to the groundwater and the stream stage should also be at lower elevation in comparison to the aquifer water levels.
- Streams lose water to groundwater by outflow through the streambed (losing stream).
- Streams gaining and losing in different stream reaches. The condition is more common considering the natural spatial variability of stream geomorphology and alluvial channel aquifer sediment deposition processes.

Groundwater abstraction from aquifers that interacts with river water can have substantial influence on the quality and quantities of water exchanged with the river system. During the abstraction from boreholes drilled into an alluvial channel aquifer that is hydraulically connected to a gaining stream, groundwater flux into the stream can be significantly reduced. Groundwater over abstraction can potentially result in the hydraulic gradient reversal hence the groundwater flow direction. Under losing stream conditions, groundwater abstraction from the adjacent alluvial channel aquifer increases stream losses. The effects of groundwater abstraction will not be investigated in this thesis because the study site comprises of ideal natural groundwater flow conditions. It is the core objective of the study to investigate GW-SW interactions that occur under natural groundwater flow conditions.

2.2.3 Components of GW-SW interaction studies

2.2.3.1 Aquifer system

Characterization of the alluvial channel aquifer system is probably the most difficult part of the GW-SW interaction studies. Unlike stream flow which is visually observable and can be conveniently measured, groundwater flow studies mostly rely on inference made from indirect measurements. The alluvial channel aquifer system has an important obligation to sustain the riparian and aquatic plants; and animal habitats.

Quantitative and qualitative assessment of aquifer recharge and discharge mechanism and rates is an important facet of GW-SW interaction studies. Analysis of stable isotopes and hydrogeochemical processes can be used to map and understand groundwater recharge and discharge mechanisms (Wood and Sanford 1995). Quantitative analysis of groundwater recharge rates is often a subjective and difficult process. A detailed discussion of the challenges associated with groundwater recharge estimation methods in Southern Africa is discussed by Xu and Beekman (2003). A comprehensive understanding of the geohydrological processes governing the aquifer behaviour is important for the development of a GW-SW interaction system conceptual model. In general, the role that groundwater has on supporting ecology at various scales of investigations is complex and intricate to quantify. The main challenges in quantifying groundwater's supporting responsibility stems from the following principal factors (Kirk 2006):

- Groundwater quantity and quality inputs into the surface and terrestrial ecosystems are variable in space and time thus difficult to measure with conventional geohydrological tools.
- The dependence of an ecosystem does not only rely on the groundwater properties but is also related to specific ecological needs. Ecological requirements of plant and animal habitat also vary according to species, age and ecosystem type.
- Identification and delineation of groundwater dependent ecosystem is important but often a difficult process because not all surface water ecosystems are dependent on groundwater.

2.2.3.2 Groundwater discharge measurements

Quantifying and understanding of groundwater discharge mechanisms is critical in GW-SW interactions studies. It therefore requires reliable methods to measure groundwater flux across streambeds and banks. In general, techniques to determine groundwater flux into surface water bodies mainly include; simple hydraulic tests, tracer tests, seepage meters and stream hydrograph separation techniques. Cey *et al.* (1998) discusses the merits and challenges associated with the application these techniques to determine groundwater fluxes into surface water bodies.

2.2.3.2.1 Hydraulic measurements

Hydraulic measurement techniques involve the use of boreholes and piezometers to measure hydraulic gradients and conductivity along the alluvial channel aquifers adjacent to stream/river surface water bodies. Darcy's law is then used to indirectly determine the groundwater fluxes. The application of Darcy's law to estimate groundwater flux requires accurate measurements of hydraulic conductivity of the porous medium and hydraulic gradients (Lee and Cherry 1978, and Landon *et al.* 2001). Aquifer hydraulic conductivities spatially vary due to the influence of geological heterogeneities, thus making it difficult to obtain representative measurements of the parameter. Hydraulic gradients in riparian zones are often small due to high hydraulic conductivity that is typically associated with alluvial gravel-sand channel deposits. In general, small hydraulic gradients are often difficult to measure with a good degree of accuracy (Lamontagne *et al.* 2002).

Bradbury and Muldoon (1990) have reported variation of hydraulic conductivity measurements that appear to increase with the scale of measurement. The influence of heterogeneity on spatial variation of the estimated hydraulic parameters from point measurements cannot be ignored. However at local scales of investigation, groundwater discharge estimated from such parameters should fall within reasonable estimates. In order to utilize point measurements, it can be assumed that groundwater flow is one dimensional (horizontal) as dominated by horizontal hydraulic conductivities. In general, alluvial channel aquifers comprise of unconsolidated channel deposits and these are typically characterised by high hydraulic conductive gravel-sand materials.

2.2.3.2.2 Tracer test

Groundwater discharge from an aquifer system can be determined using flux measurements derived from natural gradient point dilution tracer tests (NGPDTT) and Darcy's law. To perform a point dilution test under natural gradient, a tracer is injected into the test section and the dilution of the tracer is monitored by measuring the decreasing concentrations at time intervals. The test depth is determined by locating the section where the main groundwater flow occurs. The main groundwater flow zone can be located by performing EC depth profiling and analysis of geological logs. In alluvial channel aquifers, gravel-sand deposits are typically characterized by high groundwater transmissivity and would often be used for the tracer testing. In general, a range of tracers exist but table salt (NaCl) offers the best option due to its availability at relatively low cost and can be easily monitored by EC measurements.

Under natural gradient it is assumed that tracer dilution in the test section is due to the horizontal influx of fresh groundwater into the borehole test section, thus groundwater flux (Darcy velocity) can be determined. Assuming steady-state conditions and no density driven gradient, Darcy velocity is computed from the tracer dilution rate using Equation: 1 (Drost *et al.* 1968).

$$q = \frac{W}{\alpha At} \ln \frac{C}{C_0}$$

Equation: 1 Groundwater flux (Darcy velocity).

Where:

W	=	volume of fluid contained in the test section (m ³).
A	=	cross sectional area normal to the direction of flow (evaluated from πrL , assuming a radial flow model with $n = 2$) (m ²).
C ₀	=	tracer concentration at $t = 0$.
C	=	tracer concentration at time = t .
α	=	borehole distortion factor (between 0.5 and 4; = 2 for an open well) (note that $q\alpha = v^*$, where v^* = apparent velocity inside well).
t	=	time when concentration is equal to C (days).
L	=	test section length (m).

2.2.3.2.3 Seepage flow meters

Seepage flow meters provide a direct measurement of seepage fluxes. A wide range of designs exist for seepage meters, comprehensive details on the design and use of seepage meters are discussed by Lee (1977) and Lee and Cherry (1978). However, according to Boyle (1994), most of these seepage meters can be effectively used only in shallow water environments, such as the littoral zones of lakes and irrigation channels. The application of seepage meters in streams is also limited to areas with slow moving water and sandy streambed (Cey *et al.* 1998). Where the stream bed formation comprises of coarse deposits such as gravel and cobble or hard bedrock, installation and operations of the meters becomes very difficult. Quick moving stream water can easily displace and affect seepage meter measurements. When stream bed sediments consist of heavy and fine silt-clays, it will also require more time to make measurements.

Despite being a direct measurement technique, there is no guarantee that seepage meter readings can only reflect groundwater exchanges. Other sources of water influx on stream bed include; surface water circulation in the sediments and interflow. The seepage meters could not be used at the study site because of the following considerations:

- Large pools exist on the case study site bedrock river channel and these makes it extremely difficult to install seepage meters.

- Seepage meters are often used to monitor GW-SW exchanges on the river beds. Groundwater-surface water exchanges at the case study site occur through a preferential flow path at the contact plane of the unconsolidated sediments and bedrock.
- The groundwater discharge at the seepage face can be physically measured hence there was no need for a seepage meter.

2.2.3.2.4 Stream flow measurements

Stream inflow and outflow measurements are conducted to develop a water balance model of the GW-SW interaction system. These measurements help to determine the losing or gaining status of the system. The technique works on the conservation of mass principle that; inflowing rate should be equal the outflow; any difference is attributed to GW-SW exchanges and other external sources or sinks such as bank storage and evapotranspiration. In general, stream flow measurement techniques provide large-scale estimates of GW-SW exchanges in comparison to point estimates of seepage meters and hydraulic measurements (Cey *et al.* 1998). Streamflow measurements conducted during dry seasons can be used to identify the groundwater contribution to stream flow.

2.2.3.3 Riparian zone

A riparian zone is an interfaced boundary between the land and surface water bodies such as rivers, stream, lakes and wetlands. Gregory *et al.* (1991) defined a riparian zone as a region that encompass sharp gradients of environmental factors, ecological process and plant communities between surface water and terrestrial environments. The saturated zone beneath the riparian zone constitutes the alluvial channel aquifer. The riparian zone shelters and provide food requirement for the diverse plant and animal habitats. The capacity of the riparian zones to sustain habitat biodiversity is depended on factors such as rainfall, soil properties, water table depth, and hydrogeochemical and biochemical process occurring in the vadose and unsaturated zones.

Groundwater table depth fluctuations have been observed to induce dynamics in vegetation growth (Wang *et al.* 2011). Shallow water tables of at least < 1.5 mbgl have been observed to successfully support seedling establishment of woody riparian plants at numerous sites (Mahoney and Rood 1998). According to Stromberg (1998), mature riparian trees and shrubs are often associated with water tables of less than 3 mbgl. Mature riparian trees and shrubs have a fully developed root system that can tap from deep groundwaters. In general, mature trees have less water and nutritional requirements as compared to the young and growing. A number of studies have also managed to establish classes of responses for different ecosystem species to changes in groundwater depth (Groom *et al.* 2000, Pettit *et al.* 2001 and Groom *et al.* 2003).

Huge fluctuations in groundwater tables that occurs naturally or due to abstraction can result in significant alteration of the riparian ecosystem and loss of biodiversity due to retardation of seed development. The study site is mainly characterised by old trees and the limited establishment of young plants can be mainly attributed to deep water levels (> 2 mbgl) that potentially hinders seed establishment. In general, vegetation response to water table changes is mainly influenced by soil water retention properties. The soil water retention capacity is mainly influenced by soil texture and soil moisture potential properties. For instance, Cooper *et al.* (1999) noted the importance of fine-textured soils for the survival of *populus* seedlings that had never tapped the shallow water table. The effect of a particular water table decline on the riparian vegetation depends on the following interacting factors that influence both plant water requirements and uptake (Shafroth *et al.* 2000):

- The magnitude of groundwater decline relative to the pre-decline distribution of roots.
- Rate and duration of the water table decline.
- The ability of soil to retain water following the water table decline.
- Physiological ability of the plant to grow deeper roots and adjust to lowered water tables.

Besides sustaining the plant and animal habitat, the riparian zones also protect stream/river banks from the erosional effects. Green and Haney (2000) discuss in detail other environmental roles that are played by the riparian zones. The riparian zones are often rich in organic matter and high vegetation density has great potential to increase infiltration rates and consequently recharge of the shallow alluvial channel aquifer.

2.3 Summary

This chapter gives a discussion of alluvial channel aquifers, GW-SW interaction mechanisms and processes along a typical alluvial channel aquifer. An overview on the techniques that can be used for measuring GW-SW exchanges is also given. Groundwater flow properties and GW-SW interaction mechanisms in alluvial channel aquifers that can occur along the alluvial and bedrock river channels is discussed. The groundwater flow properties of alluvial channel aquifers are greatly influenced by the nature of the river channel hosting the aquifer. Alluvial channel aquifers are located in the groundwater discharge or recharge zones hence their interaction with surface water resources is an important aspect. A water balance model is essential to determine the losing or gaining status of the GW-SW system before detailed field investigations can be conducted.

The next chapter describes the application of outcrop mapping and drilling of boreholes as complimentary techniques to characterise the geological properties of the alluvial channel aquifer.

3 GEOLOGICAL CHARACTERISATION

3.1 Introduction

Geohydrologists are interested in understanding the subsurface geological properties and its influence on the groundwater flow and storage properties. Geological characterisation provides the best means to understand the subsurface. Geological characterization can be achieved using different tools depending on the research objectives and the available or accessible equipment. Conventional tools and techniques such as outcropping mapping, drilling, coring and borehole geophysics are commonly used. Despite the advancement in technology, drilling of boreholes remains the principal means to geological characterization (USEPA 2001). Valuable information on the physical and chemical properties of the geological material underlying the site is obtained from visual observations and analysis made on the borehole logs.

In Southern Africa, alluvial channel aquifers comprises mostly of sedimentary deposits, composed of various lithological components such as clay-silt, calcrete and sand (Woodford and Chevallier 2002). The lithological components are highly variable in physical and chemical properties due to the difference of depositional environment and sedimentary processes. In general, research indicates that the transport of groundwater and solutes is depended on the relevant chemical and physical properties of specific lithological components in the aquifer system (Grathwohl and Kleinedam 1995).

Coarse-grained alluvial aquifers are typically regarded as close to a homogeneous porous media when estimating hydraulic and transport parameters. Groundwater and transport flow through these unconsolidated sediments is however greatly controlled by aquifer material architecture (Zappa *et al.* 2006). It is therefore important for the practicing geohydrologists to understand and describe the spatial variations of aquifer geological materials using conventional site characterisation methods. This chapter describes the application of outcrop mapping and percussion drilling to characterise a heterogeneous alluvial channel aquifer. A geological conceptual model was constructed to highlight the observations made in the study. An attempt was also made to estimate the aquifer hydraulic conductivities based on grain size analysis.

In general, real aquifers are not directly accessible for investigation to derive aquifer parameters and drilling of boreholes provides the appropriate solution. The contribution of outcrop mapping on understanding subsurface geology cannot be underestimated. An outcrop composed of a similar

stratigraphy and lithologies as the aquifer may be viewed as a representation of the actual aquifer (Klingbeil 1999). In other words, accessible outcrops can be examined for spatial geological geometries and structures at a smaller scale investigation. The chapter aims to:

- Describe in detail the regional geology based on literature.
- Describe and represent the local geology using outcrop mapping and analysis of drilling geological logs.
- Produce a site geological conceptual model.
- Show and describe the spatial variation of the subsurface geological properties due to heterogeneities of the deposition processes.
- Use the geological understanding to delineate the alluvial channel aquifer system.
- Develop a hydrogeological conceptual framework to use for aquifer test planning.

3.2 Regional geology

The general geology of the study area is characterised by shale, sandstone and mudstone outcrops of the Beaufort Group located in the Main Karoo Basin. The Main Karoo Basin overlies the central and eastern parts of South Africa. The sediments of the lower part of Beaufort Group (Adelaide Sub-group) within the general area of the study site comprise of unconsolidated quaternary deposits of calcrete, silt-clay and gravel-sands that overlie the shale bedrock. Figure 3-1 shows a schematic of the Karoo Supergroup geological succession.








Drakensberg Volcanics			Basaltic	Jurassic
Stromberg Group	Clarens		Cross bedded sandstone	Triassic
	Elliot		Red mudstone and sandstone	
	Molteno		Sandstone, conglomerate, mudstone	
Beaufort Group	Tarkastad Subgroup		Burgersdrop Formation	
			Katberg Sandstone	
	Adelaide Subgroup		Green, grey and purple mudstones	
			Sandstone	Permian
Ecca Group			Shale and sandstone	Permian
Dwyka Group			Tillite and diamictite	Carboniferous

Figure 3-1 A schematic showing the Karoo Supergroup sequence (after Tankard *et al.* 1982).

The sedimentary stratum of the main Karoo basin is the most important geological unit and is commonly referred to as “Karoo Supergroup”. The evolving of the Karoo Supergroup is chiefly attributed to the deposition of Karoo sediments. Karoo Supergroup consists of the following major lithostratigraphic units (Woodford and Chevallier 2002):

- **Drakensberg Group** mainly consists of basaltic lavas and its formation is attributed to continental rifting.
- **Molteno formation** comprises of coarse sandstones and conglomerates with good groundwater storage potentials and is the ideal target for drilling.
- **Elliot formation** mainly consists of red mudstones of very low permeable properties which approximate aquitard conditions.
- **Clarens formation** is characterised by well sorted, fine to medium grained sandstones of high storage properties. It is poorly fractured and of relatively low permeability.
- **Beaufort Group** consists of sedimentary deposits varying from coarse-grained along braided stream environments and to more tight formations away from the river basins.
- **Ecca Group** is dominated by shales of a tight formation with very low porosities. They however form tiny fractures when weathered and these can store and transmit groundwater into the main bedding plane fractures. Because of fracturing, the Ecca group have good potential for groundwater exploration. Sedimentary deposits often form multilayered and multi-porous aquifers. Contact planes between different sedimentary units can form preferential flow paths for groundwater and these offer good drilling targets.
- **Dwyka Group sediments** have very low hydraulic properties and often result in the formation of aquitard. Water in these aquifers is often saline due to paleo marine depositional environments.

3.2.1 Quaternary deposits

According to Woodford and Chevallier (2002), quaternary deposits are a common characteristic along the major rivers in the Karoo basin. Deposits on the bed of braided streams consist mainly of coarse sediments, conglomerates and patches of finer material on their banks. Meandering streams on the other hand deposit mainly fine-grained sand, mudstone and siltstone with little or no conglomerates (Visser 1989). Gravel-sand and alluvium-silt deposits are often found along several river courses and along the alluvial channel zones. The deposition of sediments in the fluvial environments takes place either by vertical or lateral accretion resulting in the formation of three major deposits (Campbell 1980):

- **Flood basin deposits** which comprises largely of fine-grained deposits formed during heavy floods when river water flows over the levees into the flood basin. Flood deposits are mostly

made up of uniform laminated muds with intercalations of silt and in some instances sandstone.

- **Channel deposits** are formed mainly by the action of river channels, these include lag, point bar, and channel fill deposits.
- **Bank deposits** are formed on the banks during floods and, these mainly comprise of crevasse splay and levee deposits. The crevasse splay and levee deposits are typically characterised by thin alterations of sandy and silty layers.

Braided and meandering stream fluvial processes (Figure 3-2) are mainly responsible for the deposition of quaternary deposits (Botha *et al.* 1998). Braided and meandering stream fluvial processes occur in the same river or stream but takes place at different stream positions.

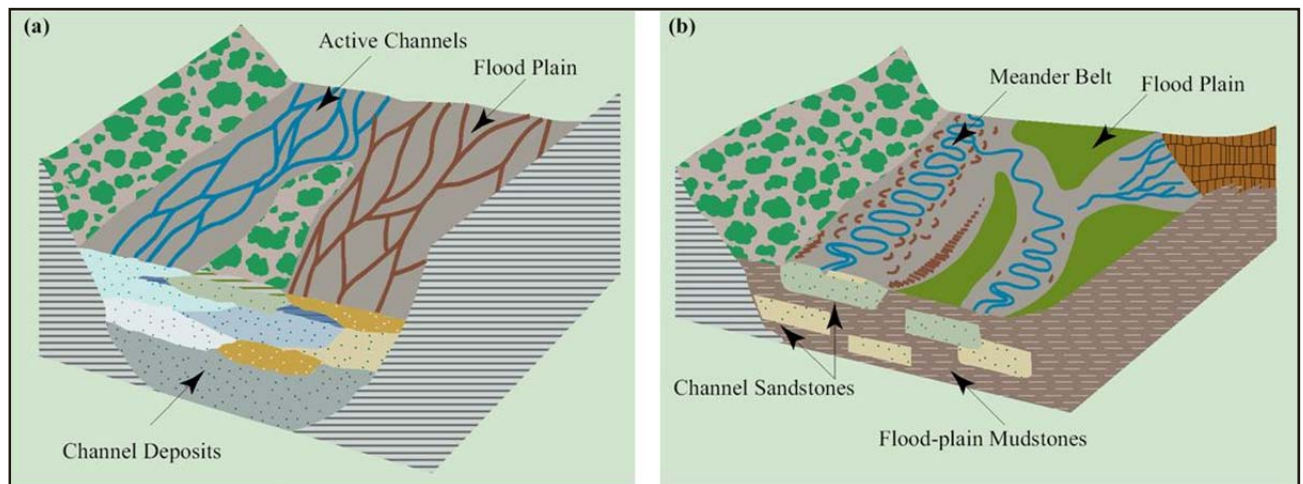


Figure 3-2 Models showing the fluvial processes associated with (a) braided stream and (b) Meandering streams (Botha *et al.* 1998).

Braided stream consist of a number of channels with high stream velocities and tends to develop on high slopes. According to Visser (1989), deposits on the beds of braided stream comprise of coarse sediments, conglomerates and patches of finer grained materials on their banks. Meandering streams often develop on flat terrain and is typically characterised by single channels with low stream velocities (Davis 1983).

3.3 Field methods and materials

3.3.1 Outcrop mapping

An outcrop is that part of a rock formation or mineral that appears at the earth's surface. In general, outcrop mapping involves the identification and description of the rock formations and minerals that

are exposed to the earth's surface. Detailed outcrop mapping can include inspection of structural geological features and their orientations.

Outcrop mapping is often conducted in the vicinity of the study area before borehole drilling explorations as part of initial site survey. Prior to borehole drilling one has to plan for the type of drilling equipment and borehole construction logistics. The general knowledge of site geology acquired through outcropping mapping is pivotal. Detailed outcrop mapping can still be conducted after borehole drilling to confirm the validity of borehole geological logs. In general, the analysis of borehole logs obtained through the percussion drilling method is a subjective process due to the mixing of the drill cuttings. The subjectivity and erroneous interpretation of borehole logs from percussion drilling does not put their usefulness into doubt but serves to highlight the need for the use of complimentary approaches. A comparison of borehole logs to rock outcrops can assist in the identification and description of the subsurface lithology. In this study, outcrop mapping was conducted in the vicinity of the study site through the observation and identification of outcropping rocks. The outcrops were classified based on the lithology, weathering and fracturing.

3.3.2 Borehole drilling

A total of nine and six boreholes were drilled in the alluvial channel aquifer and terrestrial aquifer respectively. The boreholes were cased to prevent collapsing of the unconsolidated sediments. Borehole geological logs were analysed to identify and describe the lithology per each meter of the drilled depth. Figure 3-3 shows the location of the boreholes drilled in the alluvial channel aquifer and terrestrial aquifer.

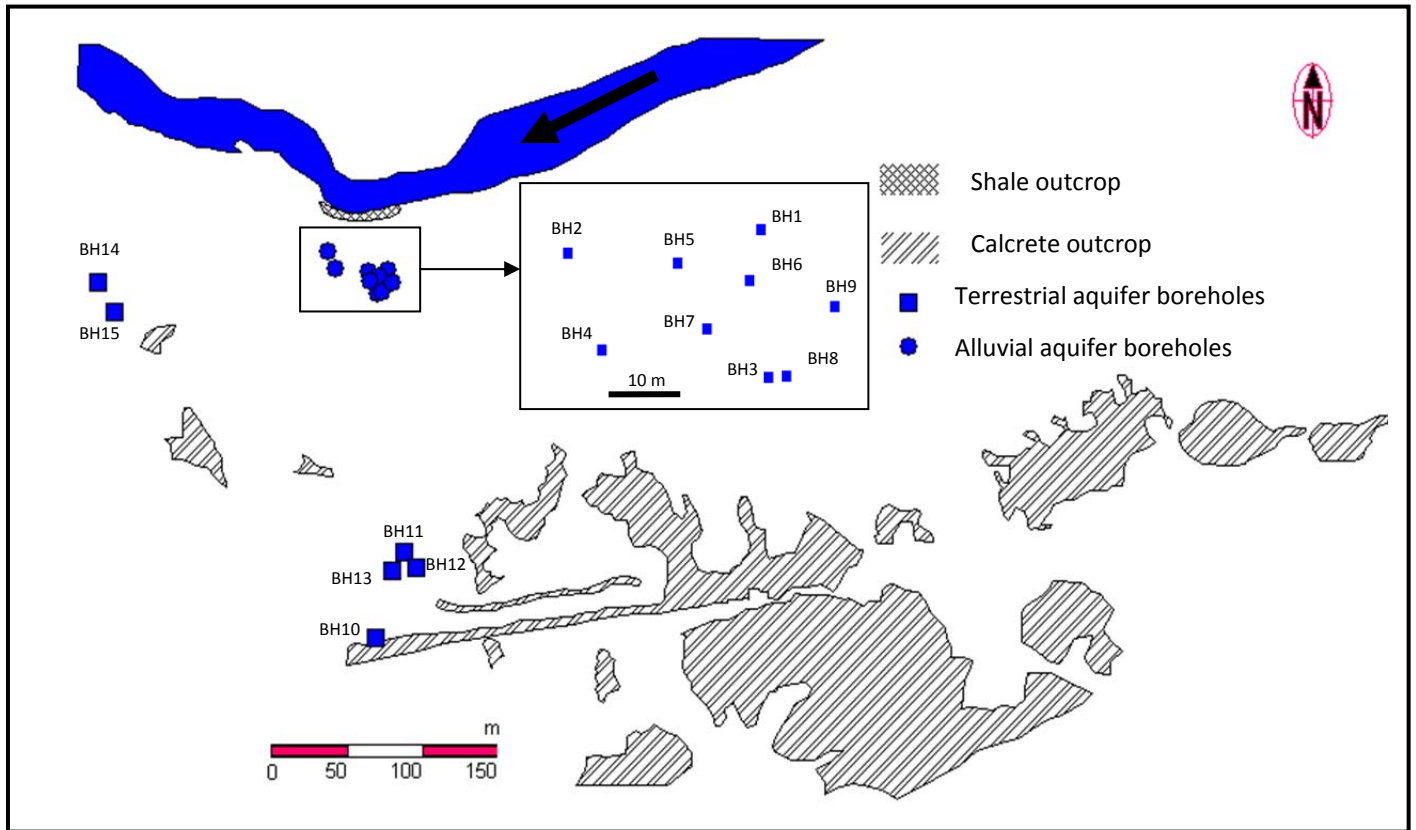


Figure 3-3 Location of the boreholes that were drilled into the alluvial channel aquifer and terrestrial background aquifer of the study site; also shown is the location of shale and calcrete outcrops.

Boreholes were drilled using the air rotary percussion drilling method (Figure 3-4). With this method, the air alone lifts the cuttings from the borehole. A large compressor provides the air which is forced into the drill pipe and escapes through small ports at the bottom of the drill bit, thereby lifting the cuttings and cooling the drill bit. The cuttings are blown out to the top of the hole and collect at the surface around the borehole. The capacity of the compressor dictates the drilling depth and diameter. Cutting removal is a function of the up-hole velocity of the air, which lift them to the surface.

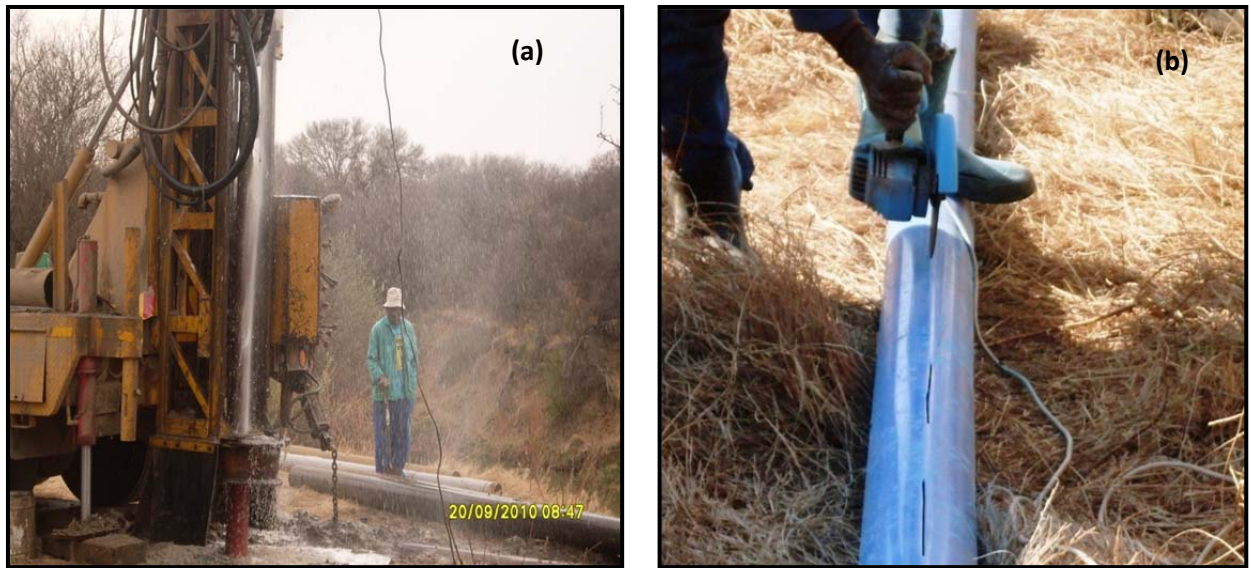


Figure 3-4 Photos of the showing: (a) Air percussion drilling equipment used for borehole drilling and (b) Poly Vinyl Chloride pipes used for boreholes casing; perforations on the pipe were handmade using a grinder machine.

The drilling depth was determined based on the initial site understanding which had been gained through outcrop mapping and initial site walk. Poly Vinyl Chloride (PVC) materials was used for borehole construction at the study site. The boreholes are cased to prevent collapsing of the unconsolidated channel deposits. Table 1 shows a summary of important drilling information. Due to technical reasons, the drilling company did not measure the blow yields. All boreholes were drilled to a diameter of 160 mm.

Hundred grams of disturbed samples were randomly collected from calcrete, alluvium-silt, clay and gravel-sand unconsolidated formations of the boreholes drilled into the alluvial channel aquifer. The samples from different boreholes were then thoroughly mixed to obtain a representative sample of each lithology. Grain size distribution on the representative samples of lithologies was determined using sieve analysis.

Table 1 Information about borehole depth, casing and main water strikes, the boreholes were named according to their drilling order. The water levels were measured after one week after drilling but prior to construction.

Borehole name	Depth [mbgl]	Casing depth [mbgl] and description	Main water strike [mbgl]	Water level [mbgl]	Surface topography [mbgl]
BH1	42	24 - closed, sealed with concrete	5.0	3.32	1240.99
BH2	24	12 - closed	5.5	2.66	1241.28
BH3	24	8 - fully perforated	7.0	2.63	1241.77
BH4	24	12 - closed	6.0	3.25	1241.55
BH5	12	8 - fully perforated	7.0	2.11	1241.33
BH6	12	8 - fully perforated	6.0	2.26	1241.34
BH7	12	8 - fully perforated	7.0	2.60	1241.58
BH8	6	6 - fully perforated	6.0	2.50	1241.77
BH9	12	8 - fully perforated	7	2.55	1241.52
BH10	36	13 - closed; 5 - perforated	12	8.79	1249.48
BH11	18	13 - closed; 5 - perforated	12	8.22	1248.67
BH12	18	13 - closed; 5 - perforated	12	7.97	1248.47
BH13	18	13 - closed; 5 - perforated	12	8.32	1248.77
BH14	12	13 - closed; 5 - perforated	8	6.31	1246.10
BH15	18	13 - closed; 5 - perforated	12	8.31	1248.28

3.4 Site Geology

3.4.1 Outcrops

Patches of calcrete outcrops were observed on the study site (Figure 3-3). The presence of the outcropping calcrete is mainly attributed to carbonate precipitating above a fluctuating shallow water table. The calcrete outcrops completely disappears towards the Modder River. Close to the river, calcrete formation is found beneath the ground surface. Detailed explanation on the possible processes leading to the formation of calcrete at the site is placed in section 3.4.3.2.1.

Shale outcrops were observed along the river bank adjacent to the case study site (Figure 3-3). The shale formation is the bedrock on which the overlying unconsolidated sediments have been deposited. The average thickness of the unconsolidated overlying sediments is approximated to be about 10 m above the shale bedrock. Based on outcrop mapping results, PVC casing pipes had to be

acquired prior to the drilling in order to prevent boreholes from collapsing on the upper unconsolidated section. A hypothesis that a deep fractured-rock aquifer system existed on the site was developed after observation of weathered shale outcrops. It is always difficult to infer the existence of weathered and fractured-rock aquifer based on observations made solely on outcropping rocks. Naturally, outcropping rocks are exposed to atmospheric conditions with various agents of weathering that can result in fracturing; hence such observations should be treated with caution.

The contact plane between the overlying unconsolidated sediments and the shale of the underlying bedrock has formed a preferential flow path for groundwater thus creating a discharge zone at the river bank. Bedding plane fractures between the contacts of different sedimentary formation of the Karoo basin are often characterized by high transmissivities (Van Tonder *et al.* 2001). In such instances, the preferential flow paths can accelerate the movement of both groundwater and contaminants.

3.4.2 Geological logs and borehole construction

3.4.2.1 Alluvial channel aquifer

3.4.2.1.1 BH1 borehole

BH1 borehole (Figure 3-5) is the deepest at the site. The borehole was drilled to 42 mbgl based on the hypothesis that the site had two aquifer systems. The first aquifer system was believed to be a perched gravel-sand shallow aquifer overlying a deep fractured aquifer of the shale bedrock. The shale deep aquifer system was hypothesized to be heavily fractured given the high prevalence of fractured-rock aquifers in the typical Karoo sediments (Botha *et al.* 1998, Botha and Cloot 2004). Figure 3-5 shows the lithology and construction of BH1.

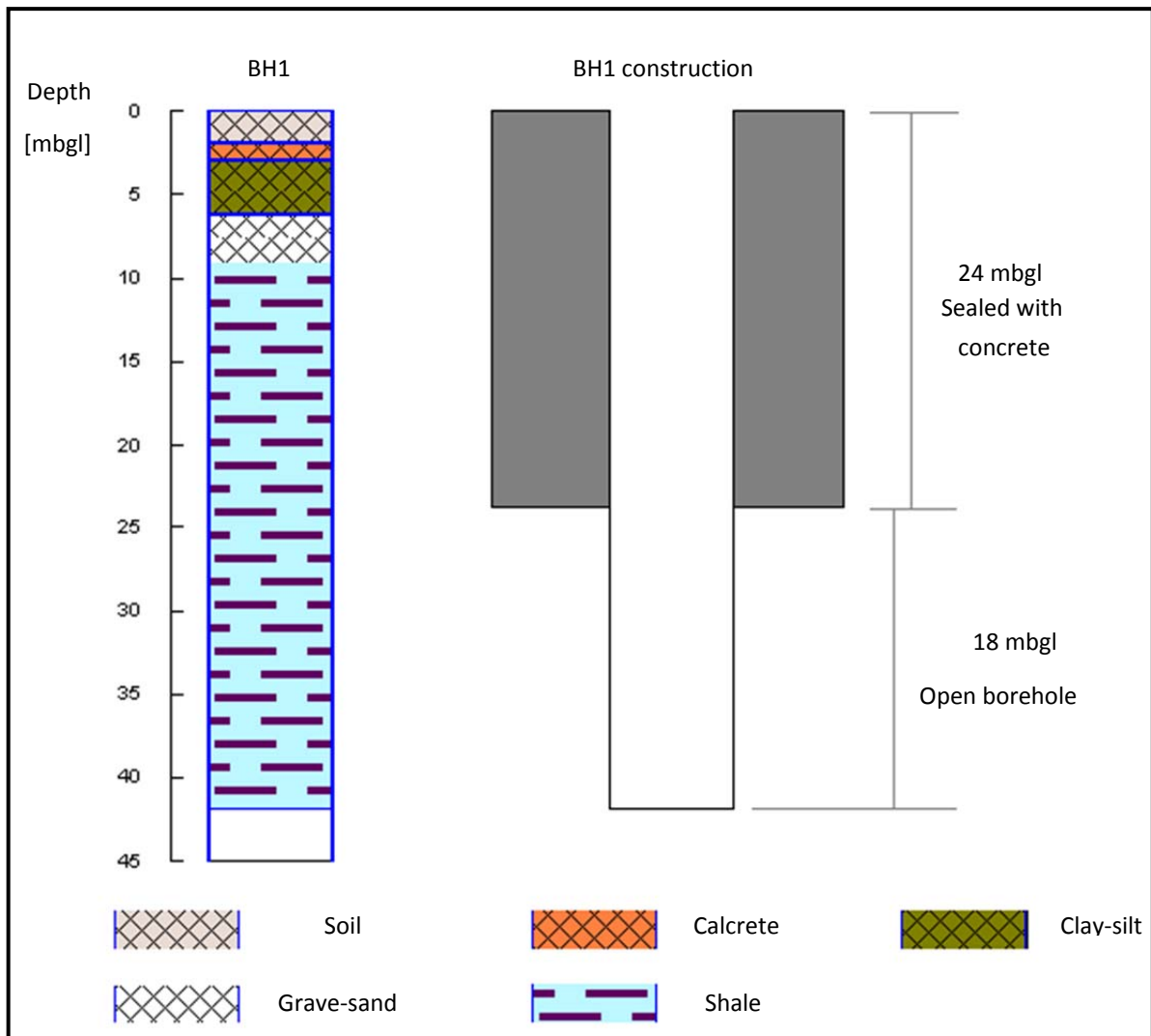


Figure 3-5 A schematic diagram showing the lithology and construction of BH1; the bold and dashed lines shows the average water levels measured before and after sealing with concrete respectively.

There was only one water strike at 7 m in the gravel-sand material. After hitting the first water strike at 7 mbgl, it was only imperative to drill deeper with the hope of reaching the deep aquifer system. There was however no visible water strike that was encountered between 7 to 42 mbgl to infer the existence of a deep aquifer system at the site. The idea of the deep aquifer system however persisted and there was need for further investigations.

An attempt was made to seal off the first 24 mbgl section of BH1 using a concrete mix. The objective of sealing was to isolate the idealized deep aquifer from the shallow gravel-sand aquifer system. After construction the borehole was pumped dry and when the borehole had fully recovered a water level 6.65 mbgl was measured. The deeper water level after construction suggested the existence of a deep aquifer system underlying the shallow alluvial aquifer system. However during the recovery

of the borehole, water could be heard dripping from the upper shallow aquifer into the borehole thus implying potential connectivity with the upper shallow aquifer system. Based on the geology and main water strikes in BH1, a preliminary conclusion that the gravel-sand material is the main aquifer system was made and the next set of boreholes were then drilled to 24 mbgl (BH2, BH3 and BH4) and 12 (BH5, BH6, BH7 and BH9) mbgl. Borehole BH8 was drilled to 6 mbgl into the calcrete and clay-silt formation.

3.4.2.1.2 BH2, BH3 and BH4

The boreholes were drilled to a depth of 24 m. The boreholes were drilled to fully penetrate shallow main aquifer system and partially into the deep fractured aquifer systems that were hypothesized to occur at the site. Just like the rest of the boreholes, BH2 and BH4 intersect calcrete, silt-clay and gravel-sand unconsolidated formations that overlie the consolidated shale formation (Figure 3-6).

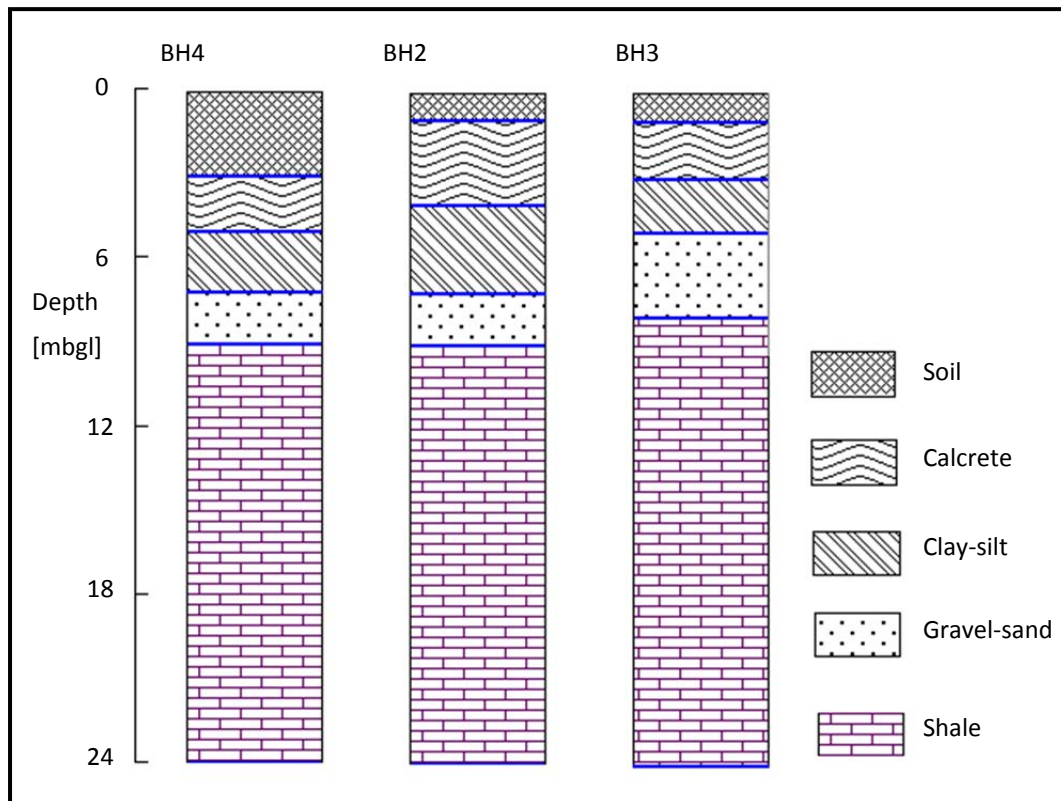


Figure 3-6 Geological logs showing the lithologies intersected in 24 m deep boreholes (BH2, BH3 and BH4).

Closed 12 m PVC casings were placed in these BH2 and BH4 boreholes. The closed casing was installed to seal off first 12 mbgl of the borehole column and the bottom 12 m was left open to the shale formation that had been hypothesized as the deep aquifer system. This construction was meant to ensure that the boreholes can be used to test separately the deep aquifer system.

No concrete or bentonite material was placed to assist the sealing. It was assumed that the closed PVC casing would ensure complete sealing. In BH3 borehole, a perforated 8 m casing was installed. It therefore implies that BH3 borehole was left open to both the shallow and deep aquifer systems.

In all the boreholes the measured water levels prior to construction was above the water strikes (<3mbgl) (Table 1). After construction the boreholes were pumped dry and water levels of 7.88 mbgl and 6.04 mbgl were measured after full recovery in BH2 and BH4 boreholes. Deeper water levels after construction suggested the existence of a deep aquifer system underlying the shallow alluvial aquifer system. During recovery of the borehole of BH2 and BH4 water could be heard dripping from the upper shallow aquifer into the borehole suggesting the potential of connectivity between the two aquifers. In BH3, the water level could only be lowered by 1 m during pumping after construction and it managed to recover to the water level ranges of the shallow boreholes (Appendix 3.1).

3.4.2.1.3 Other boreholes

The 12 m deep boreholes are drilled to fully penetrate the gravel-sand layer aquifer layer of the site. The boreholes are cased with perforated PVC pipes for the first 8 mbgl to prevent collapsing of the unconsolidated sediments. All the 12 m deep boreholes intersect calcrete, alluvium-silt, clay and gravel-sands unconsolidated sediments with the exception of BH5 (Figure 3-7). Borehole BH5 lithology consist of soil and fine alluvium-silt. The most likely explanation is that BH5 is situated in a former flood plain channel characterised by fine sediment deposits. The unconsolidated sediments of calcrete, alluvium-silt, clay and gravel-sands conceptually form the site aquifer system.

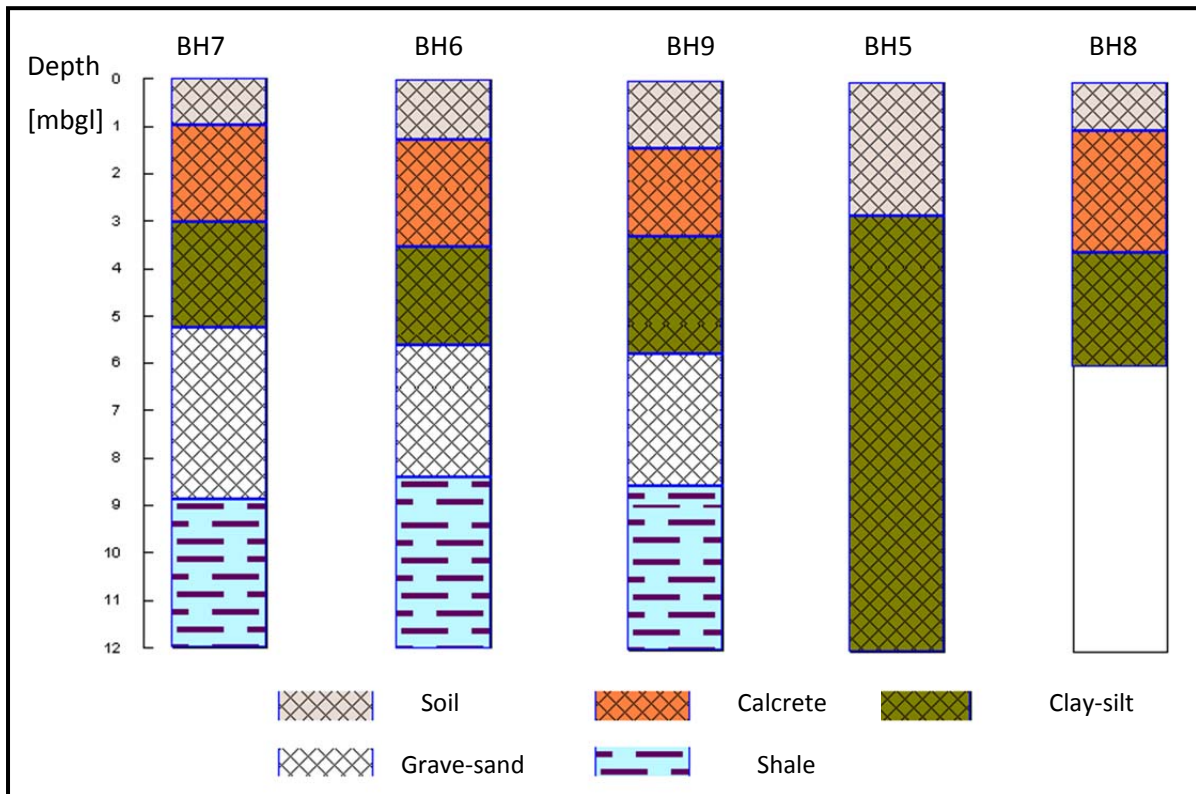


Figure 3-7 Geological logs showing the lithology intersected in BH6, BH5, BH7, BH9 and BH8 boreholes; the groundwater levels shown in bold lines were measured after borehole construction.

Borehole BH8 (6 mbgl) is the shallowest borehole at the site. The borehole intersects calcrete and clay-silt unconsolidated sediments. The borehole was drilled to assess the influence that overlying calcrete and silt-clay has on groundwater flow and transport processes at the site.

3.4.2.1.4 Lithological hydrofacies

The term hydrofacies is used to describe a sediment geohydrological unit with similar characteristic of groundwater hydraulic and storage properties. According to Klingbeil (1999), hydrofacies are formed under comparable conditions and this lead to similar hydraulic properties. Sediments at the Krugersdrift study site were grouped into four separate hydrofacies (Table 2).

Table 2 Properties of major sediment hydrofacies observed at the study site.

Hydrofacies	Geologic interpretation	Drilling descriptions	texture
Calcrete	Chemical deposition	Calcareous soils	Fine grained
Clay-silt (Muddy sands)	Flood plain deposition	clay-silt	Fine to medium grained
Gravel-sands	Channel depositions	Gravel packing	Gravel and medium to coarse sands, small to medium pebbles
Shale	Bedrock	Grey fresh	Fine grained

3.4.2.1.5 Grain size analysis

Representative samples for each alluvium aquifer layer was analyzed and results are shown in Table 3. In general, the size and nature of channel deposits spatially varies between boreholes and depths indicating the presence of horizontal and vertical heterogeneity in the aquifer. The groundwater hydraulic conductivity (Table 3) for the gravel-sand material was estimated using Hazen's (1911) empirical relationship (Equation 2) using average grain sizes from the representative samples.

$$K = C(d_{10})^2$$

Equation 2: Hazen (1911) hydraulic conductivity.

Where, K- Hydraulic conductivity (cm/s), d_{10} - Effective grain size = grain-size diameter at which 10% by weight are finer and 90 % are coarser (cm), C = is a coefficient based on grain sizes and sorting.

Table 3 Results of grain size analysis and estimated hydraulic conductivity for representative gravel-sand aquifer materials.

Geological Lithology	Weight [%]				K [m/d]
	Clay <0.002 mm	Silt 0.002-0.07 mm	Sand 0.07-2.0 mm	Gravel >2.0 mm	
Calcrete	81.3	18.7	0	0	- ^a
Silt	14.42	85.58	0	0	-
Clay	87.21	12.79	0	0	-
Gravel-sand	1.8	4.7	65.3	28.2	1.0

a- Formation consist less than 90 % coarser particles and the Hazen (1911) could not be used to determine K.

In general, the hydraulic conductivity values determined from grain-size analyses are less reliable because of distortions that occur during the drilling. However, they are still able to give a good understanding of the relative hydraulic properties between different sediment layers. The Hazen Method (1911) was used to estimate the hydraulic conductivity of the gravel-sand material. At least 90 % of the gravel-sand material was composed of coarser particles thereby meeting the Hazen method's requirement.

3.4.2.2 Background terrestrial aquifer

Six boreholes were drilled in the background terrestrial aquifer (Figure 3-3). All the boreholes intersected unconsolidated sediments of calcrete, silt-clay, sand-gravel that overlies the shale consolidated formation (Figure 3-8). The geological material of the adjacent terrestrial is just similar to the alluvial. There is however a huge difference on the thickness of the overburden unconsolidated sediments and subsequently the depth to the water levels (Table 1). The terrestrial land is characterised by thicker unconsolidated vadose zone sediments and deep water levels as compared to the shallow alluvial channel aquifer. The presence of thick unconsolidated sediments on the terrestrial background aquifer can be attributed low erosional effects when compared to the riparian zone. Figure 3-8 shows the lithologies that were intersected in the background boreholes. The geological log for BH10 in Figure 3-8 shows only up to 18 mbgl although the borehole was drilled to 36 mbgl. The bottom 18 m of the borehole also intersected hard shale formation. BH14 is generally located closest to the riparian zone and it intersected a thick soil layer closer to the ground surface. Organic matter from decaying plant in the riparian zone potentially enhances the formation of soil materials.

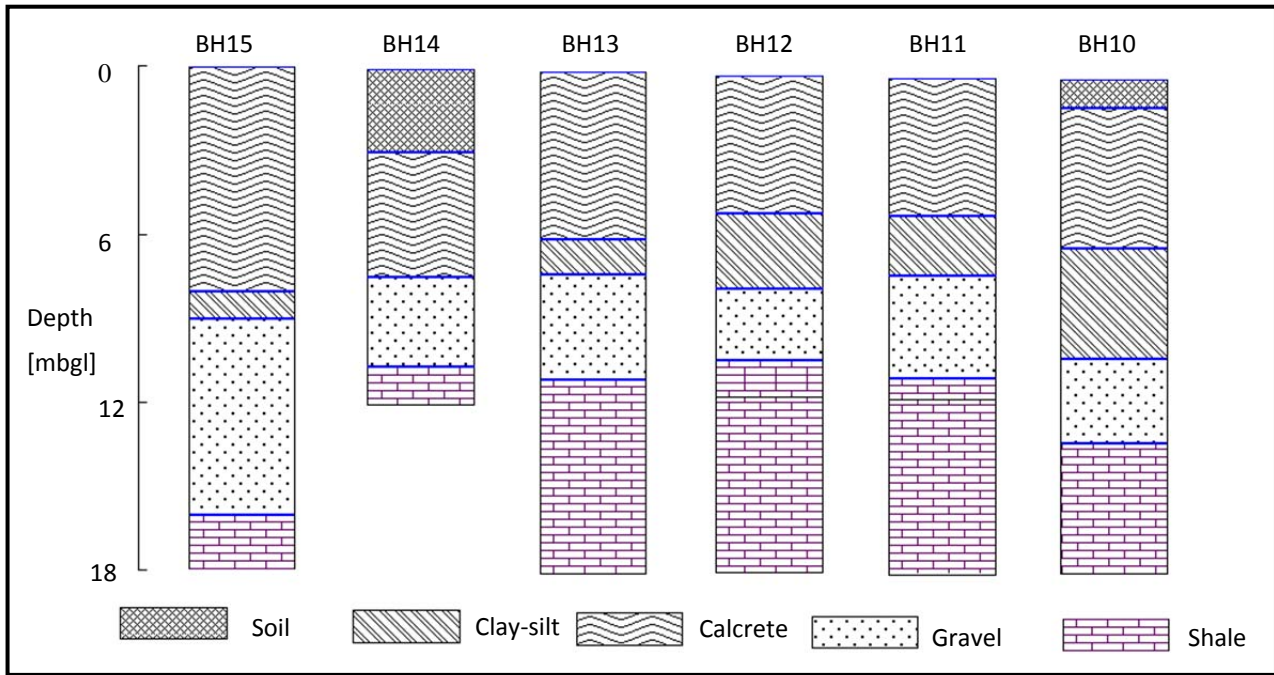


Figure 3-8 Geological logs showing the lithologies intersected in the background boreholes.

On the terrestrial land, calcrete formation outcrops on the surface (Figure 3-3) while it is found below the surface on the riparian zone of the alluvial channel aquifer (See more explanation in section 3.4.3.2.1). Some of the work on background terrestrial aquifer was covered in detail by Khiliso (2011). In general, the overburden thickness above the water table increases as the surface elevation from the river increases from the riparian zone to terrestrial background aquifer. It is therefore apparent that the depth to water table recorded in the terrestrial aquifer and the shallow alluvial channel aquifer generally mimics topography as indicated by R^2 of 0.96 and 0.73 respectively (Figure 3-9).

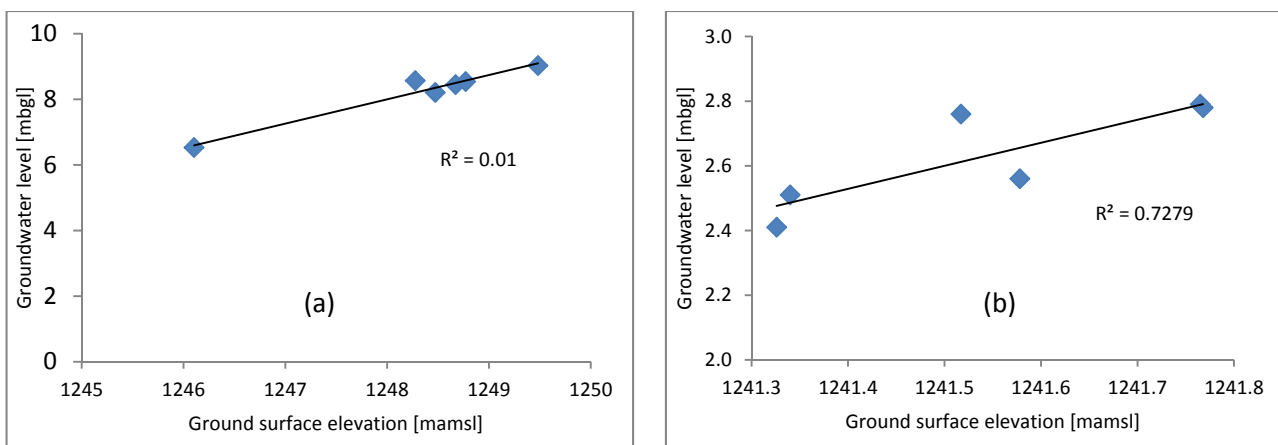


Figure 3-9 Scatter plots of groundwater level against ground surface elevation for the boreholes drilled into the terrestrial (a) and shallow alluvial channel main aquifer (b); these water levels were measured five days after drilling of each borehole.

It can be therefore concluded that the shallow main aquifer derives its groundwater from the background terrestrial aquifer as indicated by the water table continuity between the two aquifer systems (Figure 3-10). However the hydraulic flow properties are expected to differ between the two aquifers due to natural spatial variation in the distribution of aquifer geologic materials.

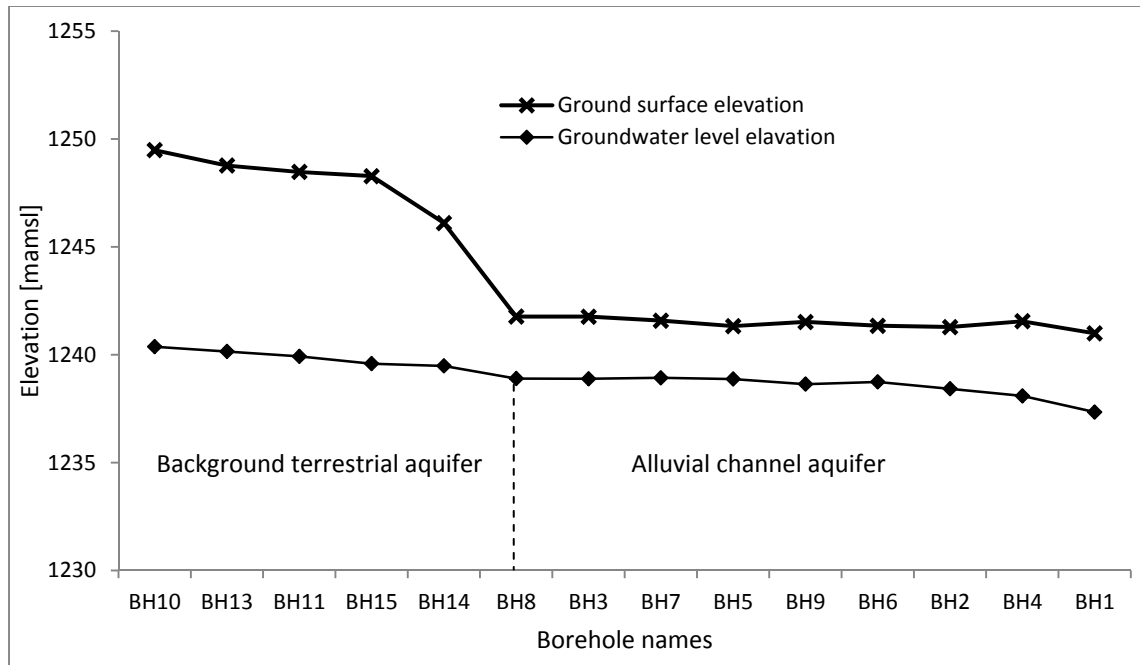


Figure 3-10 A plot showing the relationship between surface topography elevation and groundwater level elevation of the background terrestrial aquifer and the alluvial channel aquifer; groundwater level were measured 5 days after drilling of each borehole.

3.4.3 Conceptual model

3.4.3.1 Evolution of the alluvial channel aquifer

Based on theory and field observations an effort was made to try and explain the possible geomorphological processes that could have led to the formation of the alluvial channel aquifer. The presence of gravel-sand material on top of the shale bedrock was inferred to imply that the old river channel was initially flowing on top of the resistant shale bedrock. Channel deposit processes resulted in the deposition of the gravel-sand and silt-clay material on the river bed that was initially on top of the shale bedrock (Figure 3-11).

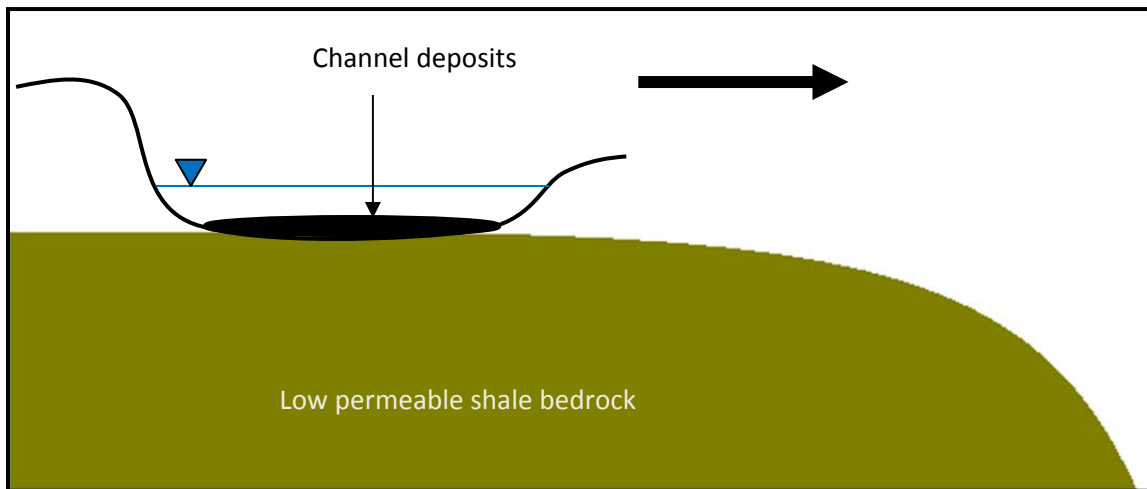


Figure 3-11 A schematic showing the idealized old river channel that was flowing on top of the shale bedrock; the arrow shows the direction towards which the river channel was shifting.

With time the river channel shifted towards the right direction most likely following the slight dip of the shale bedrock. Figure 3-12 shows the current river position at the case study site. The current river stage is characterised by erosion resistant bedrock and alluvial silt-clay on the left and right sides of the banks respectively. The river is expected to continue shifting towards the right side where the banks are characterised by unconsolidated clay-silt material that is more prone to erosion. The areal extent of the shale bedrock and depth below the current river channel is unknown. The shale formation is part of the Eccu Group and represents a paleo landscape over an extensive area.

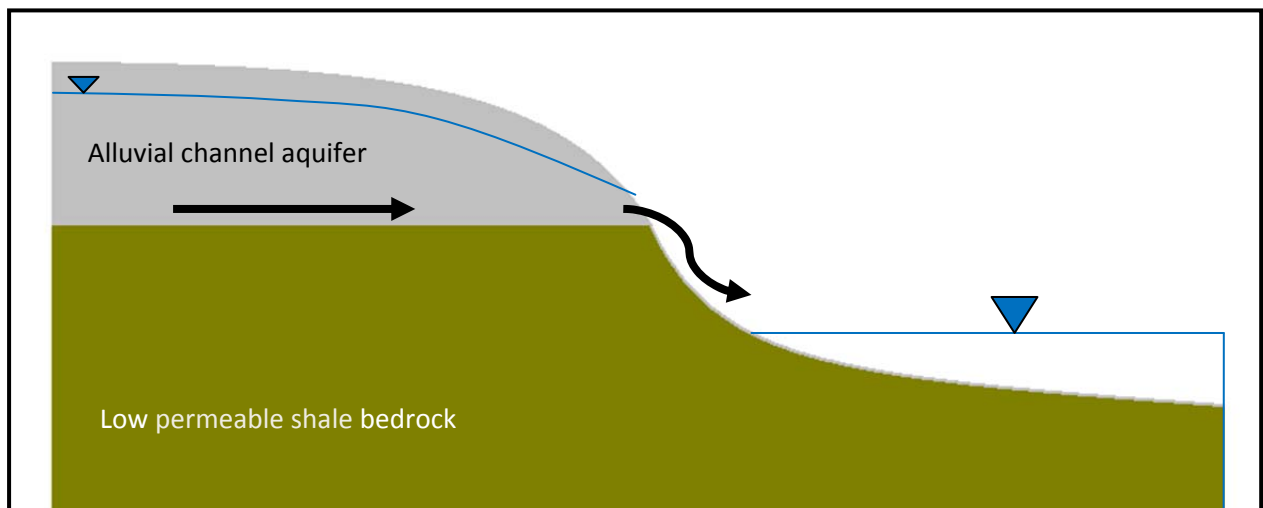


Figure 3-12 A schematic showing the idealized position of the current river channel and the alluvial channel aquifer system; the horizontal arrow shows the groundwater flow direction in the alluvial channel aquifer that eventually discharges into the river at the contact plane.

After shifting, the deposits on the former channels formed an alluvial cover channel aquifer. The presence of gravel-sand and silt-clay material on top of the shale bedrock in the alluvial channel aquifer is a reflection of channel deposition under the normal river load. When deposition occurs under extreme or catastrophic floods, cobbles and boulders are expected to dominate the sediment deposits since the river has high energy to transport them.

3.4.3.1.1 Geological conceptual model

The site geological conceptual model was developed based on two geological cross-sections made through lines A-B and C-D (Figure 3-13). The cross-sections were constructed using the geological logs of boreholes drilled into the alluvial channel aquifer. Geological characterisation of the terrestrial aquifer was conducted by (Leketa 2011). The subsurface of the site comprises of the unconsolidated sediments (soil, calcrete, clay-silt and gravel-sand) that were deposited on the shale bedrock.

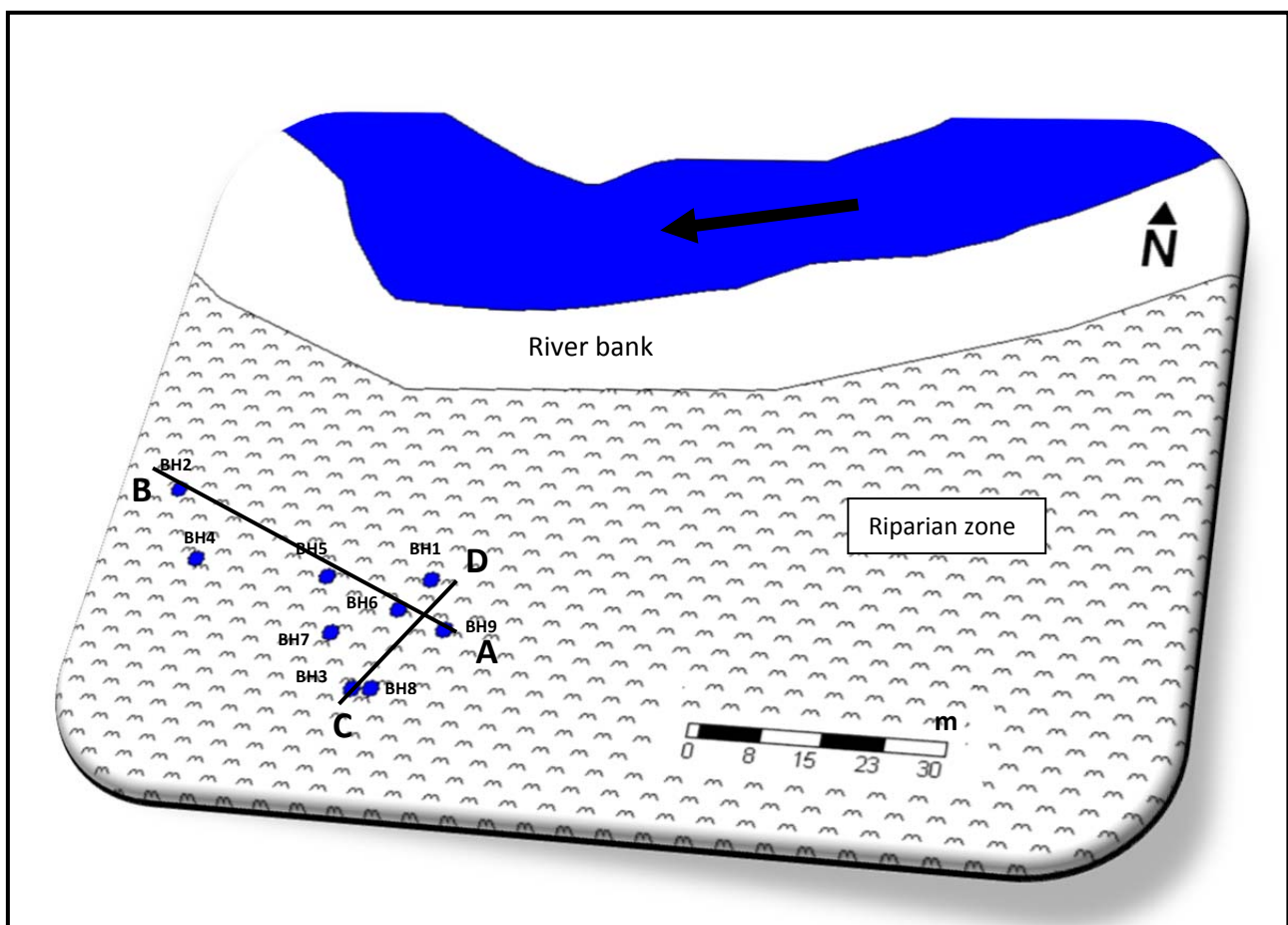


Figure 3-13 Location of boreholes drilled into the alluvial channel aquifer from which the geological cross sections were constructed.

Figure 3-14 and Figure 3-15 shows the idealized geological cross-sections taken between points A-B and C-D respectively. Cross section A-B was constructed along the river flow direction. The cross section shows that unlike the other boreholes of 12 mbgl depth, BH5 does not intersect the gravel-sand layer and shale bedrock. It is possible that the shale bedrock dips towards the river flow direction and can only be intersected by a deeper boreholes. It is however difficult to be conclusive about the complete absence or dipping of the shale bedrock towards the river because no boreholes were drilled beyond BH5 to confirm the phenomenon.

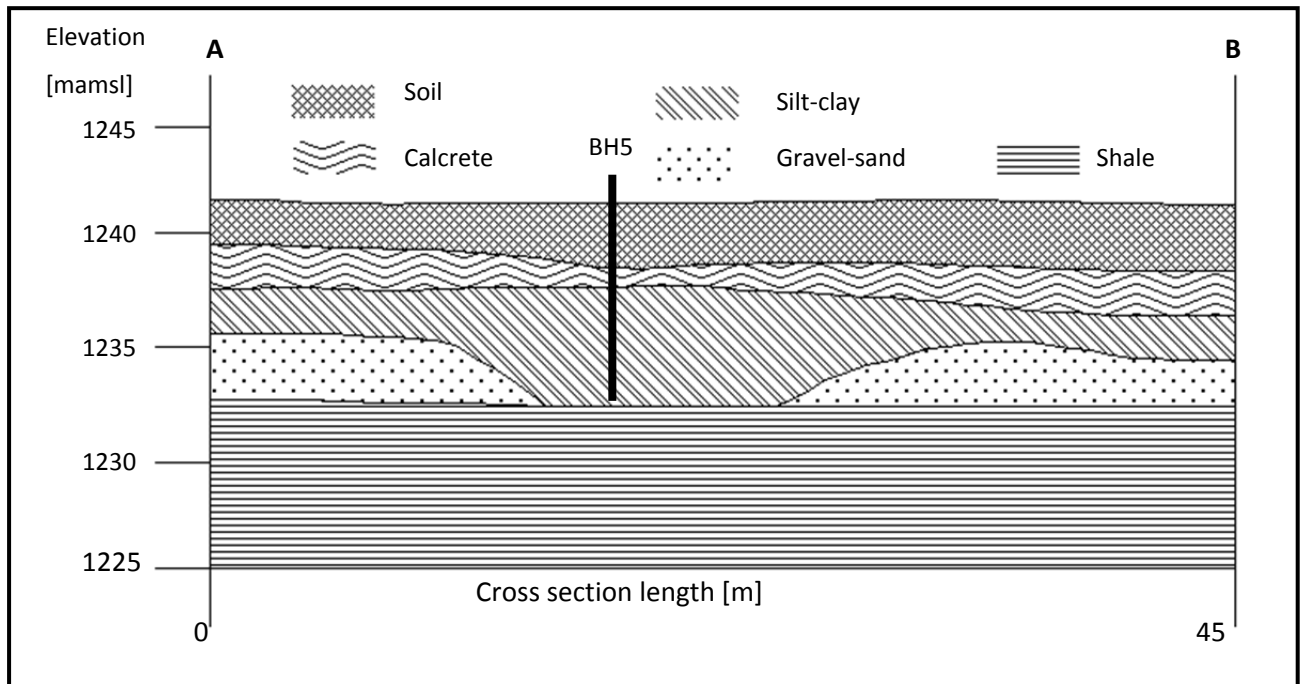


Figure 3-14 Idealized geological cross-section from point A to point B.

The cross section C-D (Figure 3-15) was constructed along the natural groundwater flow direction.

The cross section shows the following important aspects:

- Decrease in calcrete thickness towards the river.
- Increase in soil thickness towards the river.
- Slight increase of gravel-sand thickness towards the river.
- Slight dipping of the calcrete layer towards the river.
- Groundwater flow in the gravel-sand material and discharge at the contact plane of the unconsolidated channel sediments and the low permeable shale bedrock.

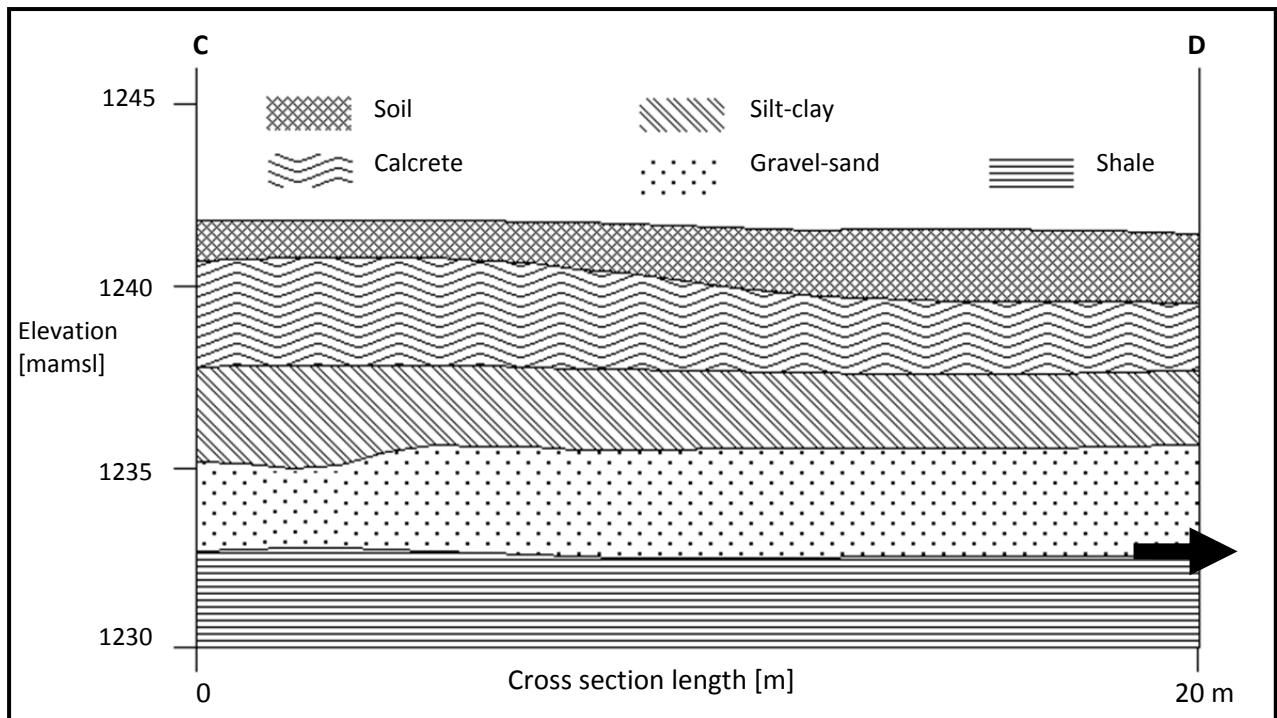


Figure 3-15 Idealized geological cross-section from point C to point D; the arrow shows the position of groundwater discharge that occurs through a seepage face created at the contact plane of the unconsolidated sediments and low permeable shale bedrock.

3.4.3.2 Unconsolidated sediments

The alluvial channel aquifer is characterised by unconsolidated sediment deposits that were deposited on top of shale bedrock. The thickness of the unconsolidated sediments gradually decreases as we move towards the river. The unconsolidated sediments consist of soil, calcrete, clay-silt, and gravel-sand deposits. In general, the riparian vegetation creates a more suitable environment for soil formation through provision of organic matter and enhanced infiltration that promotes the decay of vegetative matter. The muddy hydrofacies that comprises of silty and or clayey sands often characterises the transitional zone between channel and floodplain deposits (Fleckenstein *et al.* 2006). It is therefore important to identify, classify and describe the properties of the unconsolidated sediments before an assessment of their role on groundwater flow and transport processes can be made.

3.4.3.2.1 Calcrete

Calcrete is a sedimentary rock formed through the hardening and lithification of calcified regolith. During the formation, grains of different formations are cemented by calcium carbonates to form the calcrete rock. The site is located in an arid to semi-arid region and in such places calcrete is usually formed as a weathering product of dolerite (Woodford and Chevallier 2002). However, at the

local site scale, the following processes are more applicable in explaining the presence of calcrete at the ground surface and at shallow depth.

When carbonate precipitates above a fluctuating shallow water table, calcrete is formed very close to the earth's surface. The process typically occurs in arid regions where capillary action is a common and pronounced phenomenon (Tanji and Kielen 2002). The presence of calcrete outcrops at the site is evidence to infer the prevalence of this process. Shallow and fluctuating water table contributed to the formation of calcrete at the earth's surface through capillary action. Calcrete formation dominates the site geology between 0.3-2.5 mbgl. Uptake of water by plants leaves behind dissolved calcium carbonates that can precipitate to form calcrete (McQueen 2006).

Carbonate minerals can also be leached and transported from upper soil horizons into the lower horizons. Precipitation of carbonate and dolomite minerals occurs in the lower horizons when the saturation is reached resulting in various forms of calcrete (McQueen 2006). In arid to semi-arid areas, the removal of water by evapotranspiration greatly contributes to calcite chemical saturation conditions and hence the formation of calcrete. The study site is a semi-arid area and the existence of calcrete formation at lower horizons (0.3-2.5 mbgl) is mainly attributed to the leaching down of calcium carbonates from upper horizons.

The occurrence of calcrete in different forms and depth in the sediments possibly represent different ages and or stages of remobilisation (McQueen 2006). Although the permeability of calcrete is low because of small particle sizes and tight packing, they have high groundwater storage potential. Dissolution of calcrete often results in preferential flow paths that can increase the groundwater recharge of the aquifer from direct precipitation. The spatial variability in depths and thickness of calcrete sediments can have important influence on the groundwater recharge variation across the site.

3.4.3.2.2 Clay-silt sediments

Clay-silt sediments were deposited by the old river channel on top of the gravel-sand deposits overlying the shale bedrock. However the whitish color of the clay-silt sediments indicates the accumulation of calcium carbonate minerals from the upper calcrete layer into the lower horizons. This type of soil is collectively referred to as calcisols soils. Calcisols soils are characterised by medium to fine textured materials with good water holding capacities. Due to their medium to fine texture properties, the term clay-silt is used for the calcisols soils. Calcisols soils are formed when calcium carbonates (CaCO_3) accumulates and precipitates in the deep soil horizon forming a calcic

horizon (Deckers *et al.* 1998). In general calcisols soils are formed due to the following processes (Deckers *et al.* 1998):

- Calcium carbonates accumulate in the deep soil horizon forming a calcic layer.
- Calcium carbonates often accumulate through diffuse enrichment of soil matrix or as discrete concentrations.
- The CaCO_3 accumulates precipitates in the deep soil horizons leading to the formation of a calcic horizon.

At the site, the accumulation of CaCO_3 in the deep soil horizons is imminent given the existence of calcrete layer between 2-4 mbgl. Leaching of the overlying calcrete by infiltrating rain water over long period of time result in the build-up of CaCO_3 in the lower horizons is directly responsible for the formation of whitish silt-clay at the study site. Figure 3-16 shows a schematic of deep soil horizon of clay-silt sediments located deeper below the calcrete layer.

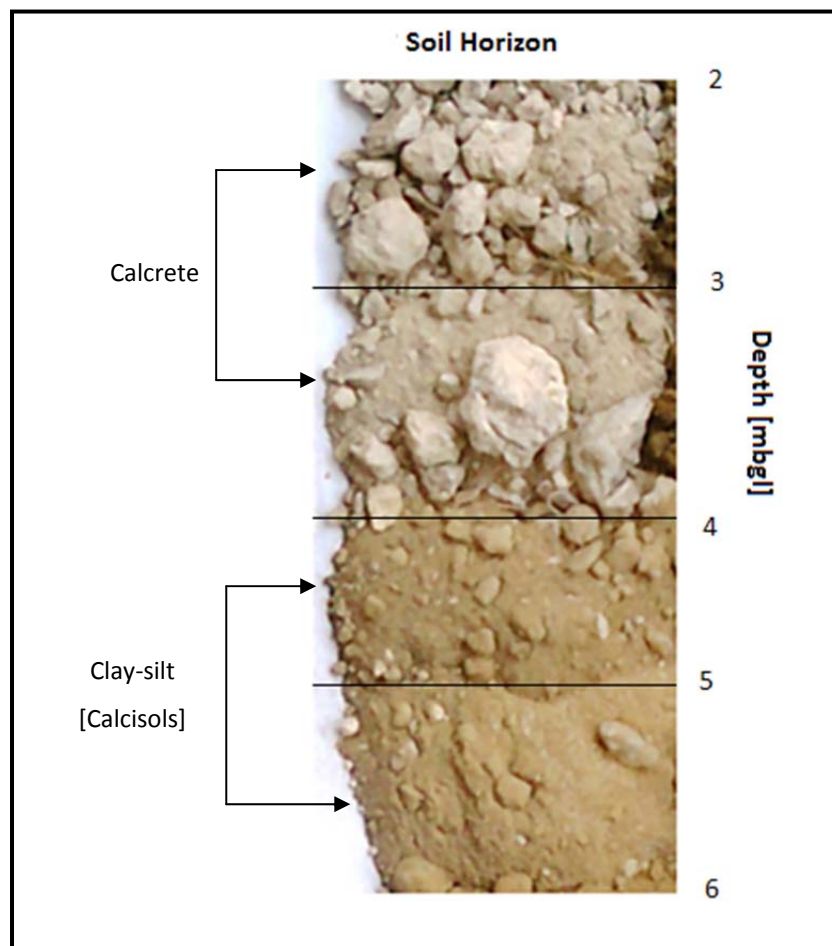


Figure 3-16 A schematic of deep soil horizon showing the clay-silt soils sediments located below the calcrete layer.

3.4.3.2.3 Gravel-sand deposits

The gravel-sand hydrofacies mainly consist of coarse sand and gravel deposited pebbles of assorted formations that represent channel deposits of different depositional environment. Gravel-sand deposits are a common phenomenon along most of the major alluvial rivers. In the European quaternary sedimentary basins, gravel-sand deposits of braided alluvial stream constitute the most extensive and productive aquifer units (Zappa *et al.* 2006). From a geohydrology perspective, detailed understanding of the distribution and connectivity of the most hydraulic zones in an aquifer is critical. The gravel-sand layer mainly comprises of quartz minerals and small to large pebbles of different origins (Figure 3-17) which have been deposited along the river channel. The gravel-sand hydrofacies are typically characterised by high hydraulic conductivities (Table 3).



Figure 3-17 Washed samples of coarse sand and gravel channel deposits that were intersected in BH7 borehole between 6-9 mbgl.

Spatial variation in sizes and packing of gravel-sand aquifer materials at the site is the most important factor contributing towards aquifer heterogeneity. Physical properties of the gravel-sand aquifer materials around a borehole have important influence on the transmissivity determined from drawdown observations made in that borehole. In general, all boreholes at the site intersect the gravel-sand layer except BH5 which is dominated by fine clay-silt. The most likely explanation is that BH5 is located in a former flood plain which is often characterised by fine muddy clay-silt deposits.

3.4.3.2.4 Shale consolidated sediments

The shale hydrofacies (Figure 3-18) which sequentially consists of fresh and hard sediments locally represent the bedrock over which the deposition of unconsolidated materials occurred. The sediments were initially deposited on an impermeable base which is eventually transformed into an aquiclude through diagenesis processes such as: cementation, dehydration and enhanced compaction. The contact plane between the low permeable shale base and grave-sand unconsolidated sediment deposits often forms a potential preferential flow path to groundwater and contaminants.



Figure 3-18 Shale bedrock outcropping at the site river bank.

The total depth of the shale bedrock at the site is not known. The deepest borehole at the site BH1 shows a shale thickness of 34 m from 9-42 mbgl. It is evident based on outcrop mapping results that the shale formation is just one of the units of the local sedimentary bedrocks. In other words, the shale bedrock is most likely underlined by other formation such mudstone, sandstone or siltstones which are typical of the Karoo Supergroup sequence. Groundwater seepage flow has been observed at the contact plane between the shale and overlying unconsolidated sediments at the river bank adjacent to the site.

3.4.4 Delineation of the aquifer system

Based on the understanding gained from the geological characterisation, EC profiling and measured water levels after drilling, an attempt was made to delineate the alluvial channel aquifer system. The main objective of this phase was to develop a geohydrological conceptual framework that could be used for the planning of hydraulic aquifer tests and natural gradient tracer tests. The average main

water strikes that ranges from 5-7 mbgl in both shallow and deep boreholes indicates shallow aquifer conditions of < 10 mbgl. It therefore implies that all boreholes drilled to 12 mbgl fully penetrate the alluvial channel aquifer. Electrical conductivity profiling conducted in 12 m deep boreholes two days after drilling further confirmed the presence of a shallow aquifer system with anomalies between 5-7 mbgl (Figure 3-19). The anomalies are associated with groundwater flow in the gravel-sand main geohydrologic unit.

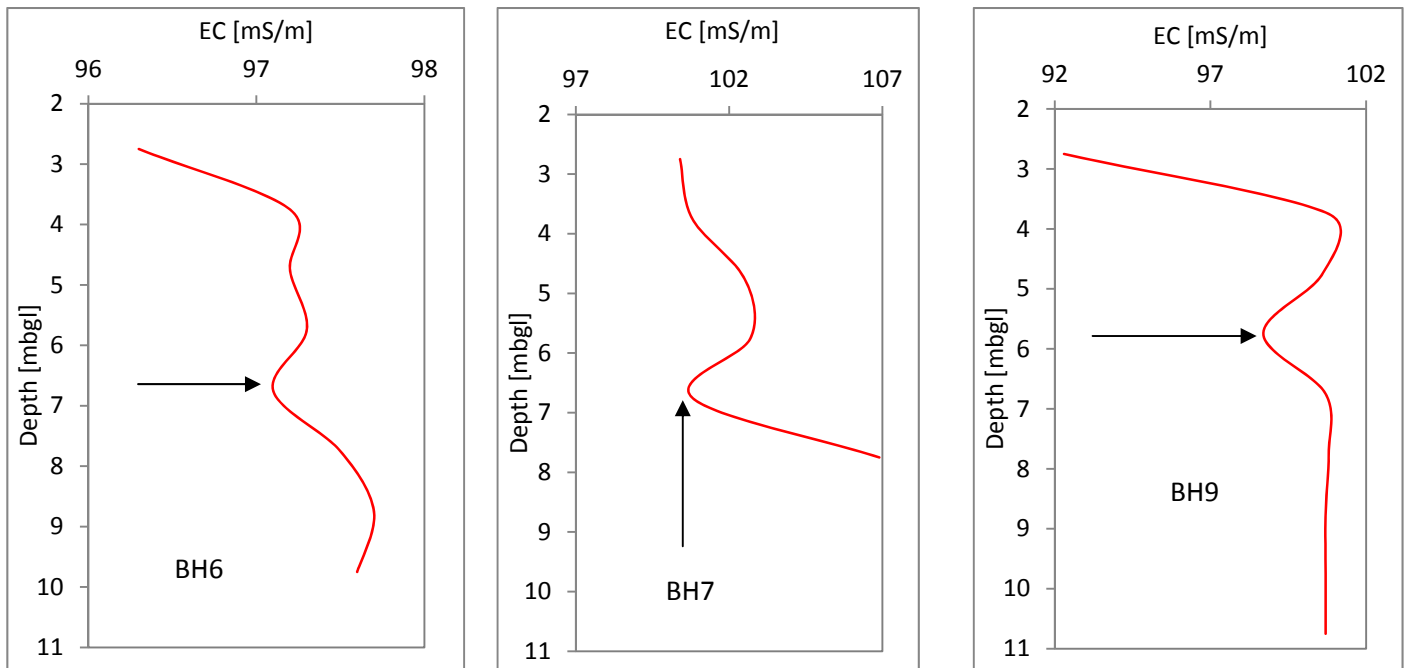


Figure 3-19 EC profiles showing anomalies associated with the groundwater flow in the gravel-sand geohydrologic zone between 5-8 mbgl; the arrow indicates the position of the main anomaly.

The gravel-sand aquifer layer which ranges in thickness between 2-3 m is the main hydraulic aquifer unit. Muddy facies of clay-silt overlies the gravel-sand aquifer unit thus potential creating semi-confining conditions. It is important to acknowledge the contribution of the low permeable shale bedrock to the formation of the shallow alluvial channel aquifer system at the site. The river bedrock practically forms the deposition floor for the unconsolidated sediments and the contact plane has become a preferential flow path for groundwater. Groundwater discharge, from the alluvial channel aquifer occurs through the seepage face that has been created at that contact plane.

Based on the groundwater levels measured in BH1, BH2 and BH4 boreholes after construction, it can be inferred that a deep aquifer system of low permeability exists on the site. However on the other hand, groundwater chemistry (Chapter 4) and stable isotopes analysis (Section 8.3 of chapter 8) does not show any difference between the groundwater in these three boreholes and the rest of the

boreholes suggesting the water is just coming from the same aquifer system. Further investigations are therefore required to determine the nature of this deep aquifer system.

3.5 Summary

Outcrop mapping and percussion drilling of boreholes were used as complimentary techniques to identify and describe the subsurface lithology of the site. In general, outcrop mapping involves the identification and description of the rock formations and minerals that are exposed to the earth's surface. Patches of calcrete outcrops were observed in the vicinity of the case study site. A total of nine and six boreholes were drilled into the alluvial channel aquifer and terrestrial aquifer respectively. Analysis of borehole geological logs indicates that site is composed of calcrete, clay-silt, and gravel-sand unconsolidated sediments overlying the impermeable shale bedrock. The gravel-sand material which is semi-confined between the upper calcretes and lower aquitard shale bedrock is conceptually the site's main geohydrologic unit. The shallow gravel-sand alluvial channel aquifer is conceptually underlined by a low permeable deep aquifer system in the shale formation. Spatial variation in sizes and packing of gravel-sand aquifer materials across the site is the most important factor contributing towards aquifer heterogeneity.

The next chapter gives a detailed description and analysis of infiltration, slug and aquifer tests conducted in the heterogeneous alluvial channel aquifer.

4 HYDRAULIC TESTS IN A TYPICAL ALLUVIAL CHANNEL AQUIFER

Hydraulic tests were designed to determine the hydraulic and storage properties of the heterogeneous alluvial channel aquifer. The chapter gives a detailed description and analysis of infiltration, slug and aquifer tests conducted in the heterogeneous alluvial channel aquifer. As a primary requirement for hydraulic tests investigation, natural principal groundwater flow direction in the main aquifer was determined based on real surveyed elevations. Infiltrations tests were conducted along the riparian zone to assess the potential contribution of piston and preferential recharge mechanism into the alluvial channel aquifer. A combination of single-borehole and multiple-borehole test was performed to evaluate and assess the behaviour, hydraulic and storage properties of a typical alluvial channel aquifer. A good understanding of the behaviour, hydraulic and storage properties of the alluvial channel aquifer is critical for; groundwater resource exploitation, GW-SW interactions studies, protection and management. Figure 4-1 shows the location of the boreholes drilled into the alluvial channel aquifer and terrestrial aquifer.

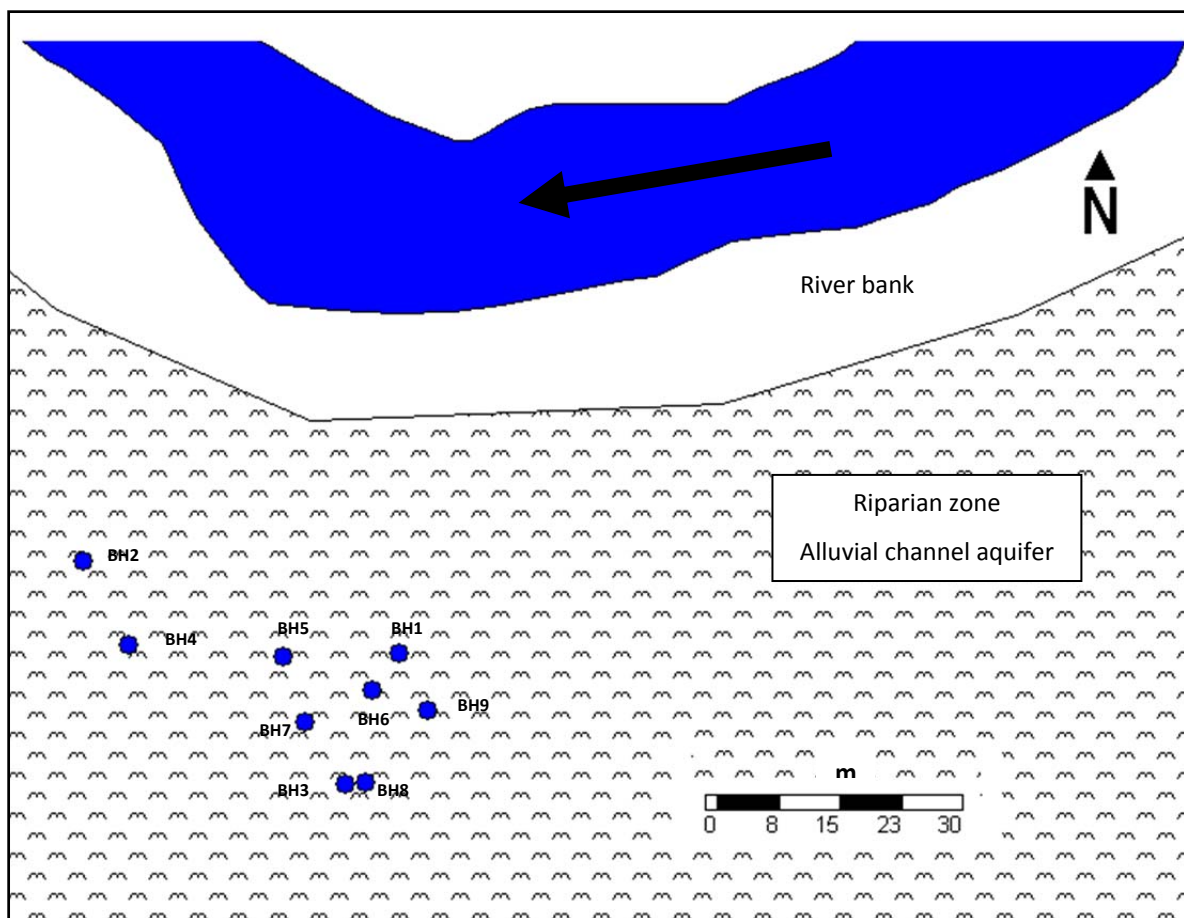


Figure 4-1 Location of the boreholes drilled into the alluvial channel aquifer.

4.1 Field measurements

4.1.1 Groundwater flow directions

Determining the natural principal groundwater flow direction is important for contamination investigations and GW-SW interaction studies. In order to understand the migration of contaminations in aquifers and make assessments about potential receptors under natural conditions, the natural principal groundwater flow direction should be precisely determined. Alluvial channel aquifers interact with stream or river channels in a number of ways. In situations where the alluvial channel aquifer discharges into stream/river surface waters, the determination of natural principal groundwater flow direction is essential for delineating the discharge zones. Measurement of natural hydraulic gradients is however a prerequisite to the determination of natural groundwater flow direction. Figure 4-2 shows the natural principal groundwater flow directions that were determined using the three groundwater level point method (Domenico and Schwartz 1990). See the location of the boreholes used for determining the principal groundwater flow direction in Figure 4-1 and Figure 3-3. It is important to note that the natural groundwater flow direction in the alluvial the alluvial was determined using the boreholes drilled into the shallow gravel-sand main aquifer. It was assumed that groundwater flow in the conceptualised deep aquifer system would follow the same trend.

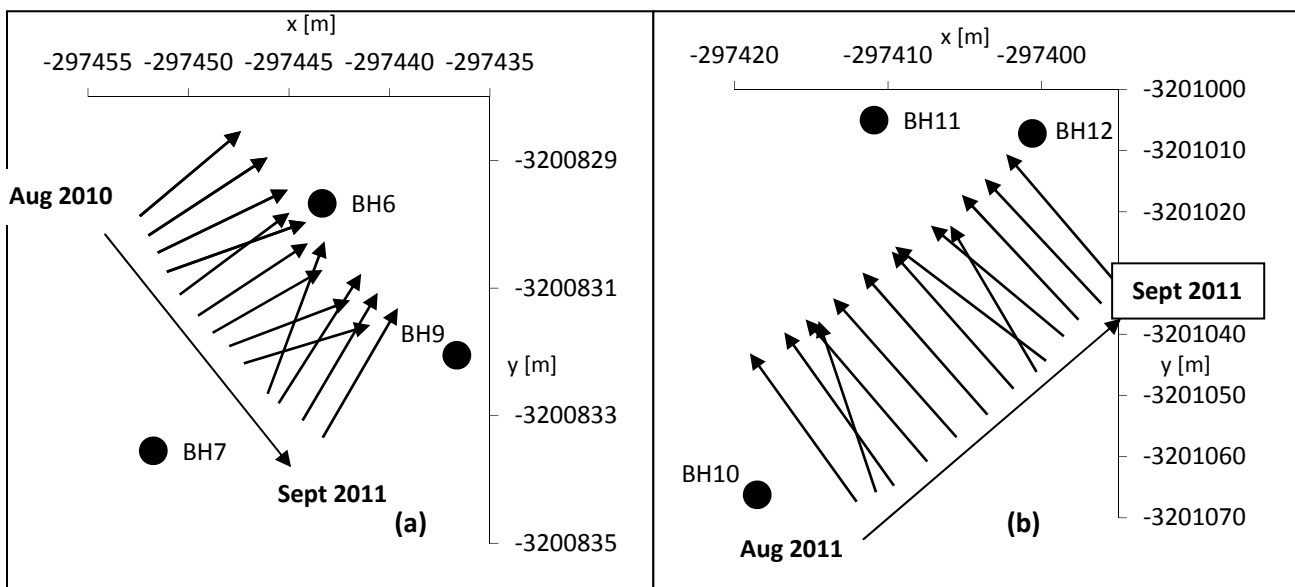


Figure 4-2 Time series principal natural groundwater flow directions monitored for 13 months (August 2010-September 2011) in the: (a) alluvial channel aquifer and (b) terrestrial aquifer; each arrow shows the principal flow direction for a specific month.

The natural groundwater flow directions in alluvial channel main aquifer (a) and terrestrial aquifer (b) show some variation with time (Figure 4-2). This variation can be mainly attributed to the differences in respond time of the boreholes to recharge and the scale effect. Boreholes are bound to respond differently to recharge events depending on their connectivity and proximity to recharge sources and pathways. The closest and more connected borehole to recharge sources and pathways has quicker responds to rainfall events irrespective of whether its located up-gradient or down-gradient of the natural principal groundwater flow direction. This phenomenon is temporary, but it can potentially offset the natural hydraulic gradient. When treating the two aquifers as separate entities, they are completely characterised by different flow directions despite that they are just < 500 m apart. In general the results reflect the significance that subsurface heterogeneity has on the spatial variation of hydraulic properties. The results also serve to indicate that groundwater flow properties in alluvial channel aquifers are greatly influenced by the spatial variation of channel deposits.

The trend however changes at a relatively large field local scale. When a combination of boreholes from both aquifers is considered, the principal groundwater flow direction remained fairly constant (Figure 4-3) which is an indication of the potential averaging effect of the subsurface heterogeneity on hydraulic properties as the scales of investigation increases. At a large scale, the relative difference in the groundwater levels between boreholes which are located far apart remains fairly constant irrespective of different recharge events and mechanisms. A constant principal groundwater flow direction is therefore a reflection of a constant hydraulic gradient between BH10, BH14 and BH7 boreholes throughout the monitoring period.

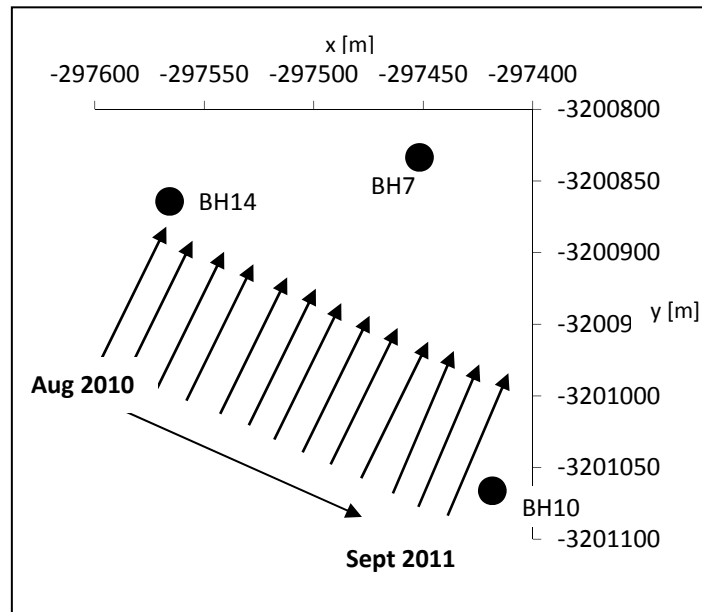


Figure 4-3 Time series principal natural groundwater flow directions monitored for 13 months (August 2010-September 2011) between the alluvial channel aquifer and terrestrial background aquifer; each arrow shows the principal flow direction for a specific month.

Figure 4-4 shows the groundwater level contours, vectors and the natural principal groundwater flow direction derived from the time series water levels measured from August 2010 to September 2011 in the shallow main alluvial channel aquifer (Appendix 3.1). The contours show the complete path of groundwater level flow lines from the terrestrial aquifer to the alluvial channel aquifer.

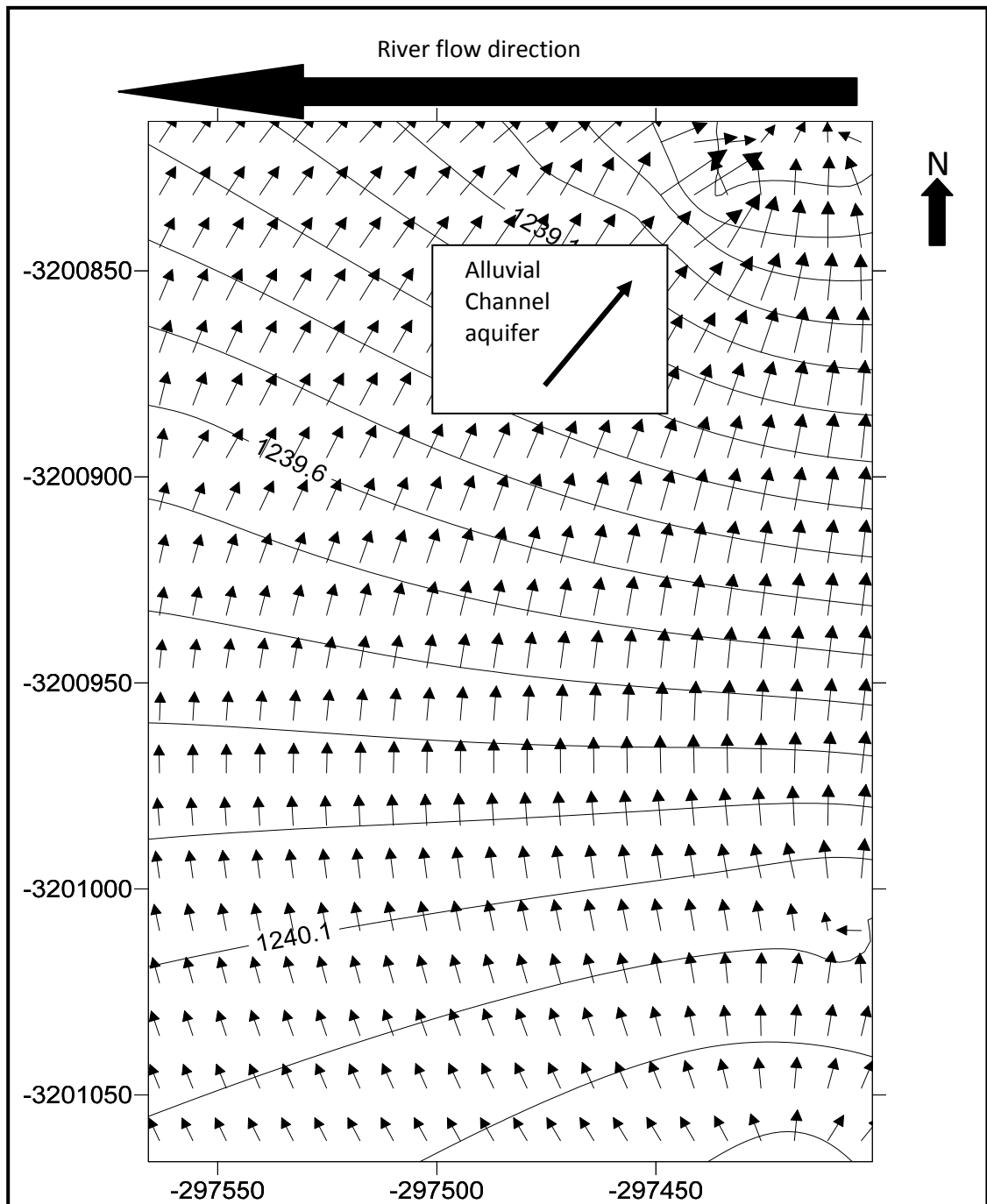


Figure 4-4 Groundwater level contours (mamsl) and vectors on the study site showing groundwater flow directions; the insert shows location of the study area on the alluvial channel aquifer; the arrow in the insert shows the natural principle groundwater flow direction as determined using water level elevation from various combinations of borehole triangles.

The groundwater generally flows from the south to north east at the site. The measured groundwater flow direction at the site is in contrast to the schematic that is often used to represent the groundwater flow direction towards a gaining river in literature (Figure 4-5). Along a gaining stream, groundwater is principally expected to flow in the same direction as the stream. The

observed groundwater flow direction at the study site shows the influence that subsurface heterogeneity has on hydraulic properties.

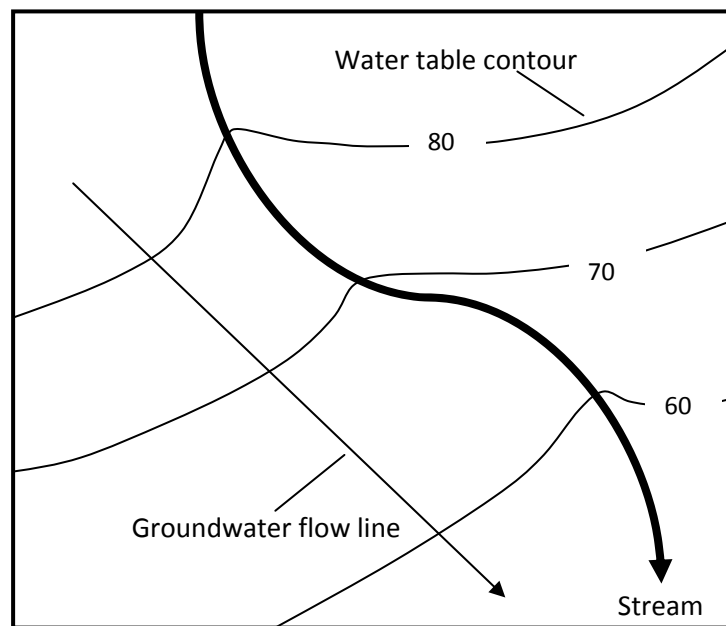


Figure 4-5 Idealized schematic used in literature to show groundwater flow direction along a gaining stream (Adapted from Winter 1998).

Naturally, groundwater flow is driven by the hydraulic gradient. Gradient can be created due to a number of factors and these include surface topography, natural discharge and abstraction. Surface topography and aquifer discharge are two important factors that are potentially driving the natural groundwater flow direction at the study site. Towards the riparian zone, the surface topography rapidly increases on the western side thus acting like geohydrology impermeable boundary to divert the groundwater flow in the north-east direction (Figure 4-4). The alluvial channel aquifer has been discharging groundwater at the seepage face for the last 50 years and it potentially act as an abstraction borehole thus forcing groundwater to flow towards the sink.

4.1.2 Infiltration tests

Infiltration tests were conducted on the riparian zone and terrestrial land with the objective of assessing the recharge mechanisms of the two aquifers. The infiltration tests were conducted in the soil horizons (0-1 mbgl) of the riparian zone and the terrestrial land. Theoretically the infiltration rates between the two lands surface is expected to vary due to different soil and vegetation cover characteristics. It was therefore vital to compare the infiltration rates between the two land surfaces and relate to their recharge mechanisms and processes.

A discussion of the infiltration tests that were conducted in the riparian zone is presented in this section. Infiltration tests in the terrestrial aquifer were conducted by Leketa (2011) under the same WRC bulk flow project. Infiltration tests were conducted on 4 sites (Figure 4-6) on the riparian zone. The infiltration holes were designed to test different sections of the unsaturated zones. Each infiltration site consisted of 3 holes of 30 cm, 60 cm and 100 cm deep respectively. The analysis of results was based on the inverse auger-hole method (Oosterbaan and Nijland 1994). In general, the following procedure was employed:

1. Identification of auguring sites and recording of coordinates.
 2. Hand auguring of the test holes.
 3. Pouring water in the holes and recoding the head.
 4. Measure the water level drop in the test holes until saturated condition is approached.
- Saturated conditions are approached when the rate of change of head nears a constant rate (See appendix 1.1 for complete procedure of the inverse whole method).

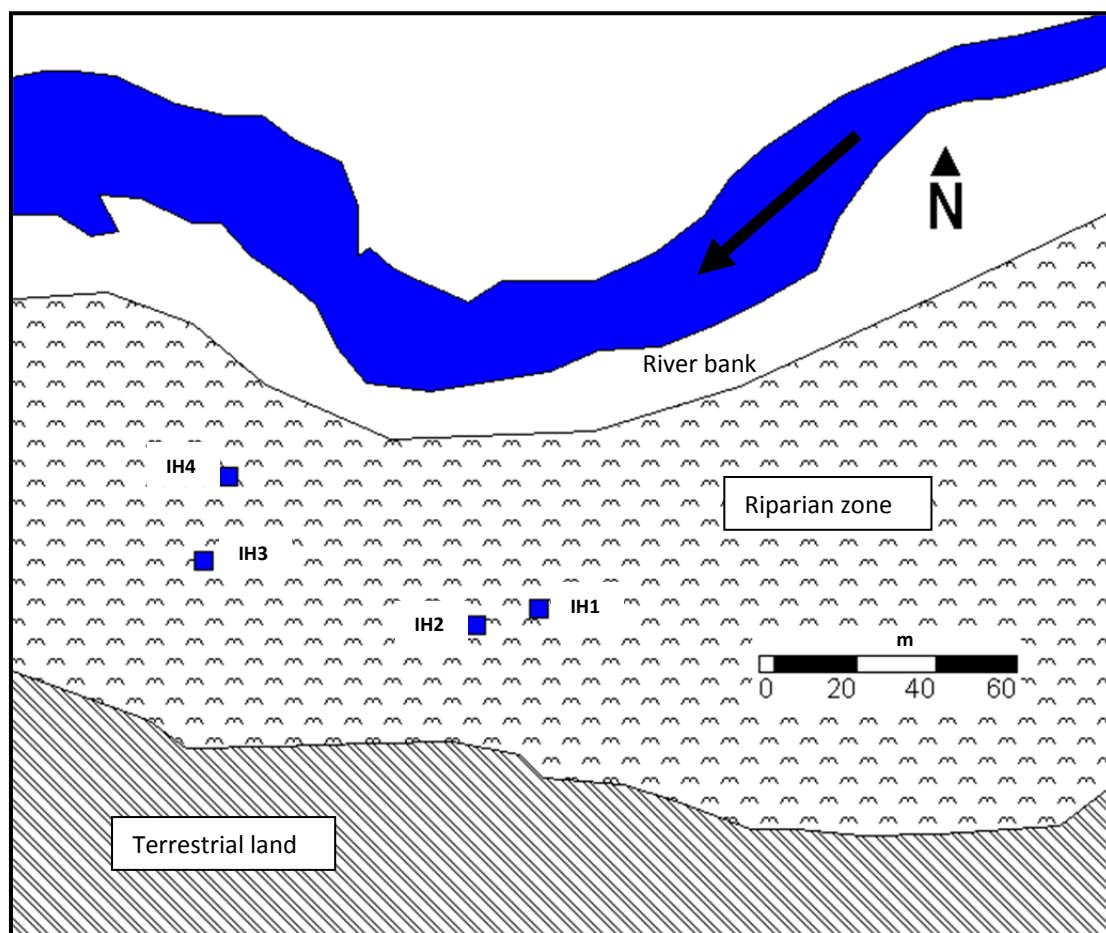


Figure 4-6 Location of the infiltration sites on the riparian zone of the alluvial channel aquifer, IH represent infiltration hole.

4.1.2.1 Infiltration rates

Table 4 shows the saturated hydraulic conductivities of the infiltration fronts determined on the riparian zone. Sites IH3 and IH4 have higher saturated hydraulic conductivity infiltration rates in excess of 1 m/d. The two sites are located on areas with dense vegetation where organic matter, tree rooting system, cavities and holes created by termites and burrowing animals are the key contributing factors. Low infiltration rates of less than 0.01 m/d were measured on the terrestrial land (Leketa 2011). The soil structure is generally poor and consists of fine clay calcareous soils resulting in low permeability. The complete set of infiltration rates calculations can be found in the appendices data disc.

Table 4 Average saturated hydraulic conductivities of the infiltrating front determined on the riparian zone.

Site name	Depth interval [cm]	K[m/s]	K[m/d]
IH1	0-30	6.E-06	0.5
	30-60	5.E-06	0.4
	60-100	1.E-06	0.1
IH2	0-30	7.E-06	0.6
	30-60	4.E-06	0.4
	60-100	3.E-06	0.3
IH3	0-30	1.E-05	0.9
	30-60	3.E-05	2.6
	60-100	2.E-05	1.7
IH4	0-30	1.E-05	1.2
	30-60	2.E-05	2.1
	60-100	2.E-05	1.3

Riparian zones are typically characterised by high infiltration rates (Bharati *et al.* 2002). High infiltration rates along the riparian zones can be mainly attributed to high vegetation density. Lange *et al.* (2008) found that dense vegetation enhances infiltration rates through preferential pathways created by tree roots. High infiltration rates along the riparian zones have important implications for increasing groundwater recharge. Riparian vegetation also assists in the buffering of nitrogen contamination (Mayer *et al.* 2005).

4.1.3 Slug tests

A total of 9 slug test were performed in the boreholes drilled into the alluvial channel aquifer with the objective of estimating borehole yield and hydraulic parameters in each borehole. The Bouwer and Rice method (1976) was used to estimate aquifer hydraulic conductivity and transmissivity from

the slug test field data. Borehole yield estimates were estimated from the log-log plot of borehole yield against recession time (Vivier *et al.* 1995).

4.1.3.1 Borehole yields and hydraulic parameters

Table 5 shows borehole yield and hydraulic parameters estimated from the slug recession time. High borehole yield estimates and hydraulic properties are expected for BH7, BH6, BH9 and BH3 boreholes because they fully penetrate the gravel-sand material of typically high hydraulic conductivity. Borehole BH5 is drilled into a tight clay-silt formation which typically has low permeable properties and that explain the low estimated borehole yield and hydraulic conductivities. BH8 was drilled 6 m depth into the calcrete and clay-silt and does not penetrate the gravel sand. Hence low hydraulic properties are expected. The time and drawdown data from the slug test can be found in the appendices data disc.

Table 5 Borehole yield and hydraulic conductivity estimates values determined from the slug test for the boreholes drilled into the alluvial channel aquifer.

Borehole name	r_w [m]	Depth [m]	Recession time [s]	Yield [l/s]	K [m/d]	T [m ² /d]
BH1	0.08	42.00	113.00	0.50	8.00E-04	0.01
BH2	0.08	24.00	100.00	0.70	5.00E-04	0.01
BH3	0.08	24.00	23.00	2.00	9.00E-03	0.09
BH4	0.08	24.00	106.00	0.60	5.00E-04	0.01
BH5	0.08	12.00	30.00	1.80	1.80E-02	0.07
BH6	0.08	12.00	13.00	4.00	5.00E-02	0.20
BH7	0.08	12.00	4.00	9.00	2.00E-01	0.80
BH8	0.08	6.00	95.00	0.70	4.00E-03	0.02
BH9	0.08	12.00	17.00	3.00	3.00E-02	0.12

Low borehole yields and hydraulic parameters estimated for BH1, BH2 and BH4 are a reflection of low permeability properties of the deep aquifer system. It should however be mentioned that the borehole construction technique used on the site might have contributed to low hydraulic properties being measured from slug tests. The boreholes perforated casings were installed without placing gravel packing between the casing and formation. The contact area between the casing and formation can be too tight and has the potential to retard the recession of water into the aquifer during the slug test leading to very low hydraulic parameters being estimated. In general all the estimated hydraulic parameters from slug tests are too low to be true when compared to parameters obtained from the constant rate aquifer testing. Unlike aquifer pump testing which can assess the contribution of the main hydraulic zones, slug test can only assess the small area in the vicinity of the borehole. It can therefore be concluded that; slug test was not a successful tool for

determining hydraulic parameters of the alluvial channel aquifer. In alluvial channel aquifers, slug tests should be rather performed in open (uncased) boreholes.

4.1.4 Aquifer pump testing

Aquifer pump test were designed to assess the hydraulic and storage properties of the shallow main aquifer and deep aquifer of the alluvial channel aquifer system. The drawdown against time that was measured during the aquifer tests can be found in the appendices data disc.

4.1.4.1 Shallow main aquifer system

Based on the geological understanding, it was conceptualised that the shallow aquifer that fully penetrates the gravel-sand layer is the main aquifer of the site. Aquifer tests were therefore performed in BH3, BH5, BH6, BH7 and BH9 to assess the hydraulic properties of the shallow alluvial channel main aquifer system. The boreholes fully penetrate the gravel-sand aquifer bottom layer and thus they ideally meet the Cooper and Jacob (1946) requirement of full aquifer penetration.

4.1.4.1.1 Aquifer pump test design

4.1.4.1.1.1 Selection of constant pumping rate (Q)

An abstraction rate of 0.5 l/s was used for testing the alluvial channel aquifer. The conservative approach was taken to avoid the potential dewatering of the alluvial channel as this could potentially disturb the natural groundwater conditions and affect the riparian ecosystems. Maintaining of natural groundwater flow conditions was very important for protecting of the riparian ecosystem and the performance of NGTT. A question was however raised on whether the rate was good enough for a constant rate aquifer testing. But maybe the biggest question should be what is a good enough abstraction rate for aquifer tests and under what circumstances can it be regarded as good enough? The starting point should be to distinguish between aquifer and pump testing because the choice of abstraction rate is greatly influenced by the objective of the test. In other words, the aim of the test should be a strong determinant when selecting an appropriate abstraction rate.

Aquifer tests in this study were conducted to determine hydraulic and storage aquifer parameters. Hydraulic and storage parameters are mainly governed by the physical properties of the aquifer material in particular grain size and sorting and not by the abstraction rate during the test. Aquifer hydraulic conductivity and storage are inherent aquifer properties which in an average homogeneous aquifer should remain constant irrespective of the abstraction rate. On the other hand, pump testing is aimed at obtaining information on the performance and efficiency of the

production borehole. It is therefore important to fully stress the aquifer during pump testing in order to assess the borehole yielding capacity which is essential for determining the sustainable yield.

Besides, the analysis of drawdown data is based on analytical equations which in principal fix the inherent aquifer properties that define hydraulic and storage aquifer parameters. The main point here is that unlike a pump test, for aquifer testing any abstraction rate that enables measurable drawdown to be observed for a reasonable time period without dewatering the aquifer is good enough. The question of what drawdown should be regarded as measurable is probably answered by resolution of the monitoring equipment. Unlike long ago when deep meters (resolution of 1 cm) was the standard equipment for measuring groundwater levels, nowadays level loggers offers great resolution that can even measure 1 mm change in drawdown. Van Tonder *et al.* (2001) recommended a maximum of eight hours in the guidelines for constant rate pumping tests in typical Karoo fractured-rock aquifers.

4.1.4.1.1.2 Equipment set-up and measurements

Water levels in the pumping and observation boreholes were monitored using Gold level loggers. The level logger effectively measures the pressure head above the logger instrument per set interval time. The drawdown is calculated by subtracting all the subsequent heads measured during the test from the initial head. The Gold level loggers have an accuracy of 0.1 cm and a resolution of 0.001. In general, level loggers offer great flexibility in selecting the monitoring intervals, allowing measurements in pumping and observation boreholes to be taken simultaneously and also in reducing the manual work. Manual measurements were also taken on a twenty minute interval to affirm the level logger readings. The interpretation and analysis of the aquifer test results aimed at selecting an appropriate aquifer model and determining of aquifer parameters is presented in the preceding sections.

4.1.4.1.1.3 Aquifer model selection

Aquifer tests are mainly conducted to determine aquifer hydraulic and storage properties; however before the determination of these parameters, one has to define the aquifer model for which an appropriate method can be selected to determine aquifer parameters. Analysis of the drawdown behavior coupled with geological understanding is vital for selecting the aquifer model that can represent the physical system. The selected aquifer model also forms the basis for groundwater flow and GW-SW interactions investigations. It is therefore critical to utilize the available tools, techniques and evidence to select the best appropriate aquifer model. This section of the study describes and illustrates how qualitative and quantitative analysis of drawdown can be used to

select an aquifer model. The alluvial channel aquifer is classified as a semi-confined aquifer based on the subsequent evidence.

4.1.4.1.1.4 Pseudo-steady state conditions

The drawdown measured in the 12 m deep boreholes that fully penetrates the alluvial channel aquifer displays a pseudo-steady state phenomenon after 50 minutes of pumping (Figure 4-7). Theoretically the water levels in the piezometers will never stabilise to a real steady state even after long pumping periods. When such a phenomena occurs, the concept of pseudo-steady state is used instead of steady state. An aquifer is said to be in pseudo-steady state when the hydraulic gradient has become constant, i.e. when the drawdown against time curves of different piezometers are parallel (Figure 4-7).

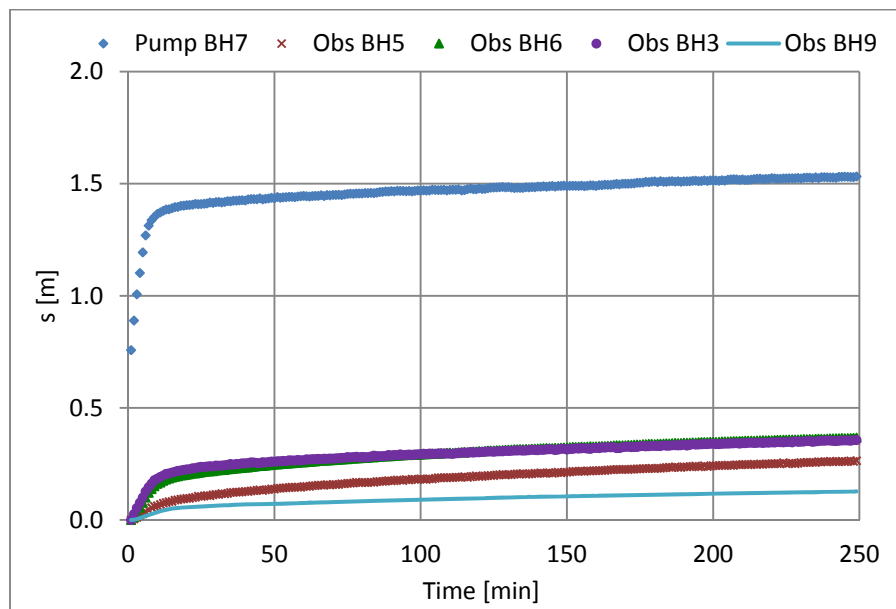


Figure 4-7 Parallel drawdown time plots showing the pseudo-steady state conditions from 50 minutes to the end of the test; borehole BH7 was being pumped and observations were made in BH3, BH5 and BH6 boreholes.

There is no evidence to show that the aquifer is being recharged by an external source and as a result the cone of depression should continue to expand and deepen at a slow rate. The slow expansion and deepening in drawdown reflect the high horizontal flow characteristics of the gravel-sand aquifer layer under semi-confining conditions. During the pumping period, significant quantities of groundwater are released from the gravel-sand and the clay-silt sediments.

4.1.4.1.1.5 Cone of depression movement

In general, the growth of the cone of depression of a borehole located in a water-table aquifer is slow in comparison to that of an artesian or semi-confined aquifer (Norvitch 1960). However, the quick spread of the depression cone from the pumping boreholes (Table 6) at the study area is a reflection of substantial horizontal hydraulic conductivities in the semi-confining gravel-sand aquifer layer. The rate of spread of the depression cone was calculated by dividing the observation distance (r) with the response time. The response time defines the time it takes for quantifiable drawdown to be measured in the observation bore since the start of the pumping. The analysis assumes that the cone of depression spreads linearly and uniformly through the high hydraulic conductivity gravel-sand materials from the pumping to observation boreholes.

Table 6 Spread rate of movement of the depression cone from the pumping boreholes to observation boreholes calculated based on the response time and observation distance (r).

Pumping borehole	Observation (Obs) borehole	r (m)	Respond Time [min]	Spread rate of depression cone [m/min]
BH7	BH3	9.00	2.00	4.50
BH7	BH5	10.00	2.00	5.60
BH7	BH6	10.00	1.00	10.00
BH6	BH7	10.00	2.00	5.00
BH6	BH3	11.90	3.00	4.60
BH9	BH8	9.60	2.00	4.80
BH9	BH6	11.50	2.00	5.80
BH9	BH7	14.70	2.00	7.40

The average response speed of the depression cone seems extremely too high gives a good measure of high horizontal flow in response to the initial induced pressure. The quick spread in the cone of depression can be only attributed to the high pressure response through the high hydraulic conductivity semi-confined gravel-sand layer.

4.1.4.1.1.6 Aquifer lithology

Site geology logs show evidence of tight clay-silt sediment material which can result in semi-confining conditions at the upper boundaries of the gravel-sand alluvial channel aquifer (Section 3.4.2.1.3, Figure 3-7). The upper bounding layer of the aquifer comprises of calcrete and clay-silt deposits and these can form semi-confining conditions. However water table conditions locally exist in the absence of low permeable upper confining aquifer material.

4.1.4.1.1.7 Derivative flow characterization

Derivative drawdown diagnostic plots are very sensitive to small changes in drawdown, thus can be easily used to identify the effects of geohydrological boundaries and establishment of various groundwater flow regimes (Samani *et al.* 2006). Typical flow regimes that can occur during alluvial channel aquifer testing include Theis, wellbore storage and radial flow conditions. In general, when derivative drawdown diagnostic plots are correctly applied, they enhance the understanding of drawdown behavior and the aquifer model development.

The drawdown derivative plot on Figure 4-8 shows the typical aquifer behaviour that characterised pumping and observation boreholes that fully penetrates the gravel-sand aquifer layer during the four hour pumping test. Derivative diagnostic plots for the boreholes that were observed during the pumping of BH7 are placed in Appendix 1.2. In general, the duration of the radial acting flow (RAF) period varies between observation boreholes as a function of aquifer heterogeneities.

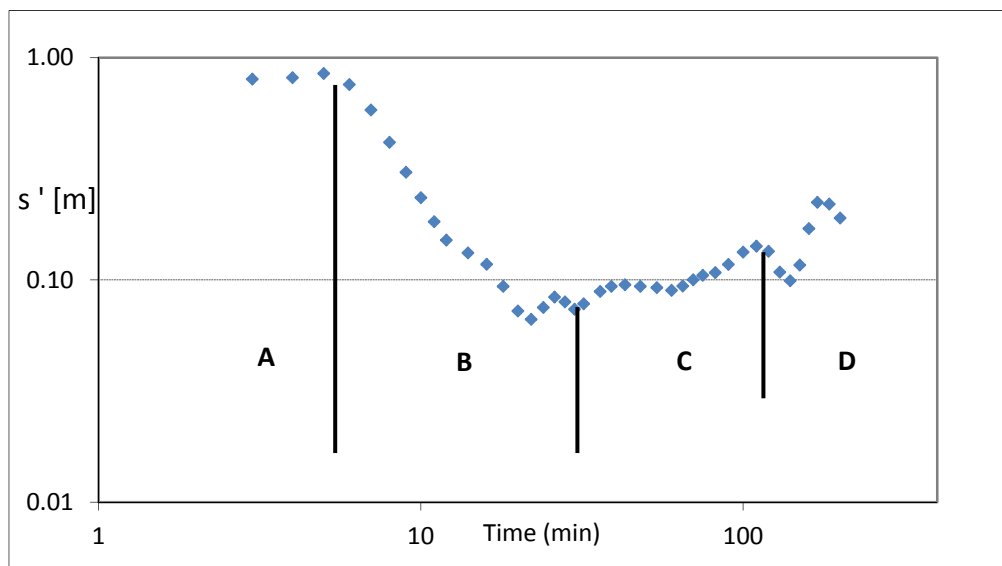


Figure 4-8 Derivative drawdown plot showing early time Theis response (A), transition period (B), RAF (C) and impermeable boundary effects flow characteristics during the abstraction from borehole BH7.

The drawdown against time derivatives analyses of the pumping and observation boreholes during the four hour aquifer testing shows four distinct groundwater flow characteristics (Figure 4-8); typical Theis response (A), transition period from the initial Theis respond to RAF (B), RAF in the gravel-sand layer (C) and the river single impermeable boundary (D).

The **transition period (B)** from the initial Theis response to the total system response (RAF) is characterised by the dip in the drawdown derivative. The dip in the drawdown derivative after the initial typical Theis curve is due to the rapid release of water from the gravel-sand storage thus appears as a recharge boundary. In general, the dip in the derivative plot after well bore storage is often attributed to the double porosity behaviour or recharge boundary (Van Tonder, 2001a). However, in this instance the dip reflects the quantitative groundwater supply from the gravel-sand layer. After the initial Theis response, the aquifer starts to experience full stress from the pumping effects and the release from storage is swiftly increased. There is no significant well bore storage because of the high transmissivity values of the gravel-sand layer result in the rapid spread of pressure as evidenced by the quick spread of drawdown to the observation boreholes (Table 6).

Radial acting flow (C) is dominated by the groundwater release and flow in the high transmissivity gravel-sand aquifer layer. The RAF period in all boreholes occurred between 20 and 65 minutes and is identified by a horizontal line (Spaine and Wurster 1992) on the derivative drawdown plot. Fitting of the straight line on a semi-log plot at the RAF period enables estimation of aquifer transmissivity and storage properties using the Cooper and Jacob straight line method (1946).

The approach of the **single river impermeable boundary (D)** signifies the end of RAF period. The approach of the impermeable boundary is marked by an increase of the drawdown derivative from 80 minutes to end of the four hour pumping period. The single impermeable boundary only acts to reduce the total inflow of water into the borehole as indicated by the reduced transmissivity values (Table 7).

It is important to note that the drawdown derivative plot shows a fluctuating up and down trend and this implies that there is gain and loss of T within the aquifer system during the testing period. The loss and gain of the T during the pumping can be attributed to the influence of lateral geological heterogeneities in the aquifer. The geological properties of the aquifer spatially vary across the site such that as the cone of depression spreads, it passes through material of various hydraulic conductivities. In other words, the drawdown observed in the pumping borehole reflects the hydraulic properties of different materials through which the water travels towards the borehole.

4.1.4.1.1.8 Groundwater flow phases

Field aquifer pump test results demonstrate three major groundwater flow characteristics of the alluvial channel aquifer that precludes its classification as a confined or semi-unconfined aquifer is presented in this section. In general, the drawdown behaviour of the pumping and observation

boreholes that fully penetrates the gravel-sand main aquifer layer are characterised by three distinct flow phases. The duration of the flow phases varies between boreholes as a function of aquifer heterogeneities. The transition period is not visible on the semi-log drawdown plots in comparison to the much sensitive derivative plots. Figure 4-9 below shows three distinct flow phases that characterise drawdown trends in the observation boreholes that fully penetrates the gravel-sand aquifer layer during the four pumping period. Semi-log graphs for BH6, BH5, BH3 and BH9 boreholes observed during the pumping of BH7 have been placed in Appendix 1.3.

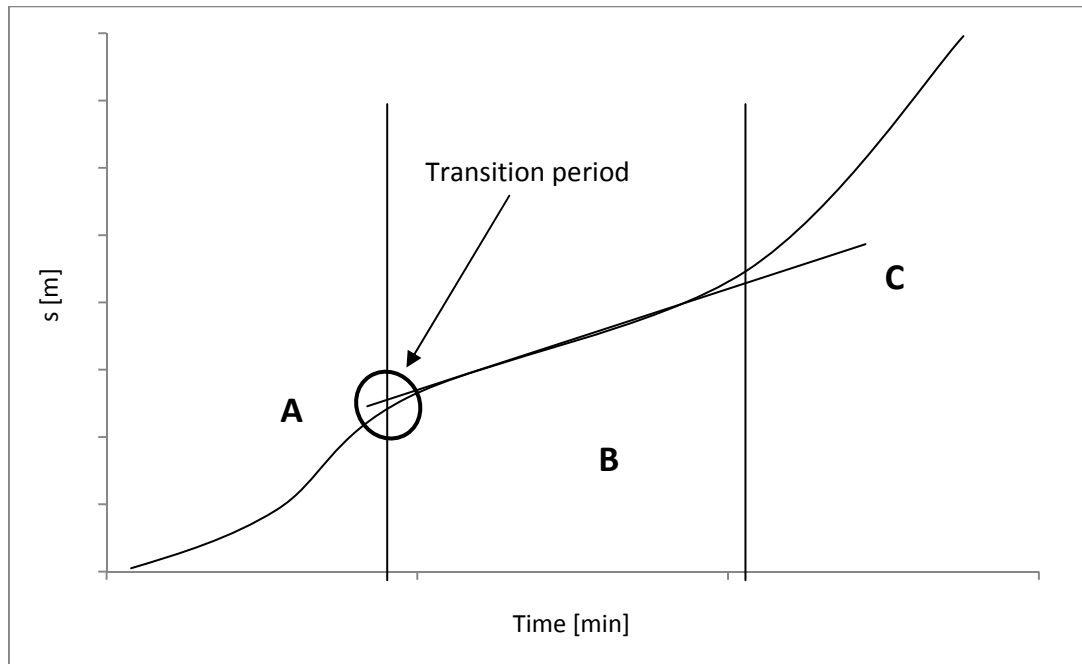


Figure 4-9 Semi-log plot of drawdown (linear scale) against time (log scale) showing three distinct flow phases (A, B and C) during a four hour aquifer test.

Flow phase A

During this initial stage of pumping the semi-confined aquifer conforms to confined aquifer behavior (Theis response). During this flow phase, free water is instantaneously released from the aquifer storage. The instantaneous quick release of groundwater from the gravel-sand layer storage is mainly attributed to aquifer compaction and groundwater expansion. Flow phase A cannot be classified as a well bore storage because observation boreholes also give the same type of response.

Flow phase B

The phase is mainly characterised by horizontal groundwater flow from the gravel-sand aquifer material. The gravel-sand aquifer material has well sorted grains which facilitate instantaneous release of water due to pressure induced from pumping. It is easier to draw water from the gravel-

sand material than from the calcretes and clay-silt overlying sediments, although the later has high storage properties.

Flow phase B should not be confused with the contribution of delayed or gravity drainage which is typical of water table (unconfined) aquifers. In unconfined aquifer conditions, the delayed respond is noted by flattening after the initial Theis respond. Although there is some deviation from the confined straight line plot, the current plots are very far from flattening (Appendix 1.3). Flow is entirely horizontal in this semi-confined gravel-sand material unlike in unconfined conditions where vertical drainage dominates the groundwater flow characteristics.

Flow phase C

Flow phase C occurs because the river bank act as an impermeable boundary that restrict the areal extend of the alluvial channel aquifer towards the river. Because of the impermeable boundary effect, the supply of water into the borehole is reduced. This effect will however only reduce the overall aquifer supply into the boreholes because the other sides of the aquifer are still able to contribute to the flow towards the pumping borehole. The transmissivity values in flow phase B are reduced by half in flow phase C (Table 7) show the influence of the approaching single impermeable boundary effect.

Table 7 Transmissivity values determined for flow phases B and C when BH7 was being pumped and observations made in BH3, BH4, BH5 and BH9 boreholes.

Borehole name	r [m]	Flow phase B T (m ² /d)	Flow phase C T (m ² /d)
Pump BH7	0.00	89.00	47.00
Obs BH3	9.00	98.00	51.00
Obs BH5	10.00	81.00	44.00
Obs BH6	10.00	93.00	39.00
Obs BH9	14.70	100.00	45.00

4.1.4.1.1.9 Aquifer parameters

Aquifer parameters can be determined from both pumping and observation boreholes' drawdown data. For the single-borehole aquifer tests, drawdown data from the pumping borehole is only used for determining aquifer transmissivity. In general, single-borehole aquifer tests provide good estimates of transmissivity where high cost and insufficient equipment hinders the performance of multi-borehole aquifer tests. Single-borehole aquifer tests are frequently analyzed with the Cooper-Jacob equation (1946) due to its simplicity (Halford 2006). Multi-borehole aquifer tests

involve the use of observation boreholes to determine aquifer transmissivity and storativity. The Cooper and Jacob straight equation (1946) was selected to determine the alluvial channel aquifer parameters based on the premise that the channel aquifer fulfills the following ideal requirements:

- The 12 m deep boreholes fully penetrate the alluvial channel aquifer layer.
- When stressed, the alluvial aquifer is dominated by horizontal groundwater flow towards the abstraction borehole in the gravel-sand aquifer layer. The dominant groundwater flow in the stressed aquifer is horizontal.
- The maximum drawdown in all observation the boreholes are less 30 cm. This implies that the saturated thickness of the aquifer did not vary significantly during test and is close to a constant.
- Flow phase B is characterised by radial acting flow (RAF) as indicated by derivative and semi-log plots (Section 4.1.4.1.1.7 and 4.1.4.1.1.8) respectively. Applying the Cooper and Jacob solution (1946) to the flow phase B would give transmissivity for the gravel-sand main aquifer layer considering the majority of the flow occurs in this layer.

Figure 4-10 shows how the Cooper and Jacob equation (1946) is used to determine aquifer transmissivity from the pumping borehole. Figure 4-11 shows how the Cooper and Jacob equation (1946) is used to determine aquifer transmissivity and storativity using data from observation boreholes. With the Cooper and Jacob method (1946), aquifer transmissivity and storativity are determined using Equation 3 and Equation 4. The straight line is fit on the semi-log plot curve during the RAF period determined from derivative drawdown diagnostic (4.1.4.1.1.7).

$$T = \frac{2.3Q}{4\pi\Delta s}$$

Equation 3: Cooper and Jacob (1946) aquifer transmissivity.

Where:

Δs is the gradient of the straight line fit on the drawdown against time semi-log plot between 10-100 log cycles (Figure 4-10); r is the distance of the piezometer from the pumped well (m); t is the time since pumping has started (days); Q is the constant well discharge (m^3/d); T is aquifer transmissivity (m^2/d) and S is the aquifer storativity.

When a line is extended until it intercepts the time axis where $s(r,t) = 0$ (Figure 4-11), the interception point will have the coordinates $s(r,t) = 0$ and $t = t_0$, t_0 is used in Equation 4 to determine S .

$$S = \frac{2.25Tt_0}{r^2}$$

Equation 4: Cooper and Jacob (1946) aquifer storativity.

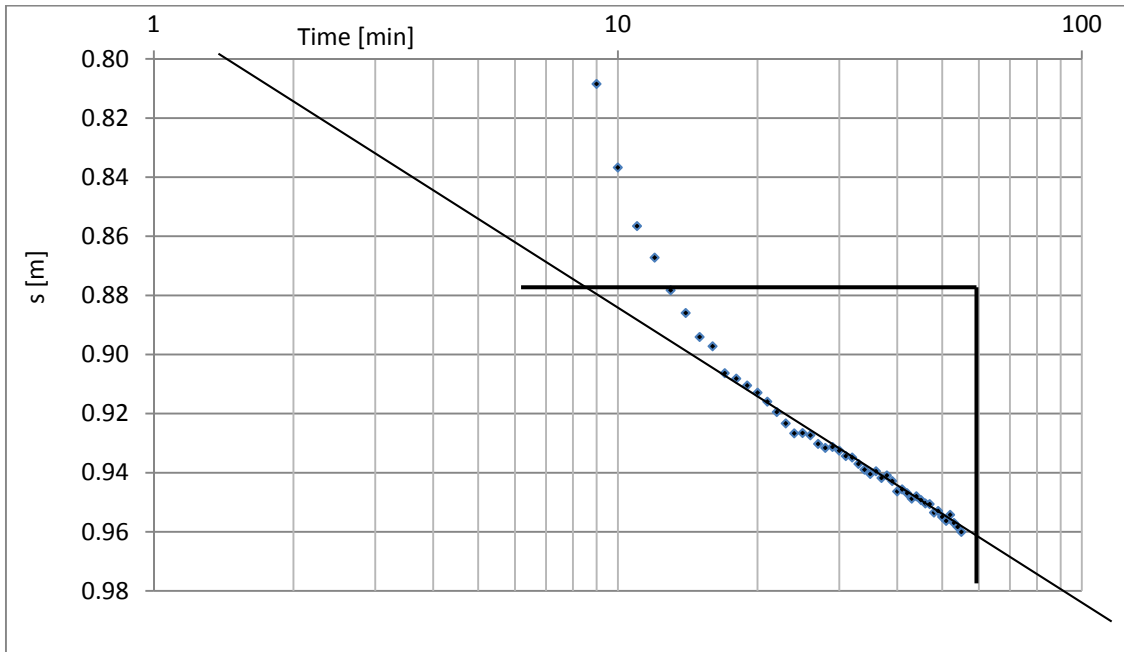


Figure 4-10 Semi-log plot of drawdown against time showing the application of Cooper and Jacob equation (1946) to get transmissivity from pumping borehole between the 10-100 log cycle.

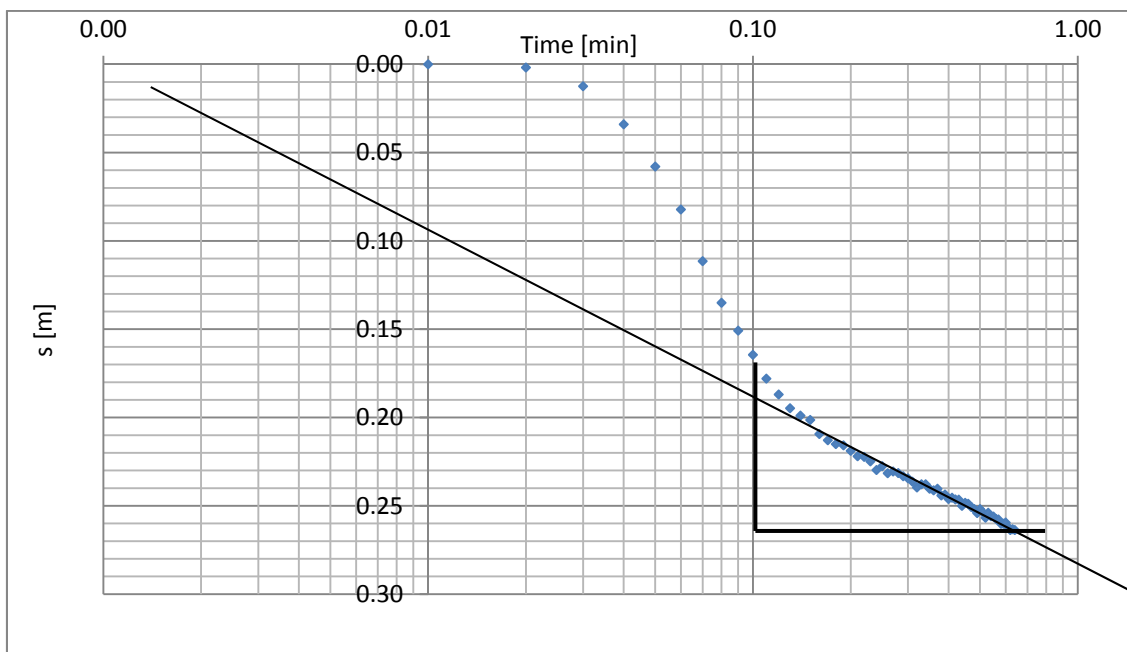


Figure 4-11 Semi-log plot of drawdown against time showing the application of Cooper and Jacob equation (1946) fit to determine aquifer transmissivity and storativity from an observation borehole between 10-100 log cycle.

4.1.4.1.1.10 Transmissivity and storage

Table 8 and Table 9 shows aquifer parameters determined using the Cooper and Jacob equation (1946) on pumping and abstraction boreholes respectively. In a homogeneous aquifer, a glance at the aquifer parameters would suggest something is definitely wrong. Aquifer test in an ideal homogeneous aquifer media should yield comparable aquifer parameters. However in heterogeneous aquifers, the physical and chemical differences in geological properties of aquifer material have great bearing on the spatial variation of aquifer parameters.

Table 8 Aquifer parameters determined from single-borehole test analysis.

Pumping borehole	T [m ² /d]
BH6	47.00
BH7	89.00
BH9	14.00
BH3	64.00
BH5	44.00

Table 9 Aquifer parameters determined from multiple-borehole test analysis.

Pumping borehole	Observation borehole	r [m]	T [m ² /d]	S
BH5	BH3	18.60	70.00	3.00E-02
BH5	BH6	10.00	54.00	6.00E-02
BH5	BH7	10.00	100.00	7.00E-02
BH5	BH9	20.30	47.00	2.00E-02
BH6	BH7	10.00	81.00	7.00E-03
BH6	BH9	11.50	48.00	3.00E-03
BH6	BH3	11.90	53.00	8.00E-03
BH6	BH5	10.00	50.00	1.00E-02
BH7	BH6	10.00	93.00	9.00E-03
BH7	BH5	10.00	81.00	3.00E-02
BH7	BH3	9.00	98.00	2.00E-03
BH7	BH9	14.70	95.00	4.00E-03
BH9	BH6	11.50	59.00	8.00E-03
BH9	BH5	20.30	43.00	6.00E-02
BH9	BH3	11.80	69.00	5.00E-3
BH9	BH7	14.70	101.00	9.00E-03

In general, alluvial channel deposits are often characterised by high hydraulic and storage properties (Wenzel 1942). High transmissivity and storage values are therefore expected for the alluvial channel aquifer. Applying the Cooper and Jacob equation (1946) on an observation borehole gives a transmissivity value of the highest hydraulic (contributing) aquifer section between the abstraction

and observation borehole. It therefore implies that the aquifer transmissivity obtained on an observation borehole can either be a reflection of hydraulic properties surrounding the observation or pumping borehole.

In alluvial channel aquifers grain size and nature of the deposits have a tremendous contribution on the hydraulic and storage properties. Under stressed aquifer conditions, it is the high transmissivity aquifer layers or segments that supplies water to the abstraction boreholes overshadowing the low permeable sections of the aquifer. Drawdown observations made in boreholes drilled into low permeable aquifer sections will yield transmissivity estimates for the high permeable sections. In general, large grain size of channel deposits materials indicate high hydraulic properties (Hazen, 1911). Figure 4-12 shows the differences between aquifer transmissivity determined from pumping and observation drawdown when borehole BH7 was being pumped and observations were made in BH3, BH5, BH6 and BH9 boreholes.

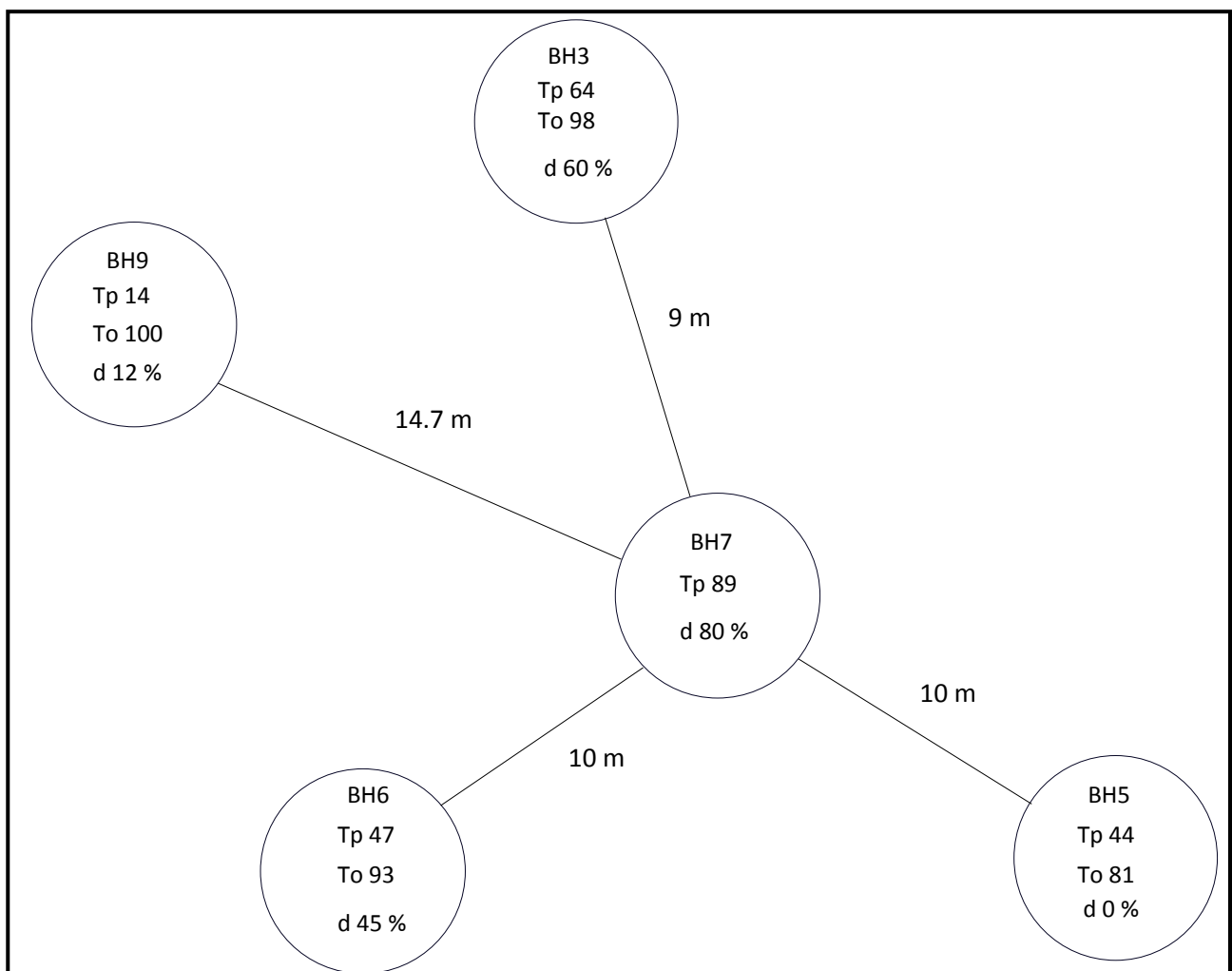


Figure 4-12 Variation between the aquifer transmissivity determined from pumping and observation drawdown; BH7 was being pumped and observations made in (BH3, BH5, BH6 and BH9); Tp is the

transmissivity obtained when the borehole is pumped and T_o is when used for observations; d is the average proportion % of gravel-sand grains of the aquifer material surrounding the borehole analysis.

The abstraction borehole BH7 intersected the largest grained gravel-sand % and the use of Cooper and Jacob (1946) on observation boreholes intersecting finer channel grains gives T for high hydraulic aquifer section around BH7 (Figure 4-12). This limitation does not render multiple-borehole aquifer testing a worthless exercise if the Cooper and Jacob method is the only available tool to determine aquifer parameters. Applying the Cooper and Jacob (1946) method on the pumping borehole gives a T value that is representative to the hydraulic properties of the surrounding layer irrespective of whether it's large or small.

The Cooper and Jacob (1946) method can still be valuably used on the observation boreholes to confirm the transmissivity values determined from pumping boreholes for aquifer sections with the highest hydraulic properties. Take for instance borehole BH7 that is surrounded by aquifer material of high transmissivity of 89 (m^2/d). The application of Cooper and Jacob method (1946) on observation boreholes (BH3, BH5, BH6 and BH9) that are surrounded by materials of low transmissivity simply confirms the high transmissivity for the BH7 abstracting borehole (Table 10). A comprehensive understanding of geological nature and spatial variation of channel aquifer deposits is thus a fundamental factor for analysis of aquifer tests conducted in alluvial channel aquifers.

Table 10 Transmissivity values obtained when Cooper and Jacob is applied on pumping and observation boreholes.

Borehole	$T [m^2/d]$
BH7 -pumping	89
BH3-observtaion	98
BH6-observation	93
BH5- observation	81
BH9-observation	100

In general, the aquifer transmissivity spatially varies along the alluvial aquifer channel aquifer due to heterogeneities brought about by the difference in nature and the grain size of channel deposits. Spatial variation of aquifer parameters is a measure of how the parameter varies in space i.e. from one point to another. The degree of variation of aquifer parameters from point to point on a small scale aquifer gives a quantitative measure of the influence that aquifer heterogeneity has on aquifer parameters. The spatial variation can also be attributed to artificial changes in groundwater flow regimes that occur due to improper borehole construction.

4.1.4.2 Deep aquifer system

Aquifer tests were performed in BH1, BH2 and BH4 to assess the hydraulic properties of the conceptualised deep aquifer system. The boreholes were pumped at 0.5 l/s until they went dry. The boreholes went dry during pumping and very low aquifer T were determined from the recovery data using the FC program (Van Tonder *et al.* 2001b) (Table 11).

Table 11 Transmissivity values determined from the boreholes drilled into the deep aquifer system.

Borehole name	T [m ² /d]
BH1	0.1
BH2	0.5
BH4	0.9

Is important to mention that during the recovery, water could be heard dripping into the borehole from the upper shallow main aquifer. Stable isotope analysis of the dripping water shows that it has similar compositions to the water samples collected from the boreholes drilled into the shallow aquifer system (Section 8.3 of chapter 8). On the other hand, deep groundwater levels (Figure 4-13) measured in BH1, BH2 and BH4 boreholes as compared to shallow boreholes indicates the possible existence of a deep aquifer system. It is however evident based on low T values (Table 11) that deep aquifer system has very low in permeability properties. Due to these contrasting evidence it is difficult to ascertain whether the deep aquifer system is leaky, confined or semi confined and further investigations are recommended to ascertain the nature of the deep aquifer system.

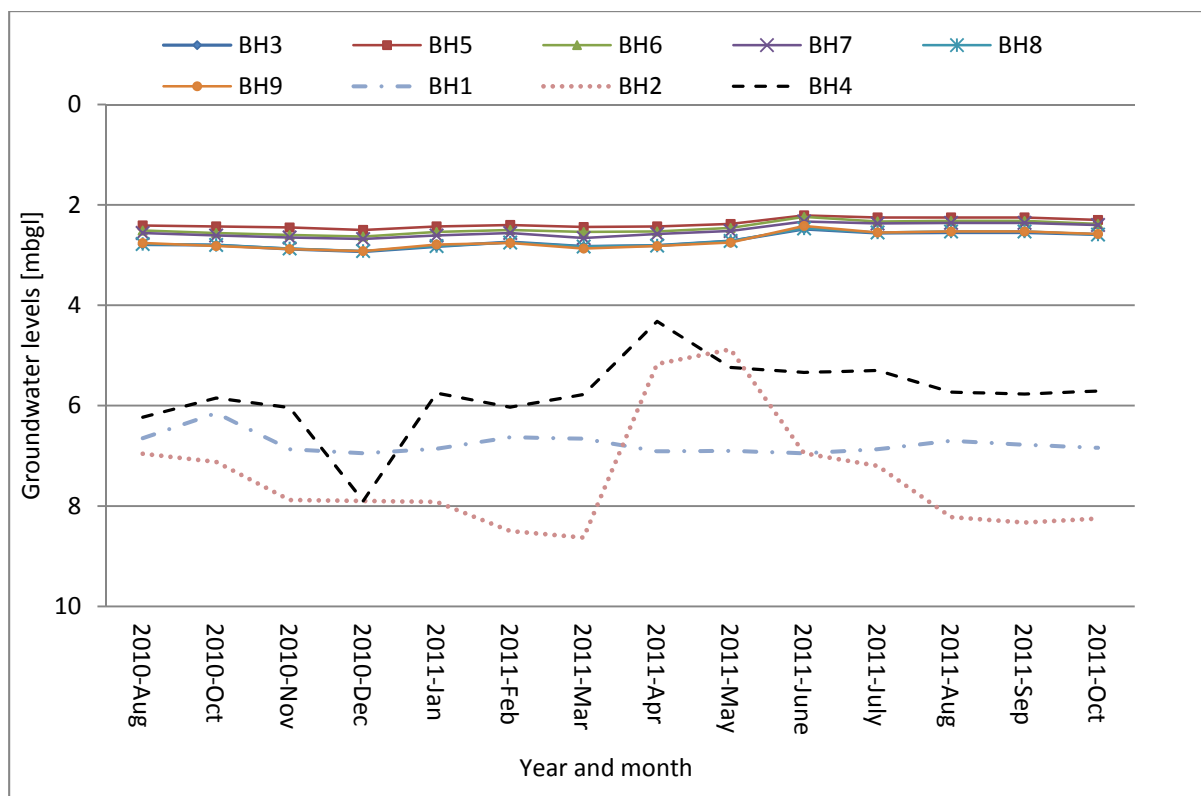


Figure 4-13 Groundwater levels measured in deep and shallow aquifers of the alluvial channel aquifer system.

4.2 Summary

The chapter gives an account of the hydraulic investigations that was performed in the alluvial channel aquifer. A total of 12 infiltration rate tests were conducted to assess the recharge mechanism of the alluvial channel aquifer. High infiltration rates exceeding 1 m/d were measured in the riparian zone. The high infiltration rates can be mainly attributed to dense tree roots, termites and burrowing animals that can create potential preferential pathways. Groundwater hydraulic and storage properties of the alluvial channel aquifer were determined using slug and aquifer tests. The shallow alluvial channel main aquifer is generally characterised by high transmissivities in the order of 10^1 m/d. The deep aquifer system is characterised by low T in the order of less 10^0 m/d. The hydraulic properties of the alluvial channel aquifer spatially vary across the site as influenced by the subsurface heterogeneity.

The next chapter discusses the investigation of the hydrogeochemical processes and its contribution to the overall water quality of the alluvial channel aquifer.

5 HYDROGEOCHEMICAL PROCESSES IN AN ALLUVIAL CHANNEL AQUIFER

5.1 Introduction

Hydrogeochemical processes in groundwater are largely controlled by the physical and chemical interactions that occur between the groundwater water and the aquifer materials. Hydrogeochemical processes are responsible for the seasonal, temporal and spatial variations of groundwater chemistry and consequently the quality (Rajmohan and Elango 2004). In alluvial channel aquifers that typically consist of unconsolidated sediments, groundwater hydrogeochemical processes are mainly influenced by the mineralogy of sediments that interacts with the infiltrating water.

Alluvial aquifers located along the major rivers of the Southern Africa Karoo basin typically comprises of unconsolidated calcrete, clay, silts and sand deposits. According to Woodford and Chevallier (2002), Quaternary deposits are a major characteristic along main rivers of the Karoo basin. Calcrete sediments at shallow depth are a common phenomenon close to river channels in semi-arid to arid climates. The case study site is characterised by arid to semi-arid conditions. The formation of calcretes close to river channels can also be related to shallow water tables and high infiltration rates that contribute to the precipitation of leached carbonates and dolomite minerals in the groundwater (Parsons and Abrahams 1994). In the riparian zones, evapotranspiration can also contribute to mineral precipitation in the vadose when the aquifer has a shallow water table.

The presence of calcrete usually as outcrops at shallow depth has significant bearing on the chemistry of the infiltrating water that recharges aquifers. Dissolution of calcite and dolomite minerals can influence the groundwater chemistry and may also create preferential flow paths for groundwater recharge at the surface and within the deposits. Ion exchange reactions involving Na^+ and Ca^{+2} often dominate geochemical processes in detrital sedimentary aquifers (Cardona *et al.* 2004). Agricultural chemicals such as fertilizers and pesticides have also been noted as significant contaminant sources for alluvial aquifers (Kelly 1997).

Geohydrological investigations of alluvial channel aquifers in Southern Africa, has largely focused on assessing the potential yield and sustainable management of the aquifers (Benito *et al.* 2009; De Hamer *et al.* 2008; Moyce *et al.* 2006 and, Mansell and Hussey 2005). Detailed studies on

hydrogeochemical process governing the groundwater evolution and its influence on water quality has not been conducted in typical Karoo Basin alluvial channel aquifers. It is upon such a background that this chapter was aimed at investigating the hydrogeochemical processes and their contribution to the overall water quality. The study utilizes the conventional Piper diagram, bivariate plots and PHREEQC model (Parkhurst and Appelo 1999) to analyze groundwater chemistry data obtained during sampling runs conducted in February, May and August of 2011.

5.2 Materials and methods

5.2.1 XRD and X-Ray analysis

The X-ray fluorescent spectrometry (XRF) and X-ray diffractometry (XRD) analysis was performed on randomly selected geological logs to determine the presence and absolute quantities of mineral species and major oxide elements in the geological samples. Six samples representative of the soil, calcrete, clay-silt, gravel-sand and shale formation were selected for the analysis. Hundred grams of disturbed samples were randomly collected from calcrete, alluvium-silt, clay and gravel-sand formations of the boreholes drilled into the alluvial channel aquifer. The logs from different boreholes were then mixed to obtain a representative sample of the lithology. The XRF and XRD analysis was conducted by the Geology laboratory of the Free State University in South Africa.

5.2.2 Groundwater sampling and analysis

A total of 16 groundwater and two river samples were collected during three sampling events in February, May and August and December 2011. Six of the groundwater samples were obtained from background boreholes (terrestrial aquifer) while one of the samples was obtained from the seepage water flowing out at the contact plane between the overlying unconsolidated sediments and the shale bedrock at the river bank. Samples from the boreholes were collected in clean polyethylene bottles using a low flow pump at an abstraction rate of 0.30 l/s. Temperature and electrical conductivity (EC) were continuously monitored in the purged water. Samples were only obtained after the stabilisation of temperature and EC. Figure 3-3 shows the location of boreholes from which the groundwater samples were collected. River samples were collected downstream and up stream of the alluvial channel aquifer.

Inorganic groundwater chemistry analyses were conducted by the Institute for Groundwater Studies (IGS) laboratory of the Free University in South Africa. The samples were analysed for major and minor ions; and silicon. The validity of the analytical measurements of the ions was determined by calculating the ionic balance error and is within the $\pm 5\%$ range. Saturation indices of quartz, calcite

and dolomite as the most dominant and major minerals respectively were calculated using PHREEQC model (Parkhurst and Appelo 1999).

5.3 Results

The groundwater chemistry analysis results have been used to identify and describe the hydrogeochemical processes governing the groundwater evolution and their contribution on the overall groundwater quality. Table 12 shows the maximum and minimum concentrations of major and other important ions in groundwater samples collected from the aquifer. A complete list of the major and minor ions detected in the groundwater and river water during the monitoring period has been placed in Appendix 2.

Table 12 Maximum and minimum concentrations of major ions and other important ions measured in the groundwater during the monitoring period, also shown in the table is the South African National Standards (SANS 1996) of drinking water quality target concentrations.

Ions	Minimum [mg/l]	Maximum [mg/l]	SANS 1996 [mg/l]
Na ⁺	82.90	209.60	≤ 100
K ⁺	4.75	8.23	≤ 50
Ca ⁺²	32.50	56.40	≤ 32
Mg ⁺²	40.09	82.80	≤ 30
Cl ⁻	48.84	107.00	≤ 100
SO ₄ ⁻²	20.02	74.83	≤ 200
F ⁻	0.25	0.73	≤ 1
NO ₃ ⁻ (N)	0.00	0.82	≤ 6
HCO ₃ ⁻	365.00	613.00	- ^a
Si ⁺⁴	19.05	23.93	-

^a- no standard available

The Ca⁺² and Mg⁺² concentrations in the all the groundwater samples exceed the SANS (1996) drinking water quality target values of 32 and 30 mg/l respectively. Abundance of the major ions is in the following order: HCO₃⁻ > Na⁺ > Cl⁻ > Mg⁺² > Ca⁺² > SO₄⁻² > K⁺. Sodium and HCO₃⁻ are the most dominant cation and anion with an average contribution to total cations and anions of at least 60 % and 80 % respectively. Based on the Piper diagram (Figure 5-1); the groundwater is classified as a Na⁺-HCO₃⁻ water type.

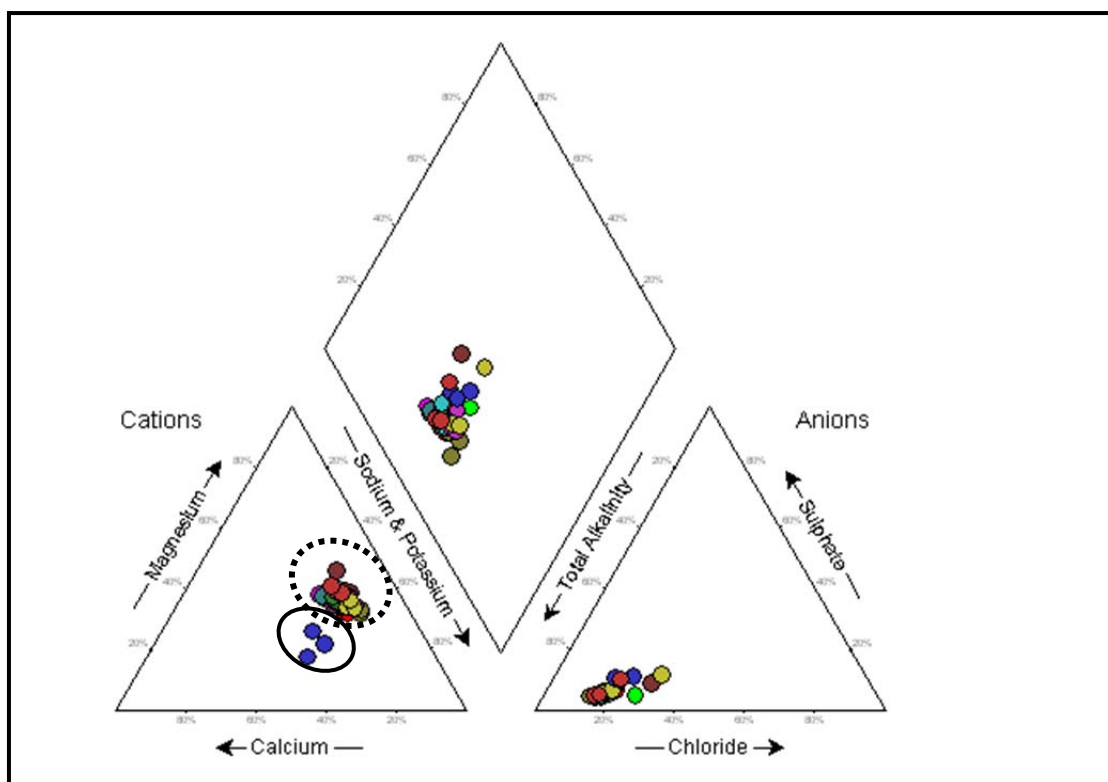


Figure 5-1 Groundwater and river samples plots on a piper diagram; groundwater samples are encircled by the dashed oval while the bold oval encircles the river water samples.

Table 13 and Table 14 show the major elements oxides and minerals detected by XRF and XRD analysis. The XRF analysis (Table 13) shows that the alluvial channel deposits are dominated by silicates, aluminum and iron oxides. Magnesium, calcium and potassium oxides in the unconsolidated channel deposits occur in relatively small contents of above 1 %. The clay-silt formation has the greatest abundance of the calcium major oxide in excess of 11 %. Anhydrite constitutes about 43 % of the fines.

Table 13 Major oxides elements detected in the channel deposits that makes the alluvial aquifer and their relative % content.

		Major oxides elements in the channel deposits and their relative % content									
Sample Description	Depth [mbgl]	SiO ₂	Al ₂ O ₃	Fe ₂ O ₃	MnO	MgO	CaO	Na ₂ O	K ₂ O	TiO ₂	P ₂ O ₅
Soil	0-1	66.04	16.67	6.17	0.08	2.09	1.16	1.40	3.90	0.75	0.18
Calcrete	1-3	63.59	12.62	8.54	0.19	4.67	5.61	1.20	1.50	0.66	0.13
Clay-silt	3-5	70.41	7.82	4.49	0.09	3.1	10.25	0.63	1.25	0.74	0.05
Gravel-sand	5-8	74.27	8.19	3.96	0.04	2.39	7.37	0.61	1.36	0.72	0.04
Shale	8-12	70.65	7.70	3.40	0.12	4.36	9.49	0.60	1.66	0.62	0.11

Table 14 Major minerals detected in the alluvial channel aquifer materials; XX - dominant (> 40 % per volume), X - major (10-40 % per volume), xx - Minor (2-10 % per volume) and x - accessory (1-2 % per volume).

		Major minerals detected in the channel deposits and their relative % content					
Sample description	Depth [mbgl]	Quartz	Calcite	Dolomite	Magnetite	Pyrite	Gypsum
Soil	0-1	XX	<x		x	<x	
Calcrete	1-3	XX		xx	xx		<x
Clay-silt	3-5	XX	X		x		
Gravel-sand	5-8	XX	xx				
Shale	8-12	XX	xx		<x		

The XRD analysis (Table 14) shows that quartz is the super dominant mineral in all samples of the channel deposits sediments that were analysed. Calcite was detected as a minor mineral in the gravel-sand and shale but is the dominant mineral constituent of the clay-silt formation. Dolomite and magnetite occurs in the calcrete deposits as major minerals.

5.4 Discussion

The discussion seeks to identify and describe the possible hydrogeochemical processes contributing to the formation of a $\text{Na}^+\text{-HCO}_3^-$ groundwater type (Figure 5-1). Attention has also been placed on levels of nitrates as nitrogen $\text{NO}_3^-(\text{N})$ in the groundwater given the proximity of the alluvial channel aquifer to agricultural farming activities. Identification of the important hydrogeochemical process in a groundwater system is not a unique exercise mainly because different reactions and weathering process can result in similar type of ions being present in the groundwater. The task of identifying the major hydrogeochemical processes is more of a diagnostic in nature. Two optional approaches can be used, firstly one can use the concentrations of the ions detected in groundwater to work backwards and try to identify their origins. On the other hand, it is also possible to start by identifying the minerals and major element oxides of the aquifer materials and then comparing their predicted potential influence on the groundwater quality to the measured ions. The relative nature of the exercise calls for the use of complimentary lines of evidence to identify and understand hydrogeochemical processes as demonstrated in this chapter.

5.4.1 Hydrogeochemical processes

5.4.1.1 Carbonate system

In general, a carbonate system consists of three soluble components; carbonic acid (H_2CO_3^*), bicarbonate (HCO_3^-) and carbonate (CO_3^{2-}). The carbonate systems of the site only consist of

bicarbonate (HCO_3^-) ion that constitutes more than 80 % of the total anion in the groundwater system (Fig. 5). The weathering and dissolution of calcite and dolomite minerals that were detected in the unconsolidated deposits is the main sources of HCO_3^- , calcium (Ca^{+2}) and magnesium (Mg^{+2}) ions in the groundwater system. The carbonate mineralogy of calcretes is mainly dominated by calcite and dolomitic minerals (Parsons and Abrahams 1994). Although calcium (Ca^{+2}) often dominates in calcrete minerals, calcite rich in magnesium (Mg^{+2}) has also been reported in the Kalahari region of Southern Africa (Watts 1980). The presence of HCO_3^- , Ca^{+2} and Mg^{+2} in the groundwater system can therefore be explained using the processes of the carbonate system. A flow diagram in Figure 5-2 shows the typical reactions that would occur as the infiltrating recharge water passes through soil, calcrete, silt-clay into the gravel-sand main aquifer layer.

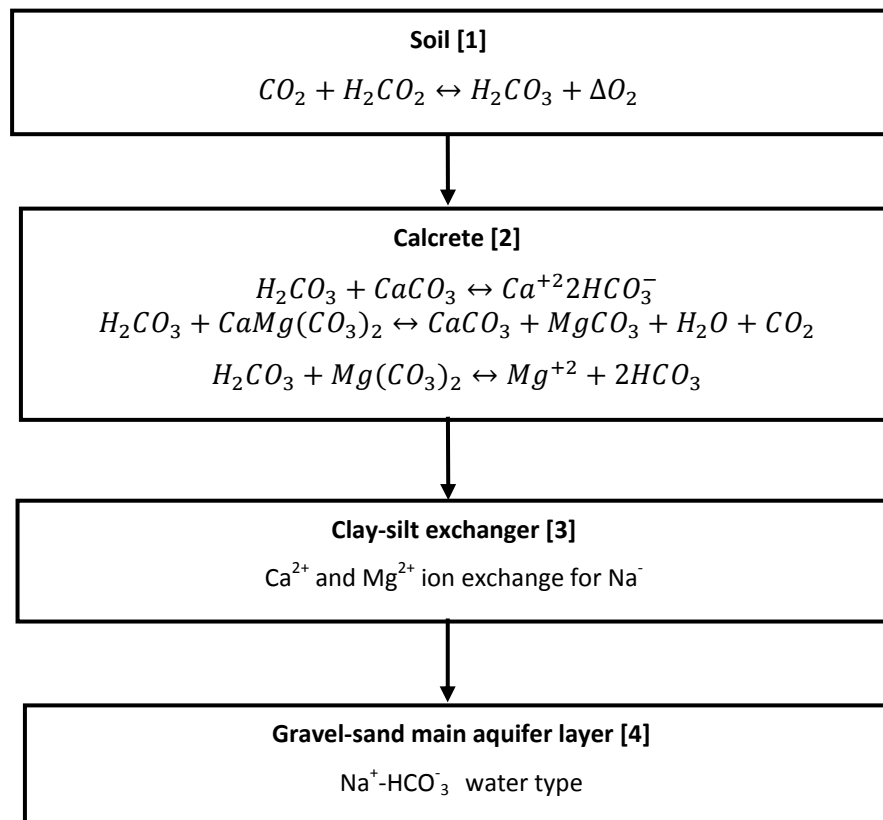


Figure 5-2 A flow diagram showing the idealised carbonate system reactions that occur during the recharge process as the water passes through the aquifer media of different chemical and physical properties.

5.4.1.1.1 Stage 1

Carbon dioxide (CO_2) in the soil medium reacts with the infiltrating rain water to form carbonic acid (H_2CO_3). Elevated levels of CO_2 are generally expected in the soil at the site from the respiration of

organic matter. The dead and decaying riparian vegetation has great potential to result in a significant built up of organic matter at the site and hence accelerated respiration rates.

5.4.1.1.2 Stage 2

Infiltrating recharging waters rich in H_2CO_3^- interacts with calcrete reacting with calcite (CaCO_3) and dolomite $\text{CaMg}(\text{CO}_3)_2$ minerals within the deposits. The reaction leads to the dissolution of calcite and dolomite minerals, thus providing Ca^{+2} , Mg^{+2} and HCO_3^- ions in the groundwater.

5.4.1.1.3 Stage 3

Stage 3 is controlled by cation exchange reactions where Ca^{+2} and Mg^{+2} exchanges for Na^+ on alluvium silt-clay sediments. The silt-clay sediment absorbs Ca^{+2} and Mg^{+2} while Na^+ is released into the groundwater solution. In general, the XRF results (Table 13) shows that silt-clay channel deposits comprises of large proportion of CaO and MgO oxides as compared Na_2O . The ion exchange is hypothesized as an ongoing process. Although no practical tests were conducted to test the occupation of the exchanger sites, the study seeks to assess the possible contribution of ion exchange process to the elevated Na^+ based on theoretical understanding and field results

5.4.1.1.4 Stage 4

Stage 4 defines the existing groundwater type from the preceding reactions in stages 1 to 3. The process typically takes place during groundwater recharge where Ca^{+2} , Mg^{+2} and HCO_3^- ions often flushes salt water out of the aquifer. The resulting groundwater in the gravel-sand main aquifer layer is $\text{Na}^+\text{-HCO}_3^-$ type. However when Ca^{+2} and Mg^{+2} ions in groundwater system are depleted, groundwater can become under saturated with respect to calcite and dolomite thus prompting dissolution.

5.4.1.2 Nitrates as nitrogen $\text{NO}_3^-(\text{N})$

In Southern Africa, farmers often rely on groundwater along alluvial channel aquifers in both ephemeral and perennial rivers to meet domestic and agricultural irrigation requirements (Seely *et al.* 2003). In these farming areas there is more risk of elevated $\text{NO}_3^-(\text{N})$ concentration levels in groundwater due to fertilizers and animal waste. Extreme $\text{NO}_3^-(\text{N})$ concentrations can result in the contamination of groundwater resources posing a huge human health risk. SANS (1996) set the target water quality concentration for nitrates in public drinking water at 10 mg/l $\text{NO}_3^-(\text{N})$ in order to protect infants from methemoglobinemia. Methemoglobinemia is a human physiological disorder that occurs in presence of a higher than normal level of methemoglobin in the blood.

Studies have also established a correlation between strong exposure to nitrates in drinking water and the incidence of gastric and intestinal cancer (Cissé and Mao 2008). It is therefore imperative to assess the evolution of $\text{NO}_3^-(\text{N})$ in a typical alluvial channel aquifer. The possible routes of $\text{NO}_3^-(\text{N})$ evolution in the alluvial channel aquifer are discussed. Identification and description of the evolution routes of groundwater chemistry can assist in identifying the source of the ions.

5.4.1.2.1 Nitrate evolution routes

A number of possible nitrate chemical evolution routes (Figure 5-3) can be used to explain the presence of low nitrate concentrations levels (0.004-0.82 mg/l) in the alluvial channel aquifer during the wet and dry season. The groundwater samples for chemistry analysis were obtained through purging at a low flow rate of 0.30 l/s for 20 minutes. During the 20 minutes of purging, groundwater flow is from the gravel-sand aquifer layer into the abstraction borehole. The groundwater quality is accordingly expected to reflect the chemistry conditions of the gravel-sand aquifer layer.

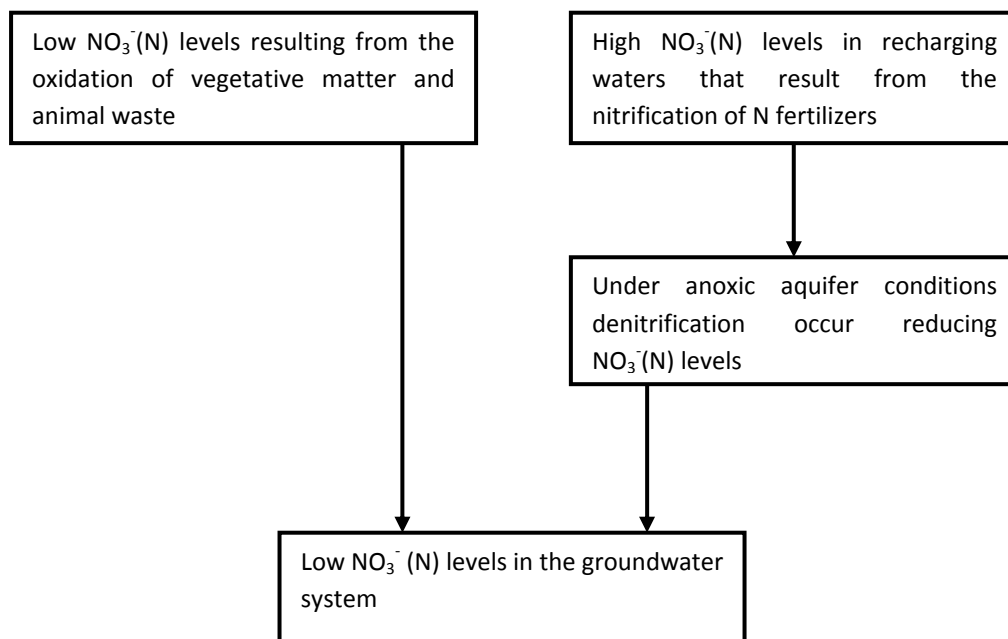


Figure 5-3 Possible routes of nitrate evolution in the alluvial channel aquifer.

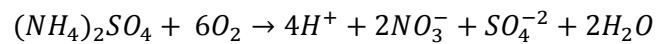
5.4.1.2.1.1 Route A

Nitrates in low concentration levels originate from oxidation of riparian vegetative matter and animal waste. The route implies that the recharging occurs after direct precipitation has interacted with the organic matter generated by the decaying riparian vegetation. According to the route, the $\text{NO}_3^-(\text{N})$ in the system only comes from the oxidation process of the organic matter. In general, nitrates leaching from forests are low in concentrations and possess little potential of contaminating groundwater in comparison to N fertilizers (Alley 1991). It has also been reported that riparian

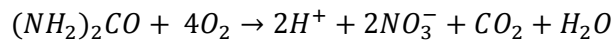
vegetation can even act as nitrogen buffers in shallow water tables (Snyder *et al.* 1998 and Spruill 2000). In other words, it is also possible to attribute low concentrations of $\text{NO}_3^-(\text{N})$ measured at the site to buffering capacity of the riparian vegetations.

5.4.1.2.1.2 Route B

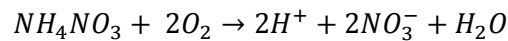
High $\text{NO}_3^-(\text{N})$ levels in recharging waters originate from the nitrification of N fertilizers that are usually used for agricultural activities. Equation 5 to Equation 7 shows reactions that represent three commonly used fertilizers (ammonium sulphate, urea and ammonia nitrate) (Adams 1984).



Equation 5: Nitrification of ammonium sulphate fertilizers.



Equation 6: Nitrification of urea fertilizer.



Equation 7: Nitrification of ammonia nitrate fertilizer.

This route implies that recharging of the aquifer occurs via the infiltration of water through the agricultural fields. However considering the significant accumulation of vegetative organic matter at the site, it is most likely that the soils are heavily depleted in oxygen levels. Several studies have also shown that groundwaters in aquifers beneath the soils of low permeability often show low nitrate levels due to low infiltration rates and/or anoxic conditions (Postma *et al.* 1991, Cey *et al.* 1999 and Panno *et al.* 2001).

The vadose zone of the background aquifer mainly comprises of clay and silt soils of calcareous origin. Low saturated hydraulic conductivities in the order of 10^{-6} m/d were determined for the vadose zone of the background aquifer. It is expected that the groundwater that flows from the background aquifer through the alluvial channel towards the river (Figure 4-4) would transport $\text{NO}_3^-(\text{N})$ generated from the agricultural activities in the background terrestrial land. However the low saturated hydraulic conductivities in the vadose zone gives infiltrating recharging waters sufficient time to go through denitrification thereby reducing the $\text{NO}_3^-(\text{N})$ levels in the water that reaches the alluvial channel aquifer. Denitrification of $\text{NO}_3^-(\text{N})$ under anoxic environments results in low $\text{NO}_3^-(\text{N})$ concentration levels being measured in the aquifer. Although route B is theoretically possible, the groundwater chemistry data at the site (Table 2) does not meet some of the criteria for sufficient denitrification ($\text{Fe}^{+2} > 7.00$ mg/l and $\text{Mn}^{+2} > 0.90$ mg/l) (Cey *et al.* 1999 and Kraft *et al.* 1999).

5.4.1.3 Sodium

Elevated Na^+ concentrations in the groundwater system can be attributed to a number of processes which include ion exchange and silicate weathering. Multiple evidences on bivariate plots to infer the contribution of the ion exchange geochemical process on the elevated Na^+ concentrations are presented.

5.4.1.3.1 Ion exchange

Ion exchange refers to the process by which an ion in a substance is replaced by similarly charged ions of a solution surrounding the substance. In the clay and silt sediments, it is expected that Ca^{+2} and Mg^{+2} ions in the groundwater would exchange for Na^+ ions. The ion exchange process implies that Na^+ ions goes into the groundwater in exchange for Ca^{+2} and Mg^{+2} ions that occupies sediments exchanger sites. The ion exchange process is used to try and explain the presence elevated Na^+ concentrations in groundwater (Table 12).

If meteoric NaCl is the source of Na^+ , then a plot of Na^+ against Cl^- ions in the ground water should fall on the 1:1 evaporation line. The Na^+ against Cl^- plot shows that all groundwater samples at the site are located above the 1:1 evaporation line (Figure 5-4) implying that the meteoric NaCl is not the source of Na^+ in the groundwater water. The shifting of the groundwater plots from the 1:1 line is due to increased Na^+ concentration and the ion exchange process can be used to explain the effect. According to (Jankowski and Beck 2000), the deviation from the simple dissolution (or evaporation) trend line indicates that Na^+ is added into the aquifer system as driven by ion exchange reactions.

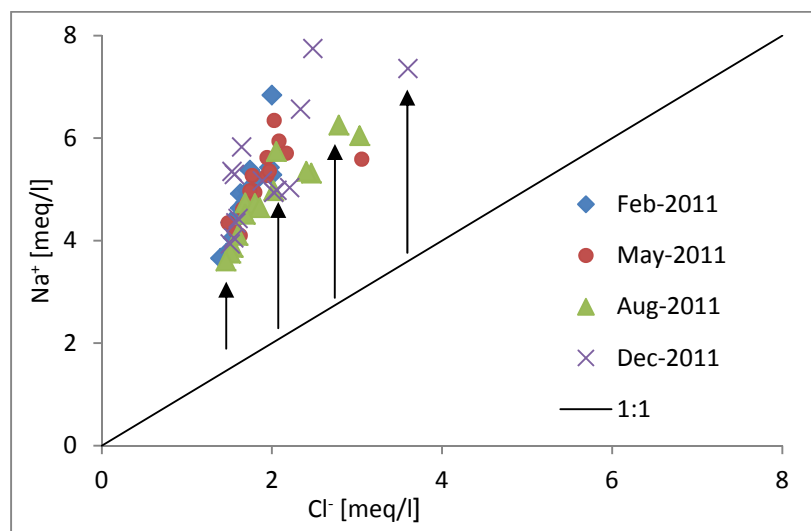


Figure 5-4 Bivariate plot of Na^+ against Cl^- at the study site; black arrows indicate the contribution of the ion-exchange process and deviation from the 1:1 evaporation line; meq/l – Milliequivalent per Liter.

The plot of $\text{Ca}^{+2} + \text{Mg}^{+2}$ versus $\text{SO}_4^{-2} + \text{HCO}_3^{-}$ will be close to the 1:1 line if dissolutions of calcite and dolomite gypsum are the dominant reactions in a system (Guler 2002). The groundwater sample plots on the right side of the 1:1 line (Figure 5-5) and according to Fisher and Mulican (1997), ion exchange process tends to shift the sample plots to right. The shift to the right of the 1:1 line is due to the decrease of $\text{Ca}^{+2} + \text{Mg}^{+2}$ cations as they leave the groundwater system to occupy the sediments exchange site left by Na^+ .

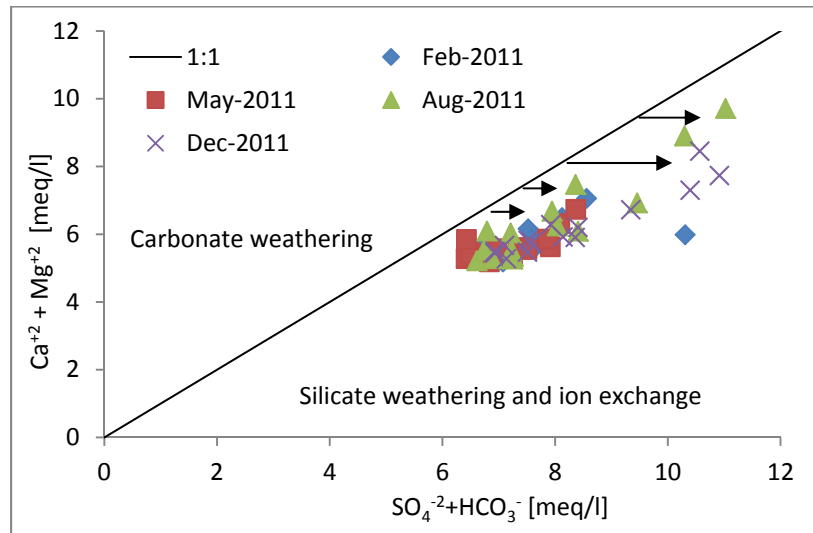


Figure 5-5 Bivariate plot showing $(\text{Ca}^{+2} + \text{Mg}^{+2})$ against $(\text{SO}_4^{-2} + \text{HCO}_3^{-})$ for the groundwater samples from the alluvial channel aquifer and terrestrial aquifer.

A plot of $(\text{Ca}^{+2} + \text{Mg}^{+2} - \text{SO}_4^{-2} - \text{HCO}_3^{-})$ against $(\text{Na}^+ - \text{Cl}^-)$ can be used to assess the existence of ion exchange reactions in the groundwater systems. By subtracting chloride from sodium chloride (considering that Cl^- is a conservative ion, and assuming that all Cl^- comes from precipitation), groundwater that are not influenced by ion exchange will plot close to zero on this axis. When sulfate and bicarbonate is subtracted from calcium and magnesium, the dissolution of calcite, dolomite and gypsum should also return values of zero assuming that dissolution is occurs at the same rate and no ion exchange occurs. If ion exchange is dominant in the system the groundwater plots should form a line with slope of -1 (Jankowski and Beck 2000).

Figure 5-6 a-d shows a plot of $(\text{Ca}^{+2} + \text{Mg}^{+2} - \text{SO}_4^{-2} - \text{HCO}_3^{-})$ against $(\text{Na}^+ - \text{Cl}^-)$ for the groundwater samples from boreholes drilled into the alluvial channel aquifer and terrestrial background aquifer.

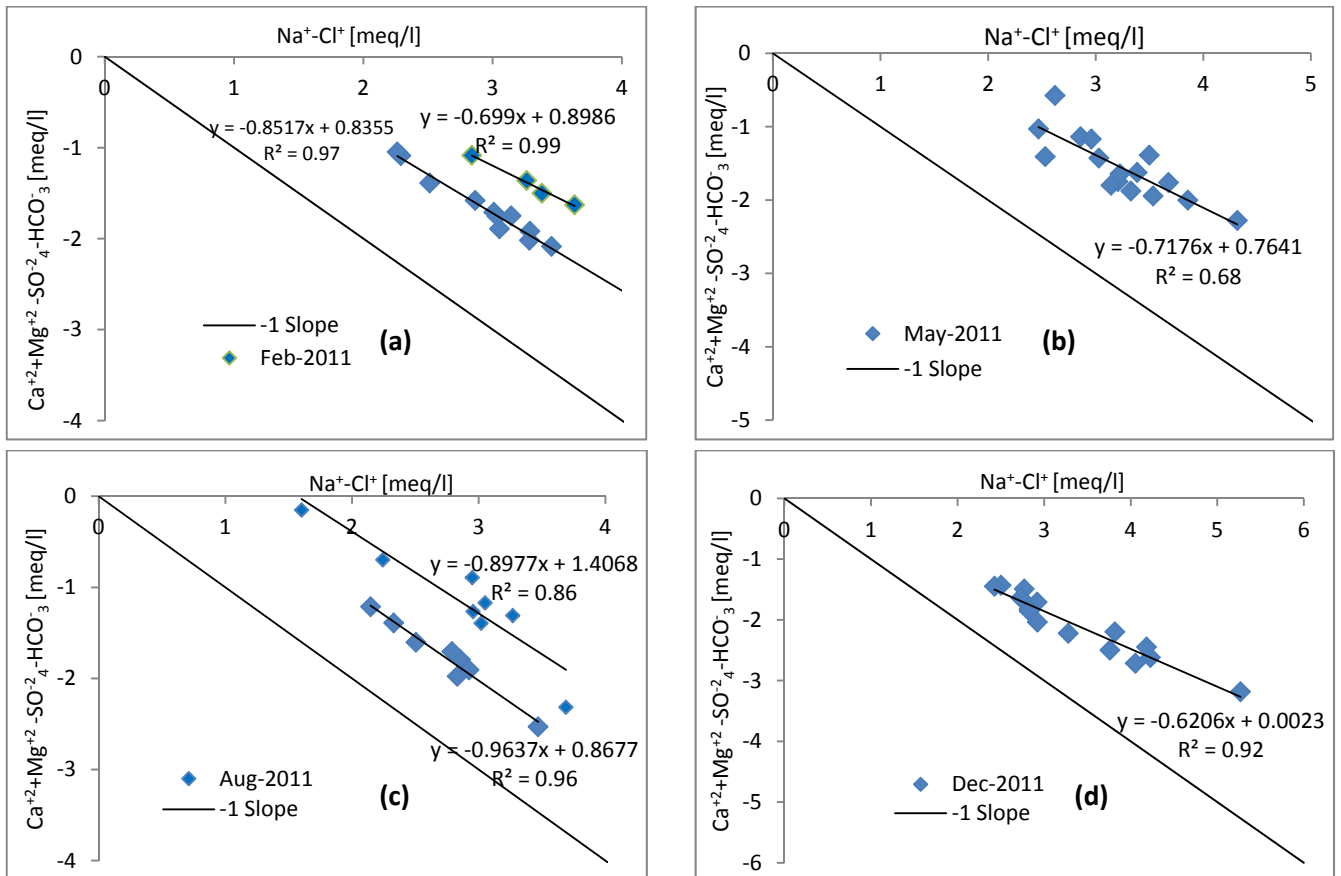


Figure 5-6 Relationship between $(\text{Ca}^{2+} + \text{Mg}^{2+} - \text{SO}_4^{2-} - \text{HCO}_3^-)$ against $(\text{Na}^+ - \text{Cl}^-)$ for groundwater sampled in February 2011 (a), May 2011 (b), August 2011(c) and December 2011 (d).

Linear regression plots on Figure 5-6 (a-d) shows that groundwater samples fit into lines that have gradients between -0.69 and -0.96. The gradients of the lines are generally close to -1 and are characterised by a goodness fit of between ($r^2 = 0.68$ and 0.99), thus enhancing evidence about the occurrence of ion exchange in the alluvial aquifer. The two different slopes on the $(\text{Ca}^{2+} + \text{Mg}^{2+} - \text{SO}_4^{2-} - \text{HCO}_3^-)$ against $(\text{Na}^+ - \text{Cl}^-)$ plot of February 2011 (Figure 5-6, a) and August 2011 (Figure 5-6, c) implies that there might be two levels of ion exchange in the groundwater system. There is however no field evidence to ascertain the existence of different levels of ion exchange. In general, chemical heterogeneities in groundwater quality can be attributed to the spatial variation in chemical properties of the aquifer (Kelly 1997).

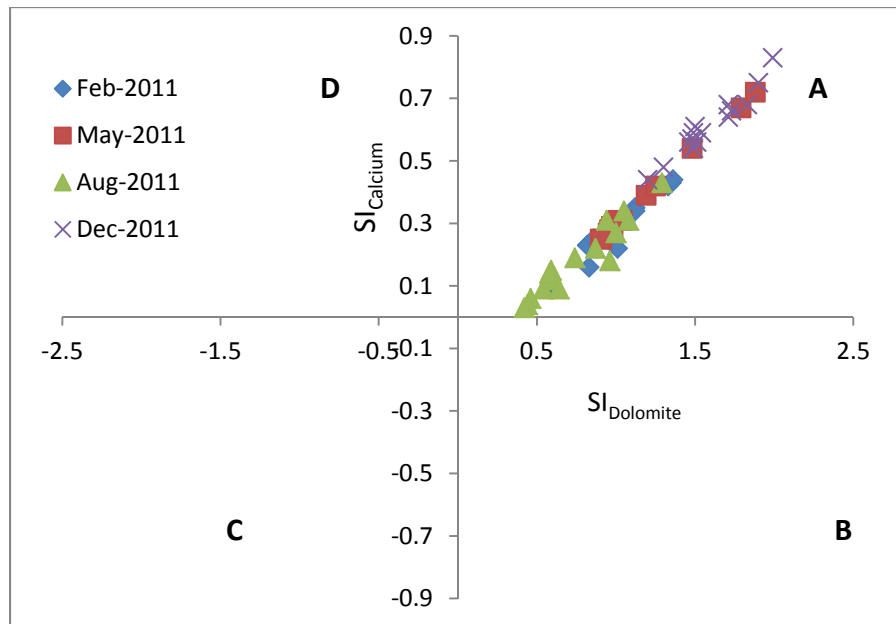


Figure 5-7 Relationship between the saturation indices for calcite and dolomite; quadrants define: A-Dolomite and calcite supersaturation, B-Dolomite undersaturation and calcite supersaturation, C-dolomite and calcite undersaturation; and D-dolomite supersaturation and calcite undersaturation.

Calcite and dolomite saturation are all positive indices and plot in quadrant A which implies that the groundwater had sufficient residence time for supersaturation to occur. The saturation index of calcite is lower than of the dolomite ($SI_{dolomite}/SI_{calcite} \geq 2$); hence the later is most likely to precipitate first. Higher saturation indices with respect to dolomite and calcite can be mainly attributed to effect of recharge rainwater that dissolves the minerals during infiltration.

The groundwater is supersaturated with respect to quartz which is the most dominant mineral in the channel deposits. Groundwater samples have low concentrations of SO_4^{-2} in the range of 20-53 mg/l, thus the water is undersaturated with respect to gypsum ($SI < -1.5$). No gypsum minerals were detected in the channel deposits and hence the most likely source of SO_4^{-2} is the old waters. It is important to note that besides mineral dissolutions, factors such common ion effect, evaporation, rapid increase in temperature and incongruent solutions processes (Langmuir 1997) can also contribute to supersaturation conditions.

5.4.1.5 Sulphate and chloride

Groundwater sulphate concentrations range from 20 mg/l to 53 mg/l throughout the monitoring period. Lower sulphate concentrations most likely originated from precipitation deposition and dry fallout that is similar to chloride. Potential natural sources of sulphate at site include:

- Sedimentary lithogenic sources (Anhydrite).
- Atmospheric deposition.
- Terrestrial aquatic sources (from the oxidation of H_2S emitted by anaerobic wetlands (Chivas *et al.* 1991)).

Figure 5-8 shows a scatter plot of chloride against sulphate ions. High correlation between chloride and sulphate ions can be a reflection of similar processes that are affecting the two ions. In shallow alluvial channel aquifers along the riparian zones, sulphate and chloride ions in groundwater can be both enriched due to the evapotranspiration process. Scanlon *et al.* (2009) reported high correlation ($r = 0.85$) of total sulfate and chloride inventories in profiles beneath natural ecosystems.

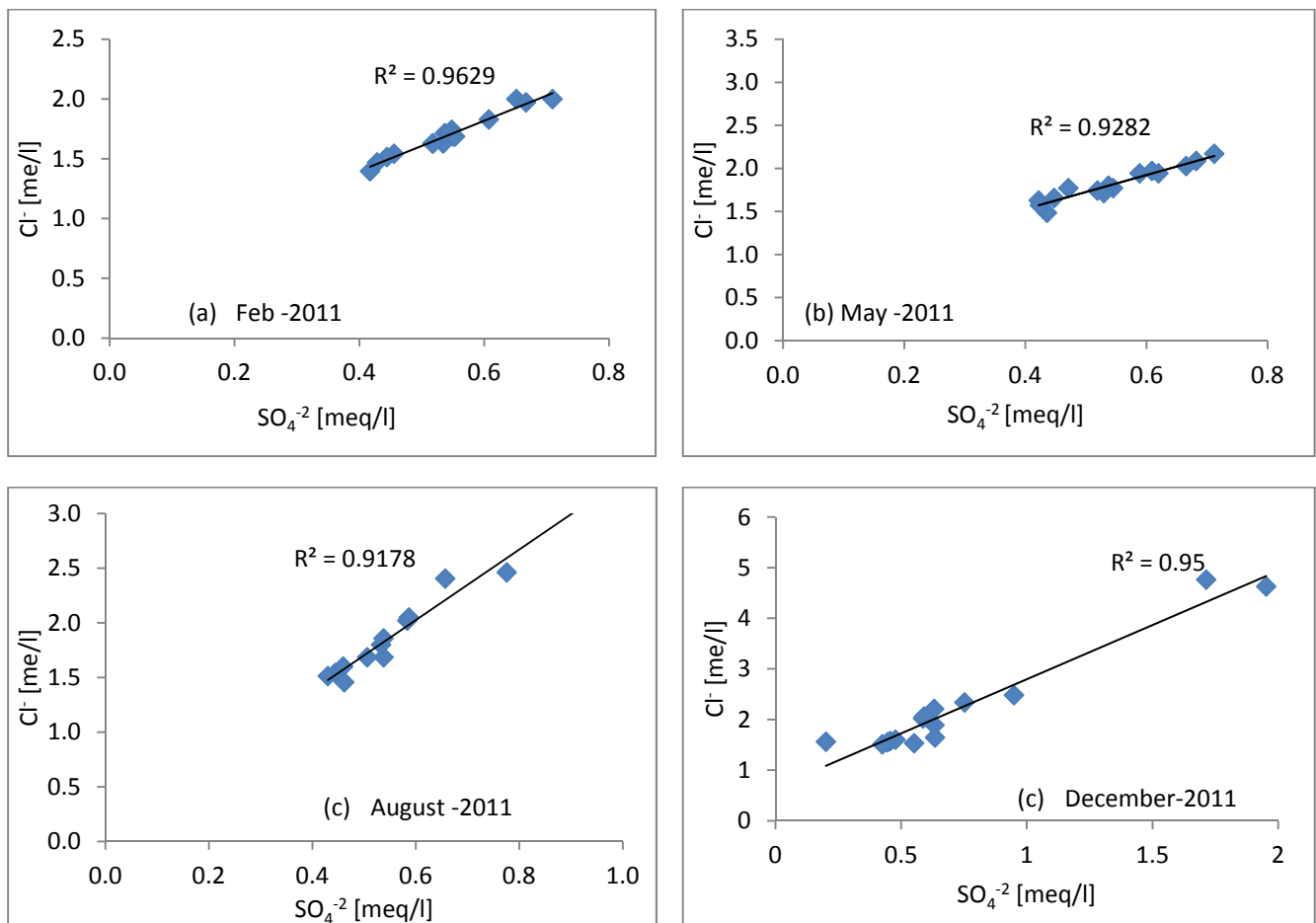


Figure 5-8 Scatter diagrams showing Cl^- against SO_4^{2-} plots for groundwater samples collected in: (a) February, (b) May 2011, (c) August and (d) Dec2011.

5.4.2 Groundwater quality

The groundwater quality is evaluated based on its suitability for drinking, agricultural, and domestic use using local and international guidelines. The possible influence that that hydrogeochemical processes has on the overall groundwater is described and explained. The maximum and minimum concentrations are compared to the South African national Standards for drinking water (SANS 1996).

Elevated concentrations of Na^+ above the (SANS 1996) target concentration of $\leq 100 \text{ mg/l}$ is due to the ion exchange and silicate weathering hydrogeochemical process. Ca^{+2} and Mg^{+2} exceeded the target levels of 32 mg/l and 30 mg/l respectively in the groundwater samples. The calcite weathering and dissolution processes are responsible for high Ca^{+2} and HCO_3^- . Dissolution and weathering of dolomite minerals in the sedimentary deposits contributes to high Mg^{+2} concentrations.

5.4.2.1 Hardness

Classification of groundwater based on total hardness shows that 81 % of the water is hard. The total hardness value ranges from 240 mg/l - 500 mg/l . The seepage groundwater sample has the highest total hardness and is mainly attributed to the accumulation of Ca^{+2} and Mg^{+2} cations along the flow path to the discharging zone. Table 15 shows the classification of groundwater based on the total hardness for the samples collected during the monitoring period.

Table 15 Classification of groundwater based on hardness (Sawyer and McMcarty 1967).

Total hardness as CaCO_3 [ppm]	Water class	Number samples
0-75	Soft	0
75-150	Moderate Hard	0
150-300	Hard	53
> 300	Very Hard	15

It is worth to point out that the total hardness is above the World Health Organization (WHO) (1993) standard of 100 mg/l . Although the total hardness exceed the international target water quality concentration levels, it does not does not constitute a serious threat because the hardness is only temporary. In general, temporary hardness can be simply removed by boiling (Van der Bruggen 2009). It can however have negative implications to aesthetic factors such as smell, appeal and colour of the water. High levels of total hardness can also lead formation of scales on water heating equipment and metal pipes. According to WHO (2010), water with hardness above 200 mg/l has potential to cause scale deposition in the water distribution system, heating and boiling equipment. On the hand, soft water (hardness $< 100 \text{ mg/l}$) often result in the corrosion of pipes and this can

lead to dissolving of heavy metals from the pipes in the drinking water (National Research Council 1977). However, the extent of these two common effects of hard water largely depends on other parameters such as PH and alkalinity.

5.4.2.2 Irrigation water quality

In general, extreme levels of sodium, bicarbonate and carbonate dissolved ions in irrigation water can potentially affect the physical and chemical soil properties thereby reducing the available water for plant growth. Accumulation of salts in ground water also leads to salinity problems which can affect plant nutrient uptake regime. Salinity effects are often more severe during crop emergence and early development stages (Tanji and Kielen 2002). The suitability of groundwater for irrigation requirements is often determined using the Sodium Adsorption Ratio (SAR) parameter mainly because it can quantify the potential effects of alkali and sodium hazard on crops (Arumugam and Elangovan 2009). Figure 5-9 shows the classification of groundwater based on salinity and alkalinity hazard of irrigation (US Salinity Laboratory Staff 1954).

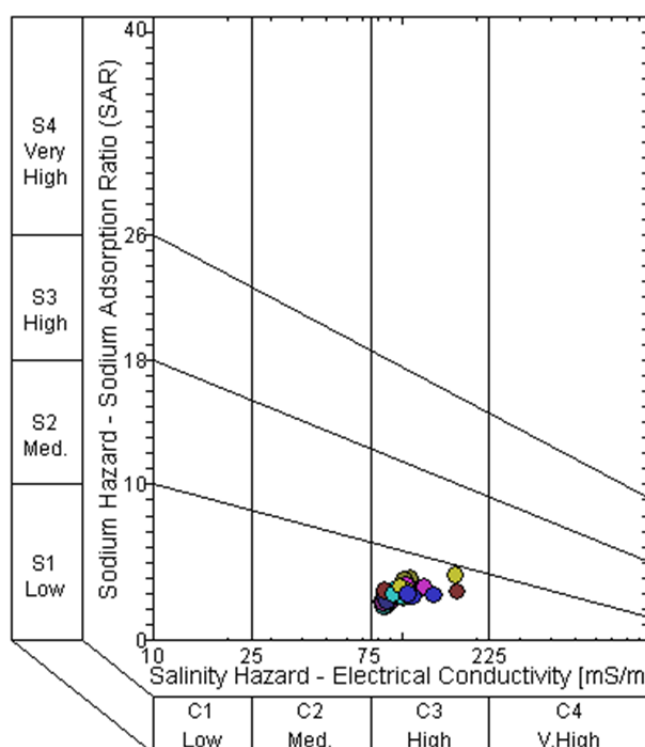


Figure 5-9 Classification of groundwater based on salinity and alkalinity hazard of irrigation requirements.

The groundwater is characterised by high salinity (C3) and would suit soils with improved drainage to flush out the salts. From a irrigation requirement point of view, the groundwater has generally low Na^+ concentration and there is less risk of harmful Na^+ effects. High HCO_3^- concentration in the

groundwater also has great potential to precipitate out of the calcium carbonate thereby increasing SAR in the groundwater. Total bicarbonate levels in the groundwater ranges from 373-613 mg/l and has a major contribution on elevated calcite and dolomite saturation indices.

5.4.2.3 Trace elements

Table 16 shows the maximum and minimum concentrations of trace elements analysed in the groundwater. The concentration levels of Fe^{+2} and Al^{+3} trace elements in the groundwater are all below the SANS (1996) target values. Manganese exceeded the water quality target value of (0.05 mg/l) in the groundwater samples and can be attributed sources of manganese oxides in the sediments. In general, trace elements in groundwater are often dissolved in very small quantities, typically less than 1 mg/l (USGS 1993). The presence of Mn^{+2} , Fe^{+2} and Al^{+3} in low concentrations is due to the dissolution of natural tracer elements from the aquifer sediments under anaerobic conditions into the groundwater.

Table 16 Maximum and minimum concentrations of trace elements analysed in the groundwater.

Ions	Minimum [mg/l]	Maximum [mg/l]	(SANS 1996) [mg/l]
Fe^{+2}	0.002	0.067	≤ 0.1
Mn^{+2}	0.006	0.090	≤ 0.05
Al^{+3}	0.008	0.049	≤ 0.15

In general, the hydrogeochemical investigation and analysis also shows that there is no distinction between the groundwater chemistry of deep and shallow boreholes. The results of this investigation can be used to ascertain the existence of one aquifer system as had been observed during borehole drilling. During groundwater abstraction at the site, water comes from the high transmissivity gravel-sand deposits which are conceptually the main aquifer yielding layer. The groundwater samples from the seepage zone also exhibit similar hydrogeochemical trend to the rest of the groundwater samples collected from the boreholes. It is therefore evident that the shallow alluvial channel aquifer is losing groundwater into the river, thereby making the river a “gaining” one

5.5 Summary

Chapter 5 discusses the investigation of the hydrogeochemical processes in an alluvial channel aquifer located in a typical Karoo basin of Southern Africa. The investigation was aimed at identifying and describing the groundwater evolution and its contribution to the overall groundwater quality. The XRF and XRD analysis was performed on representative geological samples to identify and quantify the major elements oxides and minerals in the sediments. The XRF and XRD analysis of

geological samples shows that the channel deposits are dominated by SiO_2 element oxides and quartz minerals thus elevated concentrations of Si were found in the groundwater. Samples of groundwater were collected in July 2010, February 2011, May 2011, August 2011 and December 2011. The study utilized the conventional piper diagram, bivariate plots and PHREEQC hydrogeochemical model to analyze groundwater chemistry data. Detailed studies of the hydrogeochemical processes in the alluvial aquifer system have shown that dissolution of dolomite and calcite minerals, and ion exchanges are the dominant hydrogeochemical processes that controls the groundwater quality. The study shows the potential usefulness of simple bivariate plots as a complimentary tool to the conventional methods for analyzing groundwater hydrogeochemical processes.

The next chapter discusses the investigation of groundwater recharge mechanism and process of the alluvial channel aquifer.

6 GROUNDWATER RECHARGE INVESTIGATIONS IN AN ALLUVIAL CHANNEL AQUIFER

6.1 Introduction

Identification and assessment of the sources and groundwater recharge mechanisms of the shallow alluvial channel aquifer system was performed using stable isotopes and conservative chloride. Water level fluctuations and respond to rainfall was also utilized as direct evidence to distinguish between different recharge mechanisms and quantifying the recharge rates. Groundwater recharge rates and mechanisms for the alluvial channel aquifer were extensively compared to that of the background terrestrial aquifer.

A good understanding of the groundwater recharge mechanisms and rates is important for both groundwater resource assessment (Luckey *et al.* 1986; Kearns and Hendrickx 1998) and aquifer vulnerability assessments (Scanlon and Goldsmith 1997). In general, the sustainable management and protection of groundwater resources requires a comprehensive understanding of the recharge mechanisms and rates. The study of GW-SW interactions also requires a comprehensive knowledge of groundwater recharge for both the terrestrial and alluvial channel aquifer. Groundwater discharge from the alluvial channel aquifer is an important facet of GW-SW interactions and this requires that the alluvial channel aquifer is recharged.

Alluvial channel aquifers are often characterised by shallow water table conditions and receives the majority of their recharge from rainfall through high preferential infiltration. Rapid groundwater level responds to rainfall events are therefore expected, making the water level fluctuations an important tool for estimating groundwater recharge rates in the alluvial channel aquifers. Analysis of the stable environmental isotopes can also provide qualitative information about the recharge sources and mechanisms. Although various techniques exist for recharge estimation, it is extremely difficult to assess the accuracy of any method (Healy and Cook 2002) and hence the application of multiple and complimentary methods cannot be overemphasized. This research uses stable isotopes, groundwater levels response to rainfall and infiltration tests (Section 4.1.2) as complimentary tools to identify and understand groundwater recharge processes of the alluvial channel aquifer. A comparison was drawn between the groundwater recharge processes of the alluvial channel aquifer to that of the background terrestrial aquifer.

6.1.1 Methods and materials

Groundwater and river water samples for isotope analysis were collected in February and May 2011. Samples collected in February represent the hot and wet season while May is characterised by cold and wet conditions. Groundwater samples were collected from boreholes drilled into the alluvial channel aquifer and background terrestrial aquifer. See the location of the boreholes on Figure 3-3.

Groundwater samples from the boreholes were collected after 20 minutes of purging at pumping rate of 0.3 l/s. The purged groundwater samples were collected once the pH, temperature and electrical conductivity (EC) had stabilized. One of the groundwater samples was collected from the water that discharges directly from the aquifer into the river. A bailer was used to collect river samples. The river samples were collected upstream, downstream and adjacent to the alluvial channel aquifer. All samples were collected into 1 litre plastic bottles and refrigerated until analyses. The samples were analysed for $\delta^2\text{H}$ and $\delta^{18}\text{O}$ stable isotope by iThemba Environmental Isotope Laboratory of South Africa.

6.1.1.1 Water level fluctuation method

The water level fluctuation (WLF) method (Equation 9) was used to quantify groundwater recharge rates using monitored groundwater level (Healy and Cook 2002). Groundwater levels were monitored throughout the rain season. The WLF method is based on the assumption and reasoning that increases in groundwater level is only due to groundwater recharge. In other words, any increase in groundwater levels implies that recharging waters has reached the aquifer after a rainfall event. The WLF method is therefore suited to shallow aquifers where groundwater level's respond to rainfall events is often quicker.

$$R = S_y \frac{\Delta h}{\Delta t}$$

Equation 9: Recharge (Water level fluctuation method).

Where: R is groundwater recharge, S_y is the aquifer specific yield, Δh is change in water levels and t is the time duration when the change in groundwater levels has occurred.

The WLF method was chosen as the most appropriate method to assess and quantify groundwater recharge of the alluvial channel shallow aquifer based on the following premise:

- The existence of a shallow water table to semi-confined conditions.
- There is quick and distinct rises in water levels after rainfall events (Figure 6-1).

- It was evident that groundwater recharge after precipitation was responsible for the increase in groundwater levels as compared to other factors such as barometric pressure, aquifer-inter flow and evapotranspiration.
- The method is not affected by the mechanisms through which recharging waters moves through the unsaturated zone.

The nature of the groundwater level respond to rainfall events was also used to distinguish between the recharge mechanisms of the alluvial channel shallow aquifer and terrestrial aquifer. Rapid response of groundwater levels to rainfall would imply the dominance of preferential recharge mechanism. On the other hand, slow response of groundwater level rise to rainfall events would imply the prevalence of piston/diffuse recharge mechanisms.

6.1.1.2 Chloride mass balance method

The chloride mass balance technique was utilized to determine the recharge flux for the alluvial channel aquifer and terrestrial aquifer based on Equation 10 (Wood and Stanford 1995).

$$q = \frac{P C l_p}{C l_{gw}}$$

Equation 10: Groundwater recharge flux (Chloride mass balance method).

Where: q is the groundwater recharge flux, P is the average annual precipitation, $C l_p$ is the weight-average chloride concentrations in precipitation, and $C l_{gw}$ is the average chloride concentration in the groundwater.

In South Africa, individual samples from various rainfall depths reported Cl^- concentration levels between 0.1 and 0.5 mg/l during the peak rainfall months (January and March) of the season (Van Wyk *et al.* 2011). Eriksson (1952) reported average weighted chloride concentration for dry and wet precipitation samples for the Bloemfontein city in South Africa of 0.9 mg/l. A conservative precipitation average chloride concentration of 1 mg/l was used for recharge calculations in this study. For the application of chloride mass balance recharge estimation technique in this study, the following assumptions were made:

- The major source of chloride in groundwater was precipitation.
- The alluvial channel aquifer and terrestrial aquifers receives their main recharge by direct precipitation which infiltrates through the unsaturated zone.
- There are no external sources and sinks of chloride between the surface and water table.

Considering that the alluvial channel shallow aquifer has been discharging groundwater into the river for hundred years, significant soluble chloride minerals in the deposits should have been flushed out.

6.2 Results and discussions

6.2.1 Water level fluctuations

Table 17 and Table 18 shows monthly groundwater recharge values and rates calculated for the boreholes drilled into the alluvial channel shallow aquifer and terrestrial aquifer respectively. The groundwater levels were recorded during the (2010-2011) rainy season (Appendix 3.1). Groundwater levels rises in the boreholes were recorded after rainfall events and this justifies the application of WLF method. A conservative average specific yield value of 0.1 was used based on literature. For unconfined aquifers, specific yield typically ranges from 0.1 to 0.3 (Freeze and Cherry 1979).

Table 17 Monthly groundwater recharge rates calculated using Equation 9 for the boreholes drilled into the alluvial channel aquifer during the (2010-2011) rainy season.

Borehole name	Groundwater recharge in 2011 [mm]						Total [mm]
	Jan	Feb	Mar	Apr	May	June	
BH3	10	9	9	2	9	24	63
BH5	7	3	4	1	5	17	37
BH6	9	4	4	1	7	22	47
BH7	7	5	10	8	6	19	55
BH8	10	7	8	1	8	25	59
BH9	13	3	11	5	7	33	72

Table 18 Monthly groundwater recharge values and rates calculated using Equation 9 for the boreholes drilled into the terrestrial aquifer channel aquifer during the (2010-2011) rain season.

Borehole name	Groundwater recharge in 2011 [mm]						Total [mm]
	Jan	Feb	March	May	June	July	
BH10	2	2	8	8	14	23	57
BH11	6	1	14	14	16	16	67
BH12	5	1	9	9	18	16	58
BH13	5	1	32	12	17	14	81
BH14	10	0	9	9	12	4	44
BH15	8	3	7	7	14	5	44

Harmonic mean accumulated recharge rates of 53 and 55 mm were calculated for the alluvial channel shallow aquifer and terrestrial aquifer respectively. Using a total rainfall amount of 680 mm/yr, the groundwater recharge values translate into 8 % of the total rainfall/yr for the two aquifers. Although the aquifers are characterised by different recharge mechanisms, their yearly accumulative recharge values are the same.

The alluvial channel main aquifer is characterised by a shallow water table (< 3 mbgl) which implies that recharging waters takes a short time to reach the water table in comparison to the deeper water table of the terrestrial aquifer (> 8 mbgl) (Appendix 3.2). Preferential infiltration on the riparian zone also contributes to quick recharge of the alluvial channel aquifer. While on the terrestrial aquifer, the recharging water takes longer time to reach the water table due to the thick overlying unconsolidated sediments. The thick unconsolidated overburden above the terrestrial aquifer has the potential to allow accumulation of recharging waters from different rainfall events that can be released later into the aquifer. It can therefore be inferred that the alluvial channel aquifer is characterised by quick-preferential but short lived recharge while in the terrestrial aquifer the recharge is slow and prolonged. However the amount of rainfall that reaches the two aquifer systems in a year is effectively the same.

6.2.2 Groundwater level response to rainfall

The nature and time of groundwater level respond to rainfall events was used as a qualitative tool to assess and identify recharge mechanisms. Figure 6-1 shows monthly groundwater levels and average rainfall monitored from August 2010 to September 2011. The results indicate rapid groundwater level respond to rainfall for the alluvial channel aquifer. Lagged and steady groundwater level respond characterises the terrestrial aquifer. In general, the magnitude of the water level rise in the alluvial channel aquifer is high as compared to the terrestrial aquifer. This is mainly attributed to short travelling distances and preferential recharge in the alluvial channel aquifer.

High rainfall amounts recorded in February and June 2011 were associated with flooding storms and these resulted in significant rise of the ground water levels in the alluvial channel aquifer (Figure 6-1). However, due to continuous seepage discharge, it only takes about a day before the groundwater levels start to recede again. Due to high transmissivity of the gravel-sand deposits and continuous seepage discharge, the recharged groundwater of the alluvial channel aquifer has low residence time. It therefore becomes very difficult to see the effect of low rainfall events on the alluvial channel aquifer groundwater levels. In other words, the recharging rate from a rainfall event has to surpass the seepage discharging rate, for groundwater level to start increasing in the aquifer.

Besides meeting the discharge requirements, the recharging waters will also have to fill the high pore storage spaces of the alluvial channel deposits. For instance, the low rainfall measured for October, September and November 2010 did not result in groundwater level increase in the alluvial channel aquifer (Figure 6-1).

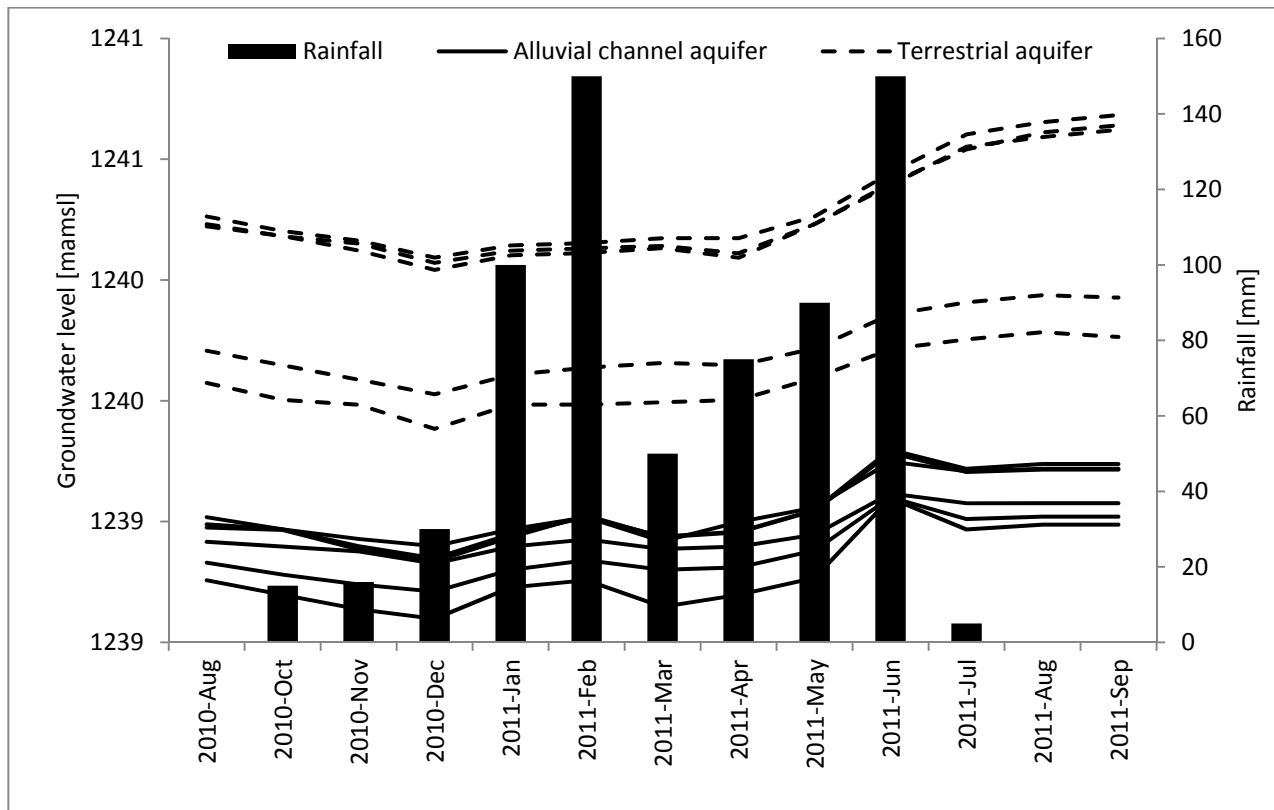


Figure 6-1 Groundwater level responds to rainfall measured during the monitoring period from August 2010 to September 2011; rainfall amounts were derived qualitatively from historical rainfall maps of the South African weather service (*WeatherSA* 2011).

The water levels for the boreholes located in the terrestrial aquifer shows steady rises in respond to rainfall as indication of the slow piston recharge process (Figure 6-1). Due to thick overburden of low permeability properties, the infiltrating water takes long time to reach the terrestrial aquifer. It therefore implies that the recharging of the terrestrial aquifer is a very slow and prolonged process. The duration of the recharging process is shown by the steady rise of water levels that continued from the June 2011 rainfall event to August 2011. During the long recharging process, there is great potential for infiltration fronts from different rainfall episodes to combine.

It is important to acknowledge the contribution of the terrestrial aquifer in recharging the alluvial channel aquifer through aquifer-interflow during the dry season. The dominance aquifer-inter flow

can be noticed by the similar steady rate of groundwater level decrease in the two aquifer systems during the dry season and early periods of the rainfall season. The similar steady rate of groundwater level decrease can be used to infer the occurrence of the same groundwater flow characteristics between the two aquifer systems during the dry period. It therefore provides further evidence to suggest that through aquifer-inter flow, the terrestrial background aquifer is an important source of recharge to the alluvial channel aquifer during this period.

A question can therefore be raised as concerning the main recharge mechanism for the alluvial channel aquifer. During the rainy season, the alluvial channel aquifer is mainly recharged through preferential infiltration from precipitation. However during the dry seasons, the alluvial channel aquifer mainly recharges through aquifer-inter flow from the terrestrial aquifer. Considering that groundwater is often used for irrigation during dry seasons in farming areas situated along perennial rivers, aquifer-inter flow from the terrestrial aquifer has an important role to sustaining the alluvial channel aquifer. A comprehensive understanding of the two aquifers is therefore needed for groundwater resource development and GW-SW interactions.

In the alluvial channel shallow aquifer, the increase in groundwater level can only be regarded as a temporary condition which cannot form the basis of quantifying average yearly groundwater recharge of the aquifer. Quantification of recharge rates in alluvial aquifer characterised by preferential recharge due to high infiltration rates has to consider both the contribution of rainfall and aquifer-inter flow from terrestrial aquifer during the dry season. During the rainfall season, the quantification of the amount of water that goes into storage during the quick rise in groundwater levels is more important than the actual rise itself because it can later be released to sustain the natural system once the episodes have elapsed.

6.2.3 Chloride mass balance

Table 19 and Table 20 shows groundwater chloride concentrations measured during two sampling runs. A total average rainfall of 680 mm/year was used for the calculations. This data is not sufficient to estimate yearly groundwater recharge as it does not incorporate other recharge events. The data will only give a reflection of recharge during these two month recharge events. A comparison of recharge rates estimated from the WLF method and CMB methods can only be between the months of February and June 2011. The two months on average received about 150 mm of rainfall.

Table 19 Average monthly groundwater chloride concentrations and the calculated recharge rate [mm] for the alluvial channel aquifer.

	2011-Feb	2011-June	2011-Feb	2011-June
Borehole name	Cl [mg/l]	Cl [mg/l]	Recharge [mm]	Recharge [mm]
BH3	70.00	71.00	1.90	1.90
BH5	61.00	68.00	2.20	2.00
BH6	60.00	62.00	2.30	2.20
BH7	60.00	63.00	2.30	2.10
BH8	69.00	73.00	2.00	1.80
BH9	70.00	76.00	1.90	1.80

Table 20 Average monthly groundwater chloride concentrations and the calculated recharge rate for the terrestrial aquifer.

	2011-Feb	2011-June	2011-Feb	2011-June
Borehole name	Cl [mg/l]	Cl [mg/l]	Recharge [mm]	Recharge [mm]
BH10	57	60	2.37	2.25
BH11	59	65	2.29	2.08
BH12	57	61	2.37	2.21
BH13	59	62	2.29	2.18
BH14	51.4	57	2.63	2.37
BH15	48.8	55	2.77	2.45

In general, the recharges rates determined based on the groundwater chloride for the samples collected after the February 2011 and June 2011 rainfall events in less as compared to those from the WLF method. The high chloride in the groundwater samples is due to elevated chloride level in the background from calcrete and halite related minerals. The CMB recharge estimation technique has very limited applications in the alluvial channel aquifer at the case study site.

6.2.4 Stable environmental isotopes ($\delta^{18}\text{O}$ and $\delta^2\text{H}$)

Figure 6-2 shows the plot of $\delta^2\text{H}$ against $\delta^{18}\text{O}$ for groundwater samples collected in February and May 2011. The groundwater $\delta^{18}\text{O}$ values ranges from - 4.95 ‰ to - 5.25 ‰ with a mean value of - 5.09 ‰ and a standard deviation of 0.08 ‰. The groundwater $\delta^2\text{H}$ ranges from -31.28 ‰ to -34.40 ‰ with a mean value of -32.78 ‰ and a standard deviation of 0.78 ‰. The negative values of $\delta^2\text{H}$ against $\delta^{18}\text{O}$ indicate depletion of the isotopes relative to the Vienna Standard Mean Ocean Water (VSMOW).

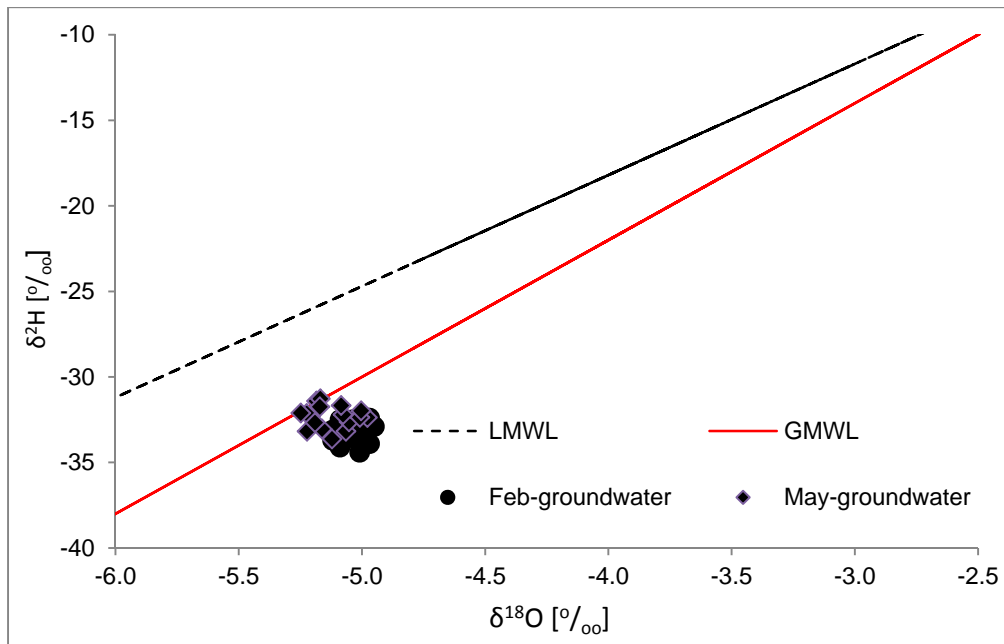


Figure 6-2 Plot of $\delta^2\text{H}$ against $\delta^{18}\text{O}$ for groundwater samples showing the deviation from the GMWL and LMWL; GMWL: $\delta^2\text{H} = 8 \cdot \delta^{18}\text{O} + 10$; LMWL Pretoria: $\delta^2\text{H} = 6.5 \cdot \delta^{18}\text{O} + 7.8$; (IAEA/WMO, 2004).

The groundwater $\delta^{18}\text{O}$ and $\delta^2\text{H}$ plot below but closer to the Global Meteoric Water Line (GMWL) of Craig (1961) (Figure 6-2). The Local Meteoric Water Line (LMWL) for Bloemfontein, or for any other place in Free State Province of South Africa, is yet to be established. The nearest available LMWL is from Pretoria which is situated about 500 km north of Bloemfontein (IAEA/WMO, 2004). Although the isotopic compositions of $\delta^{18}\text{O}$ and $\delta^2\text{H}$ of groundwater from the alluvial channel and terrestrial background aquifer plot close to the GMWL, they all plot far off below the nearest LMWL indicating evaporation effects (Figure 6-2). It can therefore be inferred that the groundwater in the aquifer was exposed to evaporation effects prior or during the recharging process.

6.3 Recharge conceptual model

The recharge conceptual model was developed to describe the location and the likely mechanisms of recharge based on the theoretical understanding and field evidence. Two different recharge mechanisms can be defined for the alluvial channel aquifer and background terrestrial aquifer respectively. Although the study has been conducted at local scale investigation, spatial variation of the recharge mechanisms and rates is highly possible due to the heterogeneity nature of the subsurface. Figure 6-3 shows the conceptualised recharge mechanisms for the two aquifer systems.

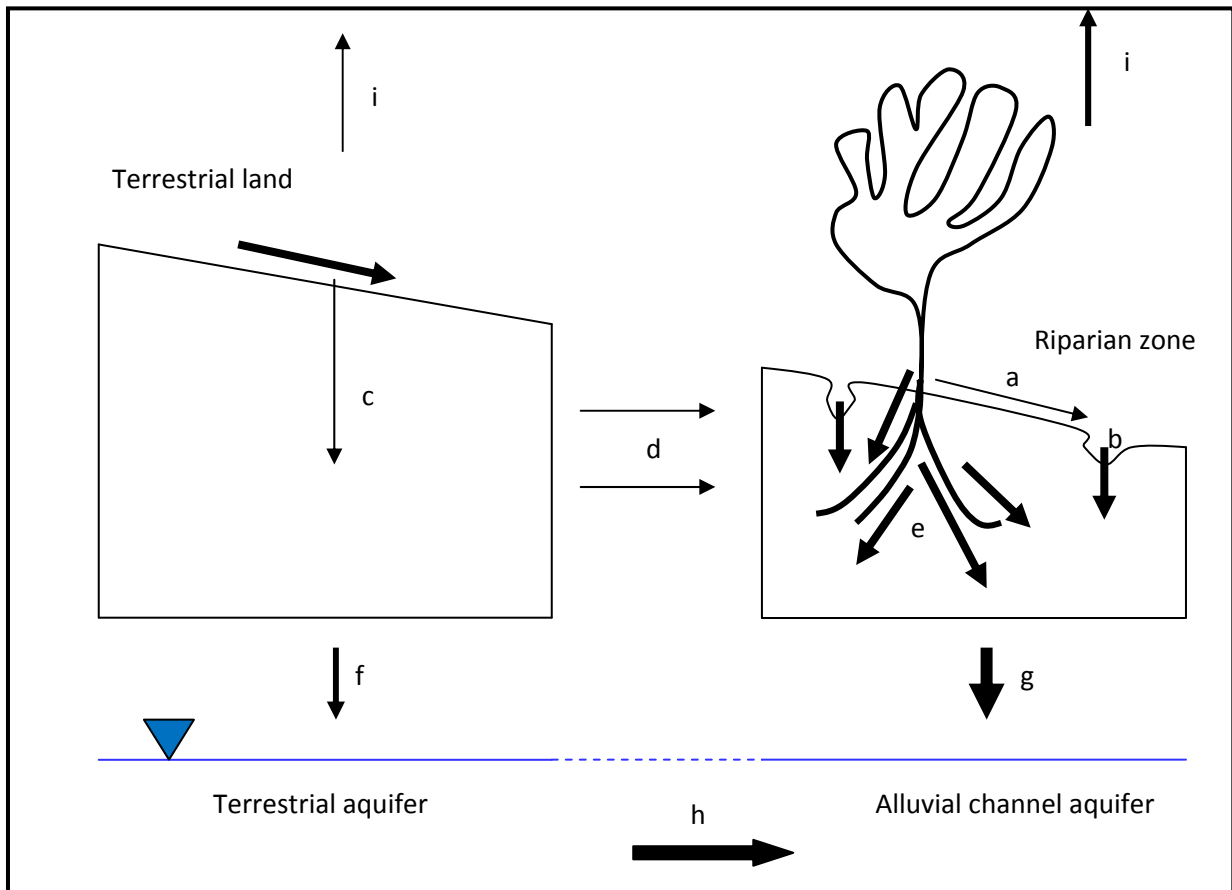


Figure 6-3 Idealized groundwater recharge processes for the alluvial channel aquifer and the terrestrial aquifer; big arrows represent large quantity parameters; the furthest borehole in the terrestrial land is located about 500 m from the river bank.

Preferential infiltration (e) of the accumulated surface runoff (a) on the riparian zone is the major recharge mechanism for the alluvial channel aquifer. Preferential infiltration is facilitated by openings created by tree rooting system. Cavities and holes (b) created by the burrowing animals also contribute to high infiltration rates on the riparian zones. Figure 6-4 shows some of the holes that have been created by burrowing animals on the riparian zone, arrows points at some of the identified holes and cavities. In general, it is expected that there will be high evapotranspiration (i) on the riparian zone in comparison to the terrestrial land.

Surface runoff from the terrestrial land also accumulates on the lower riparian zone and thereby enhancing the amount of water available to infiltrate into the shallow alluvial channel aquifer. The high slope of the terrestrial land assists in generating surface runoff (a) and unsaturated zone drainage (d) water towards lower elevated riparian zone. These processes result in high recharge rate (g) for the alluvial channel aquifer that leads to rapid groundwater level rise.



Figure 6-4 Photos showing some of the holes that have been created by burrowing animals on the riparian zone; arrows points at some of the identified holes and cavities.

Aquifer-interflow (h) from the terrestrial aquifer is also an important source of recharge for sustaining the alluvial channel aquifer particularly during the dry season. The background terrestrial aquifer mainly recharges through diffuse infiltration (c) in the soil matrix. The terrestrial zone is generally characterised by low infiltration rates as governed by low permeability of calcareous soils and sparse vegetations. Due to the thick overburden, the recharging process of the terrestrial aquifer is generally slow and prolonged.

The findings of this investigation suggest that the alluvial channel aquifer located in the riparian zone receive its recharge from the background terrestrial aquifer for the majority time of the year. It therefore implies that quantification of groundwater recharge in this type of aquifer should consider the contribution of the terrestrial background aquifer.

6.4 Summary

An investigation was conducted on the recharge mechanisms and processes of the alluvial channel shallow aquifer and terrestrial background aquifer. Qualitative analysis of stable isotopes and groundwater levels' response to rainfall events were used as complimentary tools to identify and delineate groundwater recharge of a typical alluvial channel aquifer. The WLF method was used to quantify the groundwater recharge of the two aquifers. The WLF method is more suited for shallow aquifers where groundwater levels response to rainfall events is often quicker. The alluvial channel

aquifer is characterised by shallow water table conditions (< 3 mbgl) and quick groundwater level response to rainfall events justifying the application of the WLF method. An attempt was also made to quantify groundwater recharge based on conservative groundwater chloride ions.

The recharging of the alluvial channel aquifers occurs through high preferential infiltration rates as facilitated through openings created by tree roots. Cavities and holes created by the burrowing animals also contribute to high infiltrations rates along the riparian zones. The recharge of the terrestrial aquifer mainly occurs by slow diffuse infiltration through the thick unconsolidated overburden. Harmonic mean accumulated recharge rates of 53 and 55 mm/yr were calculated for the alluvial channel aquifer and terrestrial aquifer respectively using the WLF method. Using a total rainfall amount of 680 mm/yr, the groundwater recharge values translate into 8 % of the total rainfall in the two aquifers.

The next chapter discusses the natural gradient tracer tests performed in the typical alluvial channel aquifer.

7 NATURAL GRADIENT TRACER TEST IN AN ALLUVIAL CHANNEL AQUIFER

Tracer tests were conducted with the main objective of estimating solute transport parameters and groundwater flux of the alluvial channel aquifer under natural conditions. Natural groundwater flux is important for estimating groundwater discharge which is an important facet of GW-SW interaction studies. In general, a good understanding of the solute transport parameters of an alluvial channel aquifer is essential for the protection and management of the GW-SW systems.

A total of four natural gradient tracer test (NGTT) were conducted in the boreholes drilled into the alluvial channel aquifer. All the boreholes used for the NGTT fully penetrate the shallow alluvial channel aquifer system. The utilization of these boreholes enabled assessment of the solute transportation properties of the gravel-sand aquifer materials. A complete set of data measured during the tracer testing is found in the appendix data disc.

7.1 Natural gradient point dilution tracer test

The field of single-borehole tracer test has seen a number of borehole logging methods being developed, for instance in; Kading 1976, Momii *et al.* 1993 and Kearl 1997. The single-borehole tracer dilution technique that measures the rate at which groundwater inflow into the borehole dilutes the tracer is still the best and appropriate method to estimate the horizontal groundwater flux (Pitrak *et al.* 2007). Diffusion and density effects can however have some influences on the tracer dilution rates, thus can affect the outcome of the test. In total, two NGPDTT were performed. The first one was conducted as a trial test to determine the appropriate quantities of the salt tracer to be injected and also assess the density effects on the rate of tracer dilution.

7.1.1 Design of the experiment and salt solute injection system

The design of the salt tracer solute injection system utilized the most basic tools and techniques which were perceived to be most likely available in any average testing environment. The salt tracer was injected into the system using a perforated 1 litre plastic bottle (Figure 7-1). The salt was poured into the container which was then lowered into the injection zone for mixing using a rope. Mixing was done manually by moving the container up and down within the injection zone until the background EC had increased significantly. The injection container was then taken out after the desired EC increase had been achieved. Two sets of NGPDTT were conducted to verify the applicability of the injection method.



Figure 7-1 A photo showing the perforated 1 litre plastic container that was used for injecting the salt solute into the testing borehole.

The salt tracer provides the best option in terms of affordability, accessibility and easy monitor. The dilution of the salt tracer was monitored by measuring EC. Although bromide, chloride and the fluorescein dye are ideal because of their conservative nature, there were no automated probes to measure their concentrations in situ. A bailer could be used for sampling, but that would most likely result in tracer mixing thus potentially offsetting the natural conditions.

7.1.1.1 Tracer testing zone

The testing zone to inject the salt solute tracer was determined based on the understanding gained from the geological logs, EC profiling and aquifer testing. BH7 borehole was selected based on its high T of 89 (m^2/d) which was inferred to imply the existence of high horizontal groundwater flux in the vicinity of the borehole. High groundwater fluxes generally imply quick dilution of the tracer which results in shorter time for performing test.

Geological logs show that the zone between 6-9 mbgl comprises of gravel-sand channel deposits (Figure 7-2) that is characterised by high hydraulic conductivities. Electrical conductivity logging in BH7 borehole indicates an anomaly between 6-8 mbgl (Figure 7-2) thus proving additional evidence to infer the location of the main flow zone.

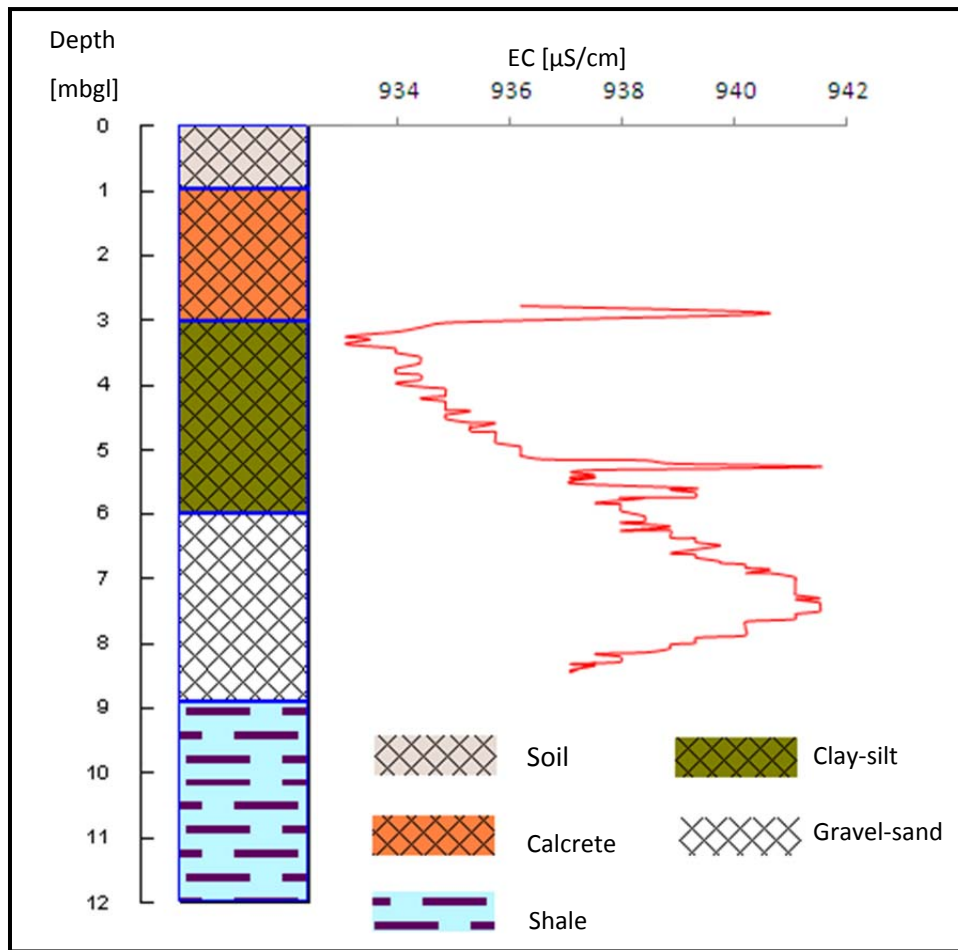


Figure 7-2 Borehole BH7 geological log and EC profiling showing EC anomaly between 6-9 mbgl that is associated with the gravel-sand main flow zone of the alluvial channel aquifer.

7.1.1.2 Measurements and accuracy

The EC was measured to monitor tracer dilution during the NGPDTT. The EC was measured using a Solinst Level Temperature Conductivity (LTC) logger junior which was placed at 7 mbgl. The logger has an accuracy of 2 % with resolution of 1 $\mu\text{S}/\text{cm}$. Although accuracy is an important facet of scientific measurements, in this point dilution test the trend and resolution was considered to have more significant implications for groundwater flux calculations. Under natural groundwater flow conditions any deviations that might occur from the true measurement due to the 2 % accuracy level were assumed to be constant. In other words, the equipment accuracy factor will have a constant effect on the measured EC readings and therefore would not affect the overall trend. The EC measurements in all the NGPDTT are within the resolution of the logger.

7.1.1.3 Data analysis

Groundwater flux was determined based on the approach that was developed by Drost *et al.* (1968) (Equation 11).

$$q = \frac{W}{\alpha A t} \ln \frac{C_0}{C}$$

Equation 11: Groundwater flux (Darcy velocity).

Where:

W	=	volume of fluid contained in the test section (m ³).
A	=	cross sectional area normal to the direction of flow (evaluated from $\pi r L$, assuming a radial flow model with $n = 2$) (m ²).
C ₀	=	tracer concentration at t = 0.
C	=	tracer concentration at time = t.
α	=	borehole distortion factor (between 0.5 and 4; = 2 for an open well) (note that $q\alpha = v^*$, where v^* = apparent velocity inside well).
t	=	time when concentration is equal to C (days).
L	=	test section length (m).

The EC measurements were standardized before calculations using Equation 12. Standardization of EC tracer solute measurements enables calculations to be done in the relative concentration ratios irrespective of the initial units of measurements.

$$C_t^* = \frac{C_t - C_b}{C_0 - C_b}$$

Equation 12: Tracer concentration standardization.

The EC measurements were standardized such that: $C_t^* = 1$ at $t = 0$ and $C_t^* = 0$ at $EC = EC$ (background).

Where: C_t^* = Standardized concentration.

C_t = Equivalent concentration at different times after tracer injection.

C_b = Background concentration in groundwater.

C_0 = Concentration in the borehole at $t=0$.

7.1.1.3.1 Density effects

When the tracer is dissolved in the borehole test section, the resulting solute becomes denser than the fresh groundwater. The overall effect is that the denser solute finds it easier to sink down than moving horizontally due to natural groundwater flux. The sinking down of tracer solute is responsible for sharp gradients at initial periods of the dilution plots (Figure 7-3). Initial slope of point dilution plots has been used in some studies for calculating groundwater fluxes (Riemann *et al.*

2002, Pretorius 2007, Gomo 2009, Shakhane 2011 and Leketa 2011). The use of the density affected portion of the dilution curve will result in extremely high groundwater fluxes being calculated. With this understanding, it therefore implies that the higher the initial concentrations of tracer solute in the test section, the greater the density effect on the initial dilution rates.

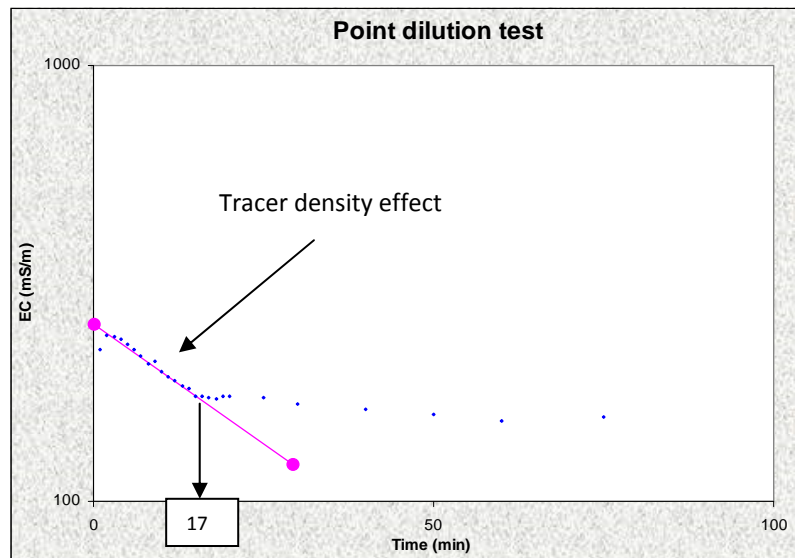


Figure 7-3 Typical influence of density effect on tracer initial dilution rates (Taken from Shakhane 2011).

Significant number of studies typically on landfill leachate plumes and tracer tests are not taking into considerations the variable density effects on plume development. The analysis of tracer dilution is often based on the assumption that density effects are small in comparison to other competing factors with no substantial justification (Simmons 2005). It has long been shown that even the tracer density effect that causes small differences in concentration can induce density driven flow on the tracer dilutions (Simmons 2001; and Diersch and Kolditz 2002). It is therefore important to understand and distinguish between the hydraulic gradient and density driven flow. Representative groundwater fluxes can only be determined from natural hydraulic gradient driven tracer dilutions. Although substantial efforts have been placed on assessing the influence of density driven flow on tracer dilutions, there is no reliable approach that has been developed to deal with the problem (Simmons 2005). Is upon such a background that a qualitative approach was developed to identify and isolate the density effects on the dilution curve prior to the calculation of groundwater flux.

7.1.1.3.1.1 Qualitative analysis

A qualitative approach was used to select the appropriate portion of the curve where the density effect on the dilution rate can be regarded as minimum. Most of the analysis of point dilution tracer tests is based on the mathematics developed by Drost *et al.* (1968) (Equation 11). Based on this

equation, for a dilution plot (concentration against time) to reflect true natural horizontal groundwater flux conditions it has to be a straight line. It therefore implies that the longest portion of the dilution curve that can be fit by a straight line should be used for horizontal groundwater flux calculations.

The straight portion of the dilution curve with the longest time period was then presumed to reflect groundwater flux under natural gradient conditions. In this experiment it was apparent that the end portion of the tracer dilution curve was the only one affected by minimum density effects because of the prevailing low concentrations gradients. With minimum density effect on the tracer dilution rate, the end time portion of the tracer dilution curve would give horizontal groundwater flux rates representative of the natural conditions. Figure 7-4 shows the EC against time dilution plots between; (a) 0-3300 minutes, (b) 400-3300 minutes and (c) 1800-3300 minutes.

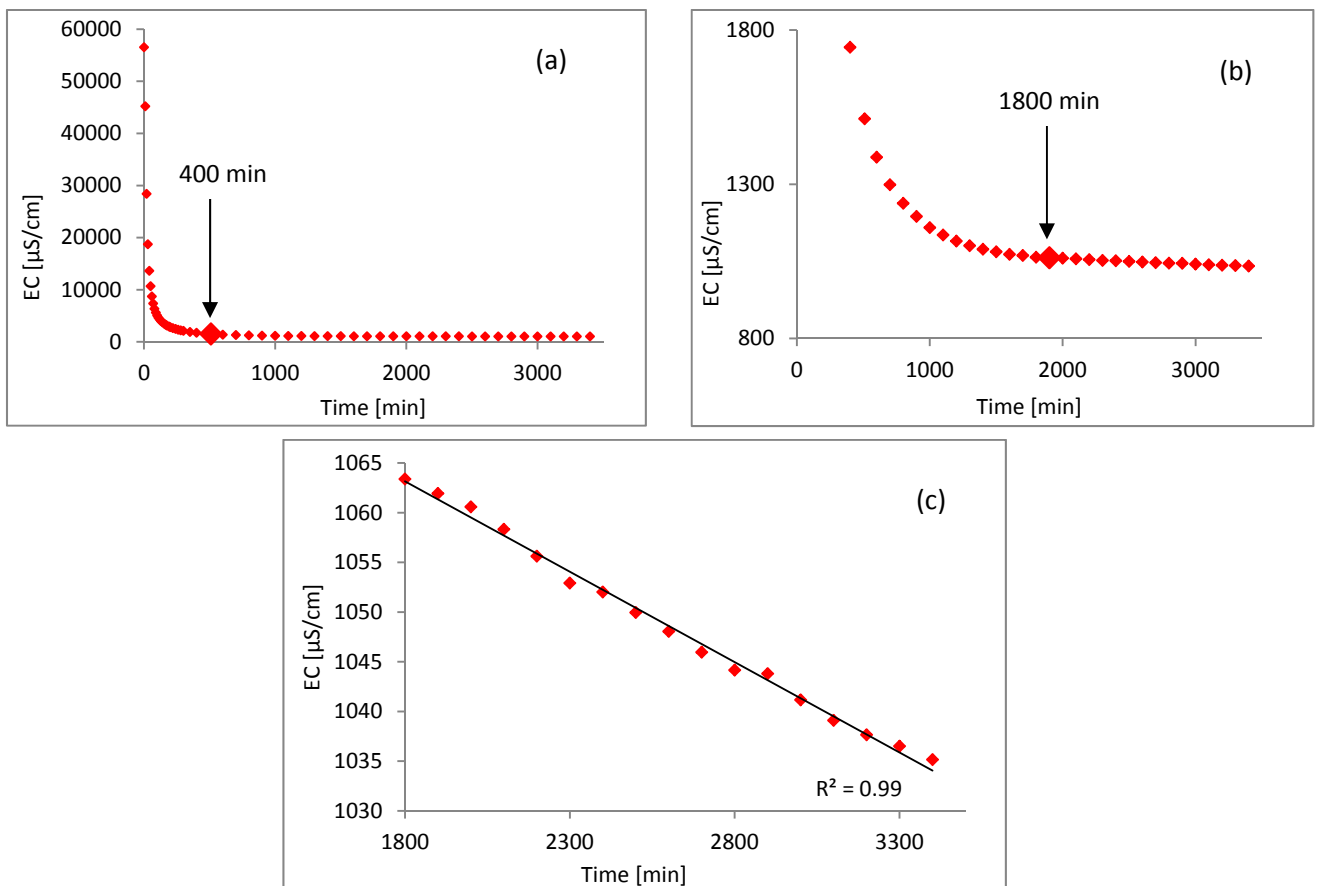


Figure 7-4 NGPDTT dilution plots of EC against time; (a) The whole dilution plot from 0-3300 minutes; (b) Dilution plot from 400-3300 minutes and (c) Dilution plot from 1800-3300 minutes.

Based on the visual inspection of plot (a) (Figure 7-4), it was presumed there was a good chance of getting a constant slope from 400 minutes. The presumption would imply that the dilution plot from

0-400 minutes is solely due to the density effects. A dilution plot from 400 minutes was then made (Figure 7-4, plot b) and from the visual inspection it was deduced that the dilution period between 400-1800 minutes is still under the density effects. The last plot (c) was then made from 1800-3300 minutes and it yielded a straight line of $r^2 = 0.99$, thus reflecting the rate of tracer dilution that is predominantly due to horizontal groundwater flux in the borehole test section. The dilution segment from 1800-3300 minutes is characterised by minimum density effects as indicated by the straight line fit. The constant dilution rate of the last segment lasted for 1621 minutes which is equivalent to more than 1 day. According to Equation 11, a constant dilution gradient is a reflection of natural horizontal groundwater flux conditions. In other words, a constant dilution gradient that was maintained for more than 24 hours can only be attributed to natural groundwater flux that is free of density effect.

7.1.1.4 Dilution plots

The first NGPDTT was performed as a preliminary investigation to assess the influence of density on the tracer dilution in the single-borehole test. Figure 7-5 shows the portion of the dilution curve which was selected to determine groundwater flux after the removal of the density driven flow effects (7.1.1.3.1.1) during NGPDTT 1.

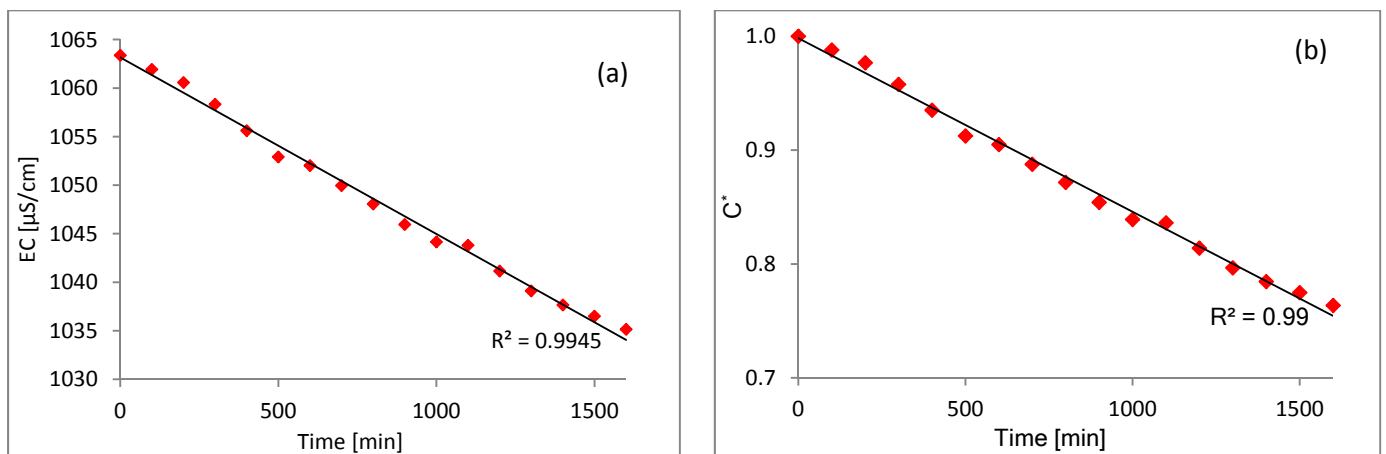


Figure 7-5 NGPDTT measurements for test 1; (a) LTC levellogger EC measurements and (b) Standardized EC measurements.

The second NGPDTT was then designed taking into consideration the possible effects of the density on the dilution curve. A salt solution of about 1500 $\mu\text{S/cm}$ EC was prepared and injected into the point dilution testing borehole BH7. The point dilution was conducted to verify the Darcy velocity (q) calculated from the first test. It was also important to test the hypothesis that there was going to be negligible density effect below an initial tracer solute concentration of 1500 $\mu\text{S/cm}$. During the

density effect correction on NGPDTT 2 dilution curve, only the first 300 minutes had to be removed from the whole dilution curve. Figure 7-6 shows the NGPDTT measurements made during test 2 and has been corrected to remove the density effects.

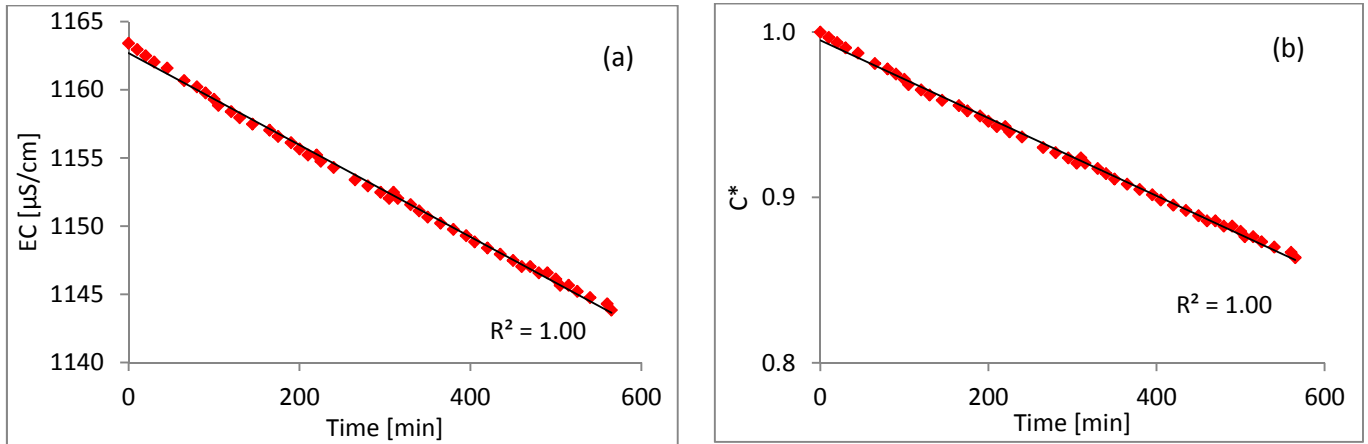


Figure 7-6 NGPDTT measurements for test 2; (a) LTC levellogger EC measurements and (b) Standardized EC measurements.

Table 21 shows the groundwater flux values determined from NGPDTT and other parameters of the equations that were utilized during the calculations. The groundwater flux values from the two NGPDTT tests are closely comparable. In general, it shows that the tests can be repeated getting very close results, thereby giving credentials to the testing and analysing procedure.

Table 21 Groundwater flux (q) determined from the NGPDTT in BH7 borehole and other parameters used during the calculations.

Test number	C ₀	r [m]	L [m]	α	Duration [min]	q [m/day]
Test 1	1061.48	0.075	0.3	3	1160	0.05
Test 2	1176.62	0.075	0.3	3	860	0.04

The alluvial channel aquifer is generally characterised by low local groundwater fluxes and can be attributed to the low localized hydraulic gradient existing in the aquifer. It is important to distinguish between the local and discharging flux. The alluvial channel aquifer can be divided into the local or main aquifer and the discharging component of the aquifer. Local flux is can therefore be defined as groundwater flux that occurs in the main aquifer itself while discharging flux occurs on the discharging component. The discharging flux should be generally high because of the high head differences between the water levels of the alluvial channel aquifer and the discharging contact plane.

7.1.1.5 Summary NGPDTT in alluvial channel aquifers

Contrary to some previous analysis of point dilution tracer tests in the typical Karoo fractured-rock aquifers where the early time fit has been used for determining groundwater fluxes (Riemann et al. 2002), it is actually the end time fit that can potentially give groundwater flux estimates which are close to natural horizontal flow conditions. Using the early time portion of the dilution curve will result in exceptionally high groundwater flux being calculated due to the density driven dilution.

After taking off the density effect, the NGPDTT tests were technically monitored until at least 24% of the initial tracer EC concentration had been diluted due to natural groundwater flux. Under natural gradient it would require exceptionally large time to achieve 90 % dilution due to groundwater flow (excluding the density effects). Riemann (2002) had recommended 90 % dilution of initial injected tracer but the analysis did not take into consideration the density effect on the dilution curve. Without excluding some of the density effect, this current study indicates that even 99 % dilution can be easily achieved.

Without any quantitative computations, it is very difficult to give some technical guidelines on how to isolate or remove the density effects on tracer dilution curves before using the data for groundwater flux calculations. However, based on the study findings, the following measures can be taken to minimize density driven flow on the tracer solute dilution and consequently on plume development:

- The aquifer should be dominated by horizontal groundwater flow and this can be assessed from determined aquifer transmissivity and also geological properties.
- Conducting a preliminary test to identify the appropriate concentration to be injected.
- Avoiding using the early time data of the dilution curve.
- Select the longest segment from the dilution curve that can be fit by a straight line.
- Target the end time segments of the dilution curve.

7.2 Natural gradient tracer breakthrough test

Natural gradient tracer breakthrough (NTGB) is obtained when the injected tracer is monitored in the observation boreholes placed down gradient of the injection borehole under natural groundwater flow conditions. The test requires a good understanding of the natural groundwater flow directions to avoid missing the tracer. Natural hydraulic gradient can be defined as that gradient which occurs under natural conditions, that is when no abstraction is taking place. However within the context of natural hydraulic gradient flow, two scenarios of low and high natural gradient

often exist in alluvial channel aquifers. During wet seasons, the quick and rapid preferential recharge potentially creates high gradients as compared to dry seasons when gradients are generally low. The high wet and low dry season natural hydraulic gradients have different effects on the tracer movement and hence contamination migration. It is therefore necessary to define the nature of the natural hydraulic gradient when conducting a natural gradient tracer breakthrough test (NGTBT). Only one of the NGTBT was successful and will be discussed under this section.

7.2.1 Test field design

The NGTBT was designed to assess contamination migration in 1-Dimension along the natural principal groundwater flow direction. Considering the high hydraulic properties of the alluvial channel aquifer, it was expected that advection process would be the main important transportation mechanism. The anticipated dominance of the advection process justified the application a 1-Dimensional model along the natural principal groundwater flow direction. The main aim of the test was to obtain solute transport parameters of the gavel-sand materials under natural groundwater flow conditions. Figure 7-7 illustrates the NGTBT field design and the idealized direction of tracer plume movement from the injection borehole (BH7).

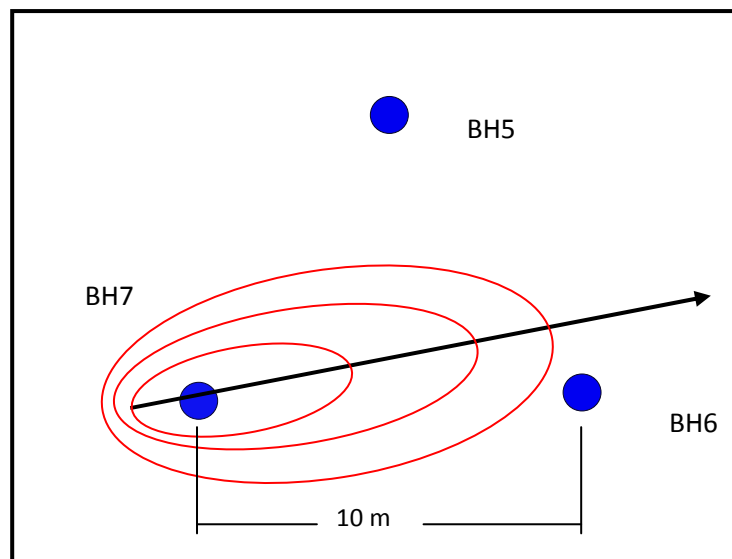


Figure 7-7 A schematic of the NGTBT field design and the idealized tracer plume movement from the injection borehole BH7; the arrow shows the principal direction of natural groundwater flow.

The salt tracer was injected in BH7 and the measurement of tracer breakthrough was done in BH6 using an LTC logger which was placed at 6.5 mbgl. The LTC provides the best way to measure tracer breakthrough under natural gradients because they often take exceptionally long time. Borehole BH6 was located closest to the principal natural groundwater flow direction and thus was used for tracer monitoring. Figure 7-8 shows an EC profile in borehole BH6 indicating an anomaly between

6-7 mbgl that is associated with the gravel-sand main flow zone. The EC profiling was conducted after the NGTBT. The elevated EC along the main flow zone is due to the salt tracer.

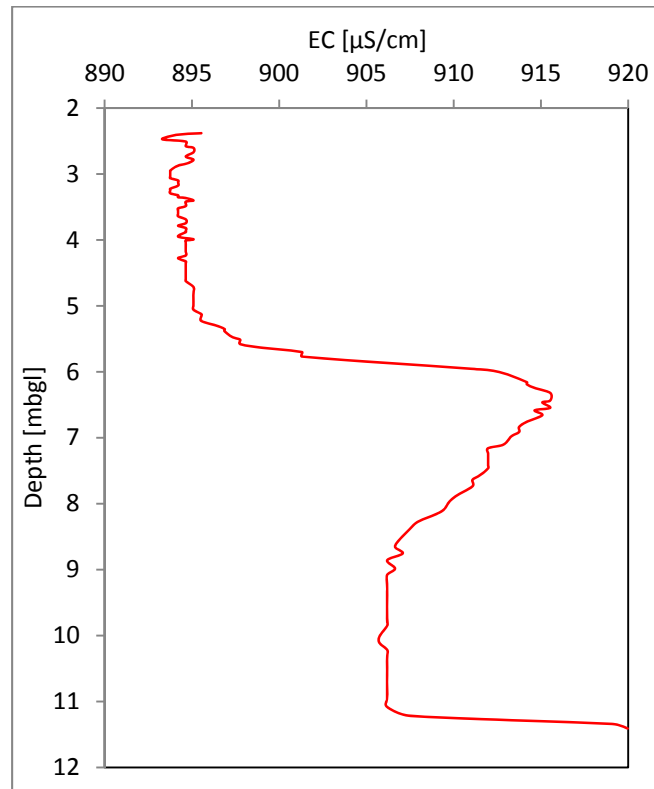


Figure 7-8 EC profile in BH6 indicating an anomaly between 6-8 mbgl that is associated with the gravel-sand main flow zone.

About 400 g of salt tracer was injected in BH7 borehole using the procedure described in section 7.1.1.1. The only difference is that for the NGTBT, the tracer source was left in the injection hole to deplete on its own. In this situation, the tracer injection can only be described as a long duration mode instead of the commonly used “instantaneous or pulse injection” mode. High salt tracer mass had to be injected for the fear that too little would get diluted before reaching the monitoring borehole.

7.2.2 Tracer breakthrough

Figure 7-9 shows the EC tracer breakthrough curve obtained from EC measurements made in BH6 borehole. In total, it took about six days for the front of the tracer solute to start appearing at the monitoring borehole. The tracer solute started appearing a day after an intense storm in which rainfall amount in excess of 150 mm was recorded (*WeatherSA* 2011). Due to the preferential recharge in the alluvial channel aquifer, groundwater levels rapidly increased one day after the start of the rainfall event (Figure 7-9). The rapid increase of the groundwater levels due to recharging event created a high natural hydraulic gradient in the aquifer leading to the quick movement of the

tracer than would have happened in the absence of the rainfall event. Practically, the recharging waters created an exceptionally high natural hydraulic gradient which is however difficult to calculate because the rapid increase in groundwater levels due to the excessive rainfall event was only captured in one borehole.

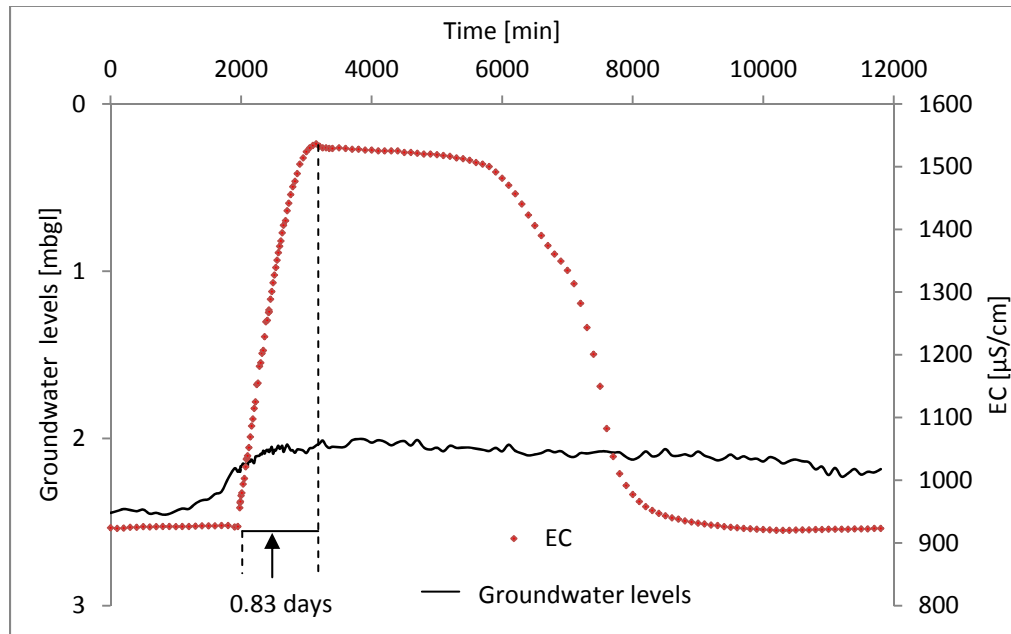


Figure 7-9 Salt solute tracer breakthrough curve and rapid increase of water levels measured in BH6 during the NGTBT.

Under natural hydraulic gradient during a recharge episode, it took the tracer peak about 0.83 days (1200 minutes) to arrive at the monitoring borehole that is located 10 m from the injection borehole. Without taking into consideration the tortuosity of the gravel-sand material, an average natural linear groundwater velocity of 12 m/d can be estimated under the natural conditions at the site. However in the reality the effective path travelled by the tracer solute is not straight and as a result higher groundwater velocities are expected. The total distance travelled by the tracer is much longer because the solute has to move through the interconnected pores.

The whole salt solute plume took about 6 days to pass and clear at the monitoring borehole. It can therefore be deduced that high groundwater velocities in the alluvial channel aquifer can also be important for flushing salt contaminants out of the aquifer system. Unfortunately such rapid flushing of solute contaminants out of the alluvial channel aquifer system would directly imply more contaminant load on the gaining surface water resources. Nevertheless, besides those highlighted limitations, the NGTBT in the alluvial channel aquifer indicates the following important aspects:

- The high groundwater velocity for the gravel-sand materials of the alluvial channel aquifer which implies the dominance of advection process on solute transportation.
- The potential capacity of the preferential recharge through infiltration to enhance solute contaminant migration in the alluvial channel aquifer. The findings of this study suggest that contamination investigations should assess solute transportation of contaminants under abstraction, dry (discharging) and wet (recharging) scenarios. These three scenarios result in different hydraulic gradients, potentially creating various mass transport characteristics.

This is probably the best solute tracer breakthrough curve under natural conditions (without abstraction) that the author has witnessed both in practice and literature. The following attributes makes this particular breakthrough curve unique and exceptional:

- No pumping was used to force the salt tracer to move, natural recharge created the hydraulic gradient to transport the tracer solute.
- The test captured the recharging event practically driving the tracer solute towards the monitoring borehole as shown by the rapid water level increases.
- A complete tail end of the tracer solute breakthrough curve was obtained as indicated by end time EC measurements that are equal to the background values.

It is however important to highlight that no analytical solutions in literature were found with the capacity to analyse the NGTBT tracer curve when a “long duration tracer injection mode” is used. Developed analytical solutions (Sauty 1980, Wang and Yang 1984; and Fetter 1993) are suitable for analyzing tracer breakthrough curves measured when the tracer is injected in an “instantaneous pulse” mode. It is recommended that significant efforts be directed at developing some analytical solutions that can be used to analyse NGTBT curves when a long duration tracer injection mode is used.

The outcome of the test in terms of solute transportation is an indication of the travelling time and linear groundwater flow velocity of solute migration under natural gradients. However, the most important achievement of the test was the successful detection of the solute tracer breakthrough under natural groundwater flow conditions. This test can be used as the basis to provide some general guidelines on performing of NGTBT tests in typical alluvial channel aquifers. Natural gradient tracer breakthrough tests are important for simulating contaminant transportation under natural groundwater flow conditions.

7.2.3 Challenges of the NGTBT

A number of setbacks were faced during the designing and performance of the NGTBT. The biggest setback was that all boreholes at the study area were drilled without a comprehensive understanding of the natural principal groundwater flow direction thus making it difficult to design the natural tracer test field. Initially only 3 boreholes are required to determine the principal flow direction. After establishment of the natural principal groundwater flow direction, multiple boreholes can then be drilled down gradient of the proposed injection borehole to monitor the tracer (Kalbus *et al.* 2006). This would reduce the chances of missing the tracer trajectory and enable monitoring of the tracer migration in 2-Dimension (longitudinal and transverse). Figure 7-10 shows a schematic of tracer plume movement from the injection borehole towards monitoring boreholes in an ideal natural gradient testing field.

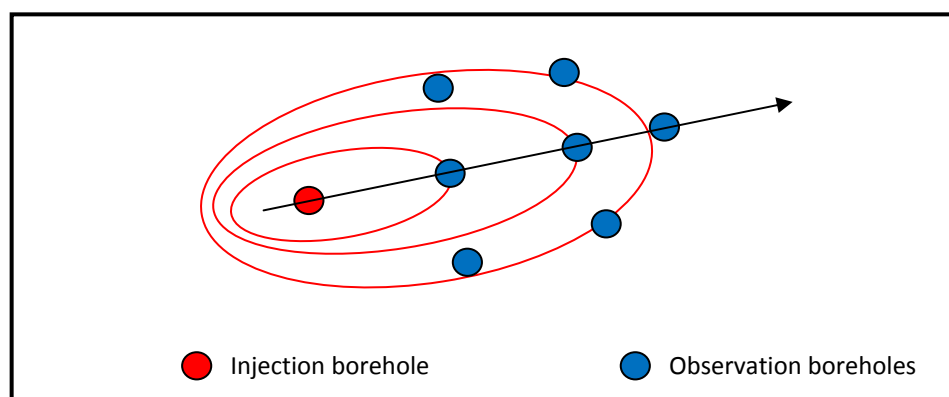


Figure 7-10 Schematic of tracer plume movement from the injection borehole towards monitoring boreholes in an ideal natural gradient testing field; the arrow shows the principal direction of natural groundwater flow.

Another major setback was poor borehole construction. Monitoring wells were not properly constructed to only allow the monitoring of tracer movements in the gravel-sand main aquifer layer. This can potentially disturb tracer movement and detections especially under natural gradients. It therefore implies that the estimated groundwater velocities could be even much higher when proper borehole construction has been done. Based on this chapter's findings and experience gained, it is recommended that the natural principal groundwater flow direction be established before the design of NGTBT field by first drilling only three boreholes.

7.2.4 General guidelines for NGTBT

Based on the experience gained from the NGTBT, the following steps are given as general guidelines for conducting a NGTBT in a typical alluvial channel aquifer:

- Drill at least three boreholes for geological characterization of the aquifer and determination of the principal natural groundwater flow direction.
- Determine the natural principal groundwater flow direction using water levels (mamsl) from a set of at least three groundwater levels that form a triangle.
- Select the injection borehole from the ones used for determining the natural principal groundwater flow direction.
- Determine the main flow zones using geological logs, EC profiling and aquifer testing. The main flow zones are important because they present the opportunity to assess the maximum solute transportation capacity of the aquifer system. Tracer should be injected and monitored in the main flow zones.
- Place monitoring boreholes on the down gradient of the proposed injection borehole along the natural principal groundwater flow direction. Monitoring boreholes can be designed to capture 1, 2 or 3-Dimension tracer movement along the longitudinal and transverse directions depending on the nature of the aquifer and levels of investigations.
- Monitoring boreholes should be constructed to enable the measurement of the moving tracer along the main flow zones.
- The tracer can be injected as a long duration pulse that is placed and expected to deplete with time.
- Automated LTC loggers should be placed in all monitoring boreholes along the flow zones to measure EC as an indicator of tracer movement. Automated in-situ probes for other conservative tracers such as; bromide, chloride and fluorescein are highly recommended when affordable.
- Groundwater levels should be automatically measured in the injection and monitoring boreholes to evaluate the natural hydraulic gradient driving the tracer.

7.3 Summary

Natural gradient tests were conducted under natural groundwater flow conditions to determine groundwater flux and transport parameters of the alluvial channel aquifer. Two NGPDTT and one NGTBT were successfully conducted in the alluvial channel aquifer. The NGTBT was designed to assess contamination migration in 1-Dimension along the natural principal groundwater flow direction. The NGTBT test requires a good understanding of the natural groundwater flow directions to avoid missing the tracer trajectory.

Natural groundwater fluxes in the order of 10^{-2} m/d were determined using the NGPDTT. No analytical solutions in literature were found with the capacity to analyse the NGTBT tracer curve when a “long duration tracer injection mode” is used. A qualitative approach was developed to remove the density effects on the tracer dilution rates during the NGPDTT before using the data for groundwater flux calculations. However, the NGTBT results indicate the high natural groundwater velocity for the gravel-sand materials of the alluvial channel aquifer which implies the dominance of advection process on solute transportation. Without taking into consideration the tortousity of the gravel-sand material, an average natural linear groundwater velocity of 12 m/d was estimated. Based on the experience gained from the NGTBT, general guidelines were developed for conducting a NGTBT.

The next chapter discusses the GW-SW interactions of the alluvial channel aquifer and the river at the site.

8 ALLUVIAL CHANNEL AQUIFER AND RIVER/STREAM INTERACTIONS

8.1 Introduction

Determining the gaining or losing status of a river/stream segment is an important primary level of any GW-SW interactions studies. It is generally easy to start working from the visible surface water resources as compared to the groundwater. A GW-SW balance model based of mass conservation, solute and isotopic mixing provides the best approach to determine if the river is gaining or losing water. A comparison of river water and groundwater water levels is another way that can be used to make an assessment of the gaining or losing status of a river system. Qualitative investigation tools such as stable isotope and geochemistry analysis are also useful as part of the secondary GW-SW investigations. The chapter describes the field application of a water balance model, stable isotopes and geochemistry analysis to investigate GW-SW interactions along an alluvial channel aquifer.

8.2 Water balance model

A water balance model is the most important primary tool for investigating GW-SW interactions before detailed field investigations can be conducted. The water balance model is fundamental for determining the gaining or losing status of the groundwater and surface water resources. In other words, the outcome of the water balance model provides direction and guidelines for the upcoming detailed GW-SW investigations. Groundwater information for the model can be obtained from available private boreholes. If private boreholes are not available, at least three boreholes should be initially drilled to provide information on groundwater solute and isotopic compositions. These three boreholes can also be used to determine the natural principal groundwater flow direction.

Due to limited funds, the current project did not have enough funds to built weirs and install flow gauges along the river channel. It is however not unusual for research projects to have limited funds especially in the developing continents such as Africa. The most important aspect whether resources are enough or not is the appropriate utilization of the available tools to collect the best possible information. Information is important for decision making and planning purposes. Sophisticated GW-SW research tools and techniques potentially increase both accuracy and efficiency. However, there is no doubt that in their absence, available basic simple tools can still provide valuable information giving at least a starting point. A basic approach that was taken to measure the river water inflow and outflow of the model is given in the next subsections.

It is important to conduct the inflow and outflow measurements made during low river flow periods. In general, low river flow volumes are easier to handle and manage. At the same time, low river flow periods also offers great opportunity to assess GW-SW exchanges when other potential external sources and sinks can be regarded to as negligible.

8.2.1 GW-SW water balance system

A GW-SW balance model is the most important primary tool for investigating GW-SW interactions before any detailed field work such as drilling of boreholes can be conducted. A water balance model is fundamental for determining the gaining or losing status of the groundwater and surface water resources. In other words, the outcome of the water balance model should provide direction and guidelines for the upcoming detailed GW-SW investigations. Figure 8-1 shows the components of the water balance model at the site.

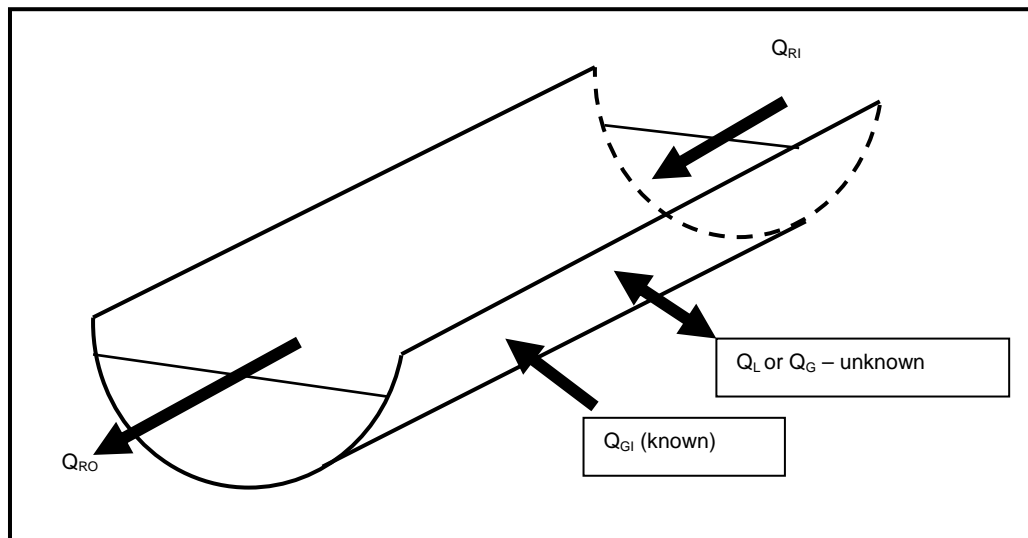


Figure 8-1 An illustration showing components of the GW-SW water balance system.

The water balance model was developed based on the conservation of mass (Equation 13); mixing of solute (Equation 14) and stable isotope (Equation 15). Based on the conservation of mass, the inflow rate into the system should be equal to the outflow rate if there is no storage, loss or additional water into the system.

$$Q_{RI} + Q_{GI} + (+Q_G \text{ or } -Q_L) = Q_{RO}$$

Equation 13: Mass balance.

Where: Q_{RI} – measured river interval inflow rate (l/s); Q_{GI} – calculated groundwater inflow rate into the system (l/s); Q_L – unknown systems loss rate (l/s); Q_G – unknown systems gain rate (l/s); Q_{RO} – measured river interval outflow rate (l/s).

Equation 13 defines the rivers' net gaining or losing status. Equation 14 and Equation 15 are then used to confirm the findings of mass balance analysis (Equation 13). The solute concentration and isotopic ratio of the system losses are taken to be equal to that of the river outflow assuming that complete mixing will have occurred prior to the losses.

$$Q_{RI}C_{RI} + Q_{GI}C_{GI} + (+Q_G C_G \text{ or } -Q_L C_L) = Q_{RO}C_{RO}$$

Equation 14: Solute mixing balance.

Where: C_{RI} – measured solute concentration of the river interval inflow; C_{GI} – measured solute concentration of groundwater inflow; C_{GI} – solute concentrations of system gains; C_L – solute concentrations of system losses; C_{RO} – measured solute concentration of the river interval outflow; solute concentrations in the equation can be measured in any unit.

$$Q_{RI}\delta_{RI} + Q_{GI}\delta_{GI} + (+Q_G\delta_G \text{ or } -Q_L\delta_L) = Q_{RO}\delta_{RO}$$

Equation 15 Stable Isotope mixing balance.

Where: δ_{RI} – measured isotopic ratio of the river interval inflow; δ_{GI} – measured isotopic ratio of the groundwater inflow; δ_G – isotopic ratio of system gains; δ_L – isotopic ratio of system losses; δ_{RO} – measured isotopic ratio of the river interval outflow; Isotopic ratio were measured in [‰].

It is important to highlight that before the output of the water balance model, one cannot tell if the system is gaining or losing water. Thus we can only have Q_G or Q_L as unknown components of the water balance model.

8.2.2 Methods and materials

8.2.2.1 Discharge measurements

The discharge measurements were conducted during the low river flow period in October 2011. In general, low river flow volumes are easier to measure and handle. At the same time, low river flow periods also offers great opportunity to assess GW-SW exchanges when other potential external sources and sinks can be regarded to be negligible.

The inflow and outflow discharge is calculated as the product of mean velocity and cross-sectional area. Measurements were therefore made to determine the mean cross section area and mean stream velocity at the river inflow and outflow positions of the model. In the absence of built weirs,

selection of the appropriate positions for measuring water outflow and inflow into the river segment was essential and the following were the key factors during considerations:

- A small and shallow river channel cross-section is preferable to avoid drowning.
- An interval that has a fairly constant channel width is desirable to reduce the effects of width heterogeneities on measurements.
- The interval should be clear of trees and any possible obstructions of water flow.

A dumpy level and staff rod were used to measure the depth from the water surface to river bed. Measurements were made at a series of points across the stream inflow and outflow positions thus dividing the cross sectional into segments. The total cross sectional area of the channel was computed from the summation of segment cross sectional areas.

Two points were marked and distance between the two points was measured. An orange peal float was thrown upstream of the first point and the time to reach the downstream point along the river interval was recorded for 5 set of readings. The average surface velocity was obtained by diving the distance travelled by the time. The surface stream velocity was multiplied by a factor of 85 % to convert it to mean velocity across the entire cross section (Costa *et al.* 2004).

Groundwater discharge from alluvial channel aquifer along the seepage face was determined using Darcy's flow equation. Hydraulic flow properties of the alluvial channel aquifer were determined in section 4.1.4.1.1 of Chapter 4. It is important to highlight that groundwater discharge into the model was visible at the seepage face and was therefore classified as a known component. A complete set of measurements and calculations made for the water balance model can be found in the appendices data disc.

8.2.2.2 Isotopes and solute measurements

The solute and isotopic ratio mixing in the model is based on the premises that complete mixing of solutes between the surface and groundwater occurs within the river interval. The concentration and isotopic composition of river outflow and loses should therefore reflect properties of a complete mixture. It is assumed that the river banks and bed sediments have a negligible influence on the solute and isotopic mixing processes.

Electrical conductivity and $\delta^2\text{H}$ were measured as indicators of the solute concentration and isotopic ratios. Measurements of these parameters were made in the discharging groundwater, river inflow and outflow components of the model. Electrical conductivity was measured using a field hand

meter. Water samples for stable isotope were analysed by iThemba Environmental Isotope Laboratory of South Africa. It was assumed that all the losses in the system would occur after completing mixing had occurred and it's solute and isotopic properties would be reflected in the river outflow water.

8.2.3 Results and discussion

8.2.3.1 Model inflow

8.2.3.1.1 River inflow (Q_{RI})

The river inflow into the system was measured at a position which is at about 50 m downstream of the dam wall. Apparently there are no flow gauges at the dam and physical measurement was the most viable technique to quantify the river outflow into the model. In general, two types of flow can be associated with dam outflow. There is a continuously maintained low flow and occasional high flows that occur during scheduled dam releases. Figure 8-2 shows the measured cross-sectional area of flow at the river inflow segment of the model.

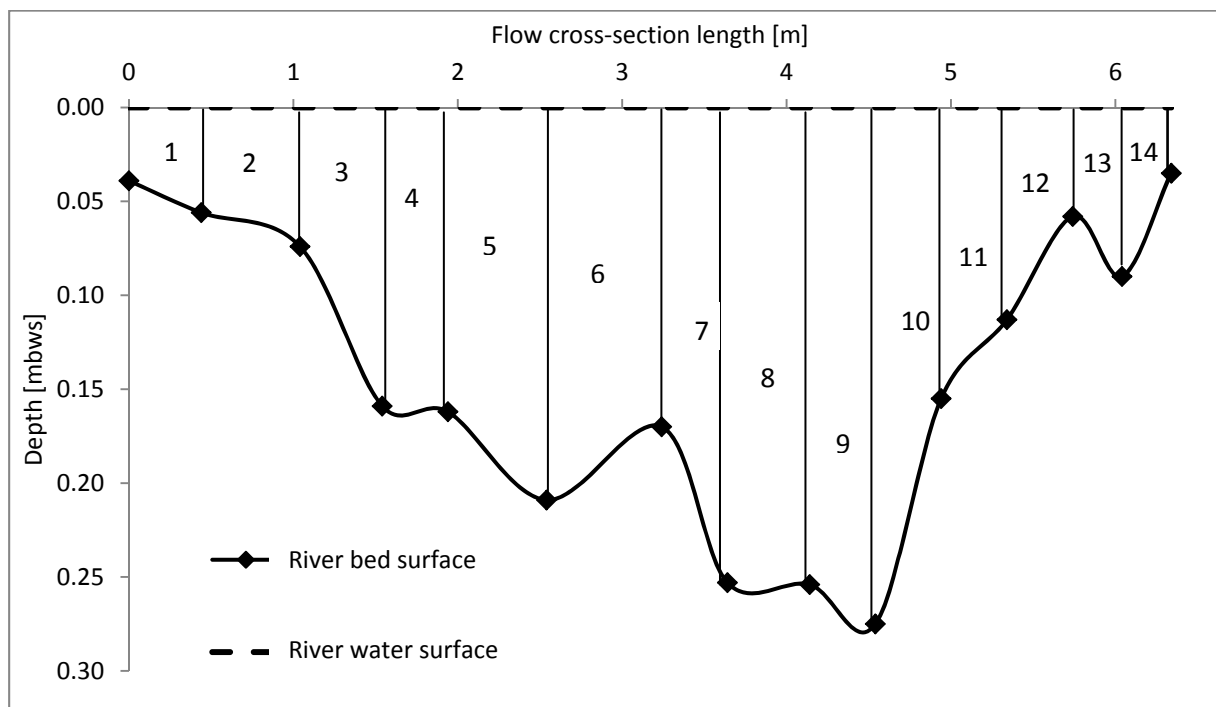


Figure 8-2 Measured river cross-sectional area of flow at the inflow segment of the GW-SW system; the numbers indicate trapezoidal segments that were used to calculate the flow cross-sectional area.

The cross-sectional area of flow was calculated manually by considering the area of each trapezium separately and then combining them to get the total area. Table 22 shows the total cross-sectional area of flow, velocity, discharge, EC and δ^2H measured at the inflow of the model. Only one cross-

sectional area of flow was measured at the inflow segment because the channel width and depth were considered to be fairly constant for at least 10 m downstream of the first measurement position. The possible influence of the cross-sectional area on the river flow rate along the inflow segment was assumed to be negligible.

Table 22 Measurements of the total cross-sectional area of flow, surface velocity, discharge, $\delta^2\text{H}$ stable isotopic ratio and EC at the inflow segment of the model.

Flow cross-sectional area [m ²]	Average surface velocity [m/s]	Mean cross-sectional velocity [m/s]	Q _{RI} [l/s]	Q _{RI} [m ³ /d]	EC [mS/m]	$\delta^2\text{H}$ [‰]
0.96	0.36	0.31	295.88	25564.30	33.40	-3.92

8.2.3.1.2 Groundwater inflow (Q_{GI})

The groundwater inflow component was determined by quantifying the alluvial channel aquifer's natural discharge rate at the seepage face. Figure 8-3 shows an illustration of the aquifer discharge zone at the seepage face. The seepage face length (L) is approximately 100 m. Based on the field observations at the seepage face, groundwater was considered to be discharging into the river through a thickness (b) of about 2 m above the shale impermeable bedrock. Hydraulic conductivity of the discharging aquifer thickness was determined using harmonic mean transmissivity derived from aquifer tests in the shallow main aquifer (Chapter 4). The discharge rate was calculated using Darcy's law (Equation 16).

$$Q = KiA$$

Equation 16: Darcy.

Where: K-harmonic horizontal hydraulic conductivity in the discharging aquifer thickness (m/d), i-hydraulic gradient from the local aquifer to the discharging face, A-cross sectional area of the discharging face perpendicular to the discharging flow (m²).

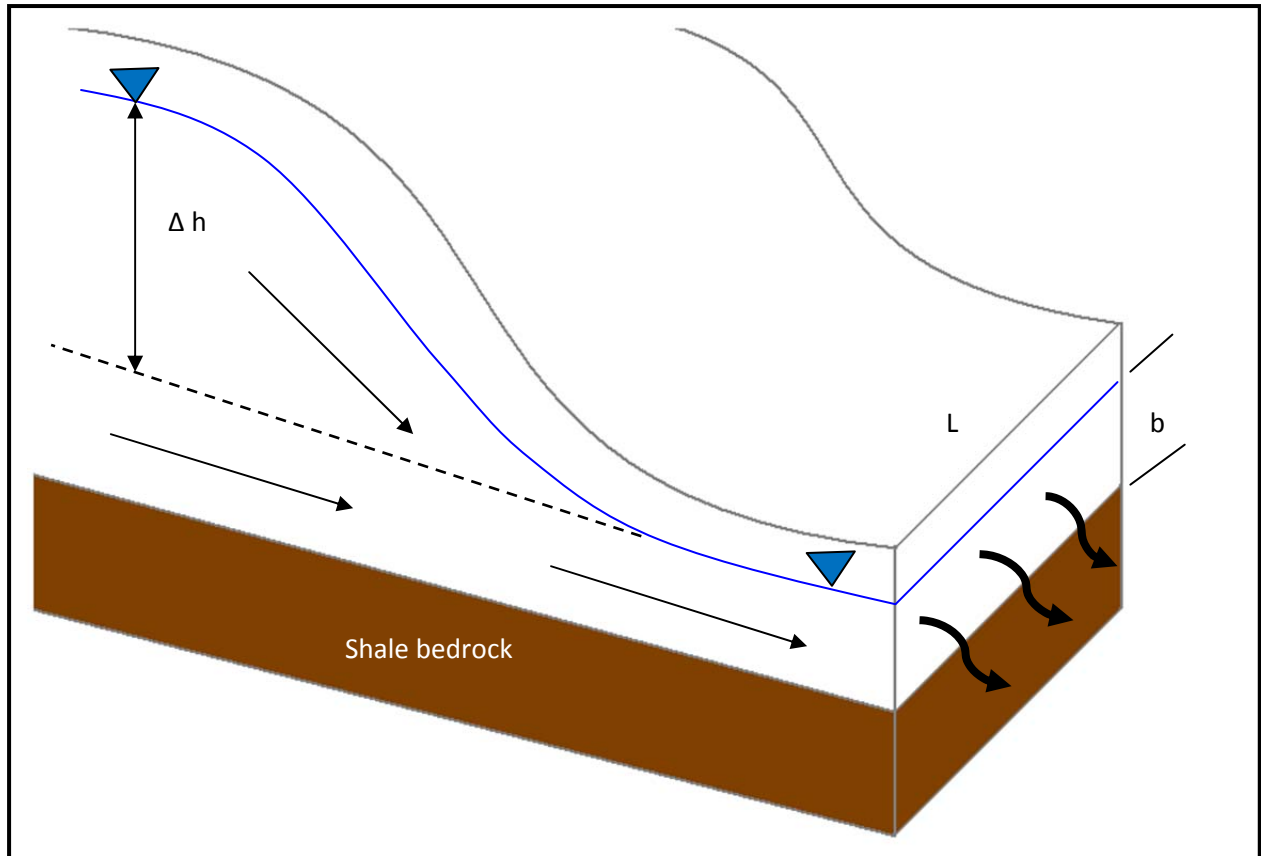


Figure 8-3 Idealized schematic showing the components of the aquifer discharge zone at the seepage face; Δh is the hydraulic head differences between local aquifer and discharging zone groundwater levels; arrows indicate groundwater discharge into the aquifer.

Table 23 shows the calculated groundwater discharge rate from the alluvial channel aquifer and the parameters that were used for the calculations. Electrical conductivity and δ^2H values in Table 23 were measured in the discharging groundwater at the seepage face.

Table 23 Calculated groundwater discharge from the alluvial channel aquifer into the river and parameters used for calculations; EC and δ^2H of the discharging waters.

L [m]	b [m]	i	T [m^2/d]	K [m/d]	Q_{GI} [l/s]	Q_{GI} [m^3/d]	EC [mS/m]	δ^2H [‰]
100.00	2.00	0.32	36.87	18.44	13.60	1174.98	126.02	-31.97

8.2.3.1.3 River outflow (Q_{RO})

The outflow from the GW-SW system was measured at the segment of the channel with the narrowest width. This segment was designated as the “outflow weir” of the GW-SW system. A shallow nick point characterises the segment of the river channel where the system outflow measurements were made. The segment of the channel is generally characterised by a compacted clay river bed of low permeability. Water loss along the designated riverbed segment was therefore

assumed to be negligible in comparison to river flow. However for the river outflow segment, two cross-section areas of flow were measured because a significant variation in the channel width within 2 m from the first measurement position was visually observed. Figure 8-4 and Figure 8-5 shows the two flow cross-section areas that were measured along the GW-SW system outflow segment. Cross-section area B is located 2 m downstream of cross-sectional area A.

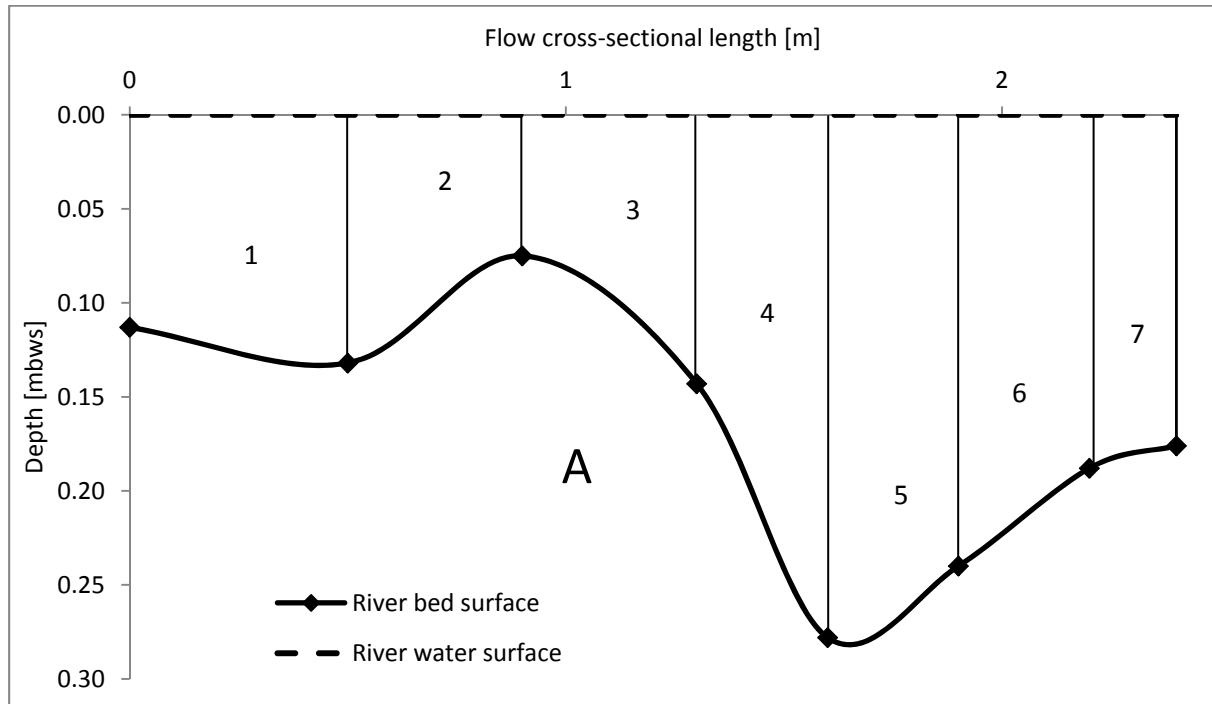


Figure 8-4 Measured cross-sectional area of flow (A) at the outflow segment of the GW-SW system; the numbers indicate trapezoidal segments that were used to calculate the flow cross-sectional area.

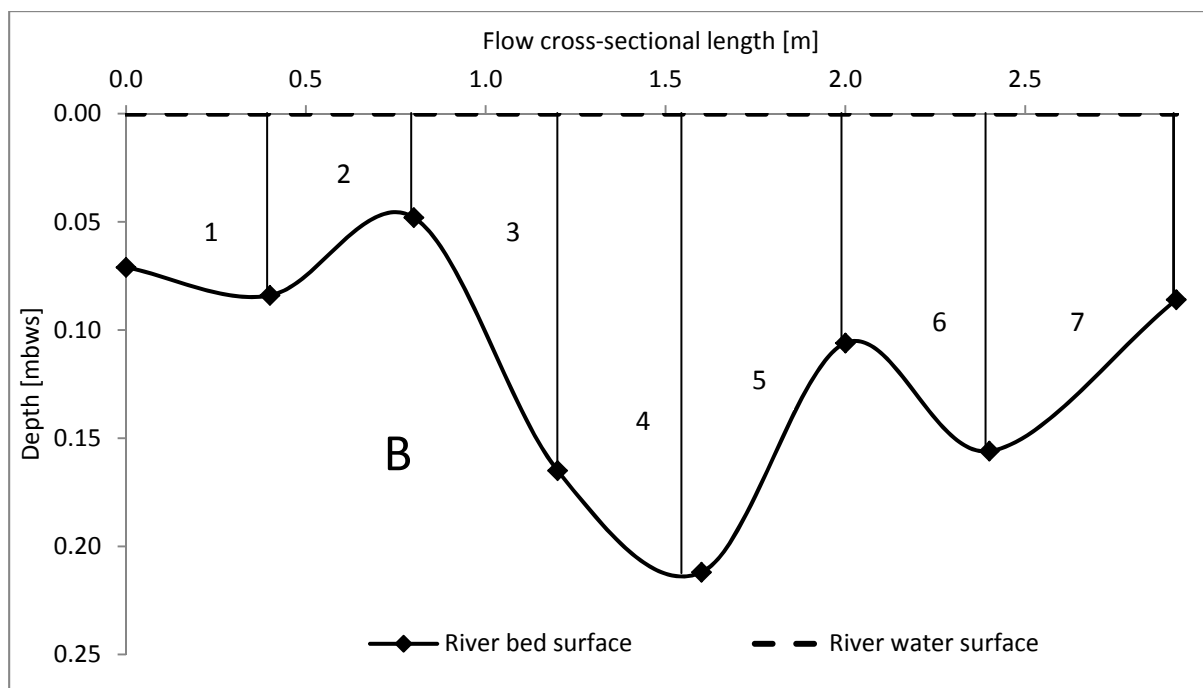


Figure 8-5 Measured cross-sectional area of flow (B) at the outflow segment of the GW-SW system; the numbers indicate the trapezoidal segments that were used to calculate the flow cross-sectional area.

Table 24 the shows measurements for the cross-sectional area of flow, flow velocity, EC, $\delta^2\text{H}$ and discharge at positions A and B along the outflow segment of the GW-SW system. Similar flow rates were calculated from the flow cross-section area and velocity measurements that were made at positions A and B which are just 2 m apart. The ability of the measurement method to produce closely comparable results is a reflection of its precision and therefore reliability. An arithmetic average of the outflow discharge measured at point A and B was used in the model.

Table 24 Measurements of the cross-sectional area of flow, velocity, flow rate, $\delta^2\text{H}$ EC and at positions A and B along the outflow segment of the GW-SW model.

Position	Flow cross-sectional area [m ²]	Average surface velocity [m/s]	Mean cross-sectional are velocity [m/s]	Q _o [l/s]	Q _o [m ³ /d]	EC [mS/m]	$\delta^2\text{H}$ [‰]
A	0.39	0.56	0.48	186.00	16070.69	37.6	-6.17
B	0.35	0.62	0.53	186.11	16079.52	37.6	-6.18

8.2.3.1.4 Model net balance

The model net balance gives an indication of whether the river channel is effectively gaining or losing water. It is however possible for the river to be gaining while at the same time losing but the net effect is important for giving an overall understanding of the GW-SW exchanges. The model net balance should quantify the unknown losses or gain thereby giving a platform for detailed field

investigations to identify the nature of the exchanges. A combination of mass, solute and isotopic mixing balances was used to determine the net balance of the model.

Based on mass balance Equation 13, a comparison of the total inflow and outflow shows that the river interval is effectively losing water (Table 25). Assuming that there is conservation of mass, solute concentration (Equation 14) and $\delta^2\text{H}$ isotopic ratio (Equation 15) in the system the three approaches should give a unique solution for the net balance. In this instance, a unique solution implies that the rate of water loss determined from the mass balance should be equal to the one determined using solute concentration and $\delta^2\text{H}$ isotopic ratio. It was assumed that that losses would occur after complete mixing of different waters in the system such that the solute concentration of the lost water will be equal to the concentration of the river outflow.

Shown in Table 24 are the measured and calculated components of the water balance model based on the mass, solute concentration and $\delta^2\text{H}$ isotopic ratio. The rate of water loss from the model determined using the mass and solute mixing balance only differs by 1.07 l/s thus providing close to a unique solution. However on the other hand, the rate of water loss from the model determined using the mass and isotopic ratio mixing balance differs by 9.48 l/s. The big differences between the losses determined by mass and isotopic ratio mixing balance approaches is most likely because the $\delta^2\text{H}$ isotopic ratio of the water is more sensitive to evaporation effects than the EC of the water. The overall effect is that the isotopic ratio balance approach would then indicate as if more loss occurs due to evaporation than from the calculations made using the solute balance approach.

Table 25 Measured and calculated components of the water balance model based on the mass, solute concentration and $\delta^2\text{H}$ isotopic ratio. A complete set of data and measured parameters used for the calculations is found in Appendix 5 of the appendices data disk.

Mass balance			
Q_{RI} [l/s]	Q_{GI} [l/s]	Q_{RO} [l/s]	Q_L [l/s]
295.88	13.60	186.05	123.43
Solute mixing balance			
$Q_{RI}C_{RI}$ [l/s mS/m]	$Q_{GW}C_{GI}$ [l/s mS/m]	$Q_{RO}C_{RO}$ [l/s mS/m]	Q_L [l/s]
9882.48	1713.79	6995.65	122.36
Isotopic ratio balance			
$Q_{RI}\delta^2\text{H}_{RI}$ [l/s ‰]	$Q_{GI}\delta^2\text{H}_{GI}$ [l/s ‰]	$Q_{RO}\delta^2\text{H}_{RO}$ [l/s ‰]	Q_L [l/s]
-1159.86	-434.77	-1147.96	113.95

In general, groundwater contributes 3 % of the total inflow into the system while about 32 % of the total inflow is lost mostly like to groundwater, bank storage, bed storage and evaporation losses. The next stage of the GW-SW investigations would then be focused on identifying the mechanisms through which the channel is losing water. It will also be important to identify the positions of GW-SW exchanges along the channel interval which will then be followed by measurements.

Although the proposed application of the water balance model to investigate GW-SW interactions does not consider changes that may occur in time and space it never the less provides a good platform for planning purposes. The effectiveness of the water balance as a preliminary tool relies much on precise and consistent measurements of the known model components. It is also important to make all the measurements in the shortest possible time to reduce the influence of external factors such evaporation on solute and isotopic compositions.

8.2.3.1.5 Model reliability

It is important to highlight that unlike the other measured model parameters; the thickness of the aquifer at the discharging seepage face was rather assigned based on geological understanding and visual observations made on the site. In other words, this parameter does not have an absolute value; it can vary depending on the observer and understanding of the site. A question can therefore be raised as to what will be the effect of changing the discharging aquifer thickness on the net balance of the model. If the aquifer thickness is assumed to vary between 0.1-2.0 m, this would decrease the groundwater discharge into the model thus effectively increasing the difference between Q_L estimated from the 3 approaches (Table 26). It is however important to mention that the difference in Q_L between mass and solute mixing approaches that result from varying the aquifer discharge thickness from 0.1-2.0 m is still within the same order (0-10 l/s) thereby justifying the use of a 2 m aquifer thickness. The mass balance approach is least sensitive to changes in aquifer discharge thickness because the calculations are based on physical measurements. The isotopic approach is more sensitive to the changes in aquifer thickness.

Table 26 Water balance model loss rates (Q_L) calculated when aquifer thickness is varied from 0.1-2.0 m.

b [m]	Q_{GW} [l/s]	Q_L [l/s] (Mass)	Q_L [l/s] (Solute)	Absolute difference of mass Q_L and solute Q_L	Q_L [l/s] (Isotopic)	Absolute Difference of mass Q_L and Isotopic Q_L
0.10	17.65	127.48	135.93	8.45	146.98	19.51
0.50	16.80	126.63	133.08	6.46	140.05	13.42
1.00	15.73	125.56	129.50	3.94	131.32	5.77
2.00	13.60	123.43	122.36	1.07	113.95	9.48
3.00	12.29	122.12	117.97	4.15	103.28	18.84
4.00	9.33	119.16	108.05	11.11	79.14	40.02
5.00	7.20	117.03	100.90	16.12	61.74	55.29

8.3 Stable isotope analysis

Analysis of the stable isotopic compositions was performed to assess the interactions between groundwater from the alluvial channel aquifer and river surface water. It was also essential to establish the characteristic isotopic signatures of groundwater and river water in the study area. A comparison was made between the measured groundwater and river water δ^2H and $\delta^{18}O$ isotopic. In general, if the river is losing water into the aquifer then isotopic signatures of the groundwater should be similar to the river water. In the case of a losing river, minimum evaporation during the movement of water is expected thus groundwater should retain the stable isotopic signature of the river water. Figure 8-3 shows the Plot of δ^2H against $\delta^{18}O$ for groundwater and river water samples showing the deviation from GMWL and LMWL. A complete set of δ^2H against $\delta^{18}O$ isotope compositions measured in the groundwater and river water is found in appendix 4.1.

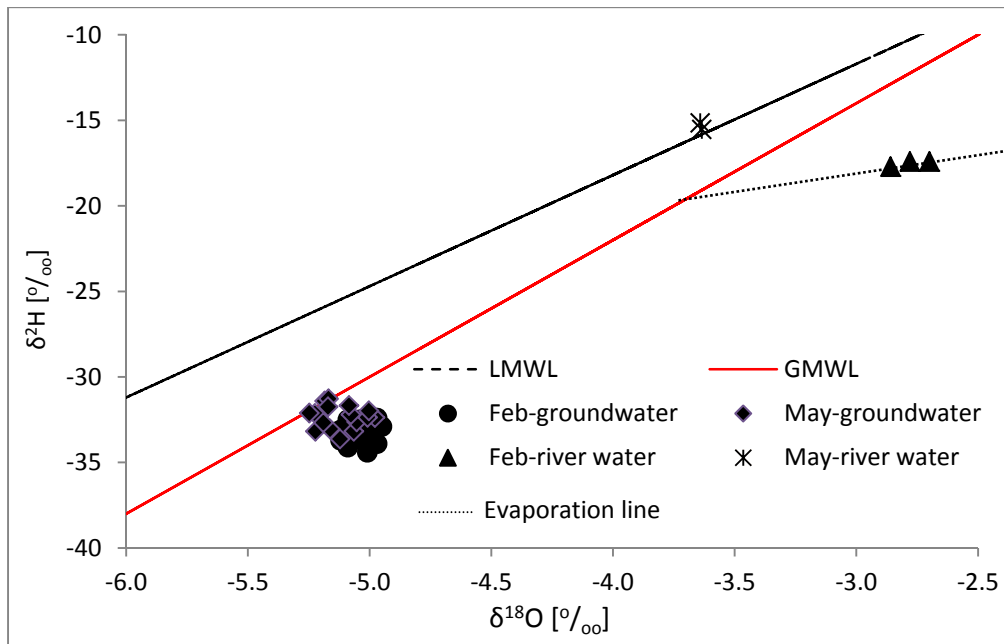


Figure 8-6 Plot of $\delta^2\text{H}$ against $\delta^{18}\text{O}$ for ground and river water samples showing the deviation from the GMWL and LMWL; GMWL: $\delta^2\text{H} = 8 \cdot \delta^{18}\text{O} + 10$; LMWL Pretoria: $\delta^2\text{H} = 6.5 \cdot \delta^{18}\text{O} + 7.8$; (IAEA/WMO, 2004).

The negative values of Oxygen-18 and deuterium indicate depletion of oxygen-18 and deuterium relative to the Vienna Standard Mean Ocean Water (VSMOW). There is a clear distinction in $\delta^2\text{H}$ and $\delta^{18}\text{O}$ between ground and river water (Figure 8-6) although it is evident that the river is gaining some water from the aquifer that discharges at the seepage face. The river water is more enriched implying that it has gone through significant evaporation in comparison to precipitation that recharges the groundwater. In February the river water had more enriched $\delta^2\text{H}$ and $\delta^{18}\text{O}$ isotopic composition than in May. It therefore implies that there was a high evaporation effect on river isotopic composition in February (hot and wet) than in May (wet and cold). The $\delta^2\text{H}$ and $\delta^{18}\text{O}$ plot of river water samples collected in February 2011 follows the evaporation line (Figure 8-6).

Even though the isotopic composition results does not confirm that the aquifer is discharging groundwater as observed, they however indirectly also ascertain that the aquifer is not gaining water from the river. If the aquifer is gaining water from the river, then its isotopic compositions should be similar to the river water since no significant evaporation is expected to occur once in the aquifer. The application of stable isotopic signatures is however limited when the river is gaining water from the aquifer. Isotopic signatures of the groundwater moving into the river cannot be maintained because the water is exposed to evaporation once it has reached the surface water body. It is however still possible to assess the contribution of the depleted groundwater $\delta^2\text{H}$ and $\delta^{18}\text{O}$ signatures into the enriched river surface water.

The $\delta^2\text{H}$ measured in the GW-SW model river outflow in October 2011 shows the contribution of the groundwater that is depleted in $\delta^2\text{H}$ on the enriched inflow (Figure 8-7). Due to the mixing effect of the groundwater that was depleted in $\delta^2\text{H}$ (-31.97 ‰) on the enriched $\delta^2\text{H}$ model inflow (-3.92 ‰), the resulting outflow had a $\delta^2\text{H}$ of -6.17 ‰ . This translates into a $\delta^2\text{H}$ depletion of -2.25 ‰ when compared to the model river inflow $\delta^2\text{H}$.

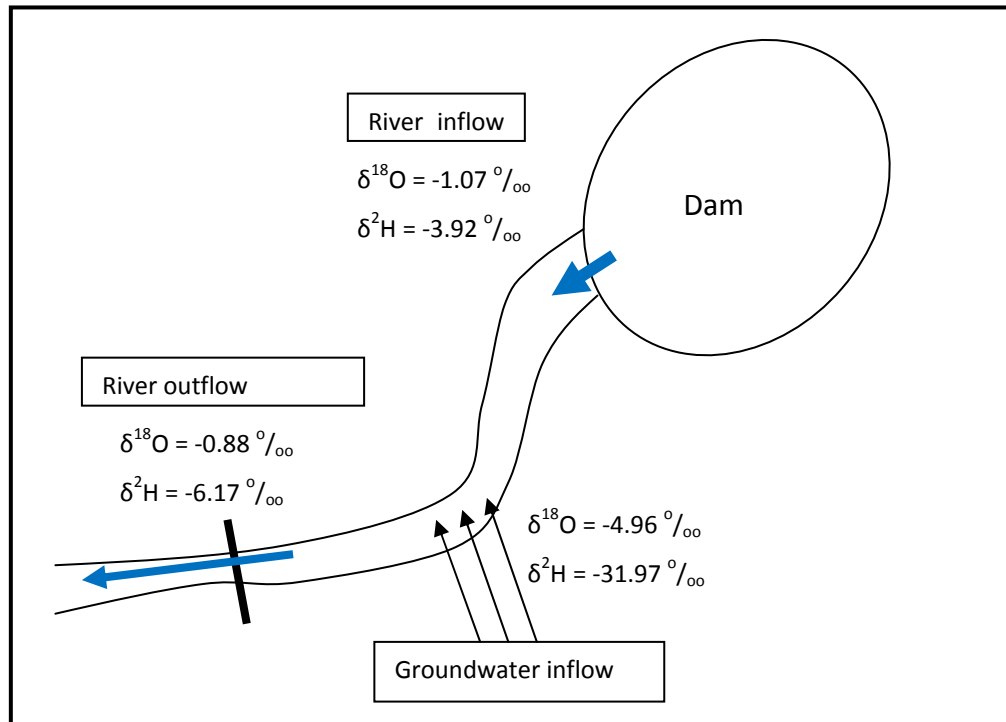


Figure 8-7 $\delta^2\text{H}$ and $\delta^{18}\text{O}$ that was measured for the water inflow and outflow of the GW-SW system measured in October 2011 during dry and low river flow conditions.

It is possible for one to argue that the monitoring period is too small to make significant conclusions about the GW-SW interactions. The fact however is that for this alluvial channel aquifer, the river remains a “gaining one” irrespective of the monitoring length or time of the season. The most likely exceptional case would occur during intense flood, when the river stage can potentially rise above aquifer water levels to reverse the hydraulic gradient. The rain season of the year 2011 presented an opportunity to assess the GW-SW interactions during the flooding conditions, when both the groundwater and river levels rose significantly. However even one most severe floods in years, could not reverse the mode of interaction of the alluvial channel aquifer losing water into the gaining river.

8.4 GW-SW interaction mechanisms at the site

The study shows a different mechanism for the GW-SW interaction which has not been overly reported in literature. Local groundwater that is driven from the distant terrestrial aquifer discharges from an alluvial channel aquifer into rivers can also occur through the seepage face created at the contact plane of the alluvial cover and impermeable river bedrock as opposed to the commonly hypothesized river/stream bed hydraulic connectivity. The photo on Figure 8-8 shows the GW-SW interaction mechanisms at the case study site. The GW-SW interactions occur through the seepage face created between the contact plane of the alluvial channel aquifer and low permeable shale bedrock.



Figure 8-8 A photo showing the seepage face where groundwater discharges from the alluvial channel into the river; arrows shows flow direction flow.

The groundwater discharging at the seepage face is solely derived from the shallow alluvial cover channel deposits and mainly constitute of local groundwater flow system (Figure 8-9). The study site provides a typical example on which significant groundwater discharge can occur through the alluvial cover and impermeable bedrock contact plane. The seepage face contact plane is located about 2 m above the average river stage elevation, implying that there is no direct hydraulic connectivity between the local groundwater system and the river, yet still there are huge interactions are taking place. The most important point is that significant GW-SW exchanges can still occur in the absence

of direct hydraulic connection between the alluvial channel aquifer and the bedrock river channel. It is therefore proposed that the definitions of the GW-SW interaction mechanisms be extended to include seepage discharge that often occurs through river banks along alluvial channel aquifers situated on low permeable bedrock river channels.

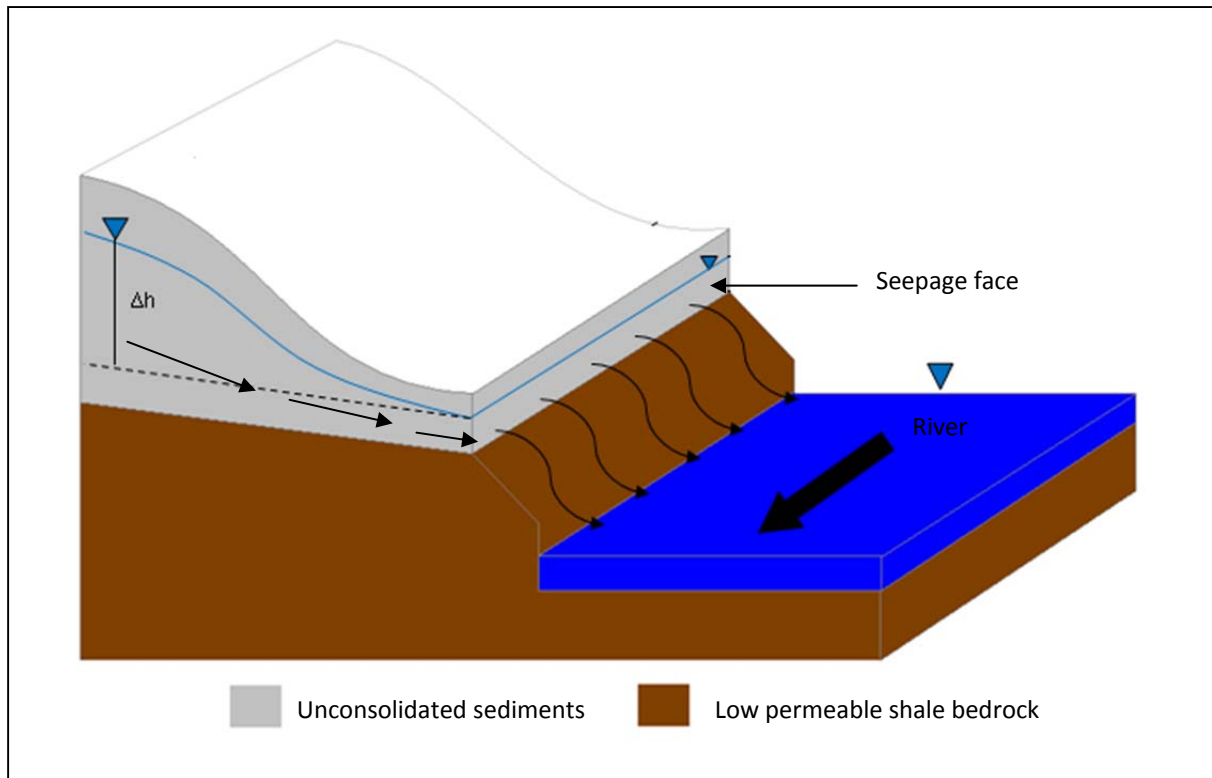


Figure 8-9 An illustration showing groundwater flow in the unconsolidated sediments of the alluvial channel main aquifer underlying the low permeable shale bedrock where discharges groundwater into the river at the seepage face; Δh is the average hydraulic head differences between alluvial channel aquifer and discharging zone; arrows shows direction of flow.

8.5 General guidelines for GW-SW interaction studies

The following steps can be very useful for investigating groundwater-river/stream interactions:

- Select the river channel segment adjacent to an alluvial channel aquifer. The combination of the river segment and alluvial channel aquifer is hereby termed a GW-SW system. The GW-SW system should be under ideal natural conditions as close as possible to reduce the potential influence of external factors affecting the results. The length of the river segment can vary but a short channel length is easier to investigate and manage. It is generally ideal to start working from the surface water resources because it's a visually observable system and hence measurements are easier to make.

- Construct a weir upstream and down stream of the channel segment under investigation. Weirs enable convenient measurement of river flow into and out of the system. The measurements should be conducted during river low flow periods for two important reasons. Making measurements during low river flow periods is generally easy. Low flow periods usually eliminate the potential influence of external sources of water inflow into the system leaving groundwater as the main source. External sources of water include; surface runoff, interflow and drainage.
- Construct a simple water balance model along the channel segment of interest as a primary objective before drilling of any boreholes. Determine inflow and outflow from the study channel segment.
- To show the scientific credibility of the GW-SW model, the mass (flow) and solute mixing (chemistry) models should give a unique solution.
- If there is a negative difference between the total inflow and total outflow, then the river system will be losing water at the study segment. Natural water losses from a river segment can be attributed to bank storage, capillary driven evaporation, groundwater gaining and evapotranspiration.
- If there is a positive difference between the total inflow and total outflow, then the river system will be gaining water. Main potential sources of water inflow to the river include groundwater and interflow. However, the interflow contribution can be minimized by performing investigations during dry and low flow river periods.
- Whether the river segment is gaining or losing, the next level of investigations should focus on identifying the exchange mechanisms and locations along the river segment. Identification of the exchange mechanisms and locations is important before any attempt to make quantifications. In other words, if you do not know where and how the exchanges are occurring then you cannot quantify them. Stable isotopes and inorganic water chemistry studies are also important for the investigations.
- Depending on the primary findings, secondary investigation efforts can be directed on some the following aspects:
 - Characterise the alluvial channel aquifer adjacent to the river segment to determine quantities and qualities of groundwater discharges
 - Install seepage meters to quantify the exchanges between the groundwater and river water.

Figure 8-10 shows the important steps and considerations for groundwater-river interactions that are summarised in a flow diagram.

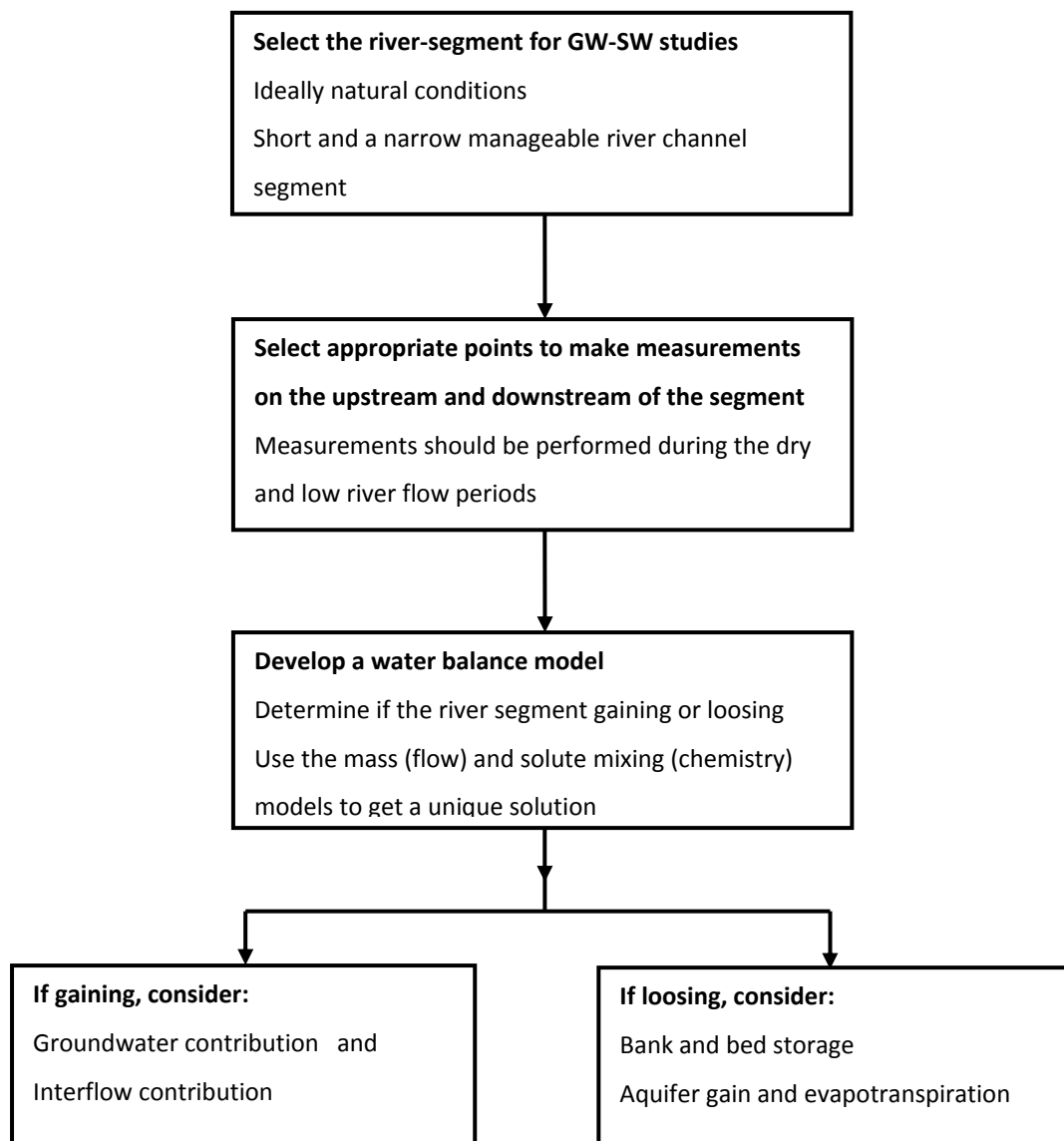


Figure 8-10 A flow diagram showing important steps and considerations for GW-SW interactions investigations.

It is important to remember that the nature and mechanisms of GW-RW interactions is always site specific. The river channel can be losing while at the same time gaining on other channel reaches. Hence no general conclusions can be made about the gaining or losing status of the entire river channel without developing a water balance model for a specific segment.

8.6 Summary

The chapter describes the field application of a water balance model, stable isotopes and geochemistry analysis to investigate groundwater river interactions along an alluvial channel aquifer. A GW-SW balance model was developed based on mass and solute mixing to determine if the system is gaining or losing water. To show the scientific credibility of the GW-SW model the two approaches of mass and solute mixing should give a unique solution. A comparison of the total water inflow and outflow of the GW-SW system showed that the system was losing water.

In general, groundwater contributes 3 % of the total inflow into the system while 32 % of the total inflow is lost mostly like to groundwater, bank storage, bed storage and evaporation. The study site provides a typical example on which significant groundwater discharge into the river can occur through the contact plane of the alluvial cover and impermeable bedrock as compared to the overly reported stream bed exchanges. A GW-SW balance model is an important primary requirement that should be developed before detailed GW-SW interaction investigations can be conducted.

The next chapter gives detailed conclusions and recommendations derived from the research thesis.

9 CONCLUSIONS AND RECOMMENDATIONS

9.1 Conclusions

Conclusions were derived for each chapter from the geological characterisation to GW-SW interaction investigations. It was decided to place the conclusions separately as they relate to specific investigations performed on the study area.

9.1.1 Geological characterisation

- An initial aquifer conceptual framework for the alluvial channel aquifer was built from geological characterization results prior to the aquifer tests and tracer tests.
- The case study alluvial channel aquifer comprises of calcrete, clay-silt and gravel sand unconsolidated channel deposits overlying the low permeable shale bedrock.
- Geological logs and groundwater levels measured after drilling shows that the alluvial channel aquifer consists of a shallow and deep low permeable aquifer system. The shallow aquifer that occurs in the calcrete, silt-clay and gravel-sand materials is the main aquifer of the system.
- The river bedrock represents the deposition floor for the unconsolidated sediments and the contact plane deposits have become a preferential flow path for groundwater.
- The gravel-sand aquifer layer that consists of medium to large pebbles is conceptually the main hydraulically conductive unit of the alluvial channel aquifer.
- Groundwater discharges from the alluvial channel shallow aquifer through the seepage face that has been created at the contact plane of the unconsolidated sediments and low permeable shale bedrock.
- Analysis of geological logs and grain size indicates the spatial variation in the physical properties of unconsolidated aquifer materials between boreholes and at different depth. The spatial variation in the physical properties of the channel deposits between boreholes and sediment layers is termed horizontal and vertical aquifer heterogeneity respectively.
- Development of the initial aquifer conceptual framework based on geological characterization has great potential to improve aquifer and tracer test planning, conductance and understanding the influence of subsurface heterogeneities.
- When exploring for groundwater resource in alluvial channel aquifers occurring along bedrock river channels, the following features can be targeted for high yield potential:

- Gravel-sand deposits.
- Contact plane between the alluvial cover and underlying bedrock.
- Bedrock when fractured.

9.1.2 Hydraulic processes and groundwater flow

- The riparian zone is characterised by exceptionally high saturated infiltration rates in excess of 1 m/d. The high infiltration rate is facilitated by the dense vegetation roots, holes and cavities created by burrowing animals and termites that create preferential infiltration paths.
- Slug test in cased boreholes yielded very low hydraulic parameters in comparison to constant rate pump test results. It is suggested that slug tests should rather be performed in open (uncased) boreholes for determining hydraulic properties.
- Based on the flow diagnosis, the alluvial channel aquifer is defined as a semi-confined to unconfined groundwater system. Semi-confined conditions occur at local scales in segments of the aquifer where tight calcrete and clay-silt sediments overlie the gravel-sand aquifer layer.
- The drawdown derivative diagnostic analysis shows that the alluvial channel aquifer system respond during pumping can be described by the following major groundwater flow characteristics:
 - Typical Theis response.
 - Transition period from initial Theis response to RAF.
 - Radial acting flow in the gravel-sand layer.
 - River single impermeable hydrogeologic boundary effects.
- The river is acting an impermeable (retarding) boundary and it indirectly implies that the river is a “gaining” one. When the river is losing, the boundary would appear as a recharging one.
- Fitting of the Cooper and Jacob (1946) equation on the drawdown of a pumping borehole gives the transmissivity of aquifer materials in the vicinity of the abstraction borehole. The method is therefore suitable for assessing spatial variation of aquifer parameters in heterogeneous alluvial channel aquifers.
- Fitting of Cooper and Jacob (1946) equation on observation wells is useful to verify the transmissivity determined for high permeable aquifer sections.
- The shallow alluvial channel main aquifer system is generally characterised by high T and storage values in the order of $10^1 \text{ m}^2/\text{d}$ and 10^{-3} respectively. The deep aquifer system that occurs in the shale formation is characterised by very low T in the range of $10^{-1} \text{ m}^2/\text{d}$.

- The determined alluvial channel aquifer transmissivity spatially varies along the alluvial aquifer channel due to heterogeneities brought about by the difference in nature and size distribution of channel deposits.
- The spatial variation of aquifer hydraulic properties at local scales underlines the significance of understanding the distribution of physical geological properties of the alluvial channel aquifer deposits prior to aquifer testing.
- The results of the aquifer tests in the alluvial channel also highlight the role of applying various geohydrological tools and techniques when selecting the representative aquifer model. Various geohydrological aspects such as water level respond to rainfall, infiltration rates, sediment grain sizes and drawdown behavior were all vital in determining the appropriate aquifer model.

9.1.3 Hydrogeochemical processes

- The groundwater evolution and quality of the alluvial channel aquifer is largely controlled by calcite and dolomite dissolutions, silicate weathering and ion exchange hydrogeochemical processes.
- The investigation revealed that the alluvial channel aquifer groundwater has evolved from $\text{Ca}^{+2}\text{-Mg}^{+2}\text{-HCO}_3^-$ recharge waters that go through ion exchange with Na^+ in the clay-silt sediments to give a $\text{Na}^+\text{-HCO}_3^-$ water type.
- Calcrete deposits are the source of Ca^{+2} , HCO_3^- and Mg^{+2} ions, while the clay-silt provides Na^+ cation exchange sites for Ca^{+2} which were detected in the sediments.
- The groundwater is supersaturated with respect to quartz, dolomite and calcite minerals.
- The hydrogeochemical investigation and analysis shows no distinction between the groundwater chemistry of deep and shallow boreholes which implies the existence of one aquifer system.
- The groundwater chemistry of the alluvial channel aquifer and terrestrial aquifer is controlled by the interactions of recharging waters and minerals of the aquifer material, rather than by a chemical evolution of water along general directions of local groundwater flow and seasonal variations.
- The study shows the potential usefulness of simple bivariate plots as a complimentary tool to the conventional methods for identification and analyzing groundwater hydrogeochemical processes. The plots simplify analysis of the groundwater chemistry processes and should be used to complement conventional tools.

- The spatial variation in chemical, hydraulic and solute transport properties is attributed to aquifer heterogeneity which is largely depended on lithology and the channel deposit processes.

9.1.4 Groundwater recharge processes and mechanisms

- Several approaches have been shown to generate information on the origin of groundwater situated in the alluvial channel and terrestrial aquifers. The investigation provided quantitative and qualitative information on the recharge processes and mechanisms of the alluvial channel aquifer.
- The alluvial channel aquifer is characterised by rapid rise of groundwater levels after rainfall events making the WFL method the most appropriate geohydrological tool for estimating recharges rates of the aquifer system.
- Water level fluctuation method provides the best geohydrological technique to determine the recharges rates of the alluvial channel.
- Cavities and holes created by the burrowing animals and dense tree rooting system contribute to preferential infiltration rates along the riparian zone resulting in quick and high recharge rates in the alluvial channel aquifer.
- Groundwater levels response to rainfall events can be used as a qualitative tool to distinguish between piston and preferential recharge mechanisms.
- Through aquifer-inter flow, the terrestrial aquifer is an important source of recharge to the alluvial channel aquifer.
- Quantification of recharge rates in alluvial channel aquifers characterised by preferential recharge due to high infiltration rates has to consider both the contribution of rainfall and flow from terrestrial aquifer during the dry season.

9.1.5 Natural gradient tracer tests in an alluvial channel aquifer

- A qualitative approach was developed to isolate and remove the density driven flow effects on the NGTBT test dilution curve before using the data for groundwater flux calculations.
- The longest duration portion of the NGPDTT dilution curve that can be fitted with a straight line should be utilized for groundwater flux calculation.
- The alluvial channel aquifer is generally characterised by low groundwater fluxes considering their low localized hydraulic heads.
- The alluvial channel aquifer is characterised by two different groundwater fluxes which are; the flux in the aquifer and the discharging flux.

- A NGTBT was successfully conducted in an alluvial channel aquifer, thus providing some advice on how to conduct tracer breakthrough tests under natural gradients in alluvial channel aquifers.
- The alluvial channel aquifer gravel-sand materials are characterised by high natural groundwater velocity in excess of 12 m/d under recharging conditions. It therefore implies that the solute transportation in the alluvial channel aquifer is dominated by the advection process.
- The findings of this study suggest that aquifer contamination investigations should assess solute transportation of contaminants under abstraction, dry (discharging) and wet (recharging) scenarios. These three scenarios result in different hydraulic gradients, potentially creating various mass transport characteristics

9.1.6 GW-SW interactions along the alluvial channel aquifer

- A GW-SW balance model is an important primary requirement that should be developed before detailed GW-SW interaction investigations can be conducted.
- To show the scientific credibility of the GW-SW model, the mass (flow) and solute mixing (chemistry) models should give a unique solution.
- Contrary to the popular concept that groundwater discharge into stream/river occurs through stream beds, the majority of GW-SW exchanges at the study site occurs through the seepage face created at the contact of plane of the alluvial cover and low impermeable bedrock. This mechanism of interaction is not dependent of the hydraulic connectivity as has been reported in literature and this is probably a special case.
- The GW-SW exchanges are dominated by local groundwater discharge into the river reach (channel segment) as enhanced by high horizontal hydraulic conductivities of the gravel-sand layer in the alluvial channel aquifer.
- Along a typical alluvial channel aquifer on a bedrock river channel, groundwater-river interactions occurs through one or more the following mechanisms:
 - Flow in the gravel-sand aquifer layer that overlies the low permeable river bedrock.
 - Preferential flow paths that occur at the contact plane of the alluvial cover sediments and the low permeable bedrock. This mechanism is not dependent on the existence of a direct hydraulic connection between the two water resources.
 - Flow in the fractured bedrock that is most likely to be in contact with the river water for most of the time. For direct hydraulic connectivity to occur, the bottom elevation of fractured-bedrock aquifer should be located at least below the river stage elevation.

- The analysis of drawdown behaviour of boreholes drilled into an alluvial channel aquifer during pump testing can be used to assess if the river is gaining or losing water into the aquifer. If the river appears as an impermeable boundary on the semi-log or derivative plot, then the aquifer will be losing into the river and the opposite is also true.

9.1.7 Proposed classification of alluvial channel aquifers

There is both theoretical and field evidence to suggest that the properties of alluvial channel aquifers are greatly influenced by the nature of the hosting river channel. Based on the review of literature and conceptual understanding gained from field investigations, it is proposed that studies be conducted to determine if alluvial channel aquifers can be further classified depending on the nature of the hosting river channel. The flow chart on Figure 9-1 shows the classification of alluvial channel aquifers and typical attributes of the aquifer that is proposed to be tested on other sites.

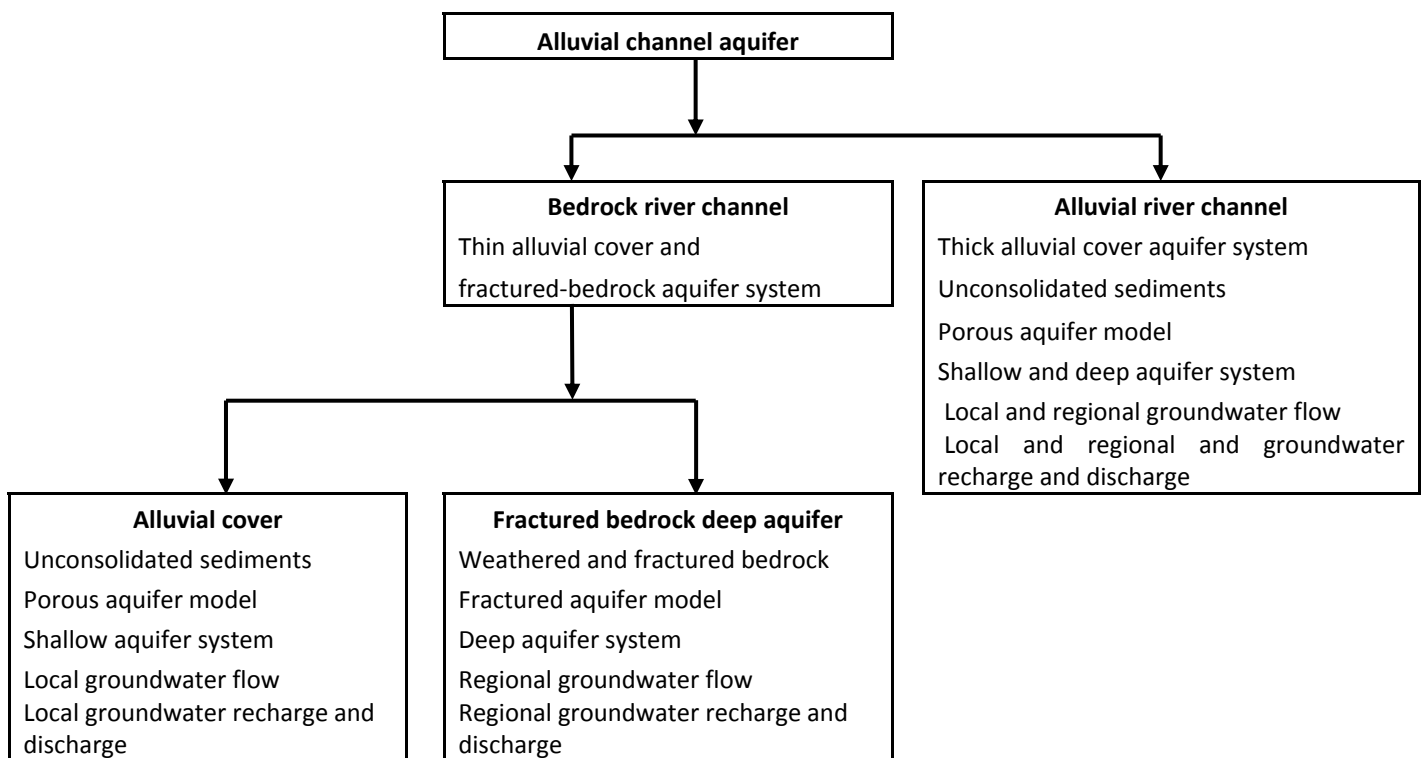


Figure 9-1 A flow diagram showing the proposed classification of alluvial channel aquifers and typical attributes of geohydrological properties.

In general, the classification suggest that a river channel segment can either be a bedrock or alluvial in nature (Figure 9-1). Along a typical bedrock river channel, two main aquifer systems can exist in the form of thin shallow alluvial cover and deep fractured bedrock aquifers. It therefore implies that groundwater would mainly occur and flow in thin alluvial cover and deep fractured bedrock aquifers.

The aquifers can be hydraulically connected or completely separated depending on the nature of the bounding geological materials.

The thin (< 10 m) alluvial cover comprises of unconsolidated material deposited by the river and this also applies to the thick alluvial aquifer that typically occurs along alluvial river channel. Sand and gravel unconsolidated deposits forms the most yielding hydrogeological unit of the thin and thick alluvial aquifer systems because of their naturally high hydraulic conductivity. Alluvial channel aquifers that mainly comprises sand and gravel unconsolidated sediments can be ideal represented by porous aquifer model. Because thin alluvial cover aquifers are located at shallow depth, they are often characterised by local groundwater flow, recharge and discharge systems.

The fractured bedrock underlying the unconsolidated sediments thin alluvial aquifer forms the deep aquifer along bedrock river channel. Continued fracturing due to pressure release during overburden removal by erosion processes can also enhance the secondary porosity of the aquifer. Groundwater occurrence and flow in the fractured bedrock can be idealised by fractured aquifer models. Regional groundwater flow, recharge and discharge are expected to dominate in the deep fractured river bedrock channel aquifers given their deep locations.

Along a typical alluvial river channel, groundwater mainly occurs and flow in thick alluvial covers of unconsolidated sediments. The groundwater flow conditions are typically similar to the thin alluvial cover except that the thick alluvial cover aquifer can have both shallow and deep groundwater flow systems. The aquifer system is therefore characterised both local and regional groundwater flow, recharge and discharge systems.

This proposed classification is aimed at providing hydrogeologists with information on the possible groundwater occurrence and flow scenarios that may occur along alluvial channel aquifers. The information can be useful for locating groundwater resources in typical alluvial channel aquifer. Planning for borehole drilling and construction also requires a good initial conceptual understanding of possible hydrogeologic conditions that might occur at the site.

9.2 Recommendations

Based on the study findings and understanding gained on the alluvial channel aquifer system and its associated interaction with the river system, the following aspects are recommended:

- Assessing the dependence of the riparian vegetation on the shallow alluvial channel aquifer. Such an investigation can address losses from the alluvial channel through evapotranspiration and also the applicability of stable isotopes to assess the dependence.
- Numerical models should be developed to assess the interactions between alluvial channel aquifers and the river systems.
- Investigations should be conducted to assess the effects of abstracting from the alluvial channel aquifer on seepage discharges.
- Geophysical mapping of the bedrock and assessment of its influence on groundwater flow direction.
- It suggested that investigation sites for GW-SW interaction studies be selected along natural river segments. Although the current site proved very useful, its positioning just downstream of the dam and the existence of a weir can potentially offset the natural conditions in the surrounding groundwater resources.
- It is proposed that the definitions of the GW-SW interaction mechanisms be extended to include seepage discharge that often occurs through river banks along alluvial channel aquifers situated on impermeable bedrock river channels.
- Research efforts should be directed towards establishing the general appropriate borehole drilling restrictive distance from river/streams as influenced by the channel type.
- In depth investigations can also be focused on determining the allowable/available drawdown that will ensure sustainable aquifer discharge for the river ecosystem. For such investigations, the ranges of aquifer discharge quantities/fluxes that can sustain the ecosystem have to be established first.
- It is recommended that deep boreholes should be drilled and properly constructed at the site to further investigate the existence of a deep aquifer system on the site. The existence of a deep aquifer system would most likely imply another mode of GW-SW interaction with the river other than the seepage face at the contact plane.
- Further investigations should be focused on identifying and characterizing river water transmission losses of the study system.
- Research should be conducted at the same case study to evaluate the influence of abstraction from both the terrestrial and alluvial channel aquifer on natural groundwater discharge quantities and qualities. The influence of the discharging quality and quantities on the riparian and aquatic ecosystem can also be investigated.
- An aquifer test conducted in the channel aquifer can be used to investigate if the river is losing or gaining water from the aquifer. If the river is gaining, then it would most likely appear as an impermeable boundary. If the river is losing, then it should appear as a recharging boundary on a semi-log drawdown against time plot.

- In unconsolidated deposits channel aquifer slug tests should be performed in open uncased holes before borehole construction.
- An automated rain gauge and levels loggers should be installed to monitor the rapid recharge process of the alluvial channel aquifer that occurs immediately after the rainfall events. Alternatively water levels can be measured immediately (a day after the rainfall event).
- Research efforts should also be placed on developing some analytical solutions that can be used to analyze NGTBT tracer curved when a long duration tracer injection mode is used.
- It is recommended that further hydraulic tests be conducted to investigate the nature of the deep low permeable aquifer system underlying the main shallow alluvial channel aquifer.

9.3 Main contribution of the thesis

This thesis made a significant contribution to understanding the geohydrological properties of a typical alluvial channel aquifer and groundwater-surface water interactions along the aquifer. Specific important outputs from the research thesis are as follows:

- A proposal to classify alluvial channel aquifers based on the nature of the river channel hosting the aquifer.
- Improved understanding of groundwater-surface water interactions along a typical alluvial channel aquifer.
- Improved understanding of groundwater flow and aquifer response during pumping of the typical alluvial channel aquifer.
- Improved understanding of the hydrogeochemical processes in a typical alluvial channel aquifer.
- Improved understanding of the recharge mechanisms and processes of a typical alluvial channel aquifer.
- A qualitative approach to isolate and remove the density effects on the point dilution tracer test dilution curve before using the data for calculations.
- General guidelines for conducting natural gradient tracer tests in a typical alluvial channel aquifer.
- Comprehensive guidelines for conducting groundwater-surface water interactions investigations along a typical alluvial channel aquifer based on the water model balance.
- Linking of the flow, chemistry and isotopic properties of the groundwater and surface water system in a water balance model to provide quantitative estimation of the system's losses.

10 REFERENCES

- Adams F (1984)** Crop response to lime in the Southern United States. In Soil Acidity and Liming. F. Adams (ed.), *Society of Agronomy, Crop Science Society of America, Soil Science Society of America (ASA-CSSA-SSSA)* 211-265.
- Alley MW (1991)** Regional Groundwater-Quality Alley, W.M., 1993, Regional Ground Water Quality, Van Nostrand Reinhold, New York.
- Arumugam K and Elangovan K (2009)** Hydrochemical characteristics and groundwater quality assessment in Tirupur Region, Coimbatore District, Tamil Nadu, India. *Environmental Geology* 58:1509-1520. Available via www.springerlink.com, accessed 18 May 2011.
- Ashley GM, Renwick WH and Haag GH (1988)** Channel form and processes in bedrock and alluvial reaches of the Raritan River, New Jersey. *Geology* 16:436-439.
- Benito G, Rohde R, Seely M, Külls C, Dahan O, Enzel Y, Todd S, Botero B, Morin E, Grodek T and Roberts C (2009)** Management of alluvial aquifers in two Southern African Ephemeral Rivers: Implications for integrated water resource management. *Water Resources Management* 24:641-667. Available via www.sciencedirect.com, accessed 25 May 2011.
- Bharati LK, Lee H, Isenhardt TM and Schultz RC (2002)** Soil-water infiltration under crops, pastures, and established riparian buffer in Midwestern USA. *Agroforestry Systems* 56: 249-257. Available via www.springerlink.com, accessed on 12 January 2011.
- Botha JF and Cloot AHJ (2004)** Deformations and the Karoo aquifers of South Africa. *Advanced Water Resources* 27:383-398. Available via www.sciencedirect.com, accessed 18 February 2011.
- Botha JF, Verwey JP, Van der Voot I, Vivier JJP, Buys J, Colliston WP and Look JC (1998)** Karoo aquifers: Their geology, geometry and physical properties. Water Research Commission, South Africa. WRC Report No. 487/01/98.
- Bouwer H and Rice RC (1976)** A slug test method for determining hydraulic conductivity of unconfined aquifers with completely or partially penetrating wells. *Water Resources Research* 12:3:423-428.
- Boyle RD (1994)** Design of a seepage meter for measuring groundwater fluxes in the nonlittoral zones of lakes- Evaluation in a boreal forest lake. *Limnology and Oceanography* 39(3):670-68.
- Bradbury KR and Muldoon MA (1990)** Hydraulic conductivity determinations in unlithified glacial and fluvial materials. In: Nielsen DM, Johnson AI (eds) Ground water and vadose zone monitoring. American Society for Testing and Materials, Special Technical Publication (ASTM STP) 1053: 138-151.
- Campbell GDM (1980)** Beaufort West groundwater investigation (1975-1977). Unpublished Technical Report GH 3155, Department of Water Affairs. South Africa.
- Cardona A, Carrillo-Rivera JJ, Huizar-Alvarez R and Graniel-Castro E (2004)** Salinization in coastal aquifers of arid zones: An example from Santo Domingo, Baja California Sur, Mexico. *Environmental Geology* 45:350-366. Available via www.sciencedirect.com, accessed 18 April 2011.

Cenderelli DA and Cluer BL (1998) Depositional processes and sediment supply in resistant-boundary channels; examples from two case studies In Rivers over rock: fluvial processes in Bedrock channels eds. Tinkler KJ and Wohl EE., 105-131, American Geophysical Union, Geophysical Monograph 107.

Cey EE, Rudolph DL, Parkin WG and Aravena R (1998) Quantifying groundwater discharge to a small perennial stream in Southern Ontario, Canada. *Journal of Hydrology* 210:21-37.

Cey EE, Rudolph, DL, Aravena R and Parkin G (1999) Role of the riparian zone in controlling the distribution and fate of agricultural nitrogen near a small stream in southern Ontario. *Journal of Contaminant Hydrology* 37:45-67. Available via www.sciencedirect.com, accessed 23 April 2011.

Chiang W and Kinzelbach W (1998) Processing Modflow-A Simulation System for Modeling Groundwater Flow and Pollution. Hamburg, Zürich <http://www.simcore.com>.

Chivas AR, Andrew AS, Lyons BW Bird IM and Donnelly HT (1991) Isotopic constraints on the origin of salts in Australian playas. 1 Sulfur, *Palaeogeography, Palaeoclimatology, Palaeoecology* 84:309-332.

Cissé IA and Mao X (2008) Nitrate: Health Effect in Drinking Water and Management for Water. *Quality Environment Research* 2:6:311-316.

Choi B, Yun S, Mayer B, Chae G, Kim K, Kim K and Koh Y (2009) Identification of groundwater recharge sources and processes in a heterogeneous alluvial aquifer: Results from multi-level monitoring of hydrochemistry and environmental isotopes in a riverside agricultural area in Korea. *Hydrological Processes* 24:317-330. Available via www.interscience.wiley.com, accessed on 4 September, 2010.

Cooper DJ, Merritt DM, Andersen DC and Chimner RA (1999) Factors controlling the establishment of Fremont cottonwood seedlings on the upper Green River, USA. *Regulated Rivers: Research and Management* 15:419-440.

Cooper HH Jr and Jacob CE (1946) A generalized graphical method for evaluating formation constants and summarizing well field history. *Transactions-American Geophysical Union* 27: 526-534.

Costa JE, Spicer KR, Cheng RT, Haeni FP, Melcher NB, Thurman EM, Plant WJ and Keller WC (2000). Measuring stream discharge by non-contact methods: A proof-of-concept experiment. *Journal of Geophysical Research* 27, 4, 553-556.

Dansgaard W (1964). Isotopic variation in meteoric waters. *Science* 133: 1702-1703.

Davis SN and Davis AG (1997) Saratoga Springs and early hydrochemistry in the United States. *Ground Water* 35:2:347-356. Available via <http://info.ngwa.org>, accessed on 06 August 2010.

Deckers JA, Nachtergaele FO and Spaargaren OC (Eds.) (1998). World Reference Base for soil resources: Introduction. ACCO Leuven/Amersfoort. Available via www.books.google.co.za, accessed on 01 February, 2011.

De Hamer W, Love D, Owen R, Booij JM and Hoekstra YA (2008) Potential water supply of a small reservoir and alluvial aquifer system in Southern Zimbabwe. *Physics and Chemistry of the Earth* 33:633-639. Available via www.sciencedirect.com, accessed 5 April 2011.

Deutsch WJ (ed.) (1997) Groundwater Geochemistry. Fundamentals and applications to contamination. Chemical Rubber Company (CRC) Press, Boca Raton, USA.

Diersch HJG and Kolditz O (2002) High-density flow and transport in porous media: approaches and challenges. *Advanced Water Resource* 25(8-12):899-944.

Domenico PA and Schwartz FW (1990) Physical and chemical hydrogeology. Wiley, New York.

Drost W, Klotz D, Koch A, Moser H, Neumaier F and Rauert W (1968) Point dilution methods of investigating groundwater flow by means of isotopes. *Water Resources* 4:1:125-146.

DWAF (2000) Policy and strategy for groundwater quality management in South Africa. Department of Water Affairs and Forestry, Republic of South Africa.

Emery JM and Cook GW (1984) A determination of the nature of recharge to a bedrock fracture system. In Proceedings of National Water Well Association, Eastern Regional Groundwater Conference, 62-77. Worthington, Ohio. Available via <http://info.ngwa.org>, accessed on 02 May 2011.

Eriksson E (1952) Composition of Atmospheric Precipitation-II. Sulfur, chloride, iodine compounds. *Bibliography Tellus* 4:4:280-303. Available via www.onlinelibrary.wiley.com, accessed 03 March 2011.

Fetter CW (1993) Contaminant hydrogeology. Prentice Hall, Englewood Cliff.

Fisher RS and Mulican WF III (1997) Hydrochemical evolution of sodium-sulfate and sodium-chloride groundwater beneath the Northern Chihuahuan desert, Trans-Pecos, Texas, USA. *Hydrogeology Journal* 10:455-474.

Fleckenstein JH, Niswonger GR and Graham FE (2006) River-Aquifer Interactions, Geologic Heterogeneity, and Low Flow Management. In press, Ground Water, Special issue from MODFLOW and more conference. Available via www.sciencedirect.com, accessed on 18 February 2010.

Freeze RA and Cherry JA (1979) Groundwater: Englewood Cliffs, NJ Prentice Hall.

Gomo M (2009) Site Characterisation of LNAPL-Contaminated Fractured-Rock Aquifer. MSc thesis at the Institute for Groundwater Studies. University of the Free State, Bloemfontein, South Africa. Available via www.etd.uovs.ac.za, accessed on 28 January 2011.

Grathwohl P and Kleinedam S (1995) Impact of heterogeneous aquifer materials on sorption capacities and sorption dynamics of organic contaminants. Available via <http://iahs.info/redbooks>, accessed on 05 November 2010.

Gregory SV, Swanson FJ, McKee WA (1991) An ecosystem perspective of riparian zones. *BioScience* 40: 540-551.

Green CH and Haney R (2000) Riparian Zones Protecting water quality. Protecting Water Quality, Phosphorus Best Management and Practices.

Groom PK (2003) Groundwater-dependency and water relations of four Myrtaceae shrub species during a prolonged summer drought. *Journal of the Royal Society of Western Australia* 86:31-40. Available via <http://espace.library.curtin.edu.au>, accessed on 15 July 2011.

- Groom PK, Froend RH and Mattiske EM (2000)** Impact of groundwater abstraction on a Banksia woodland, Swan Coastal Plain, Western Australia. *Ecological Management and Restoration* 1:117-124.
- Guglielmi Y, Mudry J, Blavoux B (1998)** Estimation of the water balance of alluvial aquifers in region of high isotopic contrast: an example from southeastern France. *Journal of Hydrology* 210: 106-115.
- Guler C, Thyne GD, McCray JE, Turner AK (2002)** Evaluation of graphical and multivariate statistical methods for classification of water chemistry data. *Hydrogeology Journal* 10:455-474. Available via <http://annmalaiuniversity.academia.edu>, accessed 8 May 2011.
- Halford JK, Weight, DW and Schreiber P (2006)** Interpretation of Transmissivity Estimates from Single-Well Pumping Aquifer Tests. *Ground Water* 44:3:467-471. Available via www.onlinelibrary.wiley.com, accessed on 27 November, 2010.
- Harvey FE and Sibray SS (2001)** Delineating ground water recharge from leaking irrigation canals using water chemistry and isotopes. *Ground Water* 39: 408-421.
- Hazen A (1911)** Discussion: dams on sand foundations. *Transactions of the American Society of Civil Engineers* 73:199-203.
- Healy RW and Cook PG (2002)** Using ground-water levels to estimate recharge. *Hydrogeology Journal* 10: 91-109. Available via www.springerlink.com, accessed on 27 March 2010.
- Hereford R (2000)** Recent Alluvial History of the Southern Colorado Plateau. Available via <http://esp.cr.usgs.gov/info/sw/scpalluvial/>, accessed on 15 August, 2011.
- Howard AD (1998)** Long Profile Development of Bedrock Channels: Interaction of Weathering, Mass Wasting, Bed Erosion, and Sediment Transport. Rivers Over Rock: Fluvial Processes in Bedrock Channels. *Geophysical Monograph* 107:297-319.
- IAEA/WMO (2004)** *Global Network of Isotopes in Precipitation*. The GNIP Database. Available via <http://isohis.iaea.org>, accessed on 12 April 2011.
- Ivkovic KM (2009)** A top-down approach to characterise aquifer-river interaction processes. *Journal of Hydrology* 365:145-155. Available via www.elsevier.com, accessed on 27 November 2010.
- Jankowski J, Acworth RI and Shekarforoush S (1998)** Reverse ion exchange in a deeply weathered porphyritic dacite fractured aquifer system, Yass, New South Wales, Australia. In: Arehart GB, Hulston JR (eds) *Proceedings of the 9th International Symposium. Water-rock interaction, Taupo, New Zealand, 30 March-3, Balkema, Rotterdam, April 1998*:243-246.
- Jankowski J and Beck P (2000)** Aquifer Heterogeneity: Hydrogeological and Hydrochemical Properties of the Botany Sands Aquifer and their Impact on Contaminant Transport. *Australian Journal of Earth Sciences* 47:1:45-64. Available via www.dx.doi.org, accessed on 18 March, 2010.
- Kading HW (1976)** Horizontal spinner, a new production logging technique. *The Log Analyst XVII* 5:3-7.
- Kalbus E, Reinstorf F and Schirmer M (2006)** Measuring methods for groundwater-surface water interactions: a review. *Hydrology and Earth System Sciences* 10:873-887.

- Kearl PM (1997)** Observations of particle movement in a monitoring well using the colloidal borescope. *Journal of Hydrology* 200(1-4):323-344.
- Kearns AK and Hendrickx JMH (1998)** Temporal variability of diffuse groundwater recharge in New Mexico. N M Water Resources Res Inst Tech Completion Rep 309:43.
- Keen-Zebert A (2007)** "Spatial Variation of Alluvial and Bedrock Channel Type in the Upper Guadalupe River, Texas" Theses and Dissertations-Geography. Paper 12. Available via <http://ecommons.txstate.edu>, accessed on 18 February 2010.
- Kelly WR (1997)** Heterogeneities in ground-water geochemistry in a sand aquifer beneath an irrigated field. *Journal of Hydrology* 198:154-176. Available via www.sciencedirect.com, accessed 4 March 2011.
- Kirk S (2006)** Interactions between groundwater-surface water and terrestrial eco-systems. *Groundwater and Ecosystems* 205-216.
- Klingbeil R, Kleineidam S, Aspiron U and Aigner T and Teutsch G (1999)** Relating lithofacies to hydrofacies: outcrop-based hydrogeological characterisation of Quaternary gravel deposits. *Sedimentary Geology* 129:299-310. Available via www.sciencedirect.com, accessed on 28 September 2010.
- Knüppe K (2011)** The challenges facing sustainable and adaptive groundwater management in South Africa. Available on www.wrc.org.za, accessed on 04 August, 2011.
- Kraft GJ, Stites W and Mechenich DJ (1999)** Impacts of irrigated vegetable agriculture on a humid north-central US sand plain aquifer. *Ground Water* 37:572-580. Available via <http://onlinelibrary.wiley.com>, accessed 18 April 2011.
- Lamontange S, Dighton, J and Ullman, W (2002)** Estimation of groundwater velocities in riparian zones using point dilution tests. CSIRO Land and Water. Technical Report 14/04. USA.
- Landon MK, Rus DL and Harvey FE (2001)** Comparison of instream methods for measuring hydraulic conductivity in sandy streambeds. *Ground Water* 39:870-885.
- Lange B, Luescher P and Germann PF (2008)** Significance of tree roots for preferential infiltration in stagnant soils. *Hydrology and Earth System Sciences* 13:1809-1821 Available via www.hydrol-earth-syst-sci-discuss.net, accessed on 10 July 2011.
- Langmuir D (1997)** Aqueous Environmental Geochemistry. Prentice-Hall, New Jersey.
- Lee DR and Cherry JA (1978)** A field exercise on groundwater flow using seepage meters and mini-piezometers. *J Geol Edu* 27:6-9.
- Lee DR (1977)** A device for measuring seepage flux in lakes and estuaries. *Limnology and Oceanography* 22:140-147.
- Leketa KC (2011)** Flow characteristics of groundwater systems: An investigation of hydraulic parameters. Unpublished MSc Thesis at the Institute for Groundwater Studies, University of the Free State, South Africa.

Luckey RR, Gutentag ED, Heimes FJ, Weeks JB (1986) Digital simulation of ground-water flow in the High Plains aquifer in parts of Colorado, Kansas, Nebraska, New Mexico, Oklahoma, South Dakota, Texas, and Wyoming. U.S. Geological Survey professional paper 1400-D: 57.

Mahoney JM and Rood SB (1991) A device for studying the influence of declining water table on poplar growth and survival. *Tree Physiology* 8:305-314.

Mansell MG and Hussey SW (2005) An investigation of flows and losses within the alluvial sands of ephemeral rivers in Zimbabwe. *Journal of Hydrology* 314:192-203. Available via www.sciencedirect.com, accessed 23 February 2011.

Mayer MP, Reynolds Jr SK, Canfield JT (2005) Riparian Buffer Width, Vegetative Cover, and Nitrogen Removal Effectiveness: A Review of Current Science and Regulations. United States Environmental Protection Agency. EPA/600/R-05/118. Available via <http://www.epa.gov/nrmrl/pubs>, accessed on 25 June 2011.

McQueen KG (2006) Calcrete Geochemistry in the Cobar-Girilambone Region, New South Wales. Cooperative Research Centre for Landscape Environments and Mineral Exploration (CRC LEME). New South Wales, Australia. Available via www.sciencedirect.com, accessed on 29 September, 2010).

Mahoney JM and Rood SB (1998) Streamflow requirements for cottonwood seedling recruitment: An interactive model. *Wetlands* 18:634-645.

Momii K, Jinno K and Hirano F (1993) Laboratory studies on a new laser Doppler velocimeter system for horizontal ground water velocity measurement in a borehole. *Water Resources Research* 29:2:283-292.

Moyce W, Mangeya P, Owen R and Love D (2006) Alluvial aquifers in the Mzingwane catchment: Their distribution, properties, current usage and potential expansion. *Physics and Chemistry of the Earth* 31:988-994. Available via www.sciencedirect.com, accessed 16 April 2011.

Murray RB, Zeppel MJB, Hose GC and Eamus D (2003) Groundwater-dependent ecosystems in Australia: It's more than just water for rivers. *Ecological Management and Restoration* 4:2:110-113.

National Research Council (1977) Drinking water and health. Washington, DC, National Academy of Sciences.

National Water Act (1998) Government Gazette, 19182. Act 38. Pretoria, South Africa.

Norvitch RF (1960) Ground water in alluvial channel deposits Nobles County, Minnesota. U. S. Geological Survey-Location of the place. Available via www.coner.com, accessed on 19 September 2010.

Oosterbaan, JR and Nijland JH (1994) Determining the saturated hydraulic conductivity. Chapter 12 in: Ritzema, P.H (Ed.), Drainage Principles and Applications. International Institute for Land Reclamation and Improvement (ILRI), Publication 16, second revised edition, 1994, Wageningen, The Netherlands. Available via www.waterlog.info, accessed on 25 May, 2010.

Panno SV, Hackley KC, Hwang HH and Kelly WR (2001) Determination of the sources of nitrate contamination in karst springs using isotopic and chemical indicators. *Chemical Geology* 179:113-128. Available via www.sciencedirect.com, accessed 26 April 2011.

- Parkhurst DL and Appelo CAJ (1999)** Phreeqc for windows version 1.4.07. A hydrogeochemical transport model. US Geological Survey Software.
- Parsons JA and Abrahams AD (Eds) (1994)** Geomorphology of desert environments. Chapman and Hall, London pp13.
- Pettit NE, Froend RH and Davies PM (2001)** Identifying the natural flow regime and the relationship with riparian vegetation for two contrasting Western Australian rivers. *Regulated Rivers: Research and Management* 17:201-215.
- Pitrak M, Mares S and Kobr M (2007)** A Simple Borehole Dilution Technique in measuring Horizontal Ground Water Flow. *Ground Water* 45:1:89-92.
- Postma D, Boesen C, Kristiansen H and Larsen F (1991)** Nitrate reduction in an unconfined sandy aquifer: water chemistry, reduction processes, and geochemical modeling. *Water Resources Research* 27:2027-2045.
- Pretorius JA (2007)** DNAPLS in South African fractured aquifers: Occurrence, fate and management. PhD Thesis at the Institute for Groundwater Studies, University of the Free State, South Africa.
- Rajmohan N and Elango L (2004)** Identification and evolution of hydrogeochemical processes in the groundwater environment in an area of the Palar and Cheyyar River Basins, Southern India. *Environmental Geology* 46:47-61. Available via www.sciencedirect.com, accessed 18 April 2011.
- Richards K (1982)** Rivers form and process in alluvial channels. Methuen, London.
- Riemann K (2002)** New developments in conducting and analyzing tracer tests in fractured-rock aquifers. Unpublished PhD Thesis at the Institute for Groundwater Studies, University of the Free State, South Africa.
- Riemann K, Van Tonder JG and Dzanga P (2002)** Interpretation of single-well tracer tests using fractional-flow dimensions Part 2: A case study. *Hydrogeology Journal* 1-29.
- Rood SB, Braatne JH and Hughes FMR (2003)** Ecophysiology of riparian cottonwoods: stream flow dependency, water relations and restoration. *Tree Physiology* 23:1113-1124. Available via www.treephys.oxfordjournals.org, accessed on 28 April 2011.
- Samani N, Pasandi M and Barry DA (2006)** Characterizing a heterogeneous aquifer by derivative analysis of pumping and recovery test data. *Journal of Geological Society of Iran* 1:29-41 Available via www.gsoi.ir, accessed on 18 November 2010.
- Sauty JP (1980)** An analysis of hydrodispersive transfer in aquifers. *Water Resources Research* 16:145-158.
- Sawyer GN and McMcarty DL (1967)** Chemistry of sanitary engineers, 2nd edition McGraw Hill, New York.
- Scanlon R B, Stonestrom A D, Reedy CR, Leaney WF, Gates J and Cresswell GR (2009)** Inventories and mobilization of unsaturated zone sulfate, fluoride, and chloride related to land use change in semiarid regions, southwestern United States and Australia. *Water Resources Research* 45:1-17.

Scanlon BR and Goldsmith RS (1997) Field study of spatial variability in unsaturated flow beneath and adjacent to playas. *Water Resources Research* 33:2239-2252.

Seaman MT, Roos JC, Watson M (2001) The State of the Modder River, First Quarter 2001-a bio-monitoring report. Report to Bloem Water by the Centre for Environmental Management. Bloemfontein: University of the Free State, South Africa.

Seely M, Henderson J, Heyns P, Jacobson P, Nakale T, Nantanga K and Schachtschneider K (2003) Ephemeral and endorheic river systems: Relevance and management challenges. In: Turton A, Ashton P and Cloete E (Eds). *Transboundary Rivers, sovereignty and development: Hydropolitical drivers in the Okavango River basin*. Pretoria, South Africa.

Shafroth B P, Stromberg CJ and Patten TD (2000) Woody riparian vegetation response to different alluvial water table regimes. *Western North American Naturalist* 60(1):66-76. Available via <https://ojs.lib.byu.edu>, accessed on 21 April 2011.

Shakhane T (2011) Coupled flow in groundwater systems: The study of bulkflow parameters. Unpublished MSc Thesis at the Institute for Groundwater Studies, University of the Free State, South Africa.

Simmons CT (2005) Variable density groundwater flow: From current challenges to future possibilities. *Hydrogeology Journal* 3:116-119.

Simmons CT, Fenstemaker TR, Sharp JM Jr (2001) Variable density groundwater flow and solute transport in heterogeneous porous media: approaches, resolutions and future challenges. *Journal of Contaminant Hydrology* 52:1-4:245-275.

Smith JWN (2005) Groundwater-surface water interactions in the hyporheic zone, Environment. Available via www.environment-agency.gov.uk, accessed on 15 July 2011.

Snyder NJ, Mostaghimi SDF, Berry DF, Reneau RB, Hong S, McClellan PW and Smith EP (1998) Impact of riparian forest buffers on agricultural nonpoint source pollution. *Journal of the American Water Resources Association* 34:385-95. Available via www.onlinelibrary.wiley.com, accessed 23 June, 2011.

Sophocleous M (2002) Interactions between groundwater and surface water: The state of the science. *Hydrogeology Journal* 10:52-67.

South African National Standards (SANS) (1996) Department of Water Affairs and Forestry South Africa Volume 1: Domestic Water Use (2nd edition). Republic of South Africa.

Spane FA Jr and Wurstner SK (1992) DERIV: A program for calculating pressure derivatives for hydrologic test data. PNL-SA-21569, Pacific Northwest Laboratory, Richland, Washington.

Spruill TB (2000) Statistical evaluation of effects of riparian buffers on nitrate and ground water quality. *Journal of Environmental Quality* 29:1523-1538. Available via <http://nc.water.usgs.gov>, accessed 15 May 2011.

Stromberg J (1998) Dynamics of Fremont cottonwood (*Populus fremontii*) and saltcedar (*Tamarix chinensis*) populations along the San Pedro River. *Arizona Journal of Arid Environments* 40:133-155.

Tanji KK and Kielen CN (2002) Agricultural drainage water management in arid and semi-arid areas. **Food and Agriculture Organization (FAO) of the United Nations** Irrigation and Drainage Paper 61. Available via www.atl.org.mx, accessed on 29 September 2010.

Tankard AJ, Eriksson KA, Hunter DR, Jackson MPA, Hobday, DK and Minter WEL (1982) Crustal Evolution of Southern Africa. Springer-Verslag, New York, pp 523.

Tooth S, Mc Carthy ST, Brandt D, Hancox PJ and Morris R (2002) Geological controls on the formation of alluvial meanders and floodplain wetlands: The example of the Klip River, Eastern Free State in South Africa. *Earth Surface Process Landforms* 27:797-815. Available via www.interscience.wiley.com, accessed on 14 March, 2011.

Tóth J (1970) Groundwater as a geologic agent: An overview of the causes, processes, and manifestations *Hydrogeology Journal* 7:1-14. Available via www.dahlhaus.com.au, accessed on 12 March 2011.

Turowski MJ, Hovius N, Wilson A and Horng M (2008) Hydraulic geometry, river sediment and the definition of bedrock channels. *Geomorphology* 99:26-38. Available via www.sciencedirect.com, accessed on 17 March, 2011.

Turowski MJ (2010) Semi-alluvial channels and sediment-flux-driven bedrock erosion Review paper for the Gravel Bed Rivers Conference 2010 Birmensdorf, Switzerland. Available via www.wsl.ch/info/mitarbeitende/turowski/download/Turowski2011, accessed on 23 July 2011.

USEPA (2001) The State-of-the Practice of Characterization and Remediation of Contaminated Ground Water at Fractured Rock Sites, Publication 542-R-01-010.

USGS (1993) National water Summary-1990-1991: Stream Water Quality United States Geological Survey. Water Supply paper 2400:590.

US Salinity Laboratory Staff (1954) Diagnosis and improvement of saline and alkalis soils US Department of Agriculture Handbook 60:160 Washington DC.

Van der Bruggen B, Goossens H, Everard PA, Stemge'e K and Rogge W (2009) Cost-benefit analysis of central softening for production of drinking water. *Journal of Environmental Management* 91:541-549. Available via www.sciencedirect.com, accessed on 19 April 2011.

Van Tonder GJ, Bardenhagen I, Riemann K, Van Bosch J, Dzanga P and Xu Y (2001a) Manual on Pumping Test, Analysis in fractured- Rock Aquifers Part A. Institute of Groundwater Studies, University of the Free State. South Africa.

Van Tonder GJ, Kunstmann H, Xu Y (2001b). FC program, software developed for DWAF by the Institute of Groundwater Studies. Institute of Groundwater Studies, University of the Free State, South Africa.

Van Wyk E, Van Tonder GJ and D Vermeulen (2011) Characteristics of local groundwater recharge cycles in South African semi-arid hard rock terrains-rainwater input Water. SA 37:2:147-154. Available via www.wrc.org.za, accessed on 5 August 2011.

Vigilar GG and Diplas P (1998) Stable channels with mobile bed: Model verification and graphical solution. *Journal of Hydraulic Engineering* 124:1097-1108.

Visser JNJ (1989) Course notes on Geology 216: Sedimentology. Lecture delivered at of the Orange Free University, Republic of South Africa.

Vivier J P J, Van Tonder GJ and Botha JF (1995) The use of Slug tests to predict borehole yields: correlation between the regression time of slug and borehole yields. Institute of groundwater Studies, University of the Free State. South Africa.

Wang B and Yang T (1984) Groundwater pollution, contamination and transport simulation. Beijing Normal University Press, Beijing.

Wang P, Zhang Y, Yu J, Fu G and Ao F (2011) Vegetation dynamics induced by groundwater fluctuations in the lower Heihe River Basin, northwestern China. *Journal of Plant Ecology* 4:1-2:77-90 Available via www.jpe.oxfordjournals.org, accessed on 13 June 2011.

Washington State Department of Ecology (1994-2011) Channel Migration. Available on http://www.ecy.wa.gov/programs/sea/sma/cma/page17_appendix.html accessed 15 August 2011.

Watts NL (1980) Quaternary pedogenic calcretes from the Kalahari (southern Africa): mineralogy, genesis and diagenesis. *Sedimentology Volume* 27:6:661-686. Available via www.onlinelibrary.wiley.com , accessed 24 April 2011.

WeatherSA (2011) <http://www.weathersa.co.za/web/Content.asp?contentID=200>.

Wenzel LK (1942) Methods for Determining Permeability of Water-Bearing Materials. U.S. Geological Survey Water-Supply Paper 887.

Weng PH, Coudrain-Ribstein A, Talbi A and Bendjoudi H (1999) Groundwater Circulations between Alluvial Aquifer and Underlying Senonian Chalk in the Seine Valley. *Physics and Chemistry of the Earth*. 24:1-2:151-154. Available via www.sciencedirect.com, accessed 10 July 2011.

WHO (1993) Guidelines for drinking water quality, Vol.1.WHO, Geneva.

WHO (2010) Hardness in Drinking-water: Background document for development of WHO Guidelines for Drinking-water Quality. Available via <http://whqlibdoc.who>, accessed 28 June 2011.

Winter TC (1999) Relation of streams, lakes, and wetlands to groundwater flow systems. *Hydrogeology Journal* 7:1:28-45.

Winter CT, Harvey WJ, Franke LO and Alley MW (1998) Ground water and surface water: A single resource. U.S. Geological Survey Circular 1139. Denver, Colorado.

Woodford AC and Chevallier L (2002) Hydrogeology of the Main Karoo Basin: Current Knowledge and Future Research Needs. Water Research Commission (WRC) of South Africa. WRC Report No. TT 179/02.

Wood WW and Sanford WE (1995) Chemical and isotopic methods for quantifying ground-water recharge in a regional, semiarid environment. *Ground Water* 33:3:458-468. Available via www.onlinelibrary.wiley.com 21 July 21 2011.

Xu Y and Beekman HE (2003) Groundwater Recharge Estimation in Southern Africa. UNESCO IHP Series No. 64. Available via www.asipohaapo.com, accessed 12 July 2011.

Yurtsever Y and Gat JR (1981) Atmospheric waters (In stable Isotope Hydrology, Eds. Gat JR and R Gonfiantini), IAEA Vienna Tech. Rep. Ser. No. 210, pp. 103-139.

Zappa G, Bersezio R, Felletti F and Giudici M (2006) Modeling heterogeneity of gravel-sand, braided stream, alluvial aquifers at the facies scale. *Journal of Hydrology* 325:134-153.

Zhang Y, Wu Y, Su J, Wen X, Liu F (2005) Groundwater replenishment analysis by using natural isotopes in Ejina Basin, Northwestern China. *Environmental Geology* 48: 6-14.

APPENDICES

Appendix 1 Hydraulic tests

Appendix 1.1 Inverse auger method

The inversed auger-hole method (Oosterbaan and Nijland 1994) is based on the principle that if an augured hole (uncased) is filled with water until the soil on its vicinity (below and sideways) is saturated the infiltration rate approaches a constant. In theory, towards saturation the average velocity (v) of the infiltrating front approximates the saturated soil hydraulic conductivity (K).

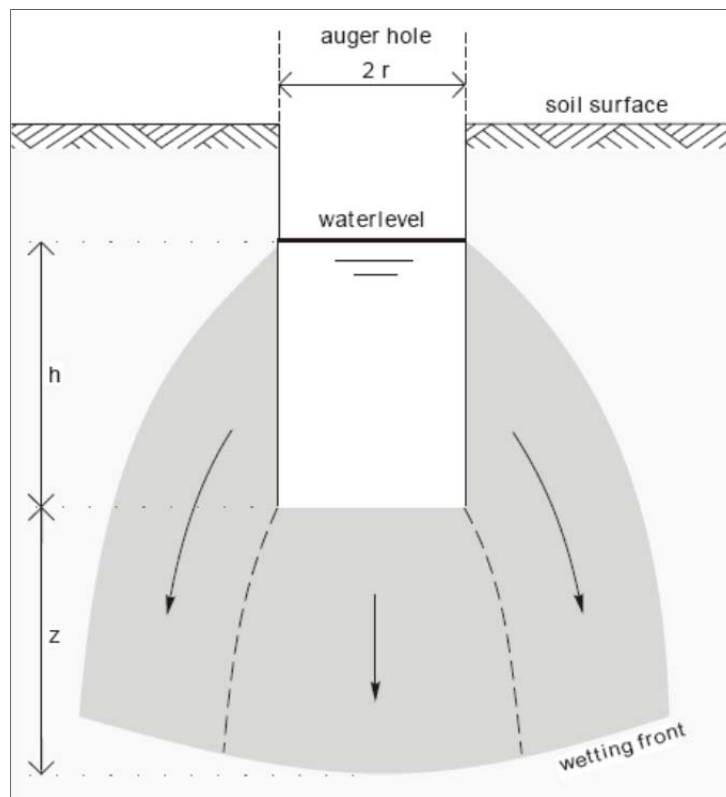


Figure 1 A schematic showing the configurations of an augured hole and the infiltrating front (Taken from Oosterbaan and Nijland).

In an uncased augured hole the following mathematics can be applied (Oosterbaan and Nijland 1994), the total infiltration into the soil Q_{in} (m^2/s) is given by Equation 16:

$$Q_{in} = vA$$

Equation 16

Where A is the surface area of infiltration (m^2) and v is average velocity of the infiltrating front (m/s). Towards saturation v (m/s) approaches K (m/s) hence:

$$Q_{in} = KA$$

Equation 17

Infiltration occurs both through the bottom and the sidewalls of the hole; hence the total infiltrating area is given by Equation 18.

$$A = \pi r^2 + 2\pi h$$

Equation 18

Where r (m) is the radius of the hole and h (m) is the height (head) of the water column in the hole). The total infiltration Q (m^3/s) is then given by Equation 19.

$$Q_{in} = 2\pi Kr \left(h + \frac{1}{2} r \right)$$

Equation 19

The total infiltration Q (m^3/s) is dependent on the rate at which the water level in the hole is lowered. The rate of fall in water level Q_{out} is given by Equation 20.

$$Q_{out} = \pi r^2 \frac{dh}{dt}$$

Equation 20

At any time (t), the flow infiltrating through the bottom and sideways of the hole (Q_{in}) should be equal to flow leaving the hole Q_{out} , hence:

$$2K \left(h + \frac{1}{2} r \right) = r \frac{dh}{dt}$$

Equation 21

Rearranging Equation 21 and integrating from time zero to time t during which the head decreases from h_0 to h yield Equation 22.

$$K = 1.15r \frac{\log \left(h_0 + \frac{1}{2} r \right) - \log \left(h_t + \frac{1}{2} r \right)}{t - t_0}$$

Equation 22

Where:

- K is the average saturated hydraulic conductivity for the infiltration front (m/s).
- r is the radius of the hole (m).
- t is time since start of measuring (s).
- h_t is the height of water column in the hole at time t (m).
- $h_0 = h_t$ at $t=0$ (m).

The scatter semi-log plot of $(h + \frac{1}{2}r)$ against (t) should yield a straight line. The straight line reflects saturation conditions. Close to saturation conditions were achieved during the infiltration tests. Figure 2 shows the straight the semi-log plot of $(h + \frac{1}{2}r)$ against (t) reflecting saturated conditions. The K value can be calculated according to Equation 22 with any two pairs of values of $h + \frac{1}{2}r$ and t .

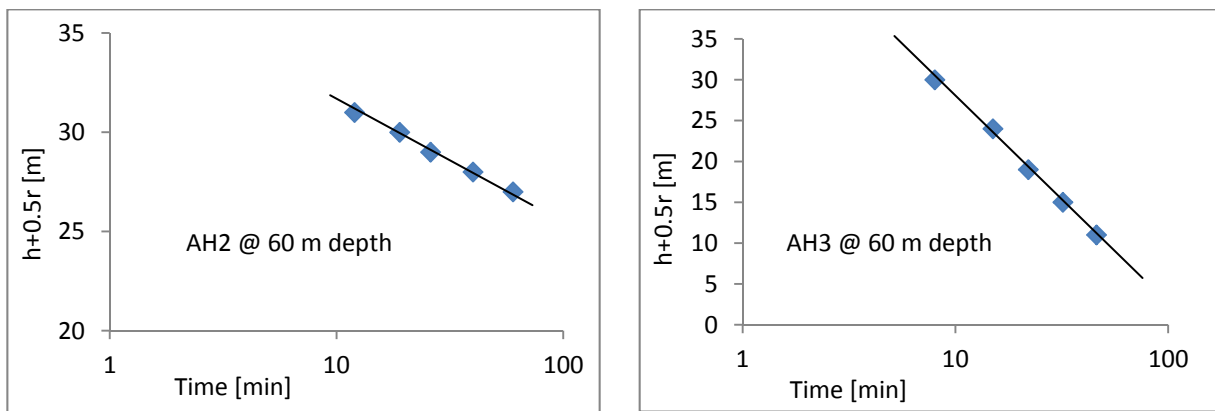


Figure 2 Straight line fit on the semi-log plot of $(h + \frac{1}{2}r)$ against (t) reflecting saturated conditions during the infiltration tests.

Appendix 1.2 Derivative plots

Drawdown derivative against time plots for BH6, BH5, BH3 and BH9 boreholes observed during the pumping of BH7 are presented in this section. The plot shows four groundwater flow segments: A-Typical Theis respond; B- transition period, C-RAF and D- impermeable river boundary effect.

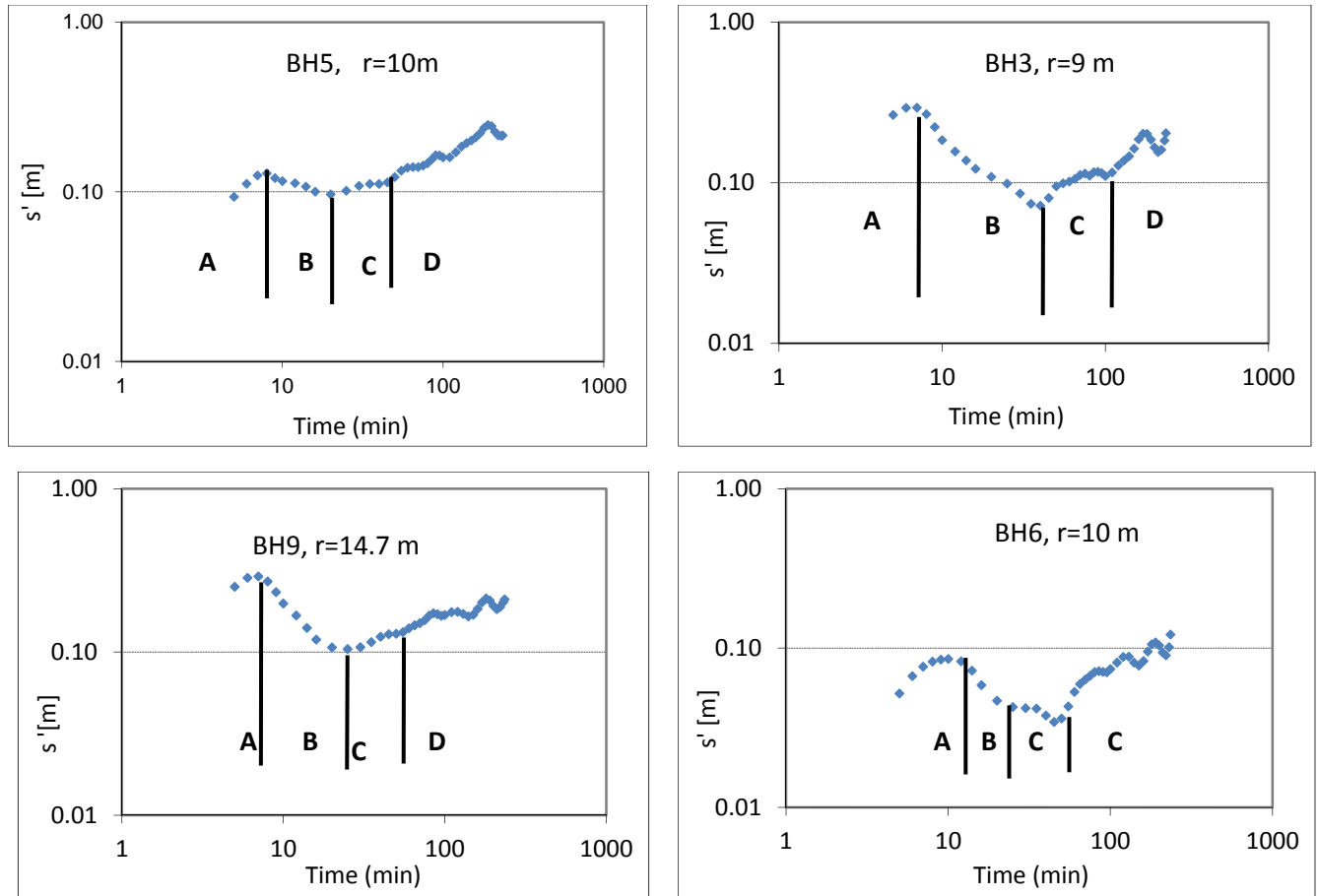
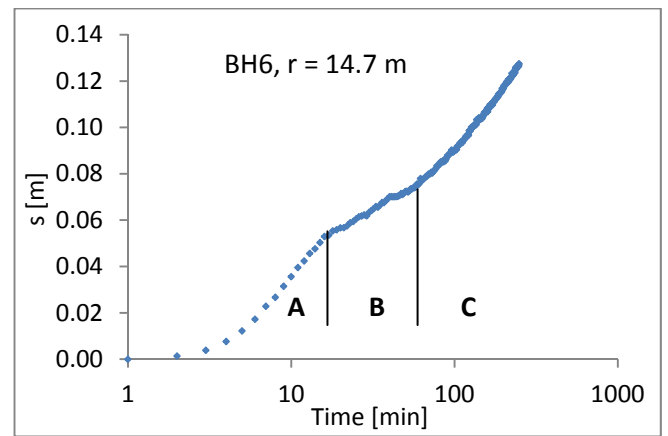
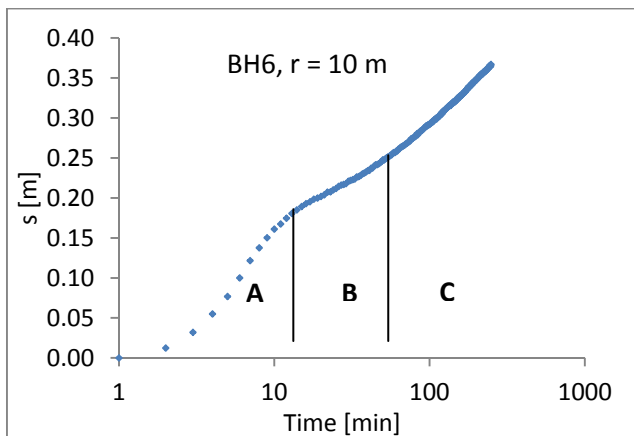
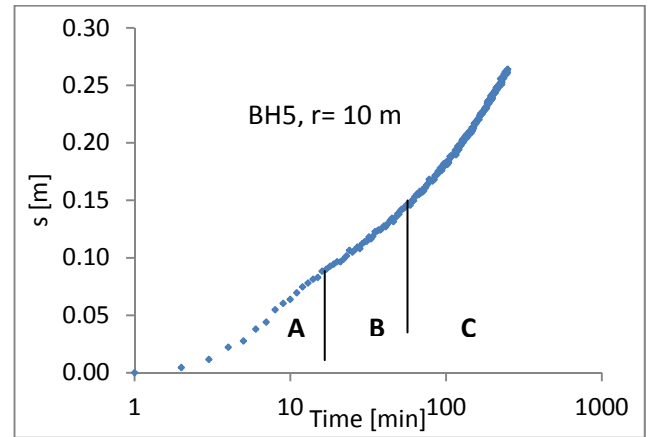
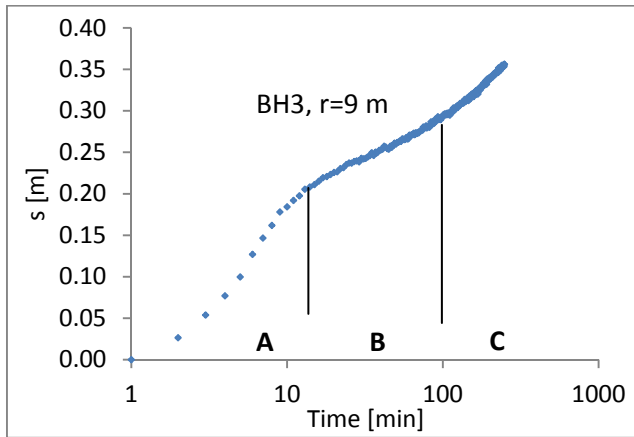


Figure 3 Drawdown derivatives against time plots for BH6, BH5, BH3 and BH9 boreholes observed during the pumping of BH7 are presented in this section.

Appendix 1.3 Semi-log plots

Semi-log graphs for BH6, BH5, BH3 and BH9 observation boreholes showing 3 dominant groundwater flow phases (A-Theis, B-RAF and C-river boundary effects) during the pumping of BH7.



Appendix 2 Groundwater and river water chemistry

Appendix 2.1 July 2010

Ions	Units	R 1	SP
pH		8.07	8.41
EC	mS/m	47.5	101
Ca ⁺²	mg/l	26.5	41.9
Mg ⁺²	mg/l	12.7	53.2
Na ⁺	mg/l	44.8	125.5
K ⁺	mg/l	8.27	6.95
P-Alk	mg/l	0	13.4
M-Alk	mg/l	171	457
F ⁻	mg/l	0.29	0.66
Cl ⁻	mg/l	35	62
Br ⁻	mg/l	0.05	0.32
NO ₃ ⁻ (N)	mg/l	0.14	0.13
PO ₄ ⁻	mg/l	<0.1	<0.1
SO ₄ ⁻²	mg/l	19.3	28
TDS	mg/l	318	776
Al ⁺³	mg/l	0.032	0.019
Fe ⁺²	mg/l	0.021	0.013
Mn ⁺²	mg/l	0.022	0.011

Appendix 2.2 February 2011

Site number	pH	EC	Concentration [mg/l]															
			Ca ⁺²	Mg ⁺²	Na ⁺	K ⁺	PAIk	MAIk	F ⁻	Cl ⁻	NO ₂ ⁻ (N)	Br ⁻	NO ₃ ⁻ (N)	PO ₄ ⁻	SO ₄ ⁻²	Al ⁺³	Fe ⁺²	Mn ⁺²
BH1	7.45	96.90	39.32	40.65	113.10	5.10	0.00	411.00	0.56	57.00	0.01	0.19	0.37	-0.10	25.65	0.03	0.04	0.00
BH2	7.36	90.10	39.42	40.09	93.29	8.23	0.00	381.00	0.49	54.00	0.30	0.24	0.82	-0.10	21.87	0.03	0.06	0.00
BH3	7.57	109.00	36.31	50.06	157.34	5.59	0.00	589.00	0.67	70.00	-0.01	0.30	0.18	-0.10	31.27	0.03	0.04	0.00
BH4	7.48	89.10	39.95	43.30	100.12	5.42	0.00	381.00	0.51	53.00	-0.01	0.29	0.37	-0.10	21.32	0.05	0.07	0.00
BH5	7.46	105.00	35.54	56.60	123.66	5.58	0.00	462.00	0.62	61.00	-0.01	0.31	0.00	-0.10	26.31	0.03	0.04	0.09
BH6	7.45	99.30	41.66	48.91	114.49	5.58	0.00	426.00	0.55	60.00	-0.01	0.32	0.23	-0.10	25.76	0.03	0.04	0.00
BH7	7.43	100.00	34.35	49.50	111.73	5.70	0.00	430.00	0.57	60.00	-0.01	0.36	0.08	-0.10	26.05	0.04	0.05	0.01
BH8	7.68	105.00	35.65	47.35	124.83	5.60	0.00	436.00	0.55	69.00	-0.01	0.36	0.25	-0.10	32.02	0.03	0.03	0.00
BH9	7.55	104.00	37.55	45.18	121.54	5.31	0.00	424.00	0.57	70.00	-0.01	0.34	0.32	-0.10	34.05	0.03	0.04	0.00
BH10	7.52	93.40	37.29	42.37	103.35	5.26	0.00	394.00	0.54	57.00	-0.01	0.20	0.34	-0.10	24.82	0.03	0.03	0.00
BH11	7.61	94.90	34.62	41.43	108.99	5.50	0.00	398.00	0.53	59.00	-0.01	0.28	0.33	-0.10	26.41	0.03	0.04	0.00
BH12	7.63	93.60	36.32	41.59	106.68	5.40	0.00	395.00	0.49	57.00	-0.01	0.28	0.31	-0.10	24.87	0.03	0.05	0.00
BH13	7.63	94.50	35.47	42.21	108.56	5.41	0.00	396.00	0.51	59.00	-0.01	0.27	0.37	-0.10	26.56	0.03	0.03	0.00
BH14	7.46	88.30	40.94	42.28	86.50	4.75	0.00	380.00	0.41	51.44	0.02	0.25	0.51	-0.10	20.56	0.03	0.04	0.00
BH15	7.49	86.50	40.45	41.53	84.14	4.85	0.00	373.00	0.36	48.84	0.02	0.31	0.51	-0.10	20.02	0.03	0.03	0.00
SP	7.57	111.00	44.02	58.28	119.83	5.85	0.00	485.00	0.65	64.00	-0.01	0.33	0.07	-0.10	29.16	0.03	0.04	0.00
R1	7.31	30.00	16.23	7.26	26.99	6.52	0.00	99.00	0.17	24.53	-0.01	0.03	0.40	-0.10	16.15	0.10	0.11	0.03
R2	7.26	29.90	21.96	8.88	23.47	6.63	0.00	99.70	0.16	22.16	-0.01	0.08	0.46	-0.10	15.08	0.09	0.11	0.02

BH-borehole water; SP-seepage groundwater; R1-river water on the site and R2-river water down gradient of the site at the designated outflow point;
negative value-below detection limit.

Appendix 2.3 May 2011

Site number	pH	EC	Concentration [mg/l]																
			Ca ⁺²	Mg ⁺²	Na ⁺	K ⁺	PAIk	MAIk	F ⁻	Cl ⁻	NO ₂ ⁻ (N)	Br ⁻	NO ₃ ⁻ (N)	PO ₄ ⁻	SO ₄ ⁻²	Al ⁺³	Fe ⁺²	Mn ⁺²	Si ⁺⁴
BH1	7.93	95.10	38.06	41.55	121.21	5.28	0.00	404.00	0.57	68.00	-0.01	0.26	0.37	-0.10	29.75	0.03	0.04	0.01	21.06
BH2	8.00	86.60	37.05	41.15	99.95	4.99	0.00	365.00	0.50	52.00	-0.01	0.25	0.45	-0.10	20.93	0.04	0.05	0.02	20.88
BH3	7.58	103.00	32.12	48.31	145.91	5.90	0.00	442.00	0.70	71.00	-0.01	0.34	0.19	-0.10	31.95	0.01	0.01	0.01	23.05
BH4	7.85	85.60	35.09	43.07	106.17	5.64	0.00	370.00	0.56	58.00	-0.01	0.28	0.44	-0.10	21.48	0.02	0.01	0.01	20.66
BH5	7.60	85.50	32.91	56.08	129.24	5.79	0.00	457.00	0.67	68.00	-0.01	0.38	0.06	-0.10	28.27	0.01	0.01	0.04	23.55
BH6	7.63	109.00	35.06	46.16	114.50	5.65	0.00	415.00	0.66	62.00	-0.01	0.38	0.25	-0.10	26.16	0.01	0.01	0.01	23.46
BH7	7.62	92.50	31.47	48.39	113.67	5.62	0.00	419.00	0.64	63.00	-0.01	0.35	0.24	-0.10	25.79	0.02	0.01	0.01	23.68
BH8	7.64	104.00	34.35	49.71	136.66	6.03	0.00	438.00	0.59	73.00	-0.01	0.39	0.19	-0.10	32.74	0.03	0.02	0.01	22.63
BH9	7.64	99.10	34.42	45.99	131.20	5.55	0.00	414.00	0.55	76.00	-0.01	0.36	0.31	-0.10	34.18	0.01	0.01	0.02	21.33
BH10	7.63	94.10	35.02	43.74	109.08	5.65	0.00	384.00	0.58	60.00	-0.01	0.25	0.33	-0.10	25.42	0.01	0.01	0.01	21.01
BH11	7.67	103.00	34.56	45.09	128.51	5.70	0.00	387.00	0.57	107.00	-0.01	0.24	0.33	-0.10	26.39	0.01	0.01	0.01	20.57
BH12	7.69	88.40	32.57	42.70	114.28	5.55	0.00	385.00	0.56	61.00	-0.01	0.27	0.30	-0.10	24.91	0.01	0.01	0.01	20.75
BH13	7.66	93.30	35.59	45.54	121.18	6.24	0.00	396.00	0.52	62.00	-0.01	0.34	0.28	-0.10	22.61	0.02	0.02	0.01	20.67
BH14	7.73	84.60	37.16	43.18	94.24	5.05	0.00	370.00	0.46	57.00	-0.01	0.26	0.55	-0.10	20.26	0.01	0.01	0.02	21.35
BH15	7.82	83.80	41.00	45.58	96.43	5.66	0.00	366.00	0.43	55.00	-0.01	0.14	0.54	-0.10	20.36	0.01	0.01	0.01	20.36
SP	7.86	106.00	39.46	57.18	123.18	5.54	0.00	473.00	0.72	69.00	-0.01	0.38	0.10	-0.10	29.24	0.01	0.01	0.01	22.75
R1	7.23	19.70	12.12	6.19	16.66	5.20	0.00	72.50	0.10	13.23	0.02	-0.04	0.56	-0.10	10.12	0.11	0.14	0.01	23.73
R2	7.25	19.90	13.48	6.68	15.31	5.22	0.00	73.60	0.13	14.76	-0.01	0.04	0.60	-0.10	10.26	0.10	0.12	0.01	24.90

BH-borehole water; SP-seepage groundwater; R1-river water on the site and R2-river water down gradient of the site at the designated outflow point; negative value-below detection limit.

Appendix 2.4 August 2011

Site number	pH	EC	Concentration [mg/l]													
			Ca ⁺²	Mg ⁺²	Na ⁺	K ⁺	PAIk	MAIk	F ⁻	Cl ⁻	NO ₂ ⁻ (N)	Br ⁻	NO ₃ ⁻ (N)	PO ₄ ⁻	SO ₄ ⁻²	Al ⁺³
BH1	7.53	107	44.5	48.3	122.3	5.6	0	443	0.55	86.2	-0.10	-0.04	0.57	-1.00	37.24	20.4
BH2	7.72	84.8	34.5	41.9	89.0	5.1	0	376	0.52	54.0	-0.01	0.20	0.52	-0.10	21.32	21.7
BH3	7.5	108	36.3	51.3	132.0	5.6	0	477	0.38	71.8	-0.10	0.34	-0.50	-1.00	28.16	23.6
BH4	7.46	87.7	36.7	41.4	94.4	5.3	0	392	0.55	56.0	-0.01	0.26	0.43	-0.10	22.06	21.8
BH5	7.25	168	53.6	107.2	172.2	7.3	0	613	0.51	206.0	-0.10	0.21	-0.50	-1.00	82.34	23.2
BH6	7.3	102	45.2	53.0	114.5	6.1	0	449	0.40	70.7	-0.10	0.30	-0.50	-1.00	28.01	23.7
BH7	7.31	109	43.5	63.5	123.2	6.6	0	470	0.25	84.2	-0.10	0.67	-0.50	-1.00	31.53	23.9
BH8	7.54	124	39.8	59.2	143.9	6.0	0	509	0.56	97.5	-0.10	0.57	-0.50	-1.00	53.30	23.0
BH9	7.36	165	56.4	82.8	209.6	6.6	0	539	0.73	204.5	-0.10	1.40	-0.50	-1.00	105.04	20.3
BH10	7.33	91.9	41.9	47.3	108.9	6.1	0	407	0.62	59.0	-0.01	0.26	0.32	-0.10	25.81	22.2
BH11	7.37	93.7	35.7	42.7	108.7	5.7	0	410	0.50	63.0	-0.01	0.29	0.31	-0.10	25.58	21.5
BH12	7.51	93.6	36.9	44.1	106.9	5.6	0	408	0.46	65.0	-0.01	0.25	0.36	-0.10	25.82	21.8
BH13	7.36	92.5	36.0	41.6	103.9	5.5	0	411	0.43	59.0	-0.01	0.21	0.30	-0.10	24.29	21.1
BH14	7.4	86.6	45.5	45.9	86.4	5.0	0	388	0.35	53.0	-0.01	0.16	0.59	-0.10	20.64	21.6
BH15	7.44	84.8	41.0	41.7	82.9	5.0	0	383	0.33	51.0	-0.01	0.19	0.55	-0.10	22.15	21.3
SP	7.52	135	54.4	74.2	139.2	5.7	0	533	0.26	106.1	-0.10	-0.40	0.11	-1.00	74.83	21.8
R1	7.41	21.8	14.6	4.3	18.2	5.3	0	76	0.11	15.0	-0.01	-0.04	0.85	-0.10	10.24	5.3
R2	7.22	22.3	14.6	4.2	19.1	5.2	0	75	0.08	16.3	-0.01	0.08	1.00	-0.10	10.74	5.2

BH-borehole water; SP-seepage groundwater; R1-river water on the site and R2-river water down gradient of the site at the designated outflow point, negative value-below detection limit.

Appendix 2.5 December 2011

	Concentration [mg/l]																		
Site	pH	EC	Ca ⁺²	Mg ⁺²	Na ⁺	K ⁺	PAIk	MAIk	F ⁻	Cl ⁻	NO ₂ ⁻ (N)	Br ⁻	NO ₃ ⁻ (N)	PO ₄ ⁻	SO ₄ ⁻²	Al ⁺³	Fe ⁺²	Mn ⁺²	Si ⁴
BH1	7.67	101	41.9	45.9	118.8	5.717	0	458	0.63	66.10	-0.01	0.32	0.29	-0.10	30.38	0.010	0.016	0.018	21.175
BH2	8.17	86.1	38.5	42.2	100.0	5.485	0	395	0.50	55.20	-0.01	0.28	0.39	0.16	21.95	0.008	0.011	0.016	19.479
BH3	7.74	122	41.4	55.8	151.0	5.950	0	524	0.33	81.81	-0.10	0.41	-0.50	-1.00	36.12	0.008	0.009	0.016	21.409
BH4	7.81	88.9	37.0	41.1	102.0	5.329	0	406	0.55	56.10	-0.01	0.29	0.41	-0.10	22.94	0.007	0.008	0.019	19.948
BH5	7.82	138	43.1	66.9	178.2	6.043	0	608	0.80	86.87	-0.10	0.58	-0.50	-1.00	45.56	0.008	0.009	0.050	21.657
BH6	7.90	105	43.2	49.5	121.7	5.849	0	471	0.32	54.60	-0.10	-0.40	-0.50	-1.00	9.65	0.010	0.009	0.016	21.348
BH7	7.91	106	38.0	51.7	123.1	5.591	0	479	0.32	53.64	-0.10	-0.40	-0.50	-1.00	26.48	0.007	0.009	0.016	21.981
BH8	7.83	106	38.3	47.9	134.1	5.686	0	471	0.34	57.58	-0.10	-0.40	-0.50	-1.00	30.47	0.010	0.008	0.017	20.893
BH9	7.77	156	53.0	69.6	202.8	6.199	0	540	0.28	166.73	-0.10	0.70	1.43	-1.00	82.24	0.010	0.008	0.019	19.054
BH10	7.84	97	40.8	45.3	113.6	5.909	0	423	0.59	70.80	-0.01	0.40	0.50	-0.10	28.18	0.011	0.009	0.014	19.827
BH12	7.86	99.9	39.4	45.4	115.8	5.900	0	424	0.72	77.30	-0.01	0.49	0.59	0.10	30.33	0.010	0.009	0.014	19.508
BH13	7.91	97.6	37.3	43.3	114.6	5.891	0	422	0.65	72.10	-0.01	0.35	0.46	-0.10	28.40	0.008	0.008	0.020	20.032
BH14	7.87	88.9	42.0	42.9	93.2	5.186	0	406	0.53	54.30	-0.01	0.34	0.49	-0.10	21.40	0.007	0.008	0.031	19.709
BH15	7.90	87.1	41.2	41.2	90.5	5.277	0	397	0.41	52.86	-0.01	0.30	0.47	0.20	20.44	0.009	0.008	0.024	19.695
R1	7.62	41.8	28.5	12.0	32.0	7.216	0	140	0.17	35.65	-0.01	0.07	0.75	-0.10	22.71	0.370	0.126	0.021	2.053
R2	7.94	58.4	33.3	18.0	53.7	6.557	0	193	0.26	56.10	-0.01	0.27	0.48	-0.10	30.43	0.360	0.120	0.022	2.524
SP	7.93	122	46.8	59.5	169.3	6.102	0	515	1.23	162.0	-0.1	1.1	-0.5	-1.0	93.7	0.011	0.008	0.019	20.732

BH-borehole water, SP-seepage groundwater; R1-river water on the designated outflow point of the water balance model, R2-river water on the designated inflow flow point of the water balance model; negative value-below detection limit.

Appendix 3 Groundwater levels

Appendix 3.1 Alluvial channel aquifer

Groundwater levels [mbgl] measured in the boreholes drilled into the alluvial channel aquifer during the monitoring period.

Year and month	BH3	BH5	BH6	BH7	BH8	BH9
2010-Aug	2.79	2.41	2.51	2.56	2.78	2.76
2010-Oct	2.80	2.43	2.56	2.61	2.80	2.82
2010-Nov	2.88	2.45	2.60	2.65	2.87	2.88
2010-Dec	2.93	2.50	2.63	2.68	2.92	2.92
2011-Jan	2.83	2.43	2.54	2.61	2.82	2.79
2011-Feb	2.74	2.40	2.50	2.56	2.75	2.76
2011-Mar	2.83	2.44	2.54	2.66	2.83	2.87
2011-Apr	2.81	2.43	2.53	2.58	2.81	2.82
2011-May	2.72	2.38	2.46	2.52	2.72	2.75
2011-June	2.48	2.21	2.24	2.33	2.47	2.42
2011-July	2.56	2.25	2.33	2.37	2.55	2.55
2011-Aug	2.55	2.25	2.32	2.36	2.53	2.53
2011-Sep	2.55	2.25	2.32	2.36	2.53	2.53

Appendix 3.2 Background terrestrial aquifer

Groundwater levels [mbgl] measured in the boreholes drilled into the terrestrial aquifer during the monitoring period.

Year and month	BH10	BH11	BH12	BH13	BH14	BH15
2010-Aug	9.03	8.45	8.21	8.54	6.53	8.57
2010-Oct	9.05	8.49	8.27	8.59	6.60	8.63
2010-Nov	9.11	8.55	8.31	8.62	6.62	8.69
2010-Dec	9.18	8.63	8.38	8.70	6.72	8.75
2011-Jan	9.16	8.57	8.33	8.65	6.62	8.67
2011-Feb	9.14	8.56	8.32	8.64	6.62	8.64
2011-Mar	9.12	8.54	8.30	8.63	6.61	8.62
2011-Apr	9.11	8.58	8.30	8.66	6.60	8.63
2011-May	9.03	8.44	8.21	8.54	6.51	8.56
2011-June	8.89	8.28	8.03	8.37	6.39	8.42
2011-July	8.66	8.12	7.87	8.23	6.35	8.37
2011-Aug	8.62	8.08	7.82	8.16	6.32	8.34
2011-Sep	8.59	8.05	7.79	8.13	6.34	8.35

Appendix 4 Isotopes

Appendix 4.1 February and May 2011

Boreholes	February-2011		May-2011	
	$\delta^{18}\text{O}$ [‰]	$\delta^2\text{H}$ [‰]	$\delta^{18}\text{O}$ [‰]	$\delta^2\text{H}$ [‰]
BH1	-4.97	-32.8	-5.19	-31.4
BH2	-4.97	-33.9	-5.22	-32.1
BH3	-5.02	-33.7	-5.17	-31.3
BH4	-5.01	-34.4	-5.17	-31.7
BH5	-5.09	-34.1	-5.25	-32.1
BH6	-5.09	-32.5	-5.12	-33.6
BH7	-5.00	-33.3	-5.07	-33.2
BH8	-5.01	-32.7	-5.05	-32.6
BH9	-4.95	-32.9	-4.98	-32.4
BH10	-4.97	-32.4	-5.01	-32.4
BH11	-5.02	-32.8	-5.08	-32.2
BH12	-5.06	-32.9	-5.00	-32.0
BH13	-5.04	-32.5	-5.08	-31.7
BH14	-5.12	-33.1	-5.22	-33.2
BH15	-5.12	-33.7	-5.16	-33.0
SP	-5.12	-33.7	-5.19	-32.7
R1	-2.86	-17.7	-3.64	-15.1
R2	-2.70	-17.4	-3.64	-15.5

BH-borehole water; SP-seepage groundwater; R1-river water on the designated outflow point of the water balance model; R2-river water on the designated inflow flow point of the water balance model.

ABSTRACT

The study describes the application complimentary geohydrologic tools to investigate the geohydrological properties of an alluvial channel aquifer and its interaction with the river surface water resources. Primary field investigations were designed to determine the geologic, hydraulic, hydrogeochemical and solute transport properties of the alluvial channel aquifer as an important component of the groundwater-surface water (GW-SW) interaction system. The secondary investigations were then aimed at assessing groundwater discharge and recharge mechanisms of the alluvial channel aquifer at a local scale (< 1000 m). A water balance model was developed for the groundwater-surface system as a tertiary level of investigation.

Geological characterisation results show the spatial variation in the physical properties of unconsolidated aquifer materials between boreholes and at different depth. The drawdown derivative diagnostic analysis shows that the alluvial channel aquifer system response during pumping can be described by the following major groundwater flow characteristics; Typical Theis response; transition period from initial Theis response to radial acting flow (RAF); radial acting flow in the gravel-sand layer and river single impermeable boundary effects. Detailed studies of the hydrogeochemical processes in the alluvial aquifer system have shown that dissolution of silicate weathering, dolomite and calcite minerals, and ion exchanges are the dominant hydrogeochemical processes that controls groundwater quality. Quantitative and qualitative investigations indicate that the alluvial channel aquifer is being recharged through preferential infiltration recharge as facilitated by cavities and holes created by the burrowing animals and dense tree rooting system. Tracer tests under natural gradient were successfully conducted in an alluvial channel aquifer, thus providing some advice on how to conduct tracer breakthrough tests under natural gradients in a typical alluvial channel aquifer.

The findings of the study also highlights the value of developing a water balance model as a preliminary requirement before detailed GW-SW interaction investigations can be conducted. Based on the theoretical conceptualizations and field evidence it is suggested that studies be conducted to determine if alluvial channel aquifers can be further classified based on the nature of the hosting river channel. The classification would split the alluvial channel aquifer into alluvial cover and fractured-bedrock, or a combination of the two. The applications of the PhD thesis findings are not only limited to the case study site, but have important implications for GW-SW interaction studies, groundwater resource development and protection in areas where groundwater occurs in alluvial channel deposits.